DIAGENESIS OF THE LANSING AND KANSAS CITY GROUPS (UPPER PENNSYLVANIAN), NORTHWESTERN KANSAS AND SOUTHWESTERN NEBRASKA

by

James E. Anderson

Kansas Geological Survey
Open-file Report 89-14

Disclaimer

Kansas Geological Survey
1930 Constant Avenue
University of Kansas
Lawrence, KS 66047-3726

89-14

Diagenesis of the Lansing and Kansas City groups (Upper Pennsylvanian), northwestern Kansas and southwestern Nebraska

by

James E. Anderson

B.S., University of Nebraska-Lincoln, 1984

Submitted to the Department of Geology and the Faculty of the Graduate School of the University of Kansas in partial fulfillment of the requirements for the degree of Master of Science.

Advisory Committee:

Robert H. Goldstein
Chairman

Donald R. Gerrow

James C. Dellwig

W. Lynn Watney

Courtney H. Wallace
For the Department

Date Thesis Accepted

TABLE OF CONTENTS

LIST OF ILLUSTRATIONS

LIST OF TABLES

ABSTRACT

The Lansing and Kansas City groups of northwestern Kansas and southwestern Nebraska are composed of interbedded limestones and shales. The porous carbonates generally are nonargillaceous wackestones, packstones, and grainstones. Argillaceous carbonates and carbonates with clayey infilling commonly are nonporous.

These carbonates contain abundant calcite and dolomite cement. Calcite cement generally postdates compaction, which suggests that it precipitated after significant burial. In places, moldic pores postdate compaction and the first generation of calcite cement, suggesting a post-burial origin for some of the moldic pores. Replacive dolomite predates all calcite cement, whereas dolomite cement commonly postdates calcite cement. Calcite cement, and to a lesser degree, dolomite cement are the main porosity destroyers. In places, porosity is enhanced by late-stage dissolution that postdates calcite and dolomite cement.

Primary, one-phase all-liquid inclusions in the first generation of calcite cement are evidence of precipitation below approximately 45°C. The composition of these inclusions indicates that this calcite precipitated from brines with approximately 22 weight-percent Ca-Na-Cl. Later calcite cements contain only two-phase inclusions. Plots of homogenization temperatures (Th) versus freezing-point depressions (Tm ice) show convergence at Th of 45-50°C and Tm ice of -22°C, indicating that later calcite cement precipitated from fluids with temperatures of 45° to 50°C and

salinities of approximately 22 weight-percent Ca-Na-Cl. Fluid-inclusion data from later dolomites suggest precipitation at 45° to 70°C from fluids with a salinity of approximately 22 weight-percent Ca-Na-Cl. Post-cementation fluids that filled some of the fluid inclusions imply a later history of increasing temperature and decreasing salinity in pore fluids. Based on fluid inclusion Th data, the maximum temperature reached was approximately 100°-110°C.

The highly saline brines responsible for precipitation of calcite and dolomite apparently moved downward 300 to 600 m from evaporating pans depositing Lower Permian anhydrite. As these fluids probably were Na-Mg-Cl brines, dolomitization, albitization, and the exchange of Na for Ca in smectite clays enhanced the calcium content of these brines as they refluxed down to eventually precipitate calcite and dolomite cement in the Lansing and Kansas City groups.

I dedicate this thesis to the Glory of my

Lord and Savior Jesus Christ,

and to the honor of my parents,

Lawrence and Maxine Anderson

ACKNOWLEDGMENTS

This thesis project originated with a summer internship with Marathon Oil Company in Casper, WY, which was a highlight of my graduate studies. Eric Potter and Dan Seamount were very helpful as I pursued the beginnings of this thesis.

During my research and writing, my advisor, Bob Goldstein, has been of tremendous help with his encouragement and scientific insight. His efforts and sacrificial help were crucial to the success of this thesis. I also appreciate the concern and help of my other committee members, Louis Dellwig, Don Sprowl, and Lynn Watney.

Financial support for this study includes an $800 1986 AAPG Grant-in-Aid and support from the Department of Geology. The Department of Geology also provided excellent facilities for the pursuit of this study. The Kansas Geological Survey has been of great help in providing a research assistantship, use of facilities, and access to the core repository, from which all samples were analyzed. I also thank the oil companies who provided these cores. Renate Hensiek and John Charlton of the Kansas Geological Survey were very helpful with drafting and the preparation of slides, which helped me to defend this thesis with *Honors* and to win the *Best Student Paper* at the 1989 South-Central Section meeting of the Geological Society of America.

Through my five years of study at KU, many students have provided insight and moral support. Some of these helpful students

include Brian McNeice, Richard Simms, Bryan Stephens, Dave Newell, Mark Bowman, Mike Lambert, Bart Douglas, Matt Wilson, and Chris Wojcik. I also appreciate the prayers and encouragements of Betty Nemecheck.

My parents, Lawrence and Maxine Anderson, were of special help with their love, concern, encouragement, and financial support.

Most of all, the greatest source of blessings and support for my work is my Lord and Savior Jesus Christ, the Creator of this entire Universe. Only through his grace and blessings, was I able to sojourn through this thesis. I so appreciate that he has redeemed me by His blood, and that I can have a personal relationship with Him, the very God of this Universe. Because of his tremendous grace and love, I have dedicated this thesis to his glory.

"Oh, the depth of the riches of the wisdom
and knowledge of God!
How unsearchable his judgments, and his paths beyond
tracing out!
Who has known the mind of the Lord?
Or who has been his counselor?
Who has given to God, that God should repay him?
For from him and through him and to him are all things.
To him be the glory forever! Amen."
-Romans 12: 33-36.

INTRODUCTION

The Upper Pennsylvanian Lansing and Kansas City groups are composed of interbedded limestones and shales. Some of the limestones are petroleum reservoirs in western Kansas and southwestern Nebraska. This thesis is a petrographic and diagenetic study of the limestones within this interval.

The first goal of this study was to determine which limestone lithologies have sufficient porosity to be petroleum reservoirs. The lithologies that commonly are porous were the focus of this study to determine what controls the presence or absence of porosity.

The second goal was to analyze the diagenetic events and determine their effect on the porosity evolution of these strata. This included petrographically analyzing the kinds and amount of porosity, processes or events that create or enhance porosity, such as dolomitization or dissolution, and processes or events that destroy porosity, such as compaction, cementation, and pressure solution. To better understand the controls of cementation, primary fluid inclusions in calcite and dolomite cements were analyzed to determine the concentration of fluids of calcite and dolomite precipitation.

The third goal was to develop a model that could predict the presence or absence of porous strata.

GEOLOGIC SETTING

The interbedded limestone and shale packages of the Lansing and Kansas City groups are cyclothems (Moore, 1936, 1949). Wanless and

Shepard (1936), Heckel (1977), and Watney (1985) interpreted that these cyclothems resulted from glacio-eustatic cyclicity. The cyclothems commonly are composed of four members: the lower carbonate, the lower shale, the upper carbonate, and the upper shale (Watney, 1980, 1985) (Figure 1). According to Heckel (1977), the lower carbonate was deposited during transgression, the lower shale was deposited during maximum transgression, the upper carbonate was deposited during regression, and the upper shale was deposited during maximum regression.

The paleogeographic reconstruction of Rascoe and Adler (1983) (Figure 2) indicated the environment of this study area was primarily marine, but there was a nearby semi-continental environment. The major structural features in the area of study (Figure 3) include the Central Kansas uplift, the Cambridge arch, the Las Animas arch, and the Hugoton embayment. The major uplift of the Central Kansas uplift and the Cambridge arch was post-Mississippian and pre-Middle Pennsylvanian (Merriam, 1963). The major uplift of the Las Animas arch was post-Cretaceous (Merriam, 1963), but Rascoe (1978) noted Pennsylvanian and Permian depositional trends paralleling the Las Animas arch which suggests some movement at these times.

Heckel (1983) proposed a diagenetic model for the Lansing and Kansas City groups in which meteoric waters percolated through the upper shale and upper carbonate during intraformational subaerial exposure events in the upper shale or upper carbonate. The meteoric

Figure 1. The typical cyclothem of the Lansing and Kansas City groups. The terms used in this study for the members of a cyclothem (Watney, 1980, 1985) are shown. Heckel (1977) used different terms, middle limestone for lower carbonate, core shale for lower shale, upper limestone for upper carbonate, and outside shale for upper shale. (modified from Heckel, 1977)

m.
Approx. thickness
Basic Cyclothem
(Kansas-type)
in Kansas-Iowa outcrop belt
Positional Member
Lithology
UPPER SHALE
UPPER CARBONATE
LOWER SHALE
LOWER CARB.
UPPER SHALE
① Gray to green, locally red Soil;
② Sandy shale w. siltstone sparse fossils
Laminated unfoss. bird's-eye calcilutite to Oolite
loc. cross-bedded Skel. calcarenite w. marine biota
Gray shaly Skel. calcilutite w. abundant marine biota
Gray-brown Shale w. loc. invert. calcarenite ~ top
Black fissile Shale w. PO4, pelagic fauna
Dense, dark Skel. calcilutite w. marine biota; loc. Calcarenite at base
Sandy shale w. marine biota
Gray to brown Sandy shale w. loc Coal, Sandstone
5
4
3
2
1
0
Depositional Environment
Nonmarine
Near-shore
Offshore
Shoreline
Shoal
Shallow w.
Eff. wave base
Intermediate depth
Eff. lwr. limit of algal CO3 production
Deep water
① Detrital influx after carbonate shoal formed
② Detrital influx before shoal conditions reached
Fossil Distribution
Algae (preserved)
Invertebrates
Conodonts
Adetognathus spp.
Anchignathodus m.
Aethotaxis adreno
Idiognathodus spp.
Neognathodus spp.
Idioprioniodus lex.
Gondolella spp.
Phase of Deposition
Direction of sea-level change
Dominant processes
Depositional member
Maximum Regression
Regression
Maxi-mum
Transgression
Max. Regr'sn
Stillstd
Sub.sed.
Detrital influx
NEARSHORE SHALE
Stillstand
Subsid.<sedimenth.
Detrital influx
NEARSHORE SHALE
Eustatic lowering of sea level - Subsidence probably < sedimentation
Still-stand
Eustatic s.l. rise
Subsid. > sedimenth.
CO3 prod.
TRANSGR. LIMEST.
-Sed.starvtn
CO3 productn~"Basin filling"
OFFSHORE SHALE
REGRESSIVE LIMESTONE

Figure 2. The paleogeography of the midcontinent during the deposition of the Lansing and Kansas City groups in relation to the area of study (modified from Rascoe and Adler, 1983).

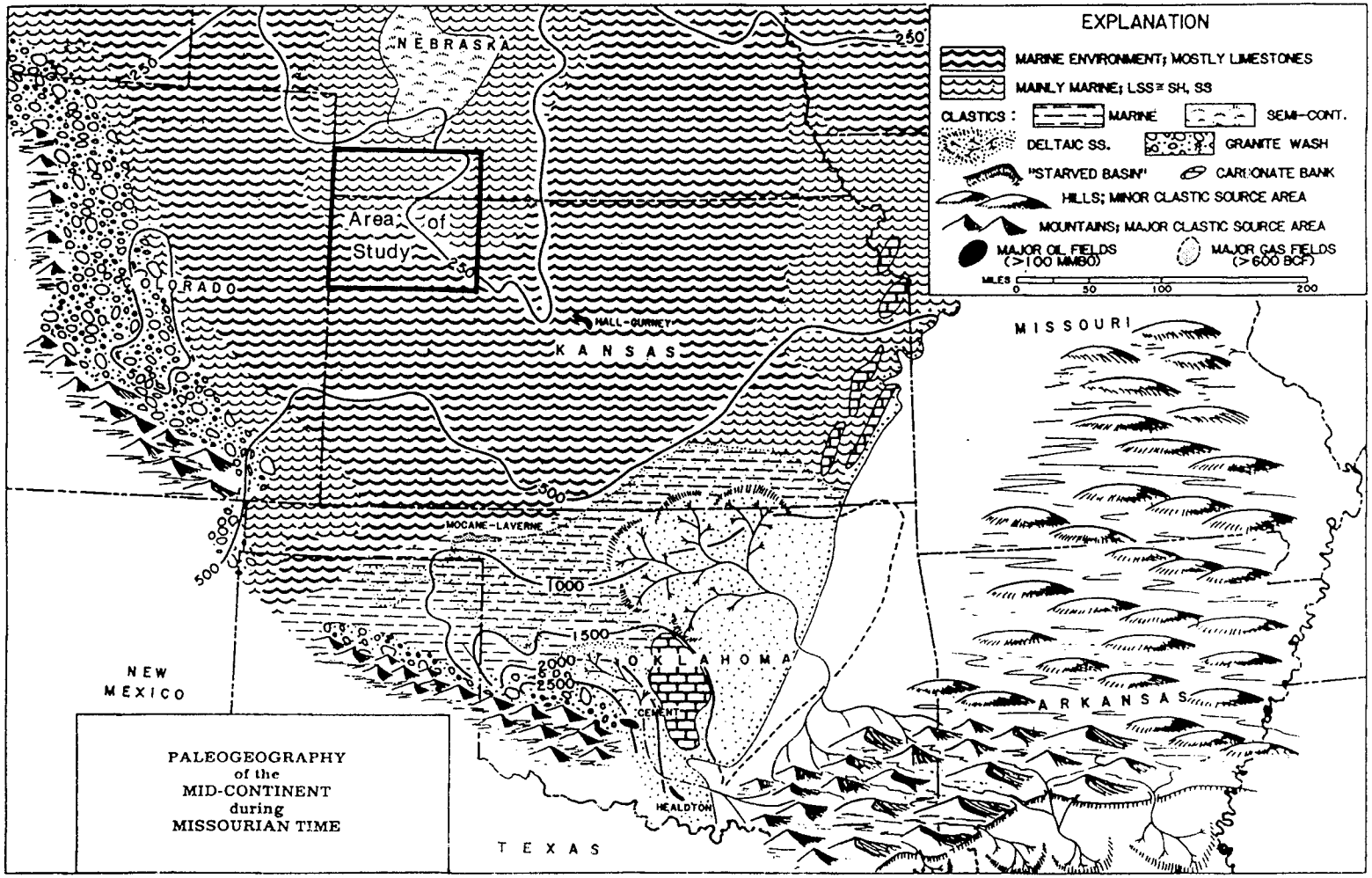
EXPLANATION
MARINE ENVIRONMENT; MOSTLY LIMESTONES
MAINLY MARINE; LSS ≥ SH, SS
CLASTICS :
MARINE
SEMI-CONT.
DELTAIC SS.
GRANITE WASH
"STARVED BASIN"
CARBONATE BANK
HILLS; MINOR CLASTIC SOURCE AREA
MOUNTAINS; MAJOR CLASTIC SOURCE AREA
MAJOR OIL FIELDS (>100 MMBO)
MAJOR GAS FIELDS (>600 BCF)
MILES
0
50
100
200
NEBRASKA
Area of Study
COLORADO
KANSAS
HALL-GURNEY
MISSOURI
MOCANE-LAVERNE
NEW MEXICO
OKLAHOMA
CEMENT
ARKANSAS
HEALDTON
TEXAS
250
500
1000
1500
2000
2500
PALEOGEOGRAPHY
of the
MID-CONTINENT
during
MISSOURIAN TIME

Figure 3. Structural features of the midcontinent. In relation to the study area, the major structural features are the Las Animas arch, the Central Kansas uplift, the Cambridge arch, and the Hugoton embayment. Precambrian structural contours are in feet; datum is mean sea level. (modified from Rascoe and Adler, 1983)

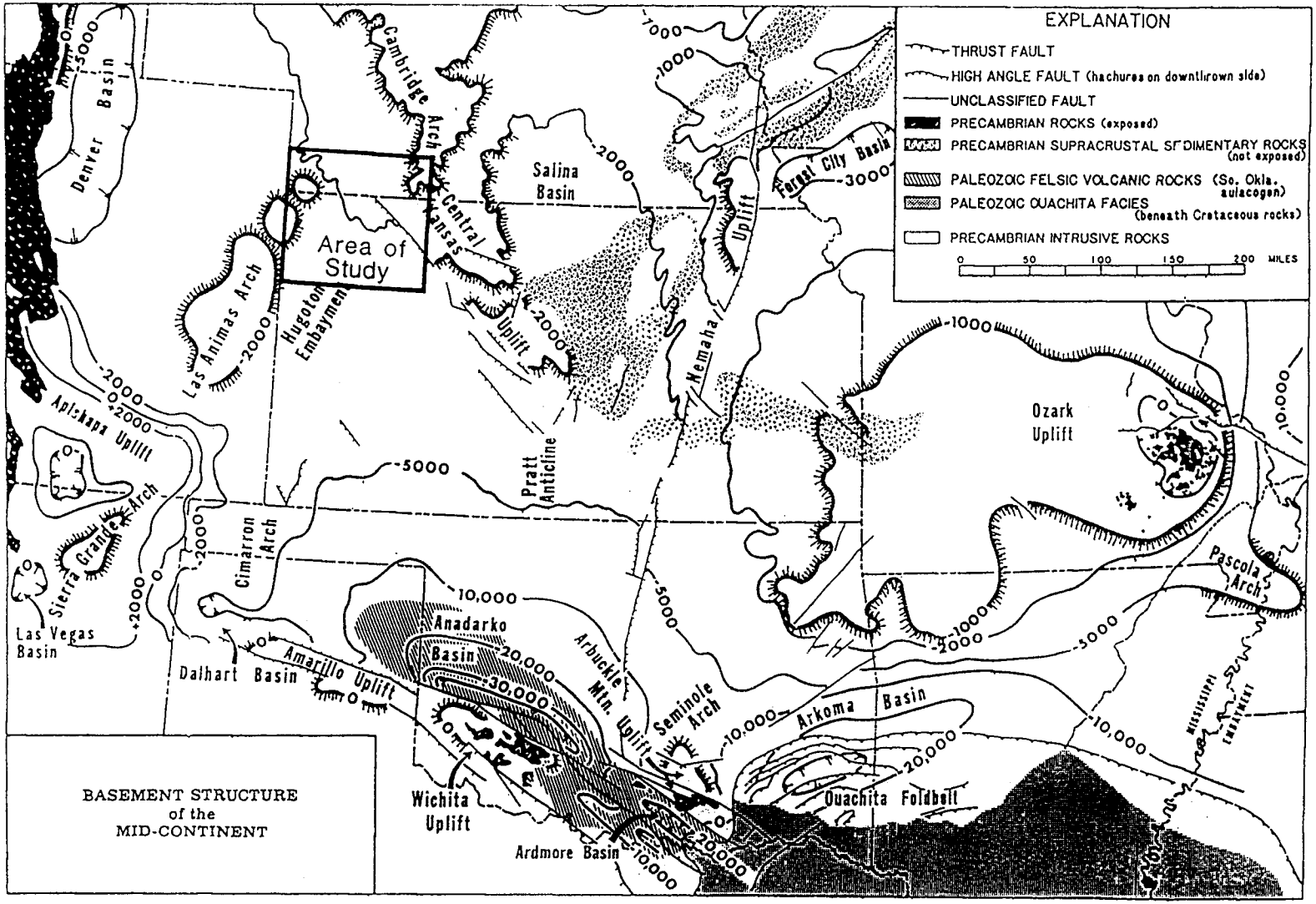
EXPLANATION
THRUST FAULT
HIGH ANGLE FAULT (hachures on downthrown side)
UNCLASSIFIED FAULT
PRECAMBRIAN ROCKS (exposed)
PRECAMBRIAN SUPRACRUSTAL SEDIMENTARY ROCKS (not exposed)
PALEOZOIC FELSIC VOLCANIC ROCKS (So. Okla. aulacogen)
PALEOZOIC OUACHITA FACIES (beneath Cretaceous rocks)
PRECAMBRIAN INTRUSIVE ROCKS
0 50 100 150 200 MILES
Area of Study
Denver Basin
Cambridge Arch
Central Kansas Uplift
Salina Basin
Forgel City Basin
Nemaha Uplift
Las Animas Arch
Hugoton Embayment
Apishapa Uplift
Sierra Grande Arch
Las Vegas Basin
Cimarron Arch
Pratt Anticline
Ozark Uplift
Pascola Arch
Dalhart Basin
Amarillo Uplift
Anadarko Basin
Arbuckle Mtn. Uplift
Seminole Arch
Arkoma Basin
Ouachita Foldbelt
Wichita Uplift
Ardmore Basin
MISSISSIPPI EMBAYMENT
BASEMENT STRUCTURE of the MID-CONTINENT

waters caused the dissolution of aragonitic grains and the precipitation of calcite cements in the upper carbonate. Heckel (1983) considered the lower carbonate to be unaffected by these meteoric waters because the lower shale was thought to be an aquiclude that prevented the percolation of meteoric waters to the lower carbonate. With burial, both the lower and upper carbonates were exposed to low-oxygen waters from which ferroan cements precipitated (Heckel, 1983).

Previous studies of the diagenesis of the Lansing and Kansas City groups in this study area (Dubois, 1979, 1985; Ebanks and Watney, 1985; Prather, 1981, 1984, 1985a, 1985b; Watney, 1980, 1985; and Watney and Ebanks, 1978) emphasized the effect of fresh water diagenesis during subaerial exposure events for the development of moldic and vuggy pores in the limestones.

STRATIGRAPHY

In western Kansas, the carbonate members of the Lansing and Kansas City groups generally are given letter designations (Morgan, 1952) (Figure 4). Most of the carbonate and shale members can be divided into cyclothems (Figure 1). The lower carbonates include the "B", "E", "G'", "H'", and "J'" limestones. The upper carbonates include the "A", "D", "G", "H", "J", and "K" limestones. In the area of study, the Lansing and Kansas City groups include six to seven complete cyclothems.

Figure 4. Well log from the Continental Oil Co. #406 Adell Unit well. The letters in the left margin are the classification system for carbonate members of the Lansing and Kansas City groups (Morgan, 1952) used in this study. The numerals in parenthesis are depths, in feet, below the top of the "A" limestone.

Where the Lansing and Kansas City groups crop out in eastern Kansas, the equivalent formations of the upper carbonates (Parkhurst, 1959; and W.L Watney, personal communication, 1988) are:

"A" Limestone - Stanton Limestone
"D" Limestone - Plattsburg Limestone
"G" Limestone - Iola Limestone
"H" Limestone - Dewey Formation
"J" Limestone - Winterset Limestone
"K" Limestone - Swope Limestone
"L" Limestone - Hertha Limestone

Vertical line segments along neutron, sonic, and core analysis define eight percent porosity. In core analysis porosity data shown along the right margin, points indicated by stars have permeability greater than 0.4 md. (modified from Watney, 1980)

CONTINENTAL OIL CO. #406 ADELL

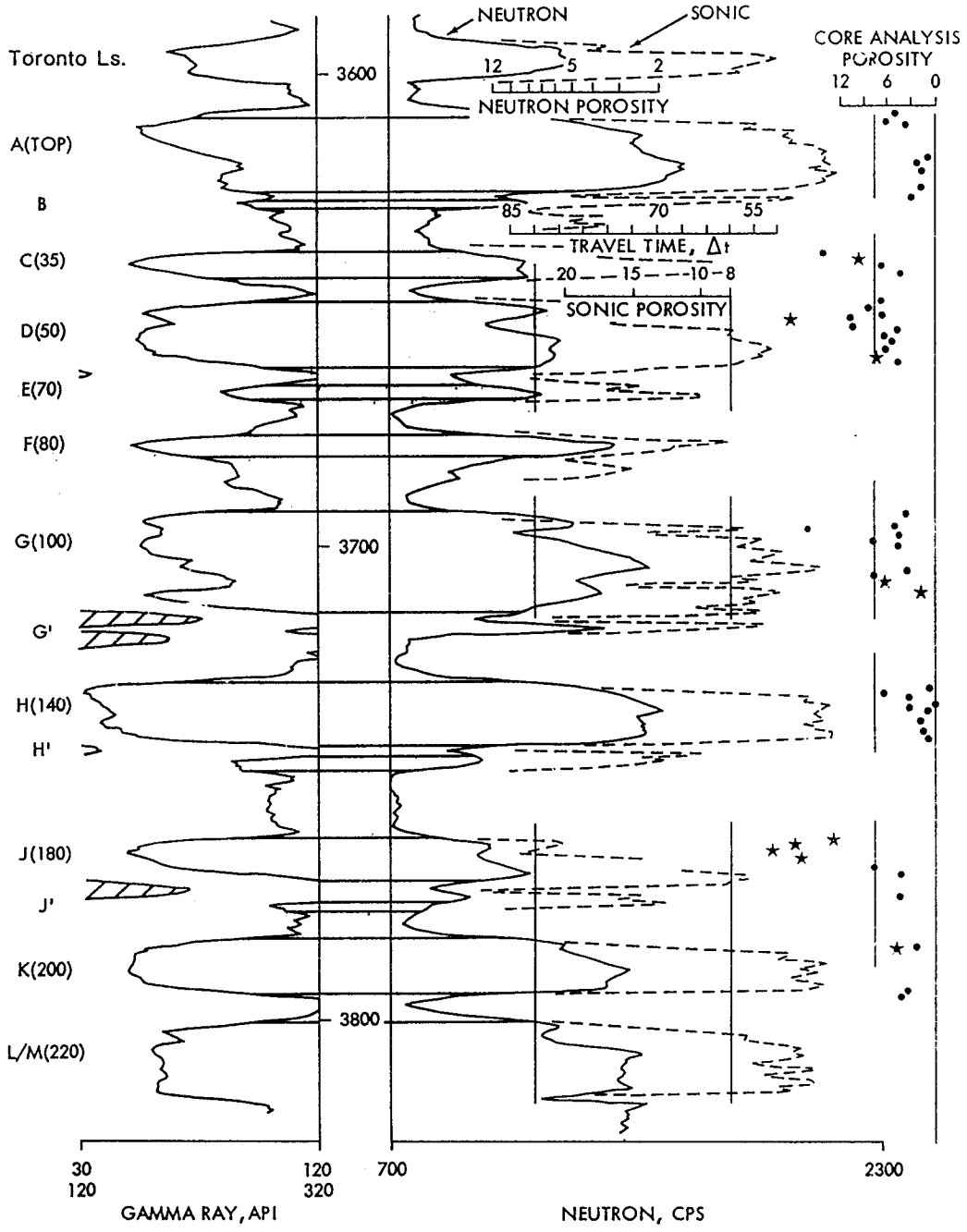

METHODS OF STUDY

Cores from 35 wells (Figure 5) with a total thickness of 1,950 feet (594 m) were described. The cored intervals were primarily from the Lansing and Kansas City groups with limited analyses of the underlying Marmaton Group and the overlying Shawnee Group. Thin sections were made from 155 nonargillaceous carbonate samples. The porous samples were impregnated with blue epoxy. Thin sections were prepared using cold-mounting techniques to avoid heating of the fluid inclusions and the thin sections were doubly polished. One side of each thin section was stained with Alizarin Red S and potassium ferricyanide (Dickson, 1965). The thin sections were petrographically studied with transmitted light, blue-light and ultra-violet epifluorescence, and a cathode beam. Primary fluid inclusions in five calcite samples, three dolomite samples, and a baroque dolomite sample were analyzed using crushing, heating, and freezing techniques. Secondary oil-filled inclusions were studied with heating techniques in five samples. Heating and freezing was performed on a Fluid Incorporated stage.

CORE DESCRIPTIONS

The various lithologies and their thicknesses in the upper and lower shales and upper and lower carbonates are from the core descriptions (Appendix XV). All designated colors are from the Munsell Soil Color Chart.

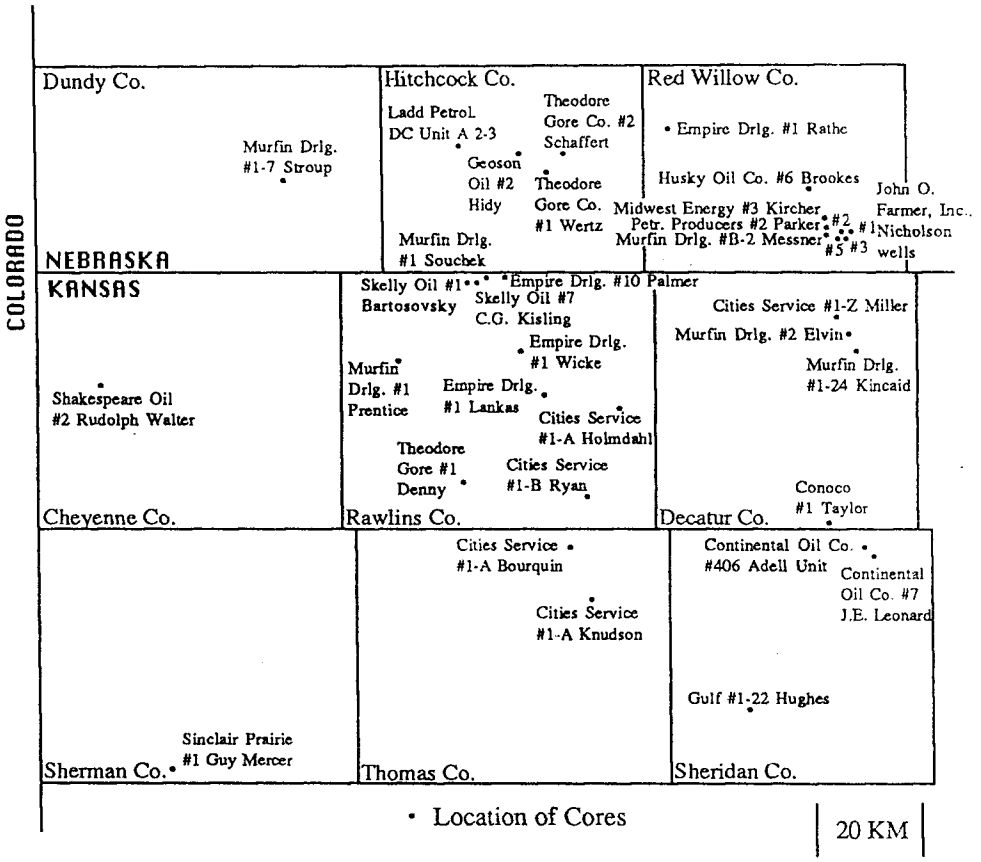

Figure 5. The location and the operators and leases of cores described and sampled for this study.

Shales

Upper Shales

The upper shales (Figure 1)(Table I-A, Appendix I) predominantly are silty. Non-silty shales, siltstones, and very-fine sandstone are present, but are uncommon. Most of these shales and silty shales are red-brown (2.5YR 3/4), but some are gray-green (5Y 5/2). The gray-green shales generally are directly above or below limestones. Where the entire upper shale intervals were cored, the average thickness is 11.1 feet (3.4 m).

Lower Shales

The lower shales (Figure 1)(Table II-A, Appendix II) generally are gray (2.5Y N5/) shales. Red-brown shales, red-brown silty shales, and gray-green silty shales are less common and are limited to the northern half of the area of study. Where the entire lower shale intervals were cored, the average thickness is 4.8 feet (1.5 m). Excluding a 20.5 feet (6.2 m) thick lower shale, the average thickness is 3.3 feet (1.0 m).

Limestones

Upper Carbonates

The upper carbonates (Figure 1)(Table 1) include mudstones, wackestones, packstones, and grainstones (Dunham, 1962), dolostones, microstylolitic carbonates, argillaceous microstylolitic carbonates, and highly argillaceous microstylolitic carbonates. These lithologies are further subdivided by whether or not they contain clayey infills.

Table 1. Lithologies and their thicknesses in the upper carbonates. Each lithology is divided by the presence of clayey infill (CI) or its absence (NI). The thickness of strata with ≥2,<8% and ≥8% porosity are listed. The remaining thickness has <2% porosity. These porosity ranges are based upon visual estimates from core. The right column is the percent of all carbonate strata with porosity ≥8% that is from that lithology. The total thickness of carbonate strata with porosity ≥8% includes carbonate strata in lower carbonates (Table 2).

LITHOLOGY	TOTAL THICKNESS	NI - No Infill CI - Clayey Infill	THICKNESS	Strata with 2-8% Porosity		Strata with Porosity ≥ 8%		% of All Carb.Strata with Porosity ≥ 8%
				Thickness	% of THICKNESS	Thickness	% of THICKNESS	
Carbonate Mudstone	20.3 ft.	NI	9.5 ft.	0 ft.	0%	0 ft.	0%	0%
		CI	10.8 ft.	0 ft.	0%	0 ft.	0%	0%
Carbonate Wackestone	456.9 ft.	NI	321.0 ft.	47.1 ft.	14.7%	91.8 ft.	28.6%	47.1%
		CI	135.9 ft.	26.4 ft.	19.4%	2.8 ft.	2.1%	1.4%
Carbonate Packstone	160.0 ft.	NI	119.9 ft.	21.9 ft.	18.3%	45.9 ft.	38.3%	23.6%
		CI	40.1 ft.	3.5 ft.	8.7%	1.3 ft.	3.2%	0.7%
Carbonate Grainstone	76.6 ft.	NI	68.9 ft.	18.2 ft.	26.4%	23.9 ft.	34.1%	12.3%
		CI	7.7 ft.	0.6 ft.	7.8%	0 ft.	0%	0%
Dolostone	17.4 ft.	NI	17.4 ft.	1.1 ft.	6.3%	10.8 ft.	62.1%	5.7%
		CI	0 ft.	0 ft.	0%	0%	0 ft.	0%
Microstylolitic Carbonates	125.9 ft.	NI	114.9 ft.	6.9 ft.	6.0%	11.8 ft.	10.3%	6.1%
		CI	11.0 ft.	0 ft.	0%	0 ft.	0%	0%
Argillaceous Microstylolitic Carbonates	229.5 ft.	NI	198.0 ft.	0.6 ft.	0.3%	0 ft.	0%	0%
		CI	31.5 ft.	0 ft.	0%	0 ft.	0%	0%
Highly Argillaceous Microstylolitic Carbonates	78.3 ft.	NI	78.3 ft.	0 ft.	0%	0 ft.	0%	0%
		CI	0 ft.	0 ft.	0%	0 ft.	0%	0%

Dolostones are recrystallized by dolomite. Microstylolitic carbonates, argillaceous microstylolitic carbonates, and highly argillaceous microstylolitic carbonates include wispy seams that have been described as microstylolites (Wanless, 1979) or clay-rich zones (McNeice, 1987). Microstylolitic carbonates (Figure 6A) have individual clay-filled seams (microstylolites) that generally are less than 5 mm thick and have a vertical concentration of at least one for each 5 cm of thickness. Argillaceous microstylolitic carbonates (Figure 6D, 6C) have a higher concentration of clay-filled or wispy seams (microstylolites); typically, there are clusters of these seams. These clusters of seams are more than 5 mm thick and have a vertical concentration of at least one for each 5 cm. The argillaceous microstylolitic carbonates generally have wavy clusters of seams divided by less altered limestone. The highly argillaceous microstylolitic carbonates lack these zones of less altered limestone and have wispy seams throughout their vertical sequence. A key difference between the microstylolitic carbonates and the argillaceous and highly argillaceous microstylolitic carbonates is the thickness of the clay-filled seams. The clay-filled seams in the microstylolitic carbonates generally are less than 5 mm thick where as the clay-filled seams in the argillaceous and highly argillaceous carbonates are greater than 5 mm thick.

The mudstones, wackestones, packstones, and grainstones (Table 1) generally do not have microstylolites. These lithologies may have one or two microstylolites, but if a carbonate interval has a

Figure 6. Photographs of microstylolitic carbonates, argillaceous microstylolitic carbonates, and carbonates with clayey infill. Scale bars are 2 cm. Arrows point to stratigraphic up. "M" are microstylolites; "S" are stylolites; "CI" is clayey infill; "CH" is chert.

(A) Microstylolitic carbonate. Microstylolitic carbonate has microstylolites (M) that are less than 5 mm thick and have a concentration of at least one/5 cm. Continental Oil #406 Adell Unit, 3609 feet.

(B) Fossiliferous wackestone with red-brown clayey infill. Where there is clayey infill (CI), microstylolite-like features have formed. Away from the clayey infill, stylolites (S) have formed. Empire Drilling #1 Lankas, 4017 feet.

(C) Argillaceous microstylolitic carbonate with red clayey infill. This sample includes microstylolites (M) similar to those described in D and clayey infill (CI). Pressure solution formed the microstylolites and altered the clayey infill. Empire Drilling #1 Rathe, 3752 feet.

(D) Argillaceous microstylolitic carbonate. The arrows point to microstylolites (M) and orange-colored chert nodules (CH). Highly argillaceous microstylolitic carbonate has clusters of whispy seams (microstylolites) that are more than 5 mm thick and have a vertical concentration of at least one/5 cm. Empire Drilling #1 Rathe, 3759 feet.

(E) Peloidal and fossiliferous packstone with gray-green clayey infill. Microstylolite-like features have formed where there has been clayey infill (CI). Theodore Gore #1 Denny, 4143 feet.

(F) Fossiliferous wackestone with autoclastic brecciation and gray clayey infill. Clayey infill (CI) surrounds <u>in situ</u> clasts of the host limestone that is brecciated. Skelly Oil #1 Bartosovsky, 3981 feet.

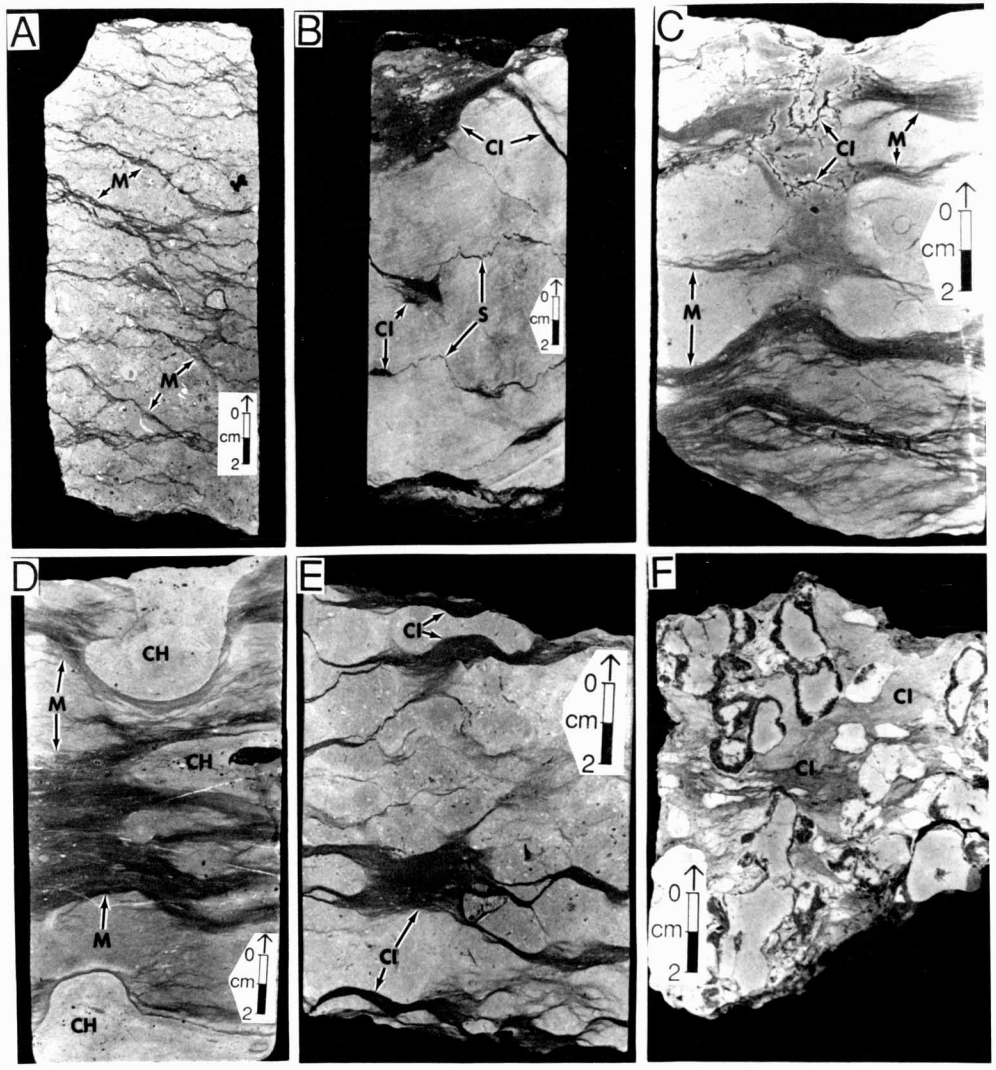
A
M
M
0
cm
2
B
Cl
Cl
S
0
cm
2
C
Cl
M
M
0
cm
2
D
CH
M
CH
M
CH
0
cm
2
E
Cl
0
cm
2
Cl
F
Cl
Cl
0
cm
2

vertical concentration of microstylolites greater than one/5 cm, it is classified as microstylolitic carbonate. The microstylolitic carbonates and argillaceous microstylolitic carbonates are commonly wackestones, but their thicknesses are only listed under those lithologies and are not included with the wackestones (Table 1).

The lithologies are further subdivided by whether they have clayey infill (Table 1). Clayey infill (Figures 6B,6C,6E, and 6F) are irregular cavities within a limestone host that are filled with clayey debris derived from overlying beds. In places, the clayey infill reduces autoclastic breccia pores. Generally, the clayey infill is altered by compaction that develops microstylolite-like features. Clayey infill is present in 48 of the 83 described upper carbonates. Typically, the clayey infill closely underlies the upper carbonate-upper shale contact. The source of the clayey infill is interpreted to be the upper shale. The average depth from the top of the upper carbonate to the base of the clayey infill is 6.8 feet (2.1 m). An average of 79 percent of the strata within this range are altered by clayey infill.

Where the entire upper carbonate intervals were cored, the average thickness is 15.2 feet (4.6 m).

Porosity The strata are classified into 2-8 percent and $\geq$8 percent porosity ranges by visual estimation (Table 1). The lithologies that are most commonly porous are the wackestones, packstones, and grainstones without clayey infill (Table 1). The lithologies less likely to be porous are the lithologies with clayey

infill, mudstones, microstylolitic carbonates, argillaceous microstylolitic carbonates, and highly argillaceous microstylolitic carbonates.

Lower Carbonates

Lower carbonates are distinguished from upper carbonates by the lower shales that are deposited between them (Figure 1). Lower carbonates (Table 2) include wackestones, packstones, grainstones, microstylolitic carbonates, and argillaceous microstylolitic carbonates.

Carbonate packstones and grainstones are more common than carbonate wackestones (Table 2); in upper carbonates, carbonate wackestones are more common (Table 1). Clayey infill is present in only two intervals.

Porosity The lithologies that are more commonly porous are wackestones, packstones, and grainstones. The microstylolitic carbonates and the highly microstylolitic carbonates rarely are porous.

Discussion of Core Descriptions

A major goal is to determine which lithologies have significant porosity. In the upper and lower carbonates, 91.9 percent of the intervals with $\geq$8 percent porosity are wackestones, packstones, grainstones, and dolostones that lack clayey infill. The lithologies less likely to be porous include carbonate mudstones, microstylolitic carbonates, argillaceous microstylolitic carbonates, highly argillaceous microstylolitic carbonates, and carbonates with

Table 2. Lithologies and their thicknesses in the lower carbonates. The thickness of strata with ≥2,<8 and ≥8% porosity are listed. The remaining thickness has <2% porosity. Porosity ranges are based on visual estimates from core. For the strata with porosity ≥8%, the percent of all carbonate strata with ≥8% porosity that is from that lithology is listed in the right column. The carbonate strata with ≥8% porosity includes the upper carbonates (Table 1). The carbonate grainstone lithology includes two intervals that have clayey infill.

LITHOLOGIES	Total Thickness	Strata with 2-8% Porosity		Strata with Porosity ≥ 8%		% of All Carb. Strata with Porosity ≥ 8%
		Thickness	% of Total Thickness	Thickness	% of Total Thickness	
Carbonate Wackestone	8.6 ft.	2.4 ft.	27.9%	1.0 ft.	11.6%	0.5%
Carbonate Packstone	12.9 ft.	3.0 ft.	23.3%	4.7 ft.	36.4%	2.4%
Carbonate Grainstone (Grainstone with Clayey Infill)	18.4 ft. (1.1 ft.)	11.3 ft.	61.4%	0.5 ft.	3.0%	0.3%
Microstylolitic Carbonate	14.7 ft.	0.2 ft.	1.4%	0.3 ft.	2.0%	0.2%
Argillaceous Microstylolitic Carbonate	9.3 ft.	0 ft.	0%	0 ft.	0%	0%

clayey infill.

An important difference between the commonly nonporous lithologies and the lithologies less likely to be porous is the clay content. The lithologies that are more commonly porous lack significant clay. The commonly nonporous microstylolitic carbonates, argillaceous microstylolitic carbonates, and the highly argillaceous microstylolitic carbonates are clay rich.

Carbonates with clayey infill are less commonly porous than the same lithologies that lack clayey infill (Table 1). Typically, the clayey infill closely underlies the contact between the upper carbonate and upper shale (Figure 1). The clayey infill is derived from the overlying upper shale. Watney (1980) interpreted that clayey infill was formed during subaerial exposure events.

PETROGRAPHY

The goal of the petrographic analyses is to determine the diagenetic history of these carbonates and the importance of the diagenetic features on the formation and preservation of porosity.

Using cathodoluminescence petrography, the percent of petrographically identifiable open pore space, the percent of cement, and the percentage of the open pore space caused by postcementation dissolution (late-stage dissolution) was estimated using comparison charts. Using these data, the percent of porosity caused by postcementation dissolution, and the percent of "precementation porosity" were calculated using the following equations:

Percent of porosity caused by postcementation dissolution: Percent porosity from postcementation dissolution = (percent open porosity x percentage of open pores caused by postcementation dissolution) /100.

"Precementation porosity": "Precementation porosity" = Percent open porosity - percent porosity from postcementation dissolution + percent cements.

"Precementation porosity" is the estimated porosity that predated cementation. The formula for "precementation porosity" implies that all compaction predated all cements, and that all moldic pores formed prior to cementation. This is commonly not true.

Extant and Occluded Pores

Moldic, interparticle, intraparticle, and vuggy pores (Choquette and Pray, 1970) are the most common pore types in the nonargillaceous carbonates. Intercrystalline pores are common in six dolomitized intervals that total less than 20 feet (6.1 m) in thickness.

Paragenesis

The diagenetic events are described in their approximate order of occurrence.

Radial-Bladed Calcite

Radial-bladed calcite cement that precipitated on ooids predates compaction and is present in only one thin section. This cement has dull luminescence.

Compaction

Compaction features are common. Evidence of compaction includes overly close packing (Figure 7A) and crushed grains (Figures 7B,7C). Overly close packing of grains (Figure 7A) results from grain deformation and minor grain-to-grain pressure dissolution. Overly close packing or crushed grains predate all cementation in 83 of the 155 thin sections. In 10 of the 155 thin sections, the first generation of calcite cement appears to predate compaction.

Moldic Pores

The most common open or occluded pore type is moldic. Moldic pores resulted from the dissolution of formerly aragonitic or poorly calcified shells or grains, such as bivalves and phylloid algae. In some grain-supported lithologies, the formation of molds postdates compaction because the grain-to-grain contacts of the molds and grains are overly close. The outline of the molds are intact and surrounding grains do not protrude into the position of the former grains (Figure 8).

For the thin sections containing greater than 5 percent of the nonluminescent calcite cement, which typically is the first generation of calcite cement, moldic pores in 48 percent of these thin sections do not contain this first generation of calcite cement whereas the surrounding interparticle and intraparticle pores do contain this cement. Therefore, mold formation postdates the precipitation of the first generation of calcite cement in these thin sections.

Figure 7. Photomicrographs of compaction features. Scale bars are 200 micrometers.

(A) Plane-polarized light photomicrograph of overly-close packing of grains. The white is calcite cement. The contacts between the large echinoderm fragment (marked E) and smaller grains (3 are marked by arrows) are overly close. Overly close packing is a compaction features. The calcite cement that fills these pores is postdates the overly close packing. Theodore Gore #2 Schaffert, 3683.9 feet.

(B,C) Paired plane-polarized light (B) and cathodoluminescence (C) photomicrographs of a broken brachiopod shell. Arrows point to a broken end of the shell. The first generation of calcite cement, which is nonluminescent in C, grows around the end of the broken shell and, therefore, postdates the breakage. Petroleum Producers #2-B Parker "B" (D) zone.

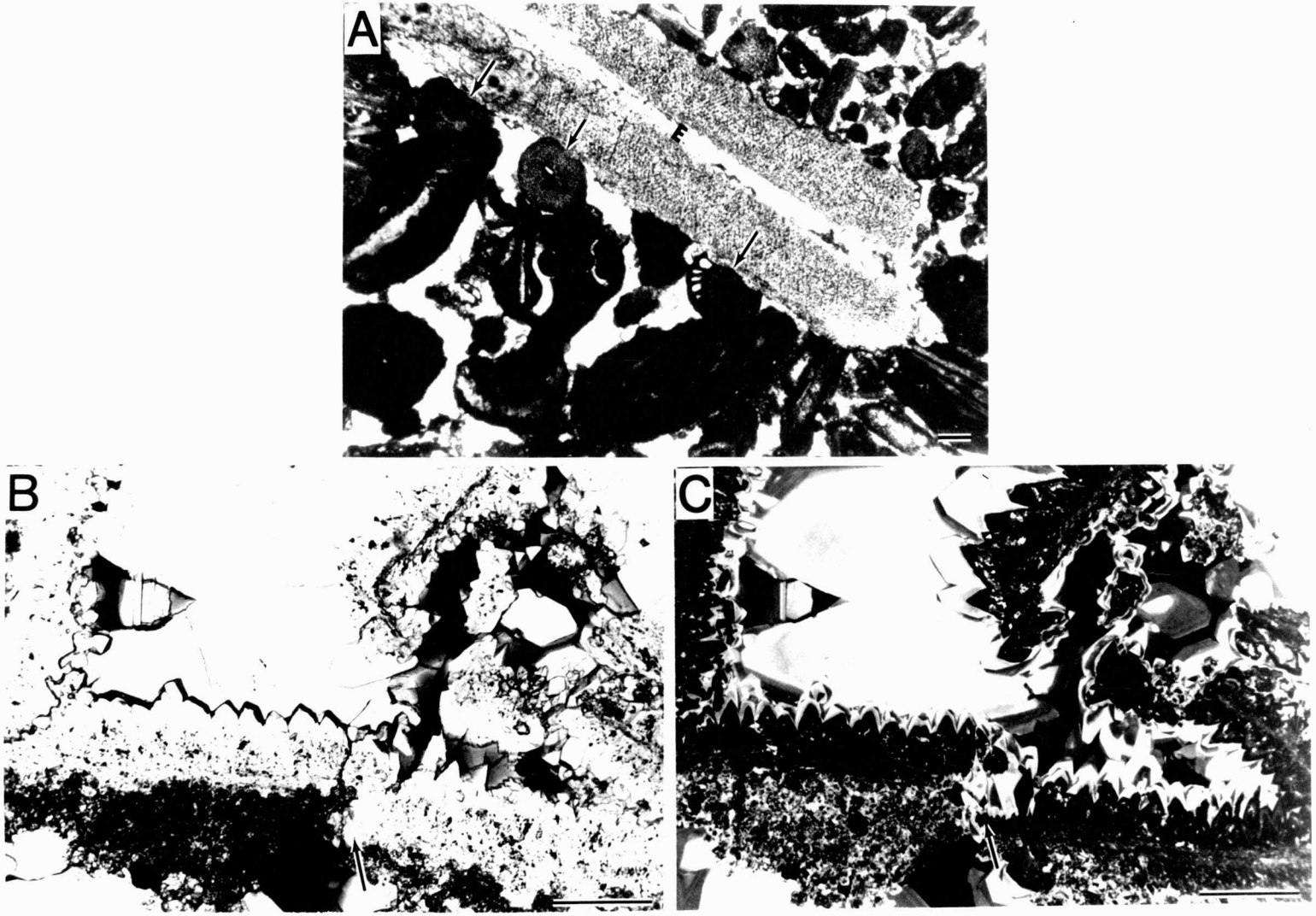
A
E
B
C

Figure 8. Photomicrographs of moldic pores in relation to compaction features. Scale bars are 200 micrometers.

(A) Plane-polarized light photomicrograph of a mold (MO). Gray is blue-colored epoxy; white is calcite cement. Contacts between echinoderm fragments (E) and surrounding grains are overly close, which is good evidence of compaction before cementation. Grains flattened against the margin of the mold (MO) but not protruding into the mold (2 are marked by arrows), indicate that the mold formed after compaction. Theodore Gore #2 Schaffert, 3816 feet.

(B) Cross-polarized light photomicrograph of a mold (MO). Mold is filled with calcite cement. An oncolite (ONC) is flattened against the margin of the mold, but does not protrude into it. This indicates that the mold formed after compaction. Skelly Oil #1 Bartosovsky, 4143 feet.

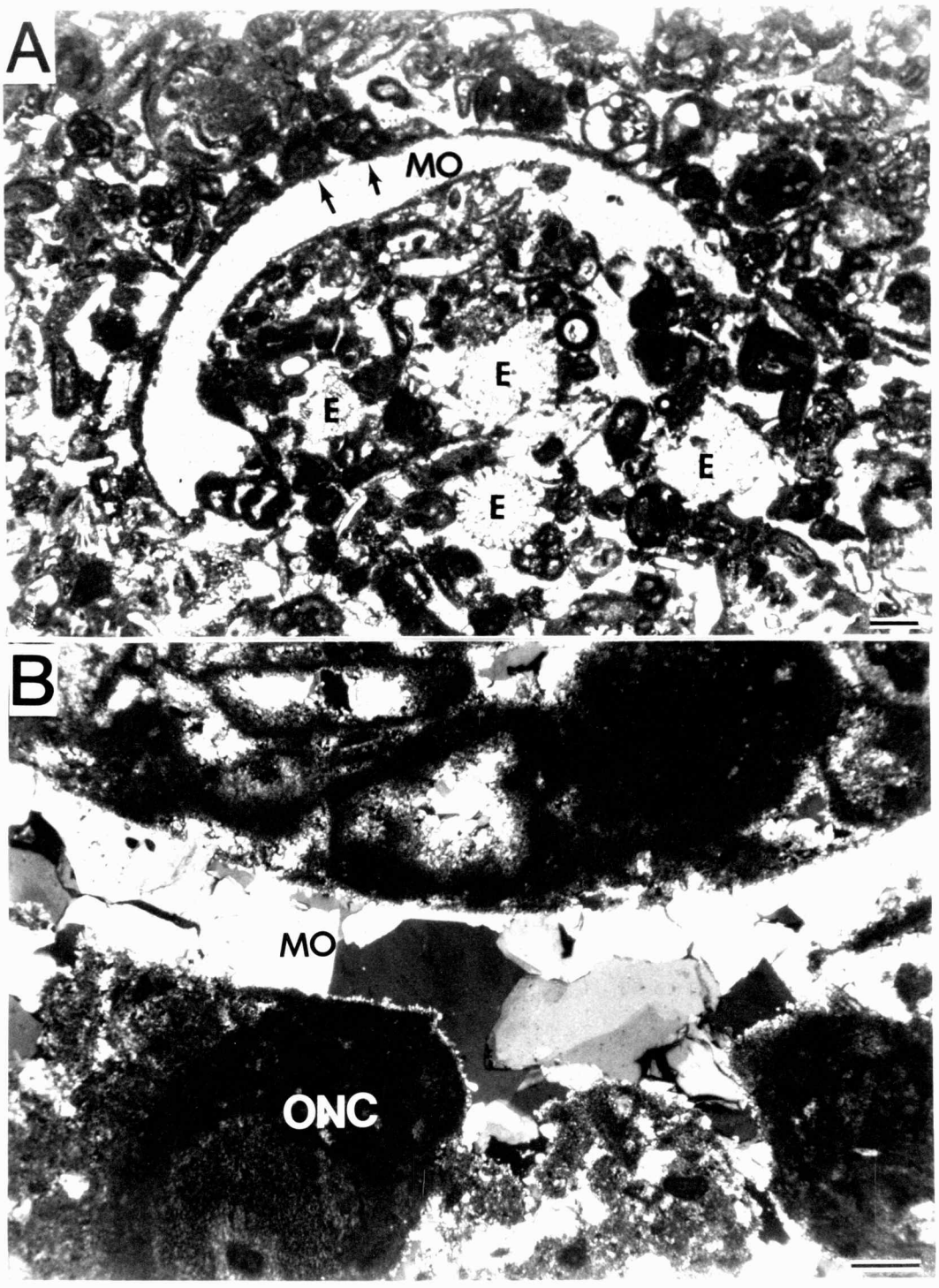
A
MO
E
E
E
E
B
MO
ONC

Heckel (1983) noted that formerly aragonitic or poorly calcified grains were neomorphosed to calcite in the lower carbonates. In this study, the formerly aragonitic or poorly calcified grains were dissolved and not neomorphosed.

Zoned Dolomite

Commonly, dolomite cement and replacive dolomite have luminescent (Figure 9 A,B) and fluorescent bands. These dolomites are nonferroan. Replacive zoned dolomite rhombs occur in 83 of the 155 thin sections. For all thin sections, replacive dolomite averages 4.9 percent. Six thin sections have been extensively dolomitized, thus creating intercrystalline pores. Zoned dolomite cement includes dolomite rhombs that reduce pores (Figure 9 A,B) and syntaxial overgrowths of echinoderm fragments (Figure 9 C,D).

Crosscutting relationships with calcite cement are rare and ambiguous. In three thin sections, zoned dolomite cement predates calcite cement (Figure 9 A,B). In two thin sections, zoned dolomite cement postdates part of the calcite cement (Figure 10). The replacive dolomitization that formed intercrystalline pores is interpreted to have predated calcite cement.

Calcite Cement

Calcite cement is divided into five types based on cathodoluminescence and staining characteristics (Figure 11).

The calcite cements generally are clear, equant cements that reduce the moldic, interparticle, and intraparticle pores. In places, the calcite cement is a bladed cement, but these cements

Figure 9. Paired plane-polarized light and cathodoluminescence photomicrographs of dolomite cement. Scale bars are 200 micrometers.

(A,B) Dolomite cement rhombs (two are marked by arrows) in relation to calcite cement. The dolomite rhombs include a moderately-bright luminescent band (in B). This dolomite predates the calcite cement that grows around the dolomite rhombs. Ladd Petroleum DC Unit A 2-3, 4109 feet.

(C,D) An echinoderm fragment (E in C.) is syntaxially overgrown by dolomite cement, The dolomite cement (D in C.) is first nonluminescent and is overgrown by red moderately bright to moderately dull luminescent dolomite cement. Theodore Gore #1 Wertz, 3779 feet.

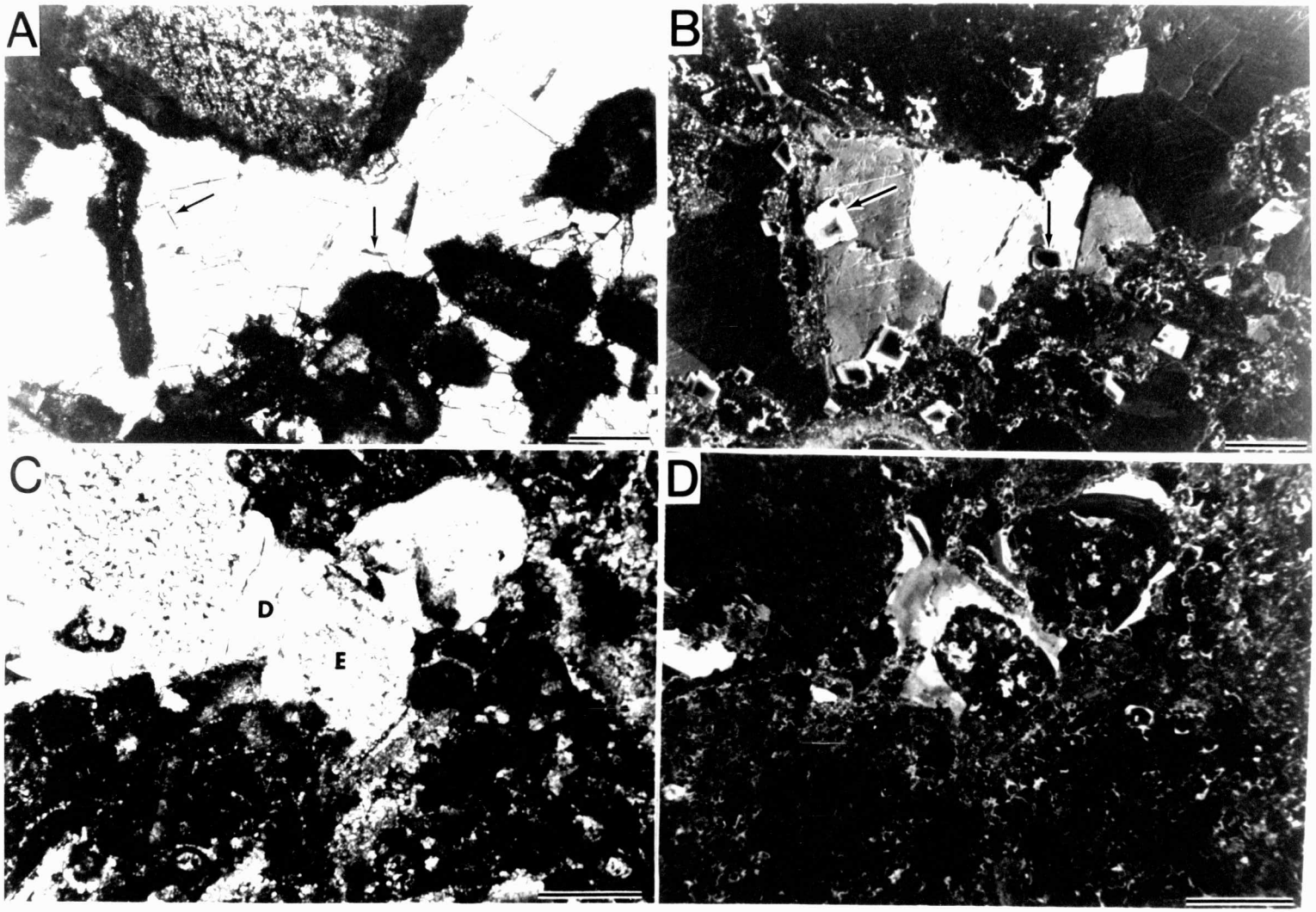
A
B
C
D
D
E

Figure 10. Paired plane-polarized light (A) and cathodoluminescence (B) photomicrographs of dolomite cement postdating calcite cement. Scale bars are 200 micrometers. The #1 and #2 calcite cements (1, 2 in B) are crosscut by dolomite cement (D in A) that has red moderately bright luminescence. Continental Oil #406 Adell Unit, 3761 feet.

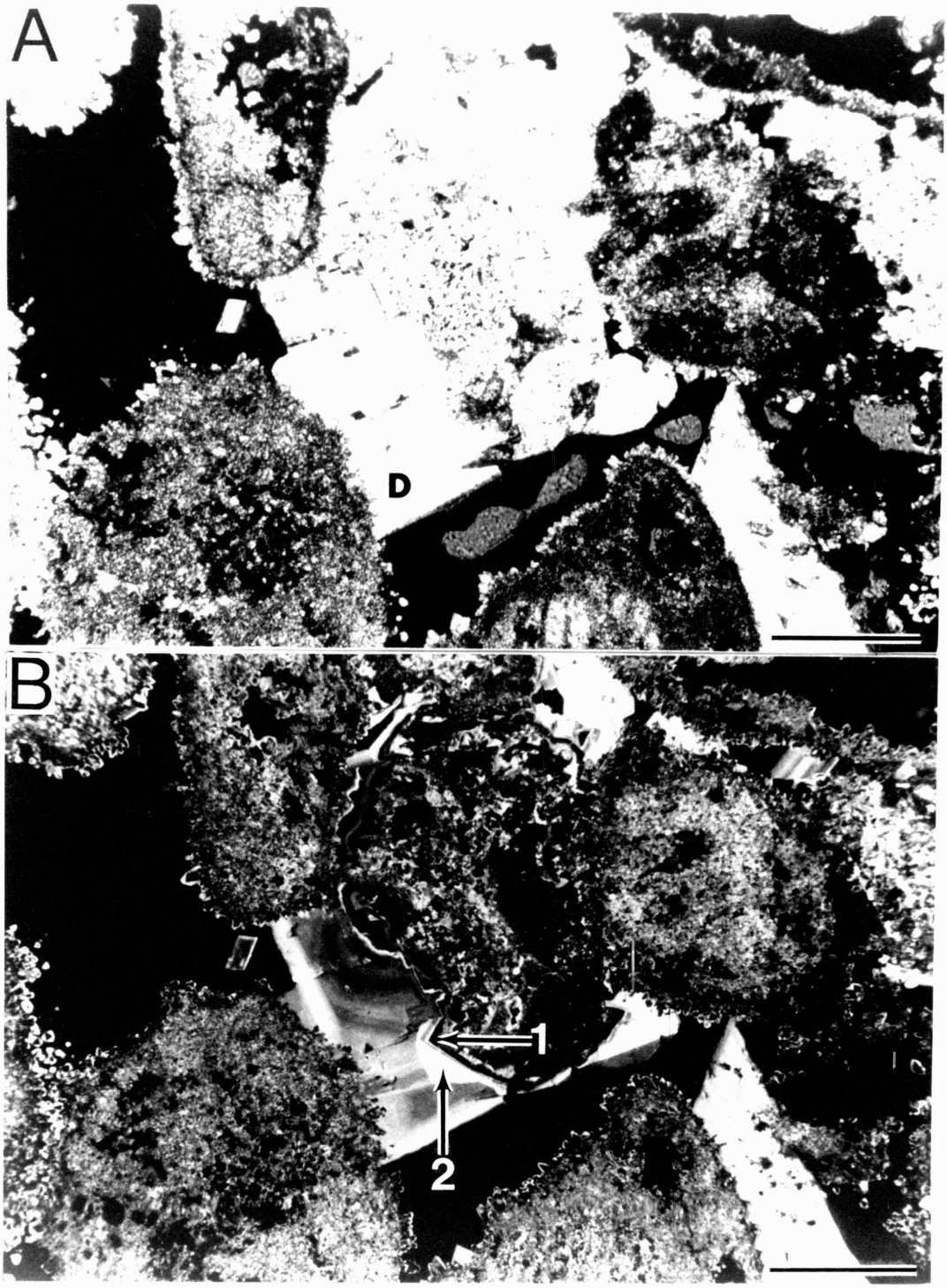
A
D
B
1
2

Figure 11. Cathodoluminescence photomicrograph (A) of the 5 calcite cements described in this study. Scale bar is 200 micrometers.

(B) Sketch illustrating the location of the #1, #2, #3, #4, and #5 calcite cements in A.

Murfin Drilling #1 Prentice, 4319 feet.

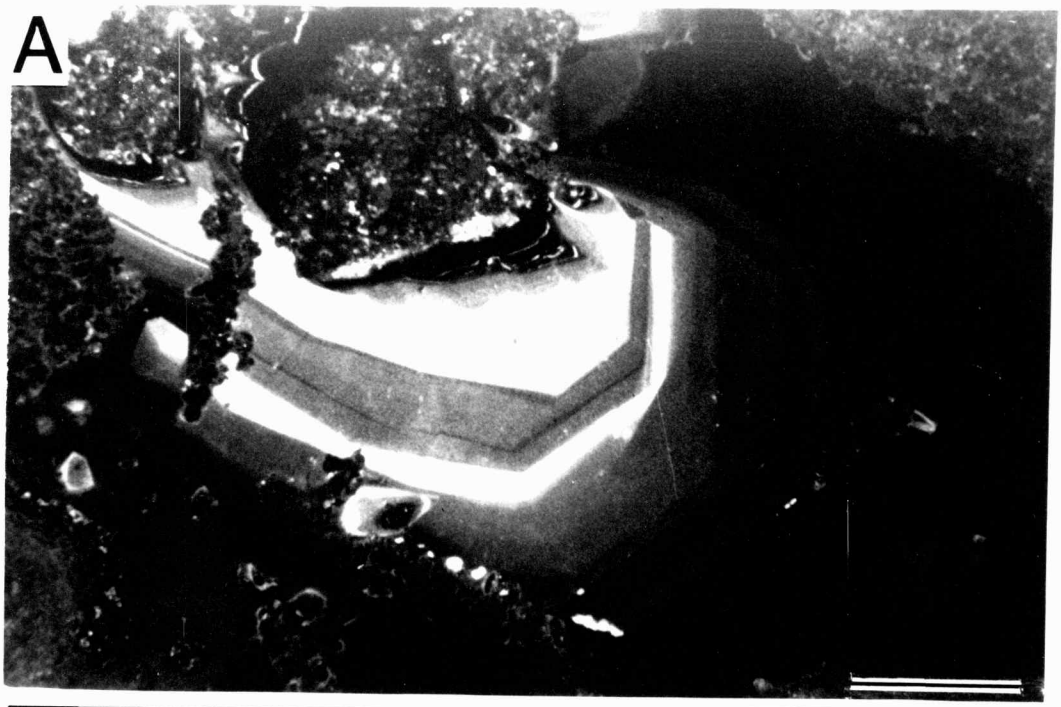
A

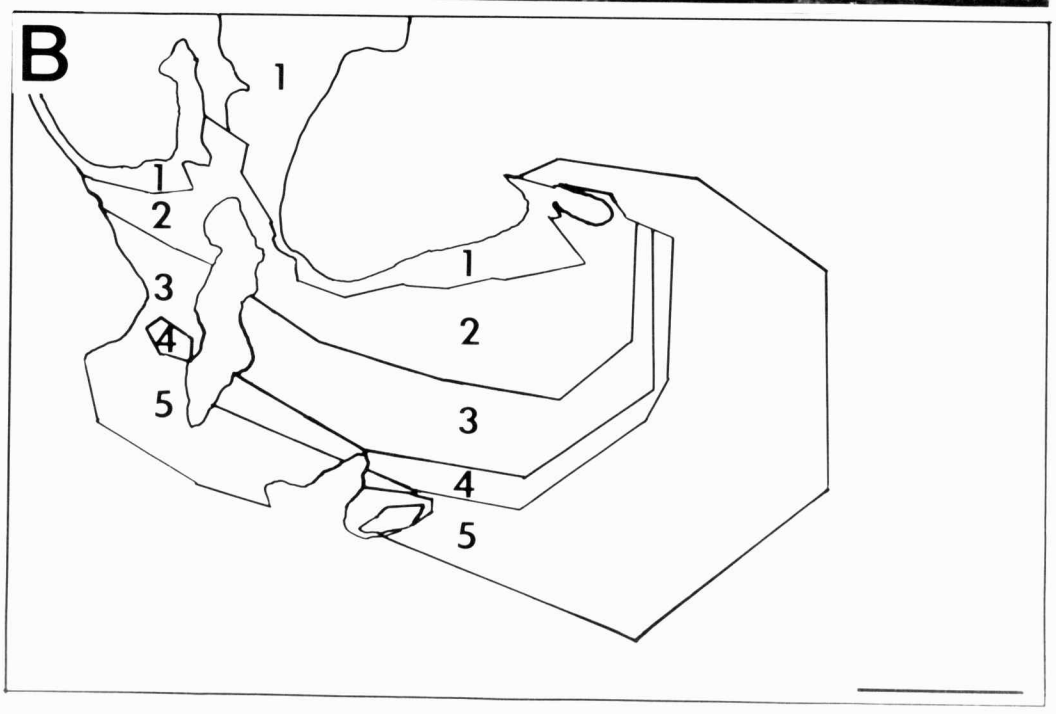
B
1
1
2
3
4
5
1
2
3
4
5

generally have the same luminescent zonation as the equant cements.

For all wackestone, packstone, and grainstone thin sections, calcite cements reduce an average of 64.4 percent of the "precementation porosity".

#1 Calcite Cement--The #1 calcite cement is a nonluminescent, nonferroan, calcite cement zone that is the first phase of calcite cementation in almost all thin sections (Figure 11). In places, this nonluminescent band includes thin bright bands (Figure 11). The #1 calcite cement is the first generation of calcite that generally postdates compaction and, in places, postdates the formation of moldic porosity.

For all wackestone, packstone, and grainstone thin sections, the #1 calcite cement reduces the "precementation porosity" by an average of 11.4 percent.

#2 Calcite Cement--The #2 calcite cement is a nonferroan calcite cement that postdates the nonluminescent #1 calcite cement. The luminescence of the #2 calcite cement is complexly subzoned and these subzones range from moderately bright to moderately dull (Figure 11). For all wackestone, packstone, and grainstone thin sections, the #2 calcite cement reduces "precementation porosity" by average of 35.6 percent.

#3 Calcite Cement--The #3 calcite cement is ferroan and has very dull luminescence without banding (Figure 11). For all wackestone, packstone, and grainstone thin sections, the #3 calcite cement reduces "precementation porosity" by an average of 13.3

percent.

#4 Calcite Cement--The #4 calcite cement is a nonferroan phase that postdates the ferroan #3 calcite cement. Its luminescence is complexly subzoned and these subzones range from moderately dull to moderately bright. The #4 calcite cement is limited to 8 of the 35 cores. For all wackestone, packstone, and grainstone thin sections, the #4 calcite cement reduces "precementation porosity" by an average of 2.6 percent.

#5 Calcite Cement--The #5 calcite cement is a ferroan phase with very dull luminescence (Figure 11). It is only recognized where it postdates the #4 calcite cement and is present in only four thin sections from three cores. Where the #4 calcite cement is absent, the outer part of the #3 may be the #5 calcite cement. For all wackestone, packstone, and grainstone thin sections, the #5 calcite cement reduces "precementation porosity" by an average of 0.2 percent.

Fractures

Fractures which occured during calcite cementation were observed in seven cores (Figure 12). The timing of the fractures, in relation to the calcite cement types, ranges from crosscutting the #1 calcite to the #4 calcite. Later calcite cements fill the fractures.

Nonzoned Dolomite and Baroque Dolomite Cement

The most common dolomite cement postdates all of the calcite cement. These dolomite cements include baroque dolomite with

Figure 12. Plane-polarized light (A) and cathodoluminescence (B) photomicrographs of a fracture in relation to calcite cement, Skelly Oil Co. #1 Bartosovsky, 4035 feet. Scale bars are 200 micrometers. A fracture (marked by an arrow in B) crosscuts the #2 calcite cement (2 in B) and is filled by the very-dull luminescent #3 calcite cement (3 in B). Skelly Oil Co. #1 Bartosovsky, 4035 feet.

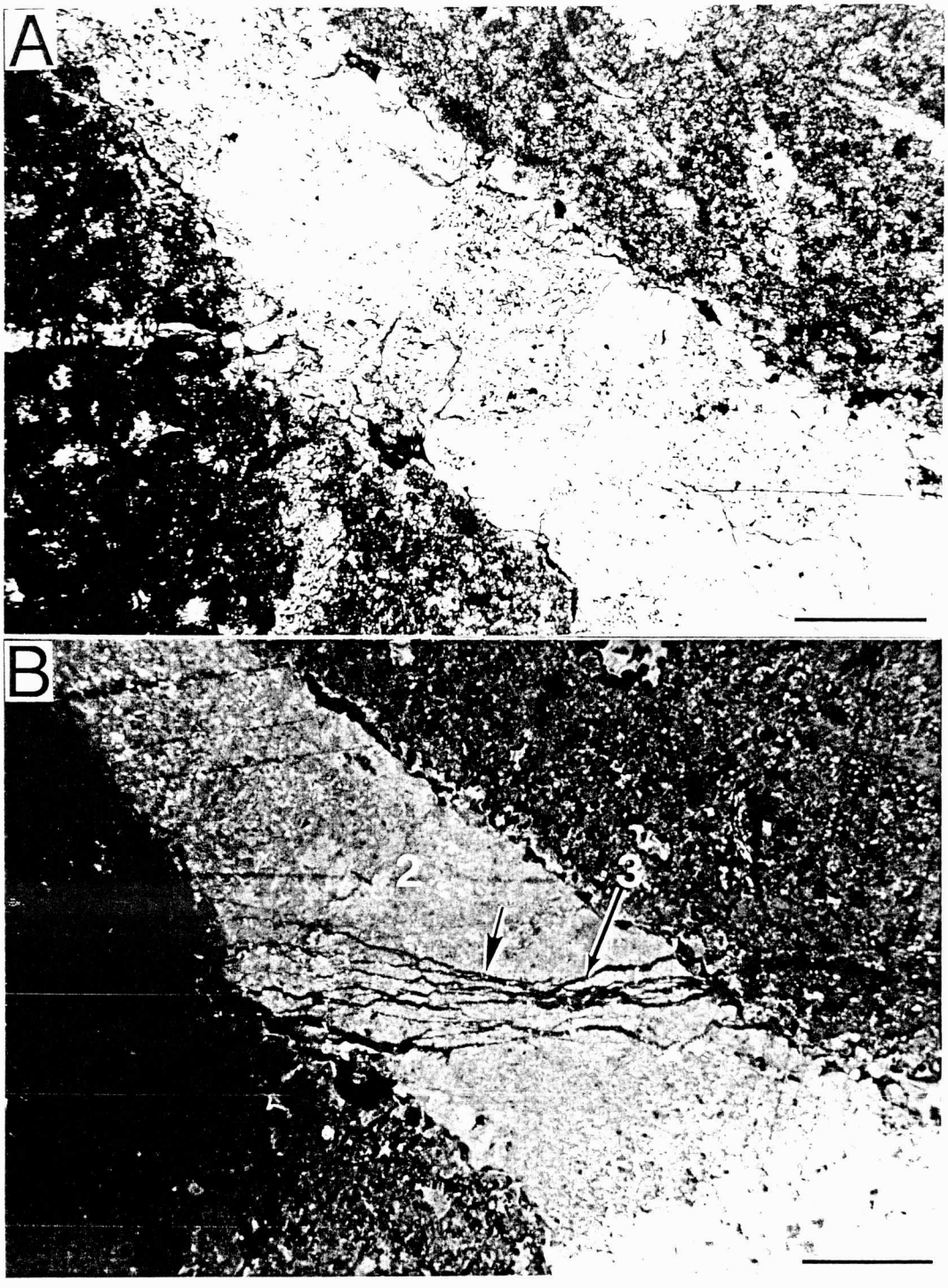
A
B
2
3

undulose extinction (Figure 13) and euhedral rhombic dolomite without undulose extinction. Generally, these dolomites lack any fluorescent or luminescent bands. In places, the outer zone of baroque dolomite takes a ferroan stain.

Dolomite cement, most of which postdates calcite cement, reduces "precementation porosity" by an average of 7.3 percent for all wackestone, packstone, and grainstone thin sections.

Siliceous Replacement and Cementation

Brachiopod and echinoderm fragments are commonly replaced by chert and chalcedony. In places, there is nodular chert and chalcedony with replacement fabrics (Figure 6D). The color of the chert and chalcedony ranges from white to red. Crosscutting relationships between chert, chalcedony and calcite are rare and ambiguous, but chert and chalcedony apparently postdate calcite (Figure 14). Silt-sized quartz crystals are present in 99 of the 155 thin sections and average 3.7 percent of all thin sections. These quartz crystals contain calcite inclusions and are probably replacive. As with replacive chert and chalcedony, crosscutting relationships with calcite cement are rare and ambiguous. There is megaquartz cement in the "J" limestone of the Theodore Gore #1 Wertz core. In this interval, quartz cement crosscuts calcite cement.

Stylolites And Microstylolites

Sutured stylolites are common in the nonargillaceous carbonates. Microstylolites generally are limited to the argillaceous carbonates and carbonates with clayey infill.

Figure 13. Paired plane-polarized light (A) and cathodoluminescence (B) photomicrographs of baroque dolomite in relation to calcite cement. Baroque dolomite cement (BD) postdates the 5 calcite cements (the #2,#3,#4, and #5 calcite cements are identified in B as 2,3,4,and 5). The baroque dolomite includes a bright luminescent band in this sample; it is rare for baroque dolomite in this study to have any luminescent banding. Murfin Drilling #1 Prentice, 4319 feet.

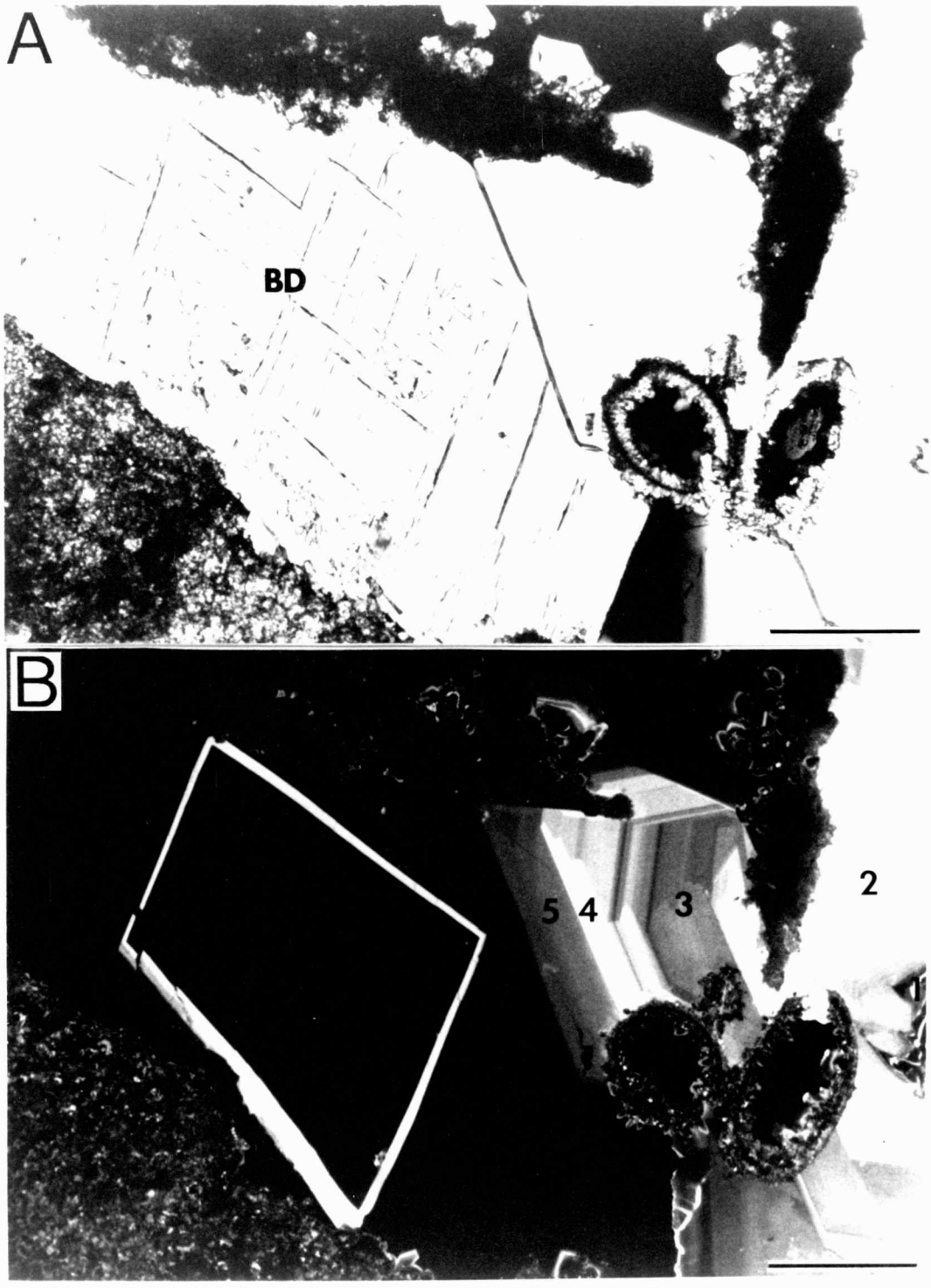
A
BD
B
5
4
3
2
1

Figure 14. Plane-polarized light photomicrograph of chalcedony in relation to calcite cement. Chalcedony (CH) has partially replaced a brachiopod shell (BR) that was syntaxially overgrown by calcite cement (CAL). Because the calcite overgrowth would not have formed overgrowth orientations on chalcedony, the chalcedony is interpreted to postdate the initial calcite cement. Scale bar is 200 micrometers. Cities Service #1-A Knudson, 4259 feet.

Figure 15. Plane-polarized light photomicrograph of pyrite in relation to a stylolite. The pyrite (PYR) is interpreted to have precipitated along a stylolite (ST), and therefore postdate the stylolite. An alternative explanation is that pyrite is a stylocumulate. A post-stylolite origin for the pyrite is accepted because pyrite is not just limited to the horizontal part of the stylolite, but is also along the vertical slickenside of the stylolite. Pyrite along the vertical side of the stylolite is less likely to be a stylocumulate and more likely to be pyrite that precipitated after the stylolite formed. Scale bar is 200 micrometers. Empire Drilling #1 Rathe, 4216.5 feet.

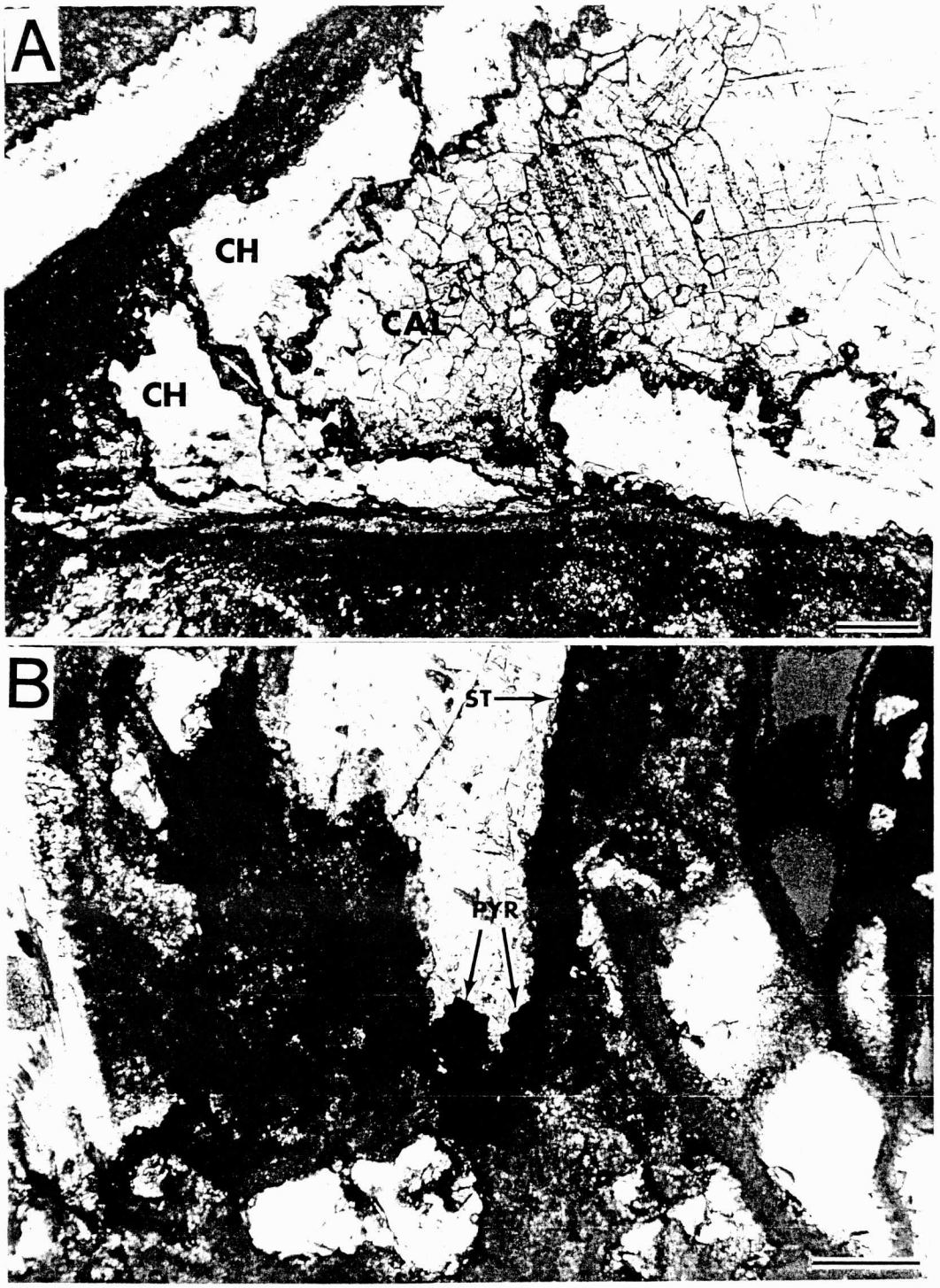
A
CH
CAL
CH
B
ST
PYR

Stylolites and microstylolites postdate all calcite and dolomite cements.

Replacive Pyrite

Pyrite replacement is common. It commonly crosscuts calcite and dolomite cement, and stylolites (Figure 15).

Late-Stage Dissolution

Late-stage dissolution (LSD) is defined herein as dissolution that postdates calcite and dolomite cementation. Evidence of LSD includes etching that crosscuts calcite cement (Figure 16A, 16C) and baroque dolomite (Figure 16B).

LSD generally creates vuggy pores. The criterion to differentiate vugs resulting from LSD from early vugs is that early vugs will likely be reduced by calcite or dolomite cement while no vugs resulting from LSD should be reduced by the calcite or dolomite cements (Figure 16E). Although some early vugs might be isolated from the calcite- or dolomite-precipitating fluids and not be reduced by these cements, almost all interparticle, intraparticle, and moldic pores are reduced by some calcite and dolomite cement, and it is assumed that early vugs should also be reduced by these cements.

In the nonargillaceous samples, almost all vuggy pores resulted from LSD; vugs resulting from early dissolution are rare. Pores resulting from LSD are present in 22 of the 35 cores (Figure 17).

LSD may enhance permeability as well as porosity. A crossplot of the estimated porosity resulting from LSD versus permeability

Figure 16. Photomicrographs of dissolution features caused by late-stage dissolution (LSD).

(A) Plane-light photomicrograph of dissolved calcite, White is calcite cement; dark gray is blue-colored epoxy. The etching of calcite (marked by an arrow) was caused by LSD. Scale bar is 200 micrometers. Husky Oil #6 Brookes, 3402 feet.

(B) Plane-light photomicrograph of dissolved baroque dolomite. White is baroque-dolomite cement; dark gray is blue-colored epoxy. The baroque dolomite was etched (marked by an arrow) by LSD. Scale bar is 200 micrometers. Continental Oil #405 Adell Unit, 3650.9 feet.

(C) Scanning electron microscope (SEM) photomicrograph of a partially dissolved calcite cement, The dissolution feature (marked by an arrow) was caused by LSD. Scale bar is 30 micrometers. Continental Oil #406 Adell Unit, 3701.5 feet.

(D) Plane-light photomicrograph of vugs. White is calcite cement; dark gray is blue-colored epoxy. Moldic pores in the sample are filled with calcite cement. The vugs are not reduced by calcite cement. If the vugs had formed prior to calcite cementation, they would probably be reduced by calcite cement. These vugs formed after calcite cementation from LSD. Scale bar is 200 micrometers. Murfin Drilling #2 Elvin, 3614 feet.

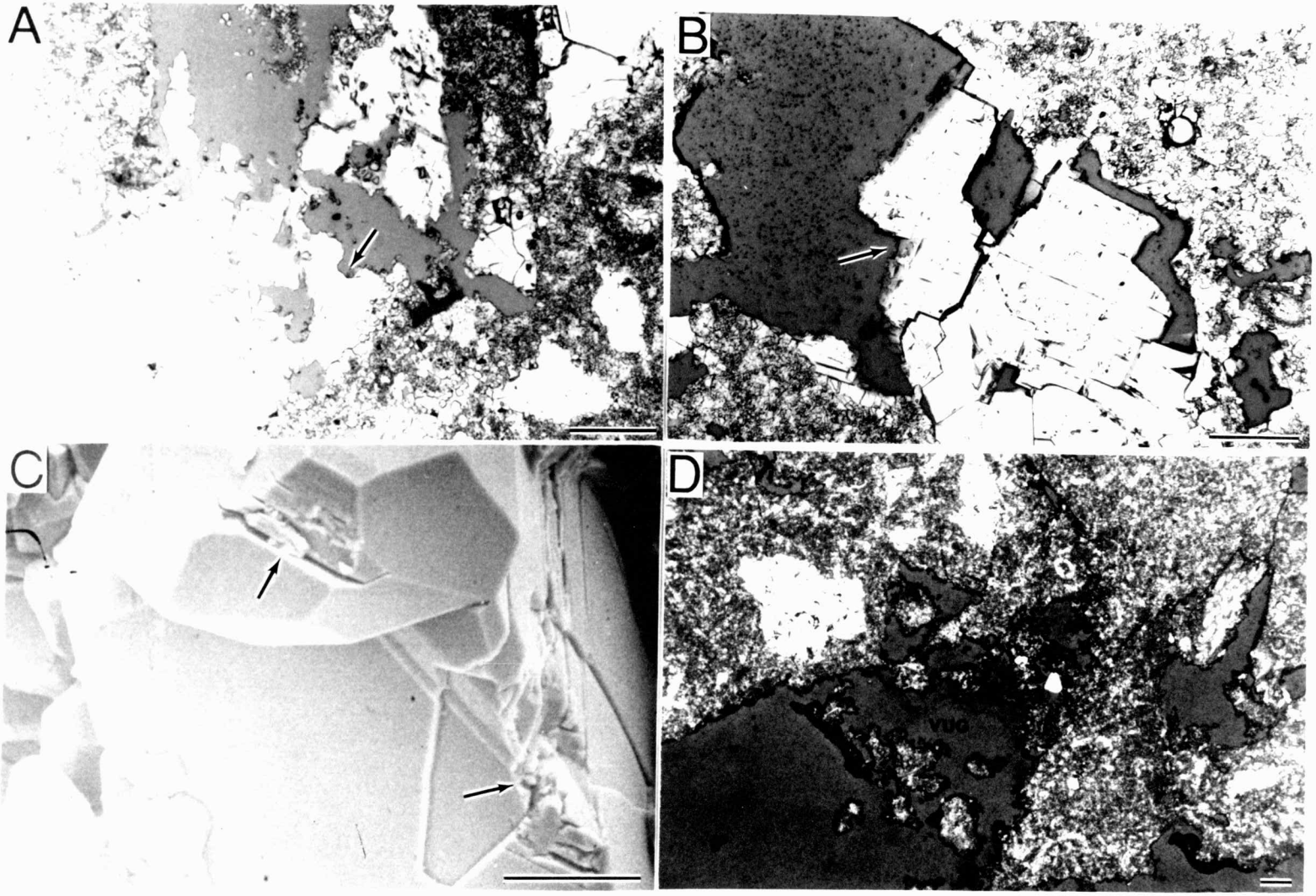
A
B
C
D
VUG

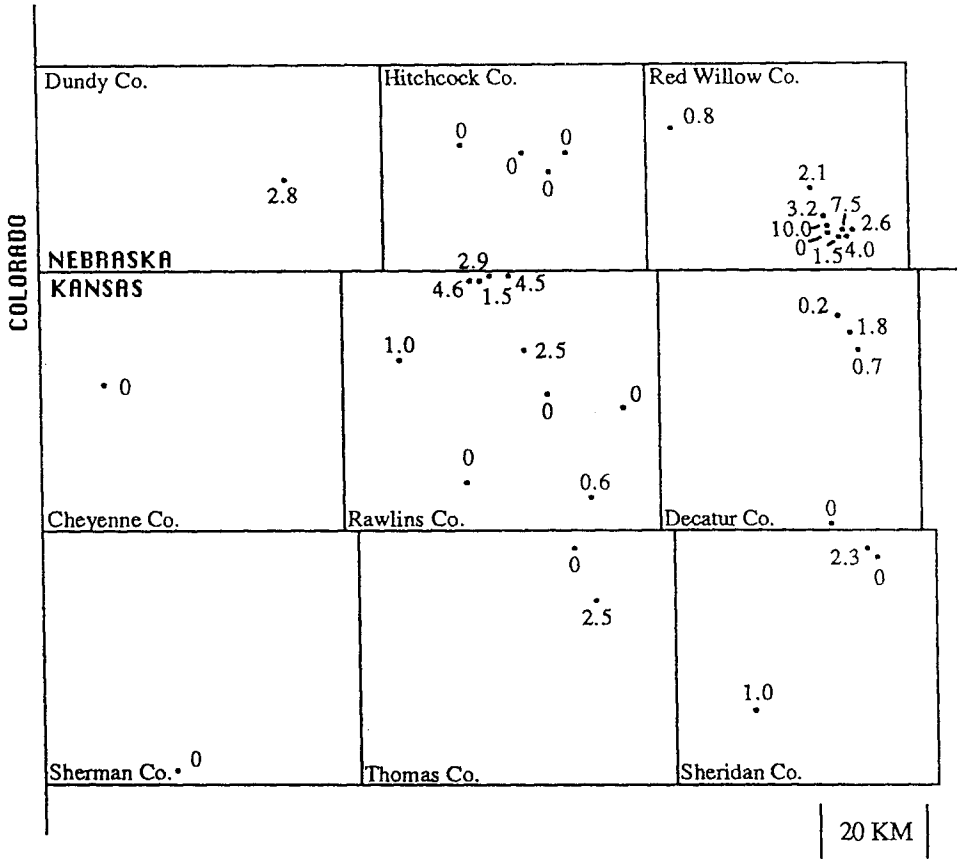

Figure 17. The average amount of open porosity (in %) that resulted from LSD for the thin sections from each core. The average amount of open porosity from LSD = (average open porosity) x (average percentage of open porosity from LSD) / 100.

(from core-plug measurements) in fossiliferous wackestones (Figure 18) shows that with increased LSD, there is higher permeability. In fossiliferous wackestones, the moldic and intraparticle pores are commonly not interconnected and have poor permeability (Moore, 1979). LSD may improve permeability by increasing the interconnectedness of the pores.

Petroleum Fluid Inclusions

Evidence of petroleum migration are petroleum-filled fluid inclusions in the calcite and dolomite cements. Under ultra-violet fluorescence, petroleum-filled fluid inclusions range from yellow to blue-white. They are secondary, trapped along healed fractures in the calcite and dolomite cements. The cores in which petroleum-filled fluid inclusions were found are shown in Figure 19.

Anhydrite Cementation

Anhydrite cements are both equant and tabular in shape. They are present in 12 of the 155 thin sections and postdate calcite and dolomite cementation. In one case, anhydrite cement reduces a pore enhanced by LSD. Anhydrite cements reduce "precementation porosity" by an average of 0.3 percent in the wackestone, packstone, and grainstone thin sections.

Altered Pyrite

The last diagenetic event was partial alteration of pyrite to a red-colored mineral. The altered pyrite is present in chert and chalcedony. The red coloration of chert and chalcedony is a result of the alteration of pyrite. Pyrite postdates stylolites, and the

Figure 18. A crossplot of the amount of porosity (in %) estimated to have resulted from LSD and the measured permeability (from core-plug analyses) for the same interval. Each of these data points are from fossiliferous wackestones. These data are tabulated in Table VI-A, Appendix VI.

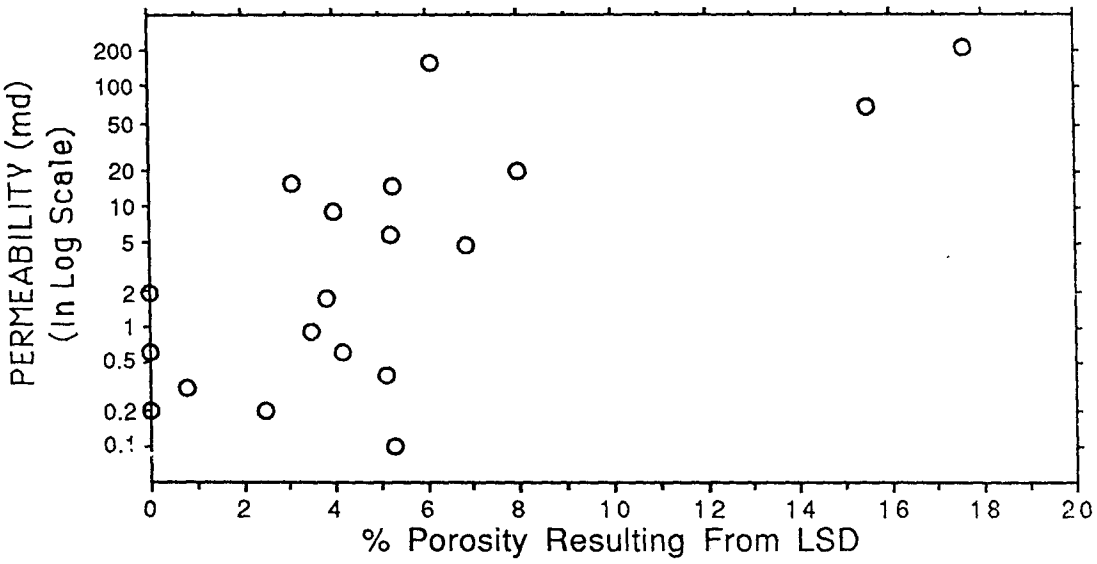
PERMEABILITY (md)
(In Log Scale)
200
100
50
20
10
5
2
1
0.5
0.2
0.1
0
2
4
6
8
10
12
14
16
18
20
% Porosity Resulting From LSD

Figure 19. The location of cores (marked by black-filled circles) which have petroleum-filled fluid inclusions in thin sections. Cores with petroleum-filled fluid inclusions are named. In general, all of these cores are near present petroleum production from the Lansing and Kansas City groups.

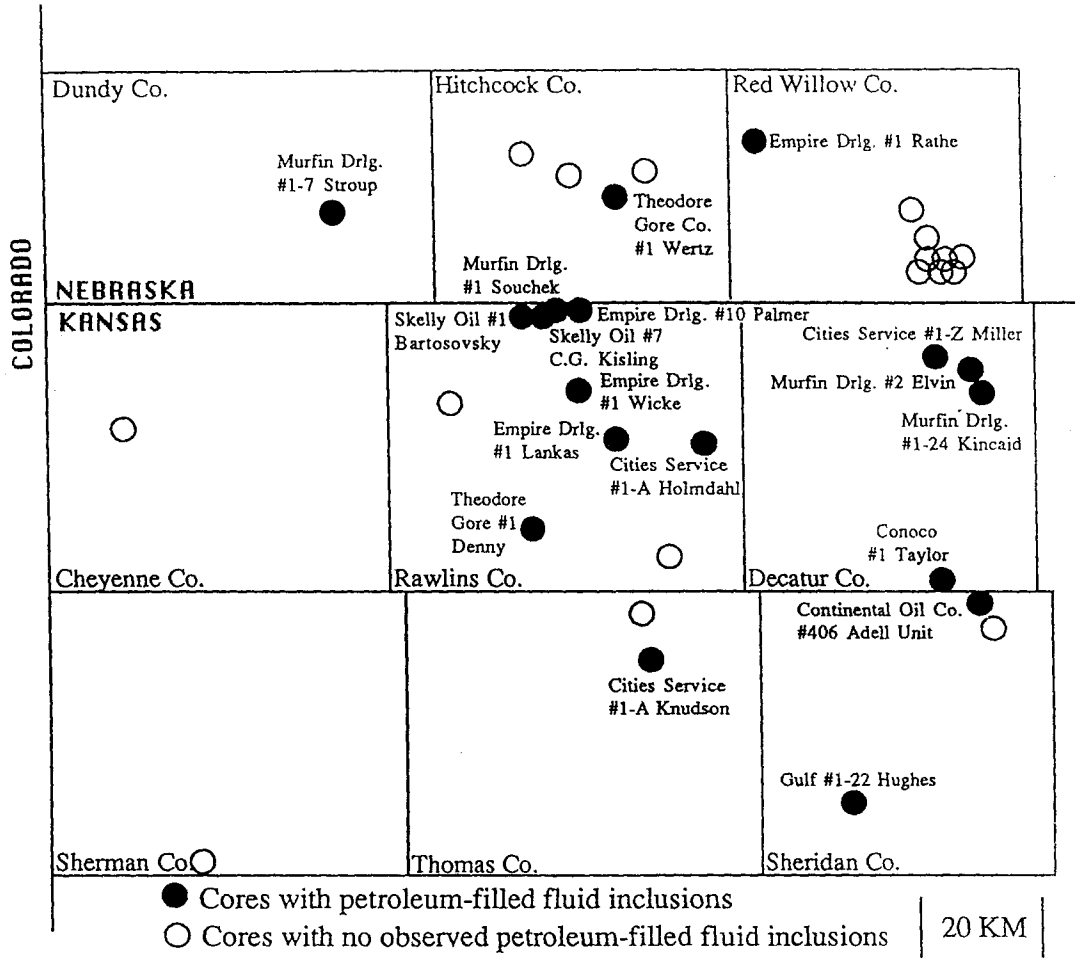
COLORADO
NEBRASKA
KANSAS
Dundy Co.
Hitchcock Co.
Red Willow Co.
Murfin Drlg.
#1-7 Stroup
Theodore
Gore Co.
#1 Wertz
Empire Drlg. #1 Rathe
Murfin Drlg.
#1 Souchek
Skelly Oil #1
Bartosovsky
Empire Drlg. #10 Palmer
Skelly Oil #7
C.G. Kisling
Empire Drlg.
#1 Wicke
Cities Service #1-Z Miller
Murfin Drlg. #2 Elvin
Murfin Drlg.
#1-24 Kincaid
Empire Drlg.
#1 Lankas
Cities Service
#1-A Holmdahl
Theodore
Gore #1
Denny
Conoco
#1 Taylor
Cheyenne Co.
Rawlins Co.
Decatur Co.
Continental Oil Co.
#406 Adell Unit
Cities Service
#1-A Knudson
Gulf #1-22 Hughes
Sherman Co.
Thomas Co.
Sheridan Co.
Cores with petroleum-filled fluid inclusions
Cores with no observed petroleum-filled fluid inclusions
20 KM

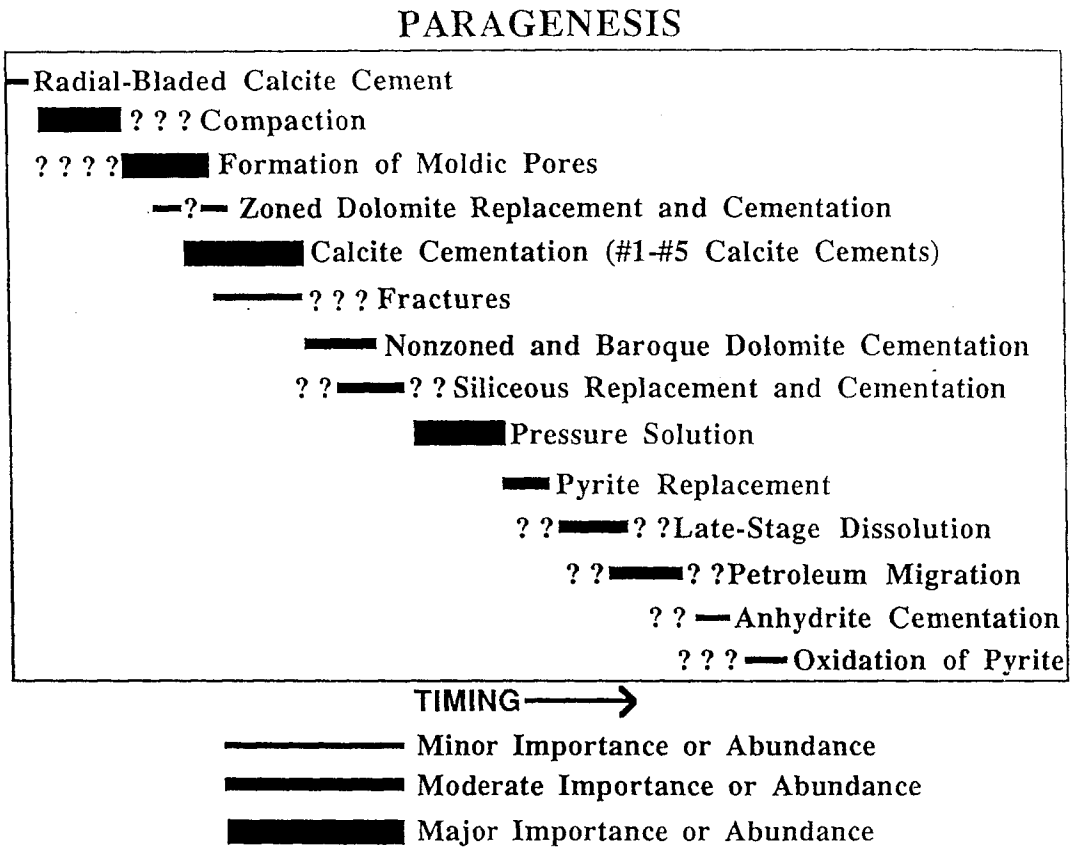

Figure 20. Interpreted paragenetic sequence of diagenetic events.

alteration of pyrite postdates stylolites because in some samples the only alteration of pyrite is within the stylolites.

Relative Abundance Of The Cements

The "precementation porosity" and the degree of reduction by the calcite, dolomite, and anhydrite cements are tabulated for the wackestone, packstone, and grainstone thin sections (Table 3) and graphically shown in Figure 21. These same data are also tabulated by stratigraphic interval (Table 4) and graphically shown in Figure 22.

Calcite cement reduces "precementation porosity" by an average of 64.4 percent for the wackestone, packstone, and grainstone thin sections. Of the calcite cements, the #2 calcite cement is the most significant, reducing an average of 36.2 percent. Open porosity caused by late-stage dissolution (LSD) accounts for an average of 1.5 percent of the rocks. LSD is most significant in the wackestone thin sections where one-third of the open porosity was caused by LSD. LSD is less significant in the packstone and grainstone thin sections.

Areal Distribution of Cements

The average reduction of "precementation porosity" for the major cements is plotted for the thin sections of each core (Figure 23). The cores are divided into two subgroups (Table 5) with <25 percent and $\geq$25 percent evaporites in the overlying Stone Corral Formation and Nippewalla Group. There is more calcite cement in the thin sections from the area with $\geq$25 percent evaporites (78.2

Table 3. Average porosity and cement-reduction data for the wackestone, packstone, and grainstone thin sections. During cathodoluminescence analysis of the thin sections, the percent of open porosity, the percent of calcite, dolomite, and anhydrite cements, and the percent of porosity resulting from late-stage dissolution (LSD) were estimated using visual standards. With these data, "precementation porosity", pre-LSD porosity, porosity from LSD, and the degree of reduction of "precementation porosity" by calcite, dolomite, and anhydrite cments were calculated.

	# of Thin Sections	% "Precementation Porosity"	% of "Precementation Porosity"								% Pre-LSD Porosity	% Porosity from LSD	% Open Porosity
			% Calcite Cement	% Calcite Cement #1	% Calcite Cement #2	% Calcite Cement #3	% Calcite Cement #4	% Calcite Cement #5	% Dolomite Cement	% Anhydrite Cement			
Wackestones, Packstones and Grainstones	153	28.3	64.6	11.6	36.3	13.5	2.7	0.3	7.3	0.3	8.9	1.5	10.5
Porosity ≥ 8%	82	32.4	46.4	9.5	23.9	11.1	1.7	0.1	7.7	0.5	15.5	2.7	18.1
Porosity > 0, < 8%	33	22.9	80.9	14.7	48.7	14.7	2.8	0	3.1	0.1	3.0	0.5	3.5
Porosity = 0%	38	24.2	89.6	13.5	52.1	17.6	4.7	0.8	10.0	0	0	0	0
Wackestones	63	22.7	72.2	12.2	40.4	14.8	4.6	0.1	5.4	0.5	5.9	3.0	8.9
Porosity ≥ 8%	34	26.4	58.7	10.3	32.8	12.0	3.5	0.2	4.1	1.0	10.1	5.3	15.4
Porosity > 0, < 8%	13	18.2	83.8	12.1	50.3	16.5	4.9	0	4.7	0	1.9	0.7	2.6
Porosity = 0%	16	18.6	91.3	16.2	48.7	19.6	6.7	0.1	8.7	0	0	0	0
Packstones	74	31.9	60.5	10.5	33.4	14.7	1.6	0.4	8.2	0.1	10.8	0.6	11.4
Porosity ≥ 8%	39	37.1	40.2	8.9	18.0	12.7	0.5	0.1	9.0	0.3	19.0	1.0	19.9
Porosity > 0, < 8%	15	24.0	77.2	14.8	43.6	16.8	2.0	0	1.8	0	3.7	0.5	4.2
Porosity = 0%	20	27.6	87.7	10.3	55.5	16.9	3.5	1.4	11.5	0	0	0	0
Grainstones	16	33.9	53.3	14.8	33.5	2.9	0	0	10.1	0.2	12.6	0	12.6
Porosity ≥ 8%	9	35.0	26.6	9.2	16.3	1.2	0	0	15.4	0	20.3	0	20.3
Porosity > 0, < 8%	5	31.4	84.3	21.1	59.7	3.4	0	0	2.8	0.6	3.8	0	3.8
Porosity = 0%	2	35.5	95.8	24.1	45.3	9.5	0	0	4.3	0	0	0	0

Figure 21. The average percent of the #1, #2, #3, #4 and #5 calcite cements that reduce the "precementation porosity" for various lithologies and porosity ranges. This data is tabulated in Table 2.

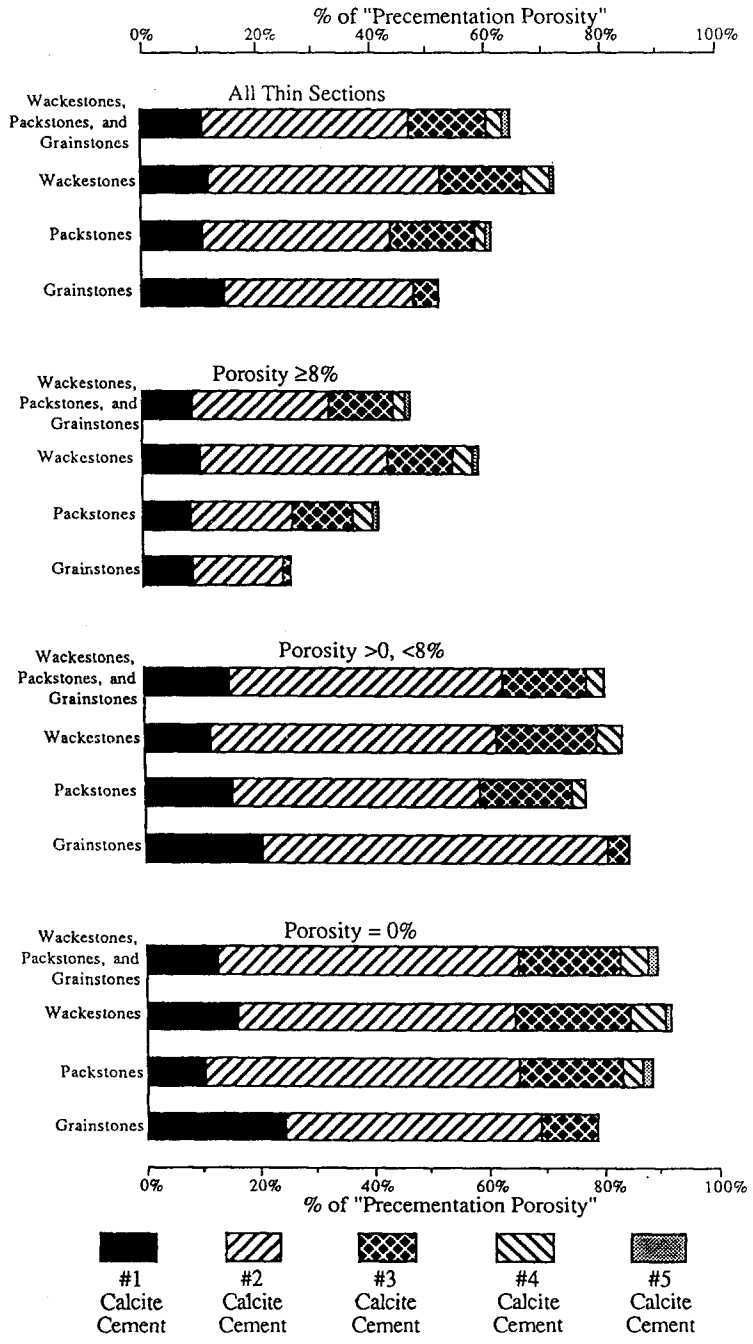
% of "Precementation Porosity"
0%
20%
40%
60%
80%
100%
All Thin Sections
Wackestones, Packstones, and Grainstones
Wackestones
Packstones
Grainstones
Porosity ≥8%
Wackestones, Packstones, and Grainstones
Wackestones
Packstones
Grainstones
Porosity >0, <8%
Wackestones, Packstones, and Grainstones
Wackestones
Packstones
Grainstones
Porosity = 0%
Wackestones, Packstones, and Grainstones
Wackestones
Packstones
Grainstones
0%
20%
40%
60%
80%
100%
% of "Precementation Porosity"
#1 Calcite Cement
#2 Calcite Cement
#3 Calcite Cement
#4 Calcite Cement
#5 Calcite Cement

Table 4. Porosity and cement-reduction data (terms described in Table 3) arranged by stratigraphic interval of the thin sections.

	# of Thin Sections	% Pre-cementation Porosity	% of Pre-cementation Porosity								% Pre-LSD Porosity	% Porosity from LSD	% Open Porosity
			% Calcite Cement	% Calcite Cement #1	% Calcite Cement #2	% Calcite Cement #3	% Calcite Cement #4	% Calcite Cement #5	% Dolomite Cement	% Anhydrite Cement			
Toronto Limest.	6	33.4	35.0	12.4	21.5	1.0	0	0	22.6	0	14.6	1.2	15.8
A Limestone	11	23.8	68.7	12.9	32.1	20.6	0	0	1.0	1.2	7.8	3.1	10.8
B Limestone	3	32.3	70.9	15.0	29.7	13.7	3.1	9.4	2.1	0	8.3	0	8.3
C Limestone	8	31.3	45.9	13.0	18.6	10.3	4.0	0	3.2	0	15.9	0	15.9
D Limestone	36	25.2	68.5	11.4	34.5	15.2	7.3	0.1	7.5	0.1	6.8	2.2	9.0
E Limestone	4	30.8	55.5	8.1	25.9	12.3	8.9	0	7.0	0	10.8	1.0	11.8
F Limestone	3	36.3	56.2	16.2	34.7	5.2	0	0	22.3	0	6.7	0	6.7
G Limestone	25	29.0	69.8	11.6	42.9	13.8	1.3	0.3	5.0	0.1	9.5	1.4	10.9
G' Limestone	3	25.0	97.5	7.1	65.8	23.1	1.6	0	0.9	0	0.3	0	0.3
H Limestone	12	28.4	71.7	16.7	48.2	6.4	0.4	0	7.8	1.3	6.3	1.8	8.1
H' Limestone	3	39.7	69.7	1.3	52.7	15.7	0	0	0.7	0.8	10.0	0	10.0
I Limestone	1	14.0	57.1	8.6	37.1	11.4	0	0	7.1	0	5.0	0	5.0
J Limestone	25	29.7	55.4	9.3	30.0	15.8	0.3	0	8.8	0.3	11.5	2.1	13.6
K Limestone	7	29.7	63.0	8.2	46.0	8.8	0	0	9.4	0.3	10.9	0	10.9
L Limestone	1	26.0	15.4	3.1	8.5	3.8	0	0	46.2	0	10.0	0	10.0

Figure 22. The average reduction of "precementation porosity" by the #1, #2, #3, #4, and #5 calcite cements arranged by the stratigraphic interval of the thin sections. These data are tabulated in Table 4.

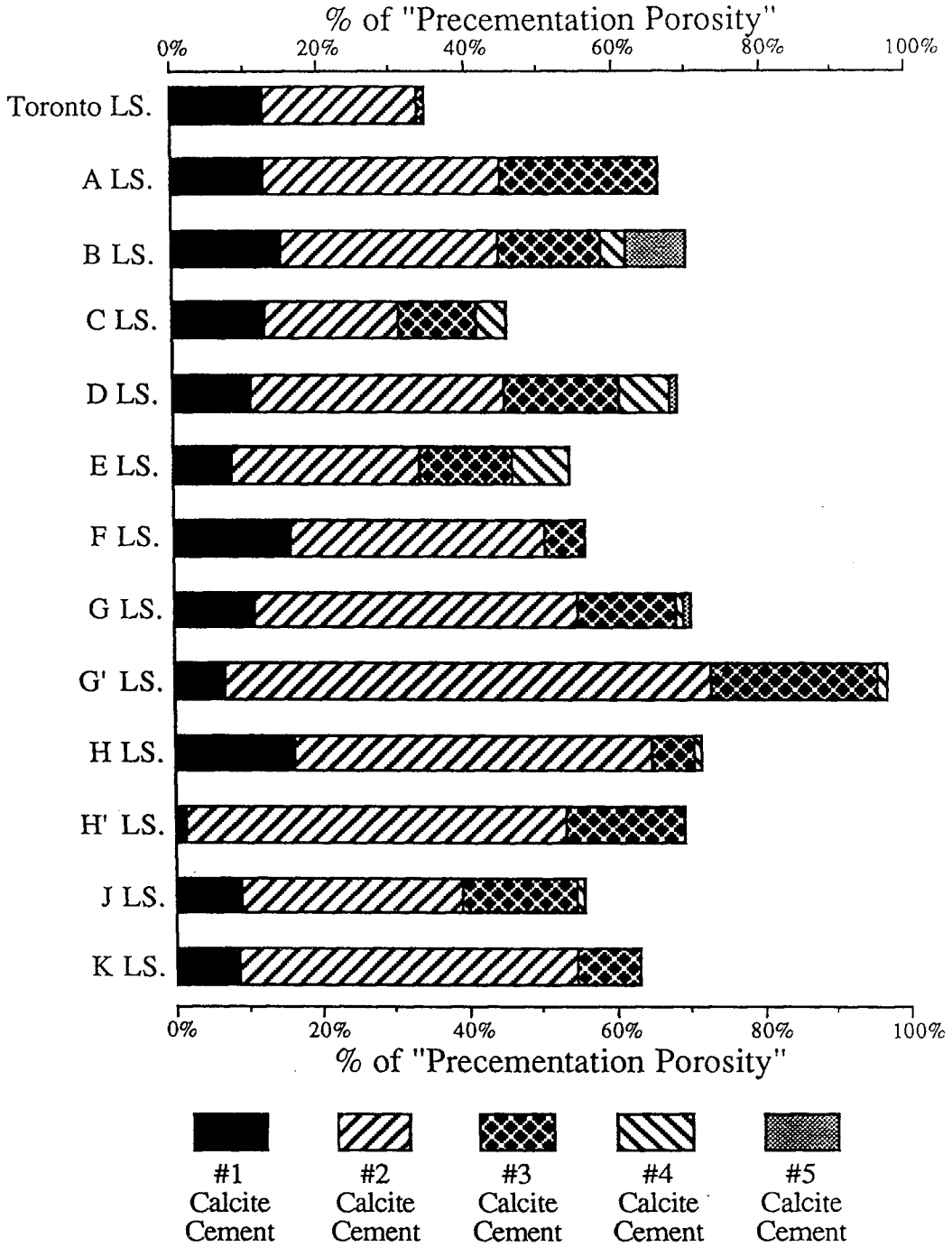
% of "Precementation Porosity"
0%
20%
40%
60%
80%
100%
Toronto LS.
A LS.
B LS.
C LS.
D LS.
E LS.
F LS.
G LS.
G' LS.
H LS.
H' LS.
J LS.
K LS.
0%
20%
40%
60%
80%
100%
% of "Precementation Porosity"
#1 Calcite Cement
#2 Calcite Cement
#3 Calcite Cement
#4 Calcite Cement
#5 Calcite Cement

Figure 23. Maps of the average reduction of "precementation porosity" by calcite and dolomite cements.

(A) #1 calcite cement, (B) #2 calcite cement, (C) #3 calcite cement, (D) #4 calcite cement, (E) all calcite cement, and (F) all dolomite cement.

Each map shows the extent of $\geq$25% and <25% evaporites in the Lower Permian Stone Corral Formation and Nippewalla Group interval (Rascoe and Baars, 1972).

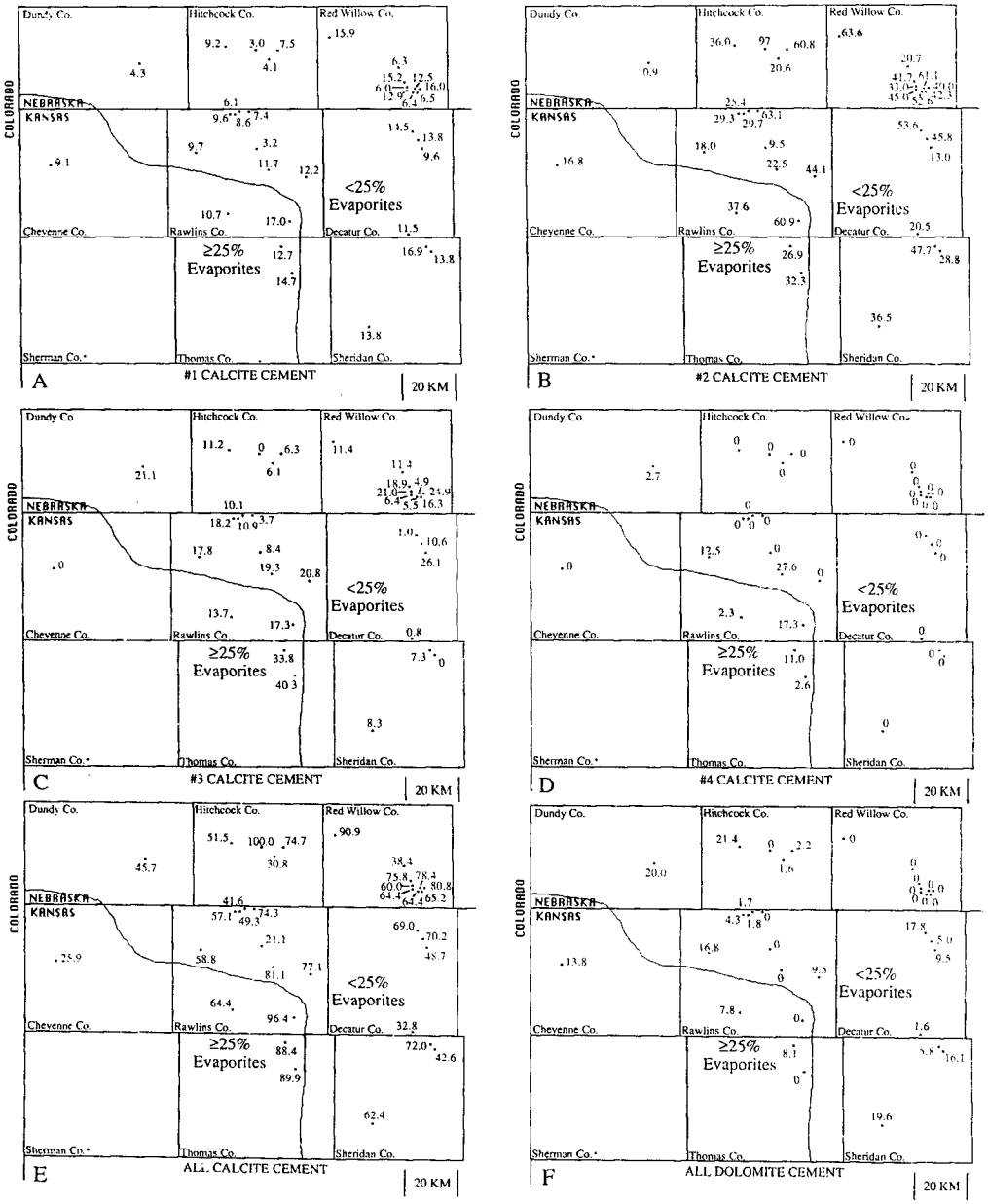
Dundy Co.
Hitchcock Co.
Red Willow Co.
COLORADO
NEBRASKA
KANSAS
Cheyenne Co.
Rawlins Co.
Decatur Co.
Sherman Co.
Thomas Co.
Sheridan Co.
<25% Evaporites
≥25% Evaporites
A
#1 CALCITE CEMENT
20 KM
B
#2 CALCITE CEMENT
C
#3 CALCITE CEMENT
D
#4 CALCITE CEMENT
E
ALL CALCITE CEMENT
F
ALL DOLOMITE CEMENT

Table 5. The amount of porosity and cement in the thin sections from areas overlain by ≥25% and <25% evaporites in the Stone Corral Formation and Nippewalla Group interval (Figure 23).

	# of Thin Sections	% "Precementation Porosity"	% of "Precementation Porosity"								% Pre-LSD Porosity	% Porosity from LSD	% Open Porosity
			% Calcite Cement	% Calcite Cement #1	% Calcite Cement #2	% Calcite Cement #3	% Calcite Cement #4	% Calcite Cement #5	% Dolomite Cement	% Anhydrite Cement			
≥25% EVAPORITES	25	29.5	78.2	13.8	35.4	23.5	4.4	1.1	6.0	0	6.7	0.4	7.1
WACKESTONES	4	16.0	92.9	20.4	41.5	30.7	0	0	6.3	0	0.3	0	0.3
PACKSTONES	20	30.8	78.0	12.7	35.1	23.3	5.5	1.4	5.5	0	6.7	0.5	7.2
GRAINSTONES	1	58.0	25.9	9.1	16.8	0	0	0	13.8	0	33.0	0	33.0
<25% EVAPORITES	128	28.1	61.9	11.2	36.5	11.6	2.3	0.1	7.5	0.4	9.4	1.8	11.1
WACKESTONES	59	23.2	70.8	11.6	40.4	13.8	4.9	0.1	5.3	0.5	6.2	3.2	9.4
PACKSTONES	54	32.3	54.1	9.6	32.7	11.5	0.1	0.1	9.2	0.2	12.2	0.7	12.9
GRAINSTONES	15	32.3	55.1	15.1	34.6	3.1	0	0	9.8	0.2	11.3	0	11.3

percent of "precementation porosity", Table 5) than in the thin sections from the area with <25 percent evaporites (61.9 percent of "precementation porosity", Table 5). For the individual calcite cements, all but the #2 calcite, are more common in the area with ≥25 percent evaporites.

Discussion Of Petrography

Generally, calcite cements postdate compaction features. In places, moldic pores also postdate compaction features. In nearly half of the thin sections with moldic pores and the #1 calcite cement, the molds are not reduced by the #1 calcite cement. As the #1 calcite cement commonly postdates compaction features, these molds also postdate compaction.

The amount of burial necessary to cause these compaction features is uncertain. Data from Shinn and Robbin (1983) and Meyers (1980) suggest that a minimum of 30 to 100 m of overburden are necessary.

In the Lansing and Kansas City groups, the average thickness of a complete cyclothem is approximately 15 m. The above data suggest that the formation of compaction features requires at least 30 meters of overburden. A post-compaction origin for calcite cement and molds would commonly require the deposition of at least two overlying cyclothems. This is evidence that calcite cementation and commonly mold formation postdate burial and are probably not related to cyclothem-capping events of subaerial diagenesis. These

observations indicate Heckel's (1983) model does not apply to these rocks.

The #1 calcite cement is nonferroan and nonluminescent; the #2 calcite cement is nonferroan and is complexly subzoned with luminescence ranging from bright to moderately dull luminescence; the #3 calcite cement is ferroan and has very dull luminescence; the #4 calcite cement is nonferroan and is complexly subzoned with luminescence ranging from moderately bright to moderately dull luminescence; and the #5 calcite cement is ferroan and has very dull luminescence. Frank et al. (1982) related nonluminescence of calcite (such as #1) to a lack of Mn^{2+} whereas bright luminescence (such as #2 and #4) is caused by Mn^{2+} in the calcite structure. They also considered weak luminescence (such as #3 and #5) to be caused by Fe/Mn ratios greater than 1.0. Frank et al. (1982) and Grover and Read (1983) related increasing Mn and Fe concentrations in calcite to a progressive reduction of pore waters. Based on these data, the sequence of the #1, #2, and #3 calcite cements represents a progression of oxidized to reduced conditions in the pore waters. The #4 calcite cement, which is less common and geographically limited (Figure 23), may indicate a return to less reduced conditions. The #5 calcite cement, however, precipitated from more reduced pore waters.

Throughout the Lansing and Kansas City groups, the limestones contain essentially the same cathodoluminescent patterns. If calcite cementation had occurred during deposition of the Lansing

and Kansas City groups, it would be expected that the cathodoluminescent patterns would be unique to stratigraphic subunits. Therefore, the calcite cementation postdates the deposition of the Lansing and Kansas City groups. This suggests that the cathodoluminescent zones may be synchronous throughout these strata. To test the synchronity of the cathodoluminescent zones, a detailed correlation of cathodoluminescent subzones is necessary.

Similar cathodoluminescent patterns throughout the Lansing and Kansas City groups suggest a progressive stagnation of pore fluids (increased reduction) that was formation wide and not isolated. If this progressive stagnation was localized, the less-permeable wackestones would probably have less #1 calcite cement and more #2 and #3 calcite cements. The distribution of the calcite cements in the thin sections, however, does not significantly vary between lithologies (Table 3, Figure 21). This supports the hypothesis that the progressive reduction of pore fluids was formation wide. The individual calcite cement zones probably formed at approximately the same time.

Zoned dolomite is present as both cement and replacement. Zoned dolomite commonly predates calcite cement, but in places, postdates part of the calcite cement. Most of the dolomite cementation, which is nonzoned and includes baroque dolomite, postdates all calcite cement.

Evidence of late-stage dissolution was observed in 22 of the 35 cores. This dissolution postdates all calcite and dolomite cement.

All petroleum-filled fluid inclusions are secondary and postdate the calcite and dolomite cements. Therefore, petroleum migration probably postdates all calcite and dolomite cementation.

The oxidation of pyrite that postdates stylolitization indicates that oxidizing fluids were present in these strata after significant burial.

FLUID INCLUSION GEOCHEMISTRY

Fluid inclusions were analyzed to determine the temperature and composition of fluids of cement precipitation and the temperature and composition of later pore fluids. The fluid inclusions studied were primary. Fluid inclusions were judged to be primary if they were confined by growth bands of the cement (Figure 24).

Fluid inclusions were analyzed from five calcite samples, three nonzoned euhedral dolomite samples, and one baroque dolomite sample. The samples were analyzed by crushing, heating, and freezing.

Inclusions were crushed while immersed in kerosene to determine the pressure and composition of gases in the bubbles of two-phase (liquid and bubble) inclusions. Measurements included (1) the change in the size of the bubble when the inclusion was initially exposed to 1 atmosphere pressure, and (2) the character of bubble dissolution into the kerosene. The crushing runs were recorded on video tape and the dimensions of the bubbles were measured before and after crushing runs. Based on Boyle's law ($V_1/V_2 = P_2/P_1$), the

Figure 24. Paired plane-light (A) and cathodoluminescent (B) photomicrographs of cloudy zones in the #1 calcite cement that contain fluid inclusions. Arrows in A. and B. point to two cloudy zones. These cloudy zones are confined to the nonluminescent #1 calcite cement. Because these cloudy zones of fluid inclusions are confined to growth zones, they are interpreted to be primary fluid inclusions that formed as the calcite precipitated. The bright bands just outside the cloudy zones in B. are the #2 calcite cement which is overgrown by the very dull #3 calcite cement. Continental Oil #7 L.E. Leonard, 3620 feet.

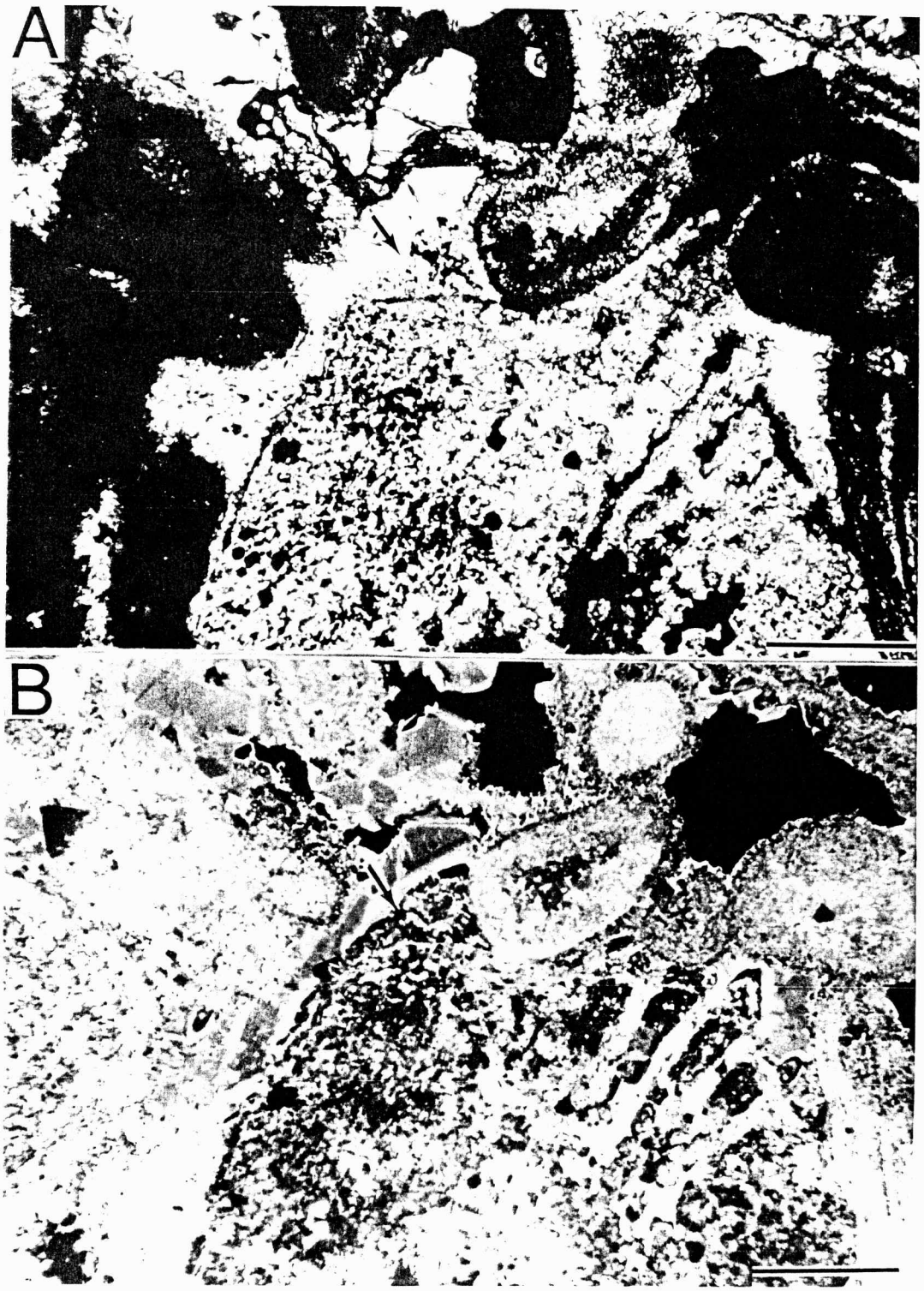
A
B

pressure of the inclusion bubble at room temperature can be determined by measuring the change in the volume of the bubble before and after crushing. Problems in determining the volume of the bubbles causes this method to be inaccurate. If the bubble dissolves in the kerosene medium, the bubble is probably a methane-rich gas (Roedder, 1984). All crushing measurements are tabulated in Appendix XII.

In all cases, the bubbles expanded when exposed to atmospheric pressure and the bubbles dissolved in the kerosene medium, which suggests the bubbles are methane-rich gas at a pressure higher than 1 atmosphere.

Zones of inclusions selected for study were mapped out to determine if the inclusions were along growth zones and to determine the distribution of the liquid-to-vapor ratios of the inclusions.

The two-phase inclusions were first heated in the fluid inclusion stage until the bubble and and liquid homogenized to all liquid. The temperature at which this occurs is the temperature of homogenization (Th). Th represents the minimum temperature of entrapment or reequilibration. Inclusions were not overheated before Th was measured. The presence of methane gas in the inclusions makes pressure correction difficult. If the volume of the inclusion has remained constant, the Th should approach the temperature of entrapment for aqueous inclusions trapped with dissolved methane (Hanor, 1980).

The inclusions were then cooled until the inclusions froze. The temperature at which freezing occurs is the temperature of nucleation (Tn). The inclusions were then heated. First, the eutectic temperature (Te), which is the temperature at which melting begins, was measured. Second, for twelve inclusions, the melting temperature of hydrohalite was measured. Third, the temperature of melting of the last piece of ice (Tm ice) was measured. Tm ice was always measured with the presence of a vapor bubble to avoid metastability problems. All-liquid inclusions were stretched so as to nucleate a vapor bubble. The freezing data yield the salinity and bulk composition of the fluids.

All observations of first melting (Te) data range from -52° to -43°C. Common aqueous solutions of chloride species with Te in this range are calcium chloride and sodium-calcium chloride (Crawford, 1981). If any sodium is in solution, the Ca/Na ratio can be determined by measuring the melting temperature of hydrohalite (NaCl * $2H_2O$) (Figure 25) (Crawford, 1981; Yanatieva, 1946). Determining the temperature at which all the hydrohalite crystals have melted is difficult. Typically, there is a clearing of the ice + aqueous solution + hydrohalite as the hydrohalite crystals melt. To more precisely observe the final melting of hydrohalite, the samples were heated very slowly and multiple measurements were made. A method which could be used to more precisely measure the melting temperature of hydrohalite is sequential freezing to isolate and enlarge the hydrohalite crystals (Haynes, 1985). In applying this

Figure 25. Phase diagram of H_2O-$CaCL_2$-NaCl (after Haynes, 1985; Crawford, 1981; Yanatieva, 1946). Point A is the eutectic temperature (Te) where hydrohalite ($NaCl \cdot H_2O$) begins to melt. Point B is a temperature of last melting of hydrohalite, and point C is the temperature of last melting of ice (Tm ice). By drawing a line from 100% H_2O through point B to the $CaCl_2$ to NaCl line, the weight ratio $CaCl_2$/NaCl can be determined. By drawing a horizontal line through point C, the salinity in weight percent Ca-Na chloride can be determined.

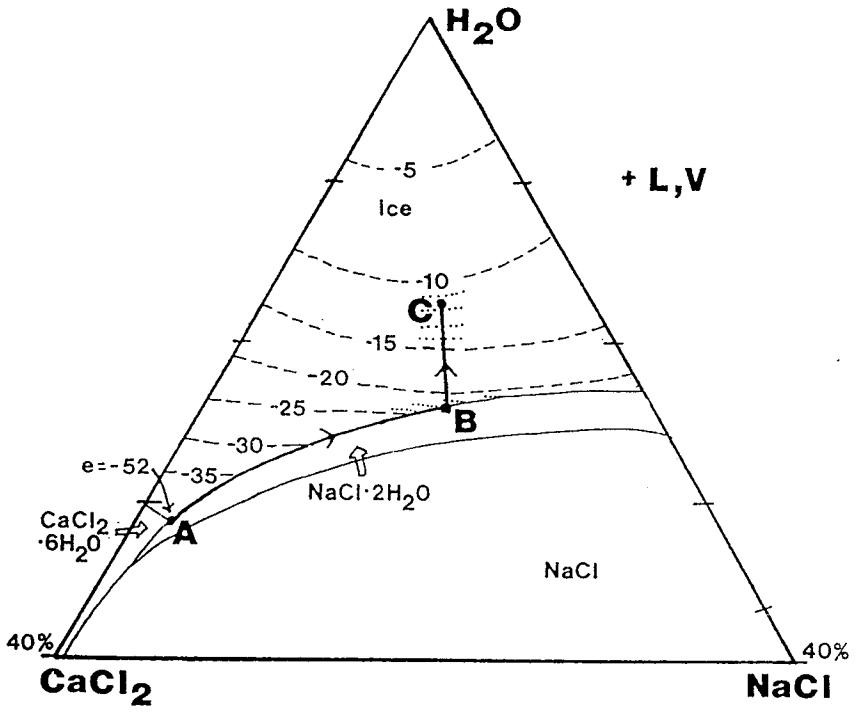
H_2O
-5
Ice
+ L,V
-10
C
-15
-20
-25
B
-30
e=-52
-35
$NaCl \cdot 2H_2O$
$CaCl_2$
$\cdot 6H_2O$
A
NaCl
40%
40%
$CaCl_2$
NaCl

method to an inclusion, hydrohalite melting was not easily observed and phases other than ice, hydrohalite, and anartacite were observed. This suggests that the brine composition is complex and that the interpreted Ca-Na ratios may be inaccurate to some unknown degree.

The melting temperature of hydrohalite was plotted on the phase diagram for H_2O-$CaCl_2$-NaCl (point B, Figure 25) to determine the $CaCl_2$/NaCl ratio. With the Tm ice and $CaCl_2$/NaCl ratio, the salinity in weight-percent Ca-Na chloride can also be determined (point C, Figure 25). All measurements of the melting temperature and the interpreted salinities are tabulated in Table 6.

The Tm ice is a measurement of salinity; higher Tm ice corresponds to lower salinity. For the Tm ice with unknown $CaCl_2$/NaCl ratios, the salinity determination is only approximate.

The presence of methane in fluid inclusions may lower the Tm ice of an inclusion due to the formation of CH_4-hydrate. High internal pressure caused by the methane could also depress the Tm ice (Hanor, 1980). However, the presence of methane in an inclusion lowers the Tm ice by "considerably less than a degree" (Hanor, 1980).

A major problem for interpreting fluid inclusion data is reequilibration of the fluid inclusions. Reequilibration includes the stretching of an inclusion or its leakage and exchange of its contents with external pore fluids (Goldstein, 1986). The stretching of a fluid inclusion may be caused by overheating above Th.

	Fluid Inclusion Data			Phase Diagram Interpretations	
	Te	Tm hydrohalite	Tm ice	$\frac{Ca}{Ca + Na}$	Salinity in Wt.% Ca-Na-Cl
#1 Calcite Cement					
Continental Oil #7 J.E. Leonard, 3620 Feet	-52	-32.0	-21.6	0.66	22.0
#3 Calcite Cement					
Theodore Gore #1 Denny, 4058 Feet	-52	-30.7,-30.4, -31.4,-31.8	-21.8	0.65	22.5
	-52	-38.5,-37.4,-36.6	-22.4	0.74	22.5
Murfin Drilling #2 Elvin, 3665 Feet	-52	-33.0 to -34.5 3 measurements	-22.2	0.69	22.5
	-52	-30.8	-19.1	0.64	21.6
	-52	-34.0,-33.0,-33.0	-22.1	0.68	22.5
	-52	-27.0	-17.0	0.46	20.8
	-52	-27.0	-14.2	0.46	18.6
Cities Service #1-A Knudson, 4052 Feet	-52	-33.0,-37.2, -35.5,-36.8	-14.3	0.72	17.8
Dolomite Cement					
Cities Service #1-A Bourquin, 3983 Feet	-52	-33.0	-18.9	0.68	21.1
	-52	-33.3,-33.7	-22.1	0.68	22.3
Murfin Drilling #1 Prentice, 4250.3 Feet.	-52	-32.2,-31.8,-33.0, -31.5,-31.0,-31.0	-22.1	0.66	22.4

Table 6. The freezing data and interpreted salinities for all inclusions in which the melting temperature of hydrohalite was measured. All measurements of Tm hydrohalite are listed. The Ca/ Ca + Na molar ratios and the salinities are from plotting the Tm hydrohalite and Tm ice on the NaCl-$CaCl_2$-H_2O phase diagram (Figure 26). The interpreted salinities and Ca/ Ca + Na molar ratios may be inaccurate due to the possible presence of phases in these inclusions that are not accounted for in the NaCl-$CaCl_2$-H_2O phase diagram.

Overheating results in high internal pressure that may stretch the inclusion wall to a larger volume (Bodnar and Bethke, 1984; Prezbindowski, 1986). The result of stretching is higher Th values which no longer represent the minimum temperature of entrapment.

The high pressures in fluid inclusions caused by natural overheating could lead to hydrofracturing of an inclusion that could allow exchange between inclusion fluids and external pore fluids. The intersection of fractures or twin lamellae with inclusions could also lead to fluid exchange (Goldstein, 1986). With such an exchange followed by healing, the inclusion fluids would no longer represent the original fluids that precipitated the host mineral.

Methods to detect and account for reequilibration of fluid inclusions include analyzing the inclusion populations from the same growth zone for variability in vapor-to-liquid ratios, determining if the populations are crosscut by twin lamellae or fractures, and analyzing trends and ranges of Th and Tm ice data. An example of inconsistent vapor-to-liquid ratios is the presence of one-phase and two-phase fluid inclusions in the same population. One-phase fluid inclusions generally indicate that the inclusion formed below 40 - 50°C; two-phase fluid inclusions generally have Th values greater than 40 - 50°C.

Where one-phase inclusions are present in a reequilibrated population, these inclusions are most likely to represent the original fluids of precipitation (R.H. Goldstein, personal communication, 1988).

#1 Calcite Cement

Continental Oil #7 J.E. Leonard, 3620 Feet

The fluid inclusions from this sample occur in fluid inclusion-rich growth zones within the nonluminescent #1 calcite cement (Figure 26). These zones parallel the outer edge of the #1 calcite cement and are interpreted to be primary (Figure 24). The diameter of these inclusions generally ranges from 3 to 8 micrometers and some are as large as 12 micrometers in diameter. The fluid inclusions generally are two-phase, vapor-liquid inclusions, but one-phase, all liquid inclusions are present. The one-phase fluid inclusions also range from 3 to 8 micrometers in diameter. Bubble pressure determinations from crushing are 8, 20, and 40 atmospheres (Appendix XII). All bubbles dissolved in the kerosene medium, suggesting the bubbles are methane-rich gas.

The Th data (Figure 26A) are broadly distributed ranging from one-phase at room temperature to 95.7°C. The Te data range from -42° to -52°C. The Tm ice data (Figure 26B) range from -22.0°C to -17.1°C. The Tm ice for the one-phase fluid inclusions (Figure 26B) cover a more narrow range between -22.0°C and -19.1°C. The melting temperature of hydrohalite and ice (Tm ice) in one two-phase inclusion indicates that it has a salinity of 22.0 weight-percent Ca-Na chloride and a Ca / Ca + Na molar ratio of 0.66 (Table 6).

The presence of one-phase and two-phase inclusions in this population suggests that the two-phase inclusions were formerly one-phase inclusions that have been reequilibrated with higher

Figure 26. Primary fluid-inclusion Th and Tm ice data, #1 calcite cement. (A) Th data, mean Th is 67.3°C. (B) Tm ice data, one-phase fluid inclusions are filled (mean Tm ice is -20.7°C), two-phase fluid inclusions are open (mean Tm ice is -20.0), overall mean Tm ice is -20.3°C. (C) Crossplot of Tm ice and Th data, one-phase fluid inclusions are plotted on the left axis. Continental Oil #7 J.E. Leonard, 3620 feet.

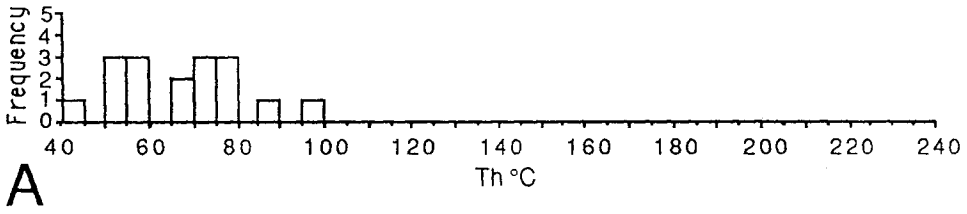

A

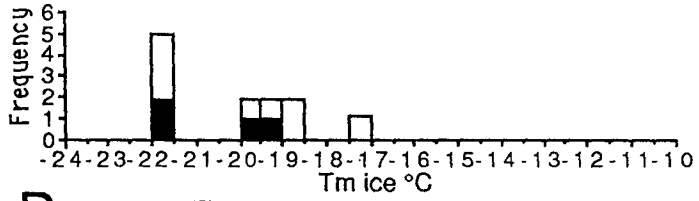

B

One-phase Fluid Inclusions

Two-phase Fluid Inclusions

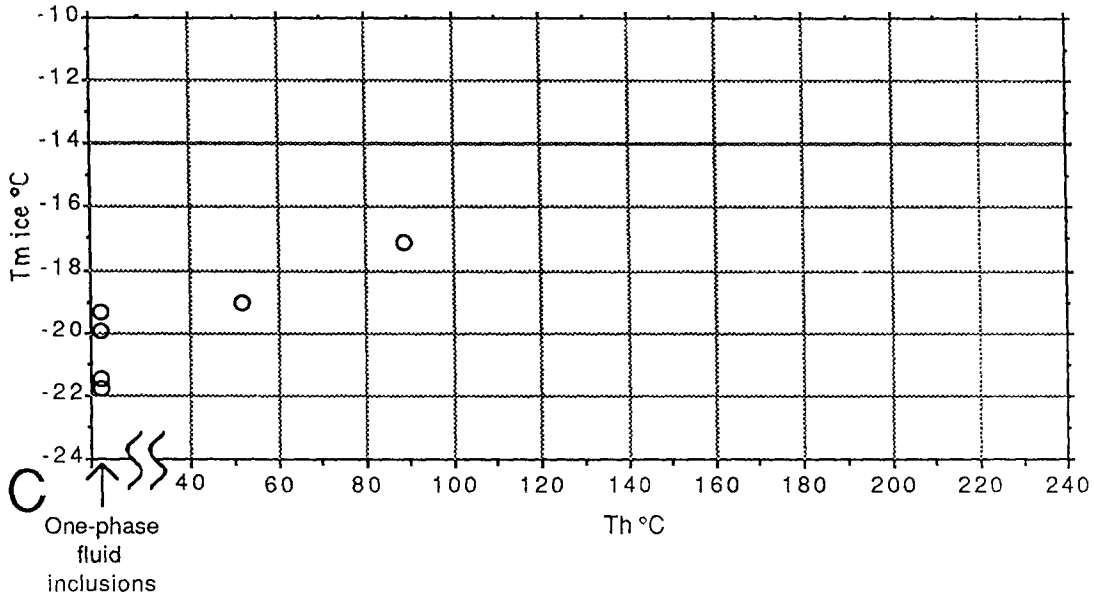

C

One-phase fluid inclusions

temperature. If one-phase fluid inclusions provide the best record of the original fluids, the one-phase inclusions indicate that this cement precipitated from fluids with Tm ice of -19.1° to -22.0°C. The Te data suggest these fluids are in the Ca-Na chloride system. For a Ca / Ca + Na ratio of 0.66 and Tm ice of -19.1° to -22.0°C, the salinity of these fluids ranges from 21.0 to 23.0 weight-percent Ca-Na chloride.

Therefore, the #1 calcite precipitated from a fluid with 21.0 to 23.0 weight-percent Ca-Na chloride at a temperature below 40°-50°C.

Cities Service Company #1-B Ryan, 4363 Feet

The fluid inclusions are in a bladed calcite cement reducing an intraparticle pore. These inclusions are confined to a growth zone in the bladed cement that is just inside a UV fluorescent band of the #1 calcite cement. Their relationship to the fluorescent and luminescent zonation suggests that they formed along a growth zone and are primary inclusions. The size of these inclusions generally ranges from 4 to 8 micrometers in diameter. Some inclusions are as large as 12 micrometers in diameter. These fluid inclusions commonly are one phase, all liquid. Two-phase inclusions are less common. Inclusions in this population were not crushed. The Th data for two-phase inclusions are 52.8°, 73.7°, and 76.4°C (Figure 27A). The Tm ice data (Figure 27B) are -20.2°C and -19.7°C; the Te for both inclusions with Tm ice is -45°C, but may be lower. The small size of the inclusions caused difficulties in .PN 61

Figure 27. Primary fluid-inclusion Th and Tm ice data, #1 calcite cement. (A) Th data, mean Th is 67.4°C. (B) Tm ice data, mean Tm ice is 20.0°C. (C) Crossplot of Th and Tm ice data. Cities Service #1-B Ryan, 4363 feet.

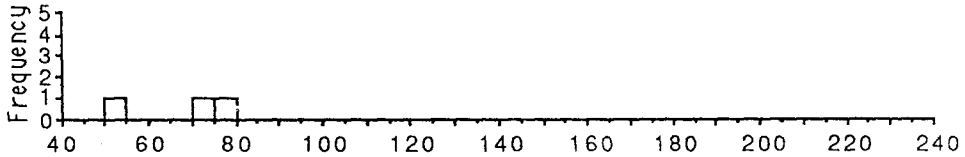
Frequency
0
1
2
3
4
5
40
60
80
100
120
140
160
180
200
220
240
Th °C

A


Frequency
0
1
2
3
4
5
6
-24
-23
-22
-21
-20
-19
-18
-17
-16
-15
-14
-13
-12
-11
-10
Tm ice °C

B

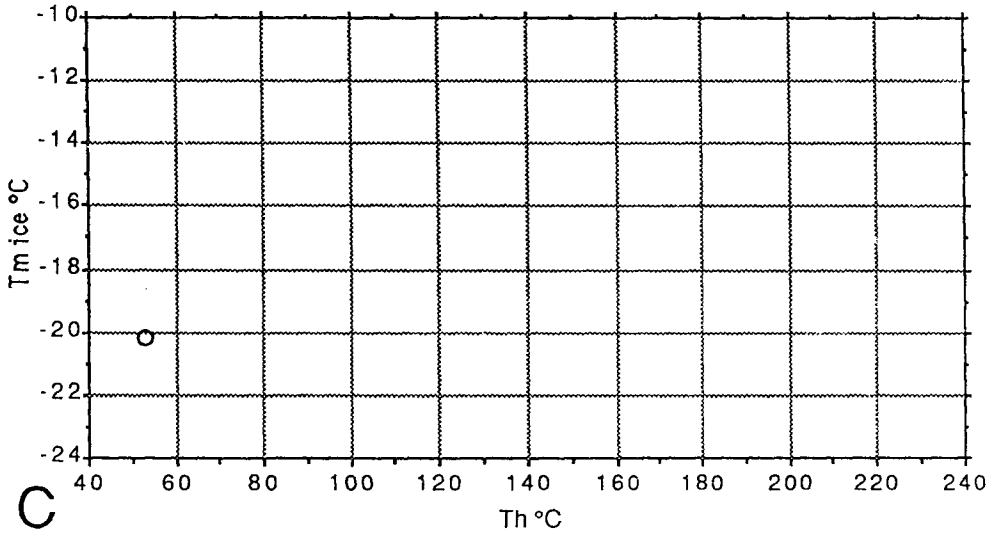
-10
-12
-14
-16
-18
-20
-22
-24
Tm ice °C
40
60
80
100
120
140
160
180
200
220
240
Th °C

C

measuring Tm ice because vapor bubbles rarely nucleated before the ice melted. Tm ice, with the presence of a vapor bubble, was only measured in two inclusions.

The presence of one-phase inclusions in this population suggests that this zone precipitated at less than 40°-50°C. The two-phase inclusions are interpreted to have resulted from stretching or fluid exchange. The Te and Tm ice data suggest that the precipitating fluid was a highly saline Ca-Na chloride brine. If the Ca / Ca + Na ratio of these fluids is near 0.66, as in the previous sample from the #1 calcite cement, the salinity for the two Tm ice data is approximately 21 to 22 weight-percent Ca-Na chloride.

Summary Of #1 Calcite Cement Fluid Inclusion Data

The fluid inclusion data from the two #1 calcite cement samples suggest that the #1 calcite cement precipitated from brines with 21-23 weight-percent Ca-Na chloride at temperatures less than 40°-50°C.

#3 Calcite Cement

Theodore Gore #1 Denny, 4058 Feet

The fluid inclusions are confined to cloudy growth zones in the very dull-luminescent #3 calcite cement. These primary fluid inclusions range from 6 to 20 micrometers in diameter. All the fluid inclusions were two phase and had relatively consistent vapor-to-liquid ratios. Two pressure measurements from crushing are 18 and 33 atmospheres (Appendix XII); because the bubbles dissolved in the kerosene, they are apparently methane-rich.

The Th and Tm ice data (Figure 28) have broad distributions which indicate the possibility of reequilibration. The Tm ice data (Figure 28B) have a mode around -22°C but range as high as -10.6°C. The Te data range from -52° to -46°C indicating a Ca-Na-Cl brine. The melting temperature of hydrohalite and ice (Tm ice) in two inclusions indicate a salinity 22.5 weight-percent Ca-Na chloride and a Ca / Ca + Na molar ratio of 0.65 in one inclusion, and a salinity of 22.5 weight-percent Ca-Na chloride and a Ca / Ca + Na molar ratio of 0.74. in the other inclusion (Table 6).

A crossplot of paired Th and Tm ice data (Figure 28C) shows two trends. One trend is horizontal and shows constant Tm ice values around -22°C with a broad range of Th data. The other trend shows increasing Tm ice values (lower salinity) and increasing Th values. Goldstein (1988) saw similar trends (Figure 29) and interpreted the trend with constant Tm ice and varying Th data to be caused by stretching of the inclusions during overheating. The trend of increasing Th with increasing Tm ice was interpreted to represent exchange with higher salinity fluids. Goldstein (1988) suggested that the point of convergence might represent the original conditions of the fluid inclusions before reequilibration.

Applying the concepts of Goldstein (1988) to the two trends in the cross-plot of Th and Tm ice (Figure 28C), the horizontal trend is interpreted to have been caused by stretching of the inclusions with increased temperature. The other trend of decreasing Tm ice with increasing Th is interpreted to have been caused by fluid

Figure 28. Primary fluid-inclusion Th and Tm ice data, #3 calcite cement. (A) Th data, mean Th is 87.4°C. (B) Tm ice data, mean Tm ice is -20.4°C. (C) Crossplot of Th and Tm ice data. There are two trends in these data: A trend of inclusions with Tm ice near -22°C and variable Th, and a trend of higher Th and higher Tm ice data. The first trend is interpreted to have resulted from the stretching of the fluid inclusions to higher Th values by higher temperature fluids. The second trend is interpreted to have resulted from fluid-exchange with higher temperature, lower salinity fluids. Theodore Gore #1 Denny, 4058 feet.

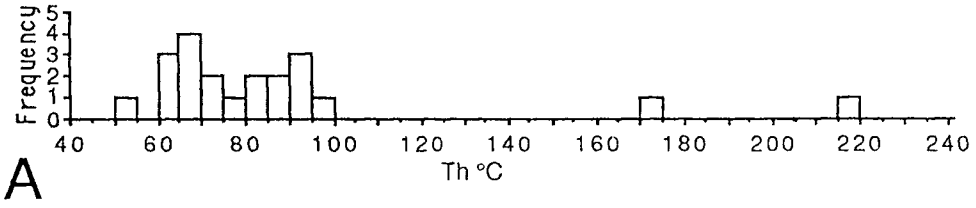

A

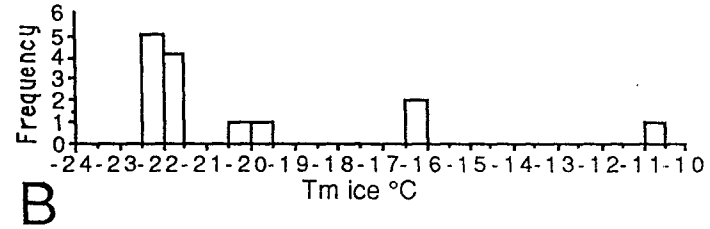

B

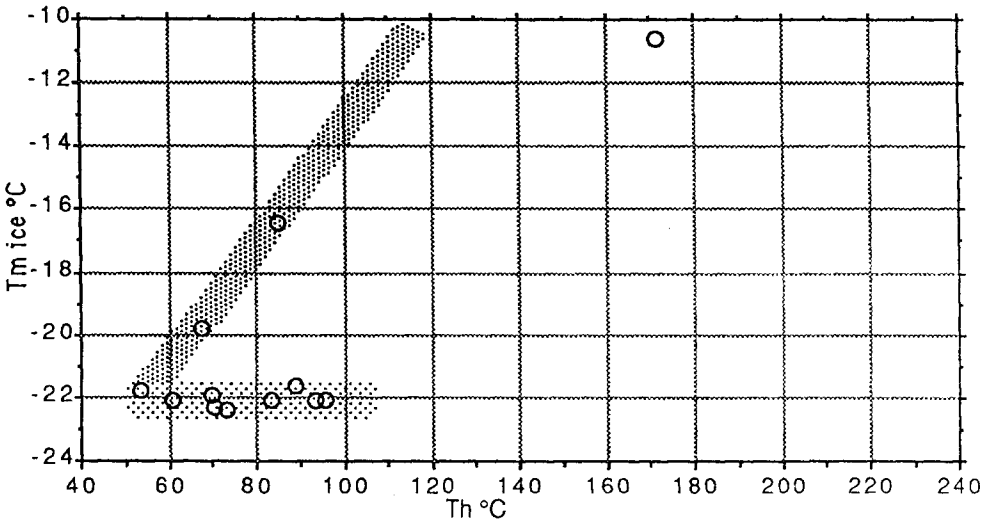

C

Fluid-exchange trend

Stretching trend

Figure 29. A crossplot of Th and Tm ice data in which trend A is interpreted to be a stretching trend and trend B is interpreted to be a fluid-exchange trend with higher temperature, higher salinity fluids. The point where the trends converge may represent the population of fluid inclusions before reequilibration. These trends are similar to those in the Theodore Gore #1 Denny data (Figure 29C). A major difference is that the Tm ice scales in the figures are reversed. In this figure, Trend B is toward higher Th, *lower* Tm ice. In Figure 29C, the fluid-exchange trend is toward higher Th, *higher* Tm ice (after Goldstein, 1988).

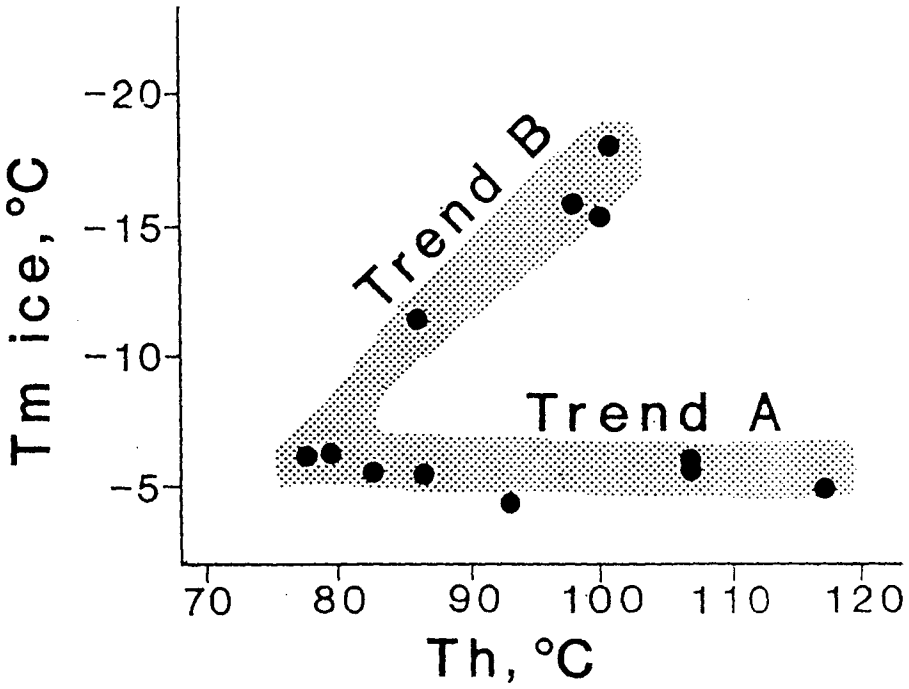
Tm ice, °C
-20
-15
-10
-5
Trend B
Trend A
70
80
90
100
110
120
Th, °C

exchange with pore fluids during decreasing salinity and increasing temperature. The convergence of these two trends is at a Th of 50°C and a Tm ice of -22°C, and this point is interpreted to represent the original conditions of the fluid inclusions before reequilibration. Due to the presence of methane gas in these inclusions, a pressure correction should not be applied (Hanor, 1980). This cement precipitated from brines with approximately 22 weight-percent Ca-Na chloride at approximately 50°C.

Murfin Drilling Co. #1 Elvin, 3665 Feet

The fluid inclusions from this sample are in cloudy growth zones confined to the #3 calcite cement. These primary fluid inclusions are all two-phase inclusions with relatively consistent vapor-to-liquid ratios. The size of the inclusions range from 5 to 17 micrometers in diameter. The pressure measurements from crushing are 7, 13, and 40 atmospheres (Appendix XII). All bubbles dissolved in kerosene, which suggests they are methane-rich gas. The Th data (Figure 30A) range from 45.5° to 81.1°C. The Tm ice data (Figure 30B) have a broad distribution ranging from -22.2° to -10.8°. The broad distribution of Th and Tm ice suggests that these inclusions have reequilibrated. The Te data range from -53° to -46°C with most data at -52°C indicating these fluids are Ca-Na chloride brines (Crawford, 1981). The melting temperatures of hydrohalite and ice (Tm ice) in five fluid inclusions from this population indicate the following salinities and Ca/ Ca + Na molar ratios: 22.5 weight-percent Ca-Na-Cl and 0.69 Ca/ Ca + Na; 21.6 weight-percent Ca-Na-Cl

Figure 30. Primary fluid-inclusion Th and Tm ice data, #3 calcite cement. (A) Th data, mean Th is 59.4°C. (B) Tm ice data, mean Tm ice is -17.0°. (C) Crossplot of Th and Tm ice data. A fluid-exchange trend is interpreted for these data. There is no data to support a stretching trend as noted in Figure 28C. Murfin Drilling #2 Elvin, 3665 feet.

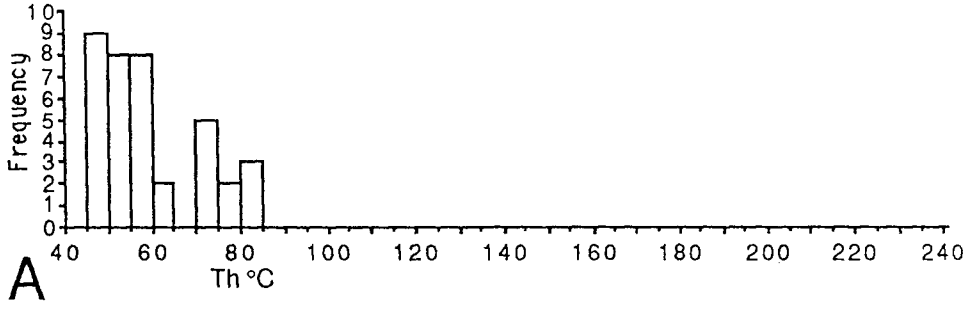
Frequency
0 1 2 3 4 5 6 7 8 9 10
40 60 80 100 120 140 160 180 200 220 240
Th °C

A

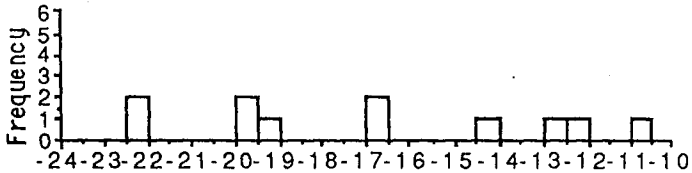
Frequency
0 1 2 3 4 5 6
-24 -23 -22 -21 -20 -19 -18 -17 -16 -15 -14 -13 -12 -11 -10
Tm ice °C

B

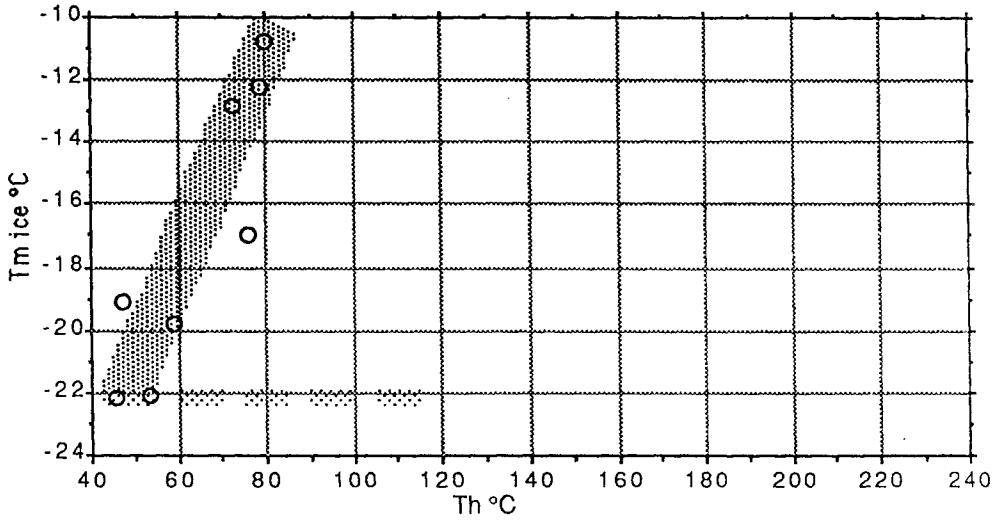
Tm ice °C
-10 -12 -14 -16 -18 -20 -22 -24
40 60 80 100 120 140 160 180 200 220 240
Th °C
Fluid-exchange trend
Missing Stretching trend

C

and 0.64 Ca/ Ca + Na; 22.5 weight-percent Ca-Na-Cl and 0.68 Ca/ Ca + Na; 20.8 weight-percent Ca-Na-Cl and 0.46 Ca/ Ca + Na; and 18.6 weight-percent Ca-Na-Cl and 0.46 Ca/ Ca + Na (Table 6).

A crossplot of the Th and Tm ice data (Figure 30C) shows increasing Th values associated with higher Tm ice values. This trend is similar to the fluid-exchange trend in the previous sample, but it has a steeper slope. This steeper slope may indicate that these two cores have had slightly different fluid temperature histories.

This crossplot (Figure 30C) lacks the stretching trend observed in the crossplot (Figure 28C) of the previous sample. Based on the interpretation of the crossplot in the previous sample (Figure 28C), the inclusions representative of the original conditions of precipitation in this sample (Figure 30C) are from the lower Th-lower Tm ice end of the fluid-exchange trend. These inclusions have a Th of approximately 45°C and a Tm ice of -22°C.

The temperature of cementation is interpreted to be approximately 45°C. Due to the presence of methane gas in these inclusions, a pressure correction should not be applied (Hanor, 1980). The cement precipitated from a brine of approximately 22 weight-percent Ca-Na chloride.

Cities Services #1-A Knudson, 4252 Feet

The fluid inclusions are from a cloudy growth zone within the #3 calcite cement. All the inclusions were two phase and had relatively consistent vapor-to-liquid ratios. The size of the

inclusions range from 6 to 20 micrometers. Pressure measurements from crushing are 20 and 23 atmospheres (Appendix XII). The bubbles dissolved in kerosene, which suggests they are methane-rich gas.

The Th data (Figure 31A) have a very broad distribution ranging from 92.3°C to 208.6°C. The Tm ice data (Figure 31B) also have a broad distribution ranging from -19.8° to -11.8°C. The broad distribution of Th and Tm ice suggests that these inclusions have reequilibrated. The Te data range from -52° to -47°C indicating that these are Ca-Na chloride brines (Crawford, 1981). The melting temperature of hydrohalite and ice (Tm ice) for an inclusion indicates a salinity of 17.8 weight-percent Ca-Na chloride and a 0.72 Ca/ Ca + Na molar ratio (Table 6).

The crossplot of Th and Tm ice data (Figure 31C) shows no trends. These data are within the wedge-shaped field interpreted for the trends in the two previous #3 calcite samples. The Tm ice data are similar to those of fluid inclusions in the previous samples interpreted to have resulted from fluid exchange. The Th data, however, are much higher.

Reappraisal of this sample shows twin lamellae to be common. Twin lamellae are a possible means for pore-fluid exchange with later brines (Goldstein, 1986). Fluid exchange of these inclusions would explain the Tm ice data (as related to the previous samples). Twin lamellae intersecting the inclusions might also cause necking down which might cause the high Th. Stretching due to methane gas under pressure might have also caused the high Th.

Figure 31. Primary fluid-inclusion Th and Tm ice data, #3 calcite cement, Cities Service #1-A Knudson, 4252 feet. (A) Th data, mean Th is 148.1°C. (B) Tm ice data, mean Tm ice is -14.0°C. (C) Crossplot of Th and Tm ice data. For comparison, the stretching and fluid-exchange trends from the Theodore Gore #1 Denny data (Figure 28C) are superimposed on this crossplot.

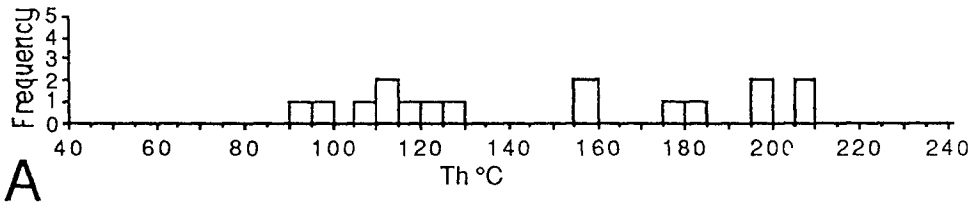

A

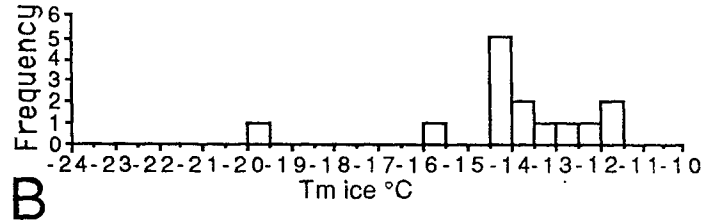

B

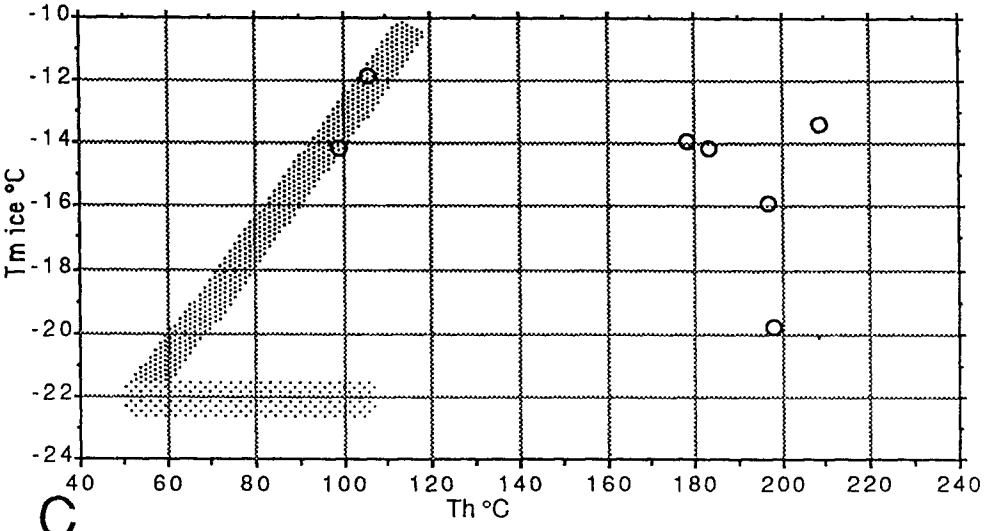

C

Both trends are from the Theodore Gore #1 Denny fluid inclusion data, #3 calcite cement (Figure 28C).

These data suggest that these inclusions have reequilibrated. The original conditions of precipitation cannot be interpreted from these data.

Summary of #3 Fluid Inclusion Data

The data from the inclusions in the #3 calcite cement interpreted to represent the original conditions indicate calcite precipitation from approximately 22 weight-percent Ca-Na chloride brines at approximately 45°-50°C, and a later history of increasing temperature and decreasing salinity.

Nonzoned Dolomite Cement

Cities Service Co. #1 Bourquin, 3981, 3983, and 4015.8 Feet

These inclusions occur in cloudy growth zones outside the luminescent and fluorescent bands of the dolomite. Petrographically, the dolomite cement outside the luminescent and fluorescent bands is interpreted to post-date all calcite cement. All fluid inclusions were two-phase and had relatively consistent vapor-to-liquid ratios. The size of these inclusions ranges from 3 to 12 micrometers in diameter. Pressure measurements from crushing are 5, 8, 8, 8, 20, 27, 32, 70, 120, 190, and 260 atmospheres (Appendix XII). The bubbles dissolved in kerosene, which suggests they are methane-rich gas. The Th data (Figure 32A) have a broad distribution ranging from 75.1° to 171.8°C. The Tm ice data (Figure 32B) also have a broad distribution ranging from -22.8° to -15.8°C. The broad distribution of the Th and Tm ice data suggests that these inclusions have reequilibrated. The Te data range from -52° to

Figure 32. Primary fluid-inclusion Th and Tm ice data from the same growth zone in post-calcite dolomite cement, Cities Service #1-A Bourquin, 3981, 3983, and 4015.8 feet. (A) Th data, mean Th is 107.7°C. (B) Tm ice data, mean Tm ice is -20.2°C. (C) Crossplot of Th and Tm ice data. For comparison, the stretching and fluid-exchange trends from the Theodore Gore #1 Denny data (Figure 28C) are superimposed on this crossplot.

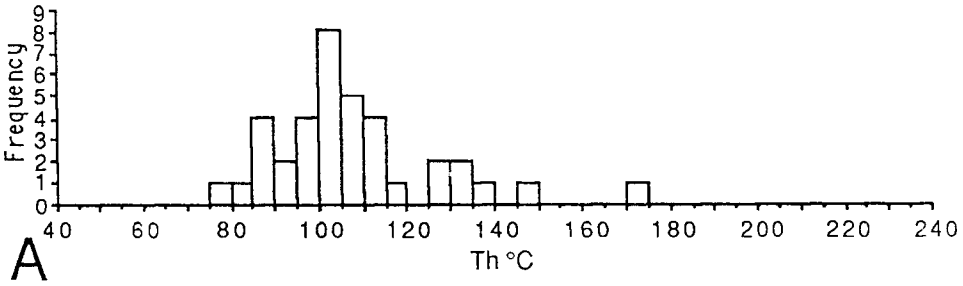

A

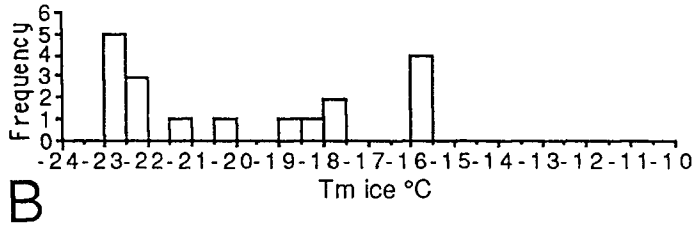

B

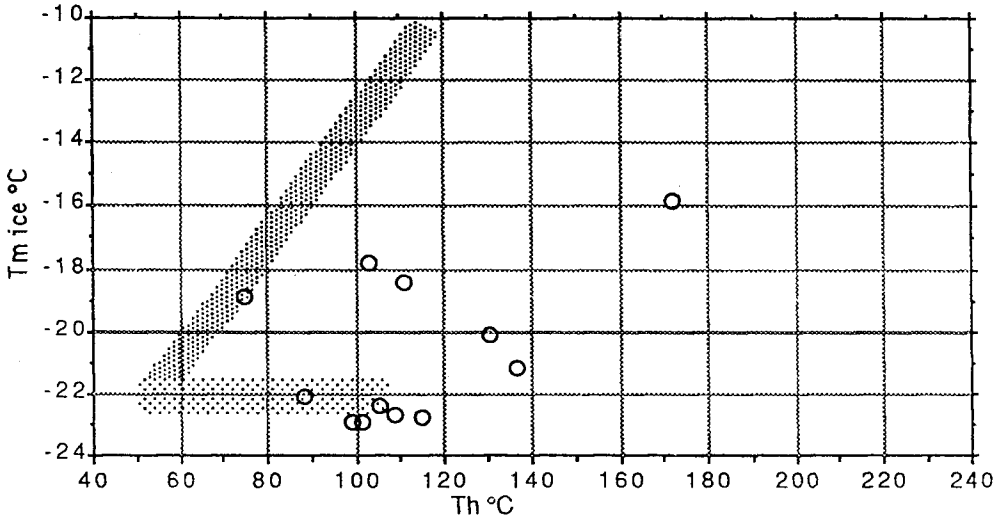

C

Fluid-exchange trend

Stretching trend

Both trends are from the Theodore Gore #1 Denny fluid inclusion data, #3 calcite cement (Figure 28C).

-49°C indicating that these fluids are Ca-Na chloride brines (Crawford, 1981). The melting temperature of hydrohalite and Tm ice in two inclusions indicate Ca/ Ca + Na molar ratios of 0.68 for both inclusions and salinities of 21.1 and 22.3 weight-percent Ca-Na chloride (Table 6).

The crossplot of Th and Tm ice data (Figure 32C) shows no clear trends, but when the trends from the Theodore Gore #1 Denny fluid-inclusion data (Figure 28C) are superimposed on the plot, all data lie within the wedge-shaped field of the trends and a large proportion of the data lies along the stretching trend. The inclusions along this stretching trend have basically the same Tm ice (salinity) and Ca/ Ca + Na molar ratio (Table 6) as the fluid from which calcite precipitated. A major difference is that these inclusions in dolomite have higher Th (88°-115°C). If the #3 calcite cement fluid-inclusion data (Figures 28 and 30) records the fluid and temperature history experienced by these strata, the temperature of fluids with Tm ice near -22°C should be approximately 45°-50°C. The fluid-exchange trends in the #3 calcite data reveal that the later, higher temperature fluids had higher Tm ice (lower salinities). Therefore, the dolomite probably precipitated from earlier fluids with Tm ice near -22°C. Because dolomite cement postdates calcite cement, the temperature of dolomite precipitation was not less than 45°C. The maximum temperature of dolomite precipitation was probably below the minimum temperature of later, lower salinity fluids (approximately 70°C, Figure 28C and 30C)

indicated by the fluid exchange trend. Therefore, the dolomite precipitated from brines with approximately 22 weight-percent Ca-Na chloride at approximately 45°-70°C. Due to the presence of methane gas in these inclusions, a pressure correction should not be applied (Hanor, 1980).

The cause of reequilibration of these inclusions in the dolomite may be related to the high pressure methane gas. Three of the measurements of pressure exceed 100 atmospheres.

Baroque Dolomite Cement

Murfin Drilling Co. #1 Prentice, 4250.3 Feet

The fluid inclusions are in cloudy growth zones in baroque dolomite cement. The primary origin is not clear because the edge of the cloudy zones is not sharp. All fluid inclusions in this population were two phase with relatively consistent vapor-to-liquid ratios. The size ranged from 5 to 14 micrometers in diameter. Pressure measurements from crushing were not made on this sample. The bubbles, however, did expand during crushing and dissolved in the kerosene medium. This suggests that the bubbles are methane-rich gas under pressure.

The Th data (Figure 33A) show a broad distribution ranging from 66.2° to 125.0°C, which suggests that these inclusions have reequilibrated. The Tm ice data (Figure 33B) range from -22.9° to -20.5°C. The Te data range from -52° to -48°C indicating that these fluids are Ca-Na chloride (Crawford, 1981). The crossplot of Th and Tm ice data (Figure 33C) shows no clear trends, but these data fit

Figure 33. Primary fluid-inclusion Th and Tm ice data, baroque dolomite cement, Murfin Drilling #1 Prentice, 4250.3 feet. (A) Th data, mean Th is 92.8°C. (B) Tm ice data, mean Tm ice is -22.2°C. (C) Crossplot of Th and Tm ice data. For comparison, the fluid-exchange and stretching trends from the Theodore Gore #1 Denny data (Figure 28C) are superimposed on this crossplot.

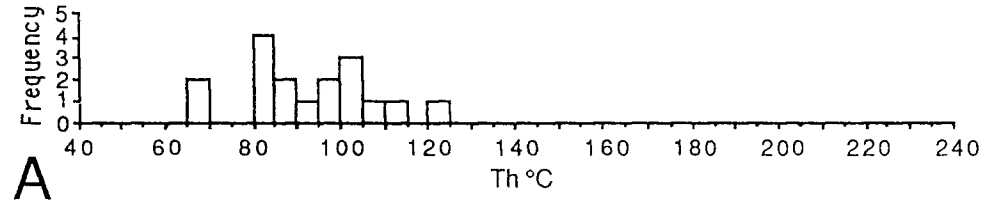

A

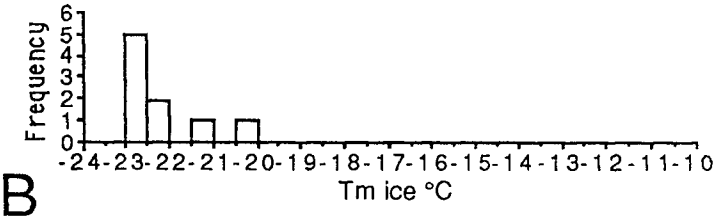

B

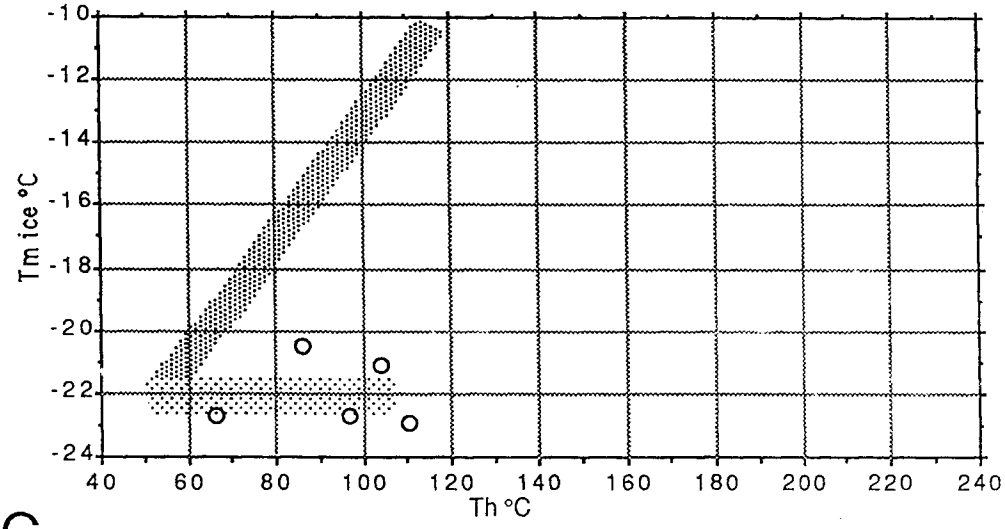

C

Both trends are from the Theodore Gore #1 Denny fluid inclusion data, #3 calcite cement (Figure 28C).

within the wedge-shaped field of the trends from the Theodore Gore #1 Denny data and three points lie along the #1 Denny stretching trend. All Tm ice data from this sample are close to the Tm ice of fluids from which the calcite precipitated. If the #3 calcite cement fluid inclusion data records the fluid and temperature history of these strata, the temperature of dolomite precipitation was approximately 45°-70°C. The dolomite probably precipitated from brines with approximately 22 weight-percent Ca-Na chloride. Due to the presence of methane gas in these inclusions, a pressure correction should not be applied (Hanor, 1980).

Petroleum-Filled Fluid Inclusion Data

The Th data for secondary petroleum-filled fluid inclusions, which postdate all calcite and dolomite cement, are shown in Figure 34. The mean Th for these inclusions is 91.0°. Excluding the Th that exceed 160°C, the mean Th is 83.0°C.

The pressure correction for these petroleum-filled fluid inclusions is unknown without the pressure-volume-temperature properties of these oils. Commonly, petroleum-filled fluid inclusions have higher pressure corrections than aqueous inclusions because petroleum generally has isochores with a lower slope than isochores for water. With lowering pressure, petroleum intercepts the liquid-vapor surface at a lower temperature than water (Burruss, 1981).

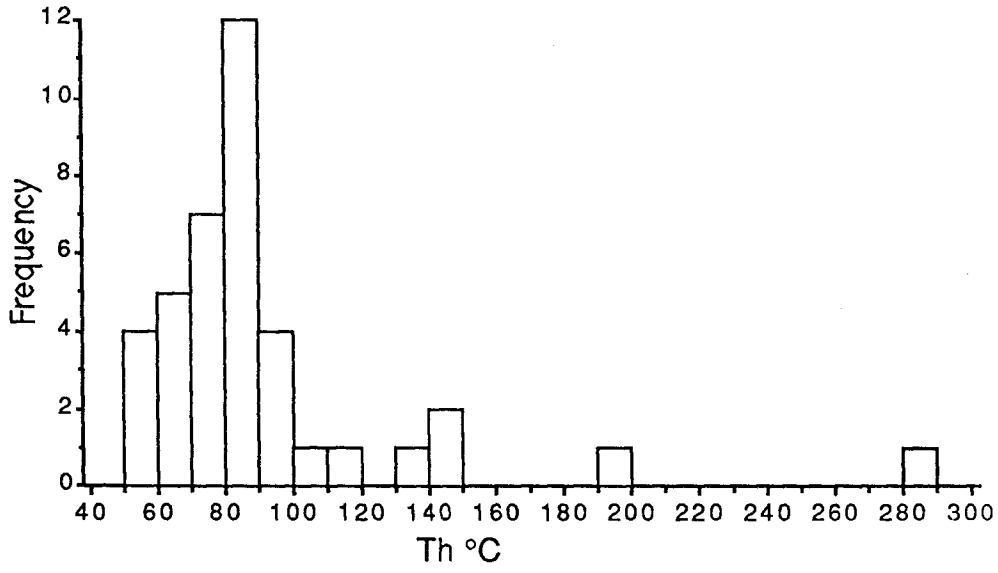

Figure 34. Secondary petroleum-filled fluid-inclusion data. The mean Th is 91.0°C; excluding the Th > 180°, the mean Th is 83.0°C; excluding the Th > 110°, the mean Th is 77.0°C.

Maximum Temperature

Petroleum migration postdates all calcite and dolomite cement and may have occurred near the maximum temperature of these strata. Without the pressure correction, the adjusted mean Th of 83.0° is a minimum estimate of maximum temperature of these strata.

For all aqueous inclusions, the mean Th is 89.7°C (Figure 35). For all aqueous inclusions in dolomite, the mean Th is 103.0°C (Figure 35), and for all aqueous inclusions in calcite, the mean Th is 82.2°C (Figure 35).

In the Smackover Formation, it has been observed that the mean Th of aqueous inclusions in calcite approximates the bottom-hole temperature of these strata (Wagner and Matthews, 1982). R.H. Goldstein (personal communication, 1988) suggested that the mean Th of aqueous inclusions in calcite plus the pressure correction or a fudge factor should approximate the maximum temperature. The mean Th of aqueous inclusions in calcite is 82.2°C. The pressure correction depends on the thickness of overlying strata during which these inclusions were formed or reequilibrated. The current depth of these strata ranges from 0.9 to 1.4 km. Based on stratigraphic reconstruction, additional overburden removed by post-Cretaceous overburden is approximately 0.6 km (Merriam, 1963). The estimated pressure correction for an overburden of 1.5 to 2.0 km overburden is approximately 20°-30°C (Potter, 1977). The sum of the mean Th aqueous inclusions in calcite (82.2°C) and the pressure correction results in a temperature of approximately 100 - 110°C. Based on the

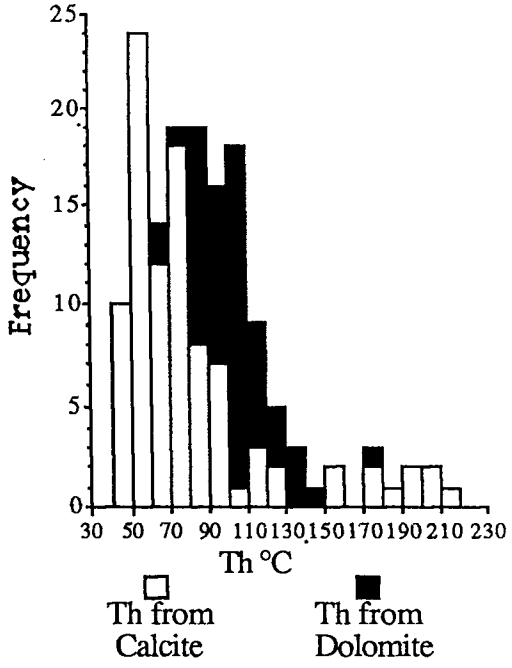

Figure 35. All Th data from aqueous two-phase inclusions in calcite and dolomite. The mean Th for all aqueous inclusions is 89.7°C. The mean Th for all aqueous inclusions in dolomite is 103.0°C, and for all aqueous inclusions in calcite, the mean Th is 82.2°C.

analogue of the Smackover Formation, 100 - 110°C may have been the maximum temperature of these strata.

Possible problems with this method are that factors other than temperature, such as high pressure methane gas, may have caused some of the high Th values. In the Smackover Formation, methane gas commonly is present in the inclusions (R.H. Goldstein, personal communication, 1988). A maximum temperature of 100 - 110°C is compatible with the non-pressure-corrected mean Th of 83.0°C for petroleum-filled fluid inclusions.

For the estimated maximum temperature of 100 - 110°C and the estimated maximum overburden of 1.5 to 2.0 km, assuming a mean surface temperature of 30°C results in an the estimated paleogeothermal gradient 35° to 53°C/km during maximum burial.

Current Temperatures

Stavnes (1982) calculated the geothermal gradient in the Kansas side of the area of study to be approximately 25°C/km based on bottom-hole temperatures from oil wells. Assuming a near-surface temperature of 56°F (13.3°C) at 50 feet (15 m) depth (an assumption used by Stavnes, 1982) and a depth range of 3000 to 4500 feet (0.9 to 1.4 km) for the Lansing and Kansas City groups, the present temperature of this stratigraphic interval should range from 35° to 50°C. Bottom-hole temperatures from the 4 of 5 wells from which most of the aqueous fluid inclusion Th data were measured (Table 7) are in this range. The 60°C temperature in the #1-A Bourquin well is from 800 feet (240 m) below the base of the Kansas City Group; at

	Depth to the base of the Kansas City Group, in feet	Bottom-Hole Temperature, °C @ Total Depth (in feet)
Theodore Gore Co. #1 Denny	4292 ft.	46°C @ 4500 ft.
Cities Service Co. #1-A Bourquin	4176 ft.	60°C @ 4963 ft.
Cities Service Co. #1-A Knudson	4324 ft.	48°C @ 4870 ft.
Murfin Drlg. Co. #2 Elvin	3744 ft.	39°C @ 4009 ft.
Murfin Drlg. Co. #1 Prentice	4460 ft.	46°C @ 4500 ft.

Table 7. Bottom-hole temperatures of the wells from which high Th values were measured in aqueous fluid inclusions.

the base of the Kansas City Group, the temperature is projected to be approximately 52°C.

This temperature range is less than the temperature of petroleum migration (at least 83°C), and less than the interpreted maximum temperature of these strata (100°-110°C).

Present-Day Brines

The present-day brines of the Lansing and Kansas City groups have been sampled and analyzed by Stell (1988) and other data are available in a Kansas Geological Survey data base compiled by Fife (1973). The salinities of 21 oil-field waters in the Lansing and Kansas City groups from the area of study ranged from 3.30 to 13.85 weight-percent total-dissolved solids. The Ca / Ca + Na molar ratio from 10 samples in the Lansing and Kansas City groups in this area were all less than 0.10. One sample from the underlying Marmaton Group in northeastern Cheyenne County had a Ca/ Ca + Na molar ratio of 0.30 (Fife, 1973). A crossplot of the salinities and Ca/Ca + Na molar ratios for the modern brines and fluid-inclusion data (Figure 36) illustrates that the modern-day brines are less saline and contain less calcium than the brines from which calcite and dolomite precipitated.

INTERPRETATION OF PETROGRAPHIC AND FLUID INCLUSION DATA

Calcite Cement

The major calcite cements are the #1, #2, and #3 calcite cements; the #4 and #5 calcite cements are minor and are not further discussed.

Figure 36. Crossplot of salinity and Ca/Ca + Na molar ratios for modern-day brine and fluid-inclusion data. The modern-day brine data (Stell, 1988; Fife,1973) are from the Lansing and Kansas City groups from the Kansas part of the area of study. The salinity for the modern-day brine data is in weight-percent total dissolved solids. The fluid inclusion data are from the 12 inclusions in which the temperature of final melting of hydrohalite was measured. This melting temperature and the Tm ice was plotted on the H_2O-$CaCl_2$-NaCl phase diagram (Figure 25) to determine the Ca/Ca + Na molar ratio and the salinity in weight-percent Ca-Na chloride. Due to the possible presence of other phases in these inclusions that are not accounted for on the phase diagram, these interpretations are in question.

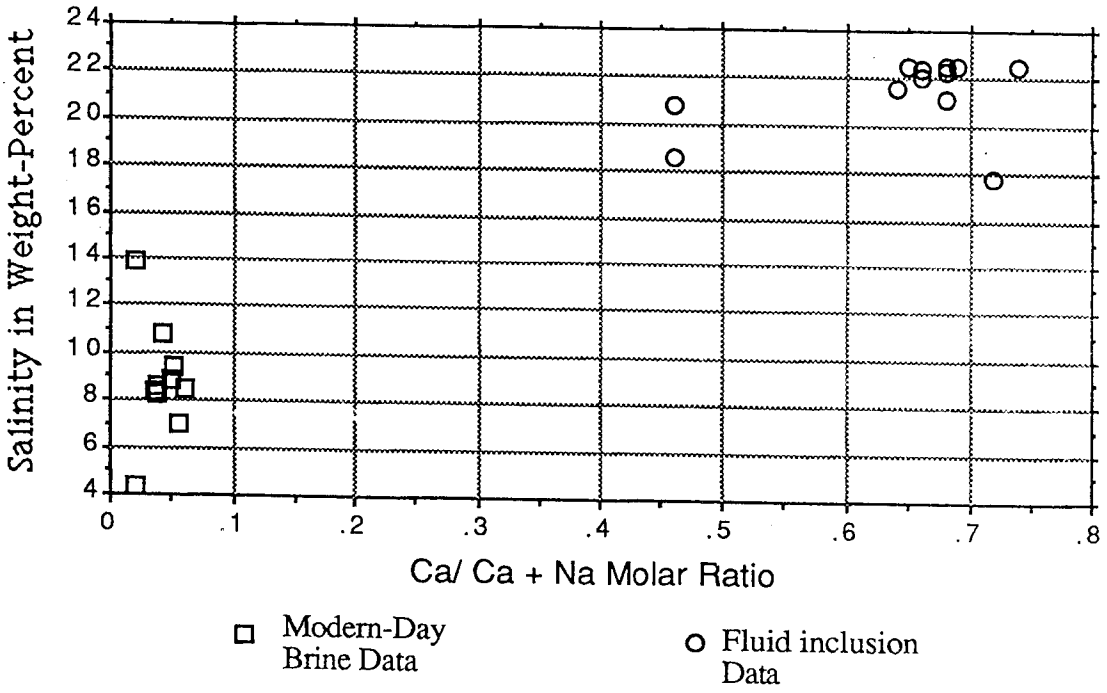
Salinity in Weight-Percent
24
22
20
18
16
14
12
10
8
6
4
0
.1
.2
.3
.4
.5
.6
.7
.8
Ca/ Ca + Na Molar Ratio
Modern-Day Brine Data
Fluid inclusion Data

The #1 calcite cement is a nonluminescent and nonferroan calcite which indicates precipitation from oxidized pore fluids. It reduces "precementation porosity" by an average of 11.6 percent and generally postdates compaction resulting from at least 30 to 100 meters of burial. It occurs throughout the Lansing and Kansas City groups (Figure 22) indicating the #1 calcite cement precipitated after deposition of the entire Lansing and Kansas City groups from oxidized pore fluids. The fluid-inclusion data indicate precipitation from a Ca-Na chloride brine with salinity of approximately 21 to 23 weight-percent Ca-Na-Cl at temperatures less than about 45°C.

The #2 calcite cement is nonferroan and its luminescence ranges from bright to moderately dull, which suggests that it precipitated from poorly oxidized waters. It reduces "precementation porosity" by an average of 36.3 percent. It postdates compaction, which suggests a postburial origin, and it occurs throughout the Lansing and Kansas City groups indicating the #2 calcite cement precipitated after the deposition of the entire Lansing and Kansas City groups from poorly oxidized pore fluids. No inclusions from this cement were analyzed.

The #3 calcite is ferroan and has very dull luminescence, which indicates precipitation from reduced pore fluids. It reduces "precementation porosity" by an average of 13.5 percent. It postdates compaction, which indicates a postburial origin, and it occurs throughout the Lansing and Kansas City groups indicating the #3 calcite cement precipitated after the deposition of the entire

Lansing and Kansas City groups from reduced pore fluids. The fluid inclusion data indicate precipitation from a Ca-Na chloride brine with a salinity of approximately 21 to 23 weight-percent Ca-Na-Cl at temperatures ranging from approximately 45° to 50°C.

Although there are no fluid-inclusion data from the #2 calcite cement, the similarity of the fluid-inclusion data from the #1 and #3 calcite cements suggests that the #2 calcite cement precipitated from the same brine. Therefore, the #1, #2, and #3 calcites precipitated from a Ca-Na chloride brine with a salinity of approximately 21 to 23 weight-percent Ca-Na-Cl at temperatures ranging from less than 45°C up to 50°C. These brines underwent progressive reduction during the precipitation of the #1, #2, and #3 cements.

Dolomite Cement

Most dolomite cement postdates calcite cement, and it occurs throughout the Lansing and Kansas City groups, which suggests that it postdates the deposition of the entire Lansing and Kansas City groups. Dolomite cement reduces "precementation porosity" by an average of 7.3 percent. Fluid-inclusion data indicate precipitation from Ca-Na chloride brines with a salinity of approximately 21 to 23 weight-percent Ca-Na chloride at temperatures ranging from approximately 45° to 70°C.

Post-Cementation Fluids

Reequilibrated fluid inclusions suggest that the later fluids had lower salinity and were higher temperature. The maximum

temperature of these fluids was approximately 100° to 110°C.

The adjusted mean Th of petroleum-filled fluid inclusions is 83.0°C. These petroleum-filled fluid inclusions probably were not reequilibrated, and this adjusted mean Th of 83° is the minimum temperature to which these strata were heated.

The modern-day brines from these strata have lower salinity, much lower Ca/Ca + Na molar ratios (Figure 36), and generally lower temperatures than the interpreted fluids of precipitation and reequilibration.

DIAGENETIC MODEL

To explain calcite and dolomite cementation after significant burial from Ca-Na chloride brines of approximately 21 to 23 weight-percent Ca-Na-Cl, at temperatures of less than 45° to 70°C, one must find a geologic explanation in which such brines could exist at significant depth at relatively low temperatures.

Based on the estimated maximum temperature and overburden, the paleogeothermal gradient was estimated to be approximately 35°-53°C. The #1 calcite cement (<45°C) would have precipitated with less than 280 to 430 m of overburden. The #3 calcite cement (45°-50°C) would have precipitated with 280 to 570 m of overburden. The dolomite cement (45°-70°) would have precipitated with 280 to 1140 m of overburden. This depth range would suggest cement precipitation during the deposition of the Permian System (Figure 37).

A typical brine from which the calcite and dolomite precipitated, based on the fluid inclusion microthermometry, would

Figure 37. The generalized Upper Pennsylvanian and Lower Permian stratigraphy of northwestern Kansas and southwestern Nebraska. Data from Holdoway (1978), Mudge (1967), and Merriam (1963).

GENERALIZED UPPER PENNSYLVANIAN-LOWER PERMIAN STRATIGRAPHY,
NORTHWESTERN KANSAS-SOUTHWESTERN NEBRASKA

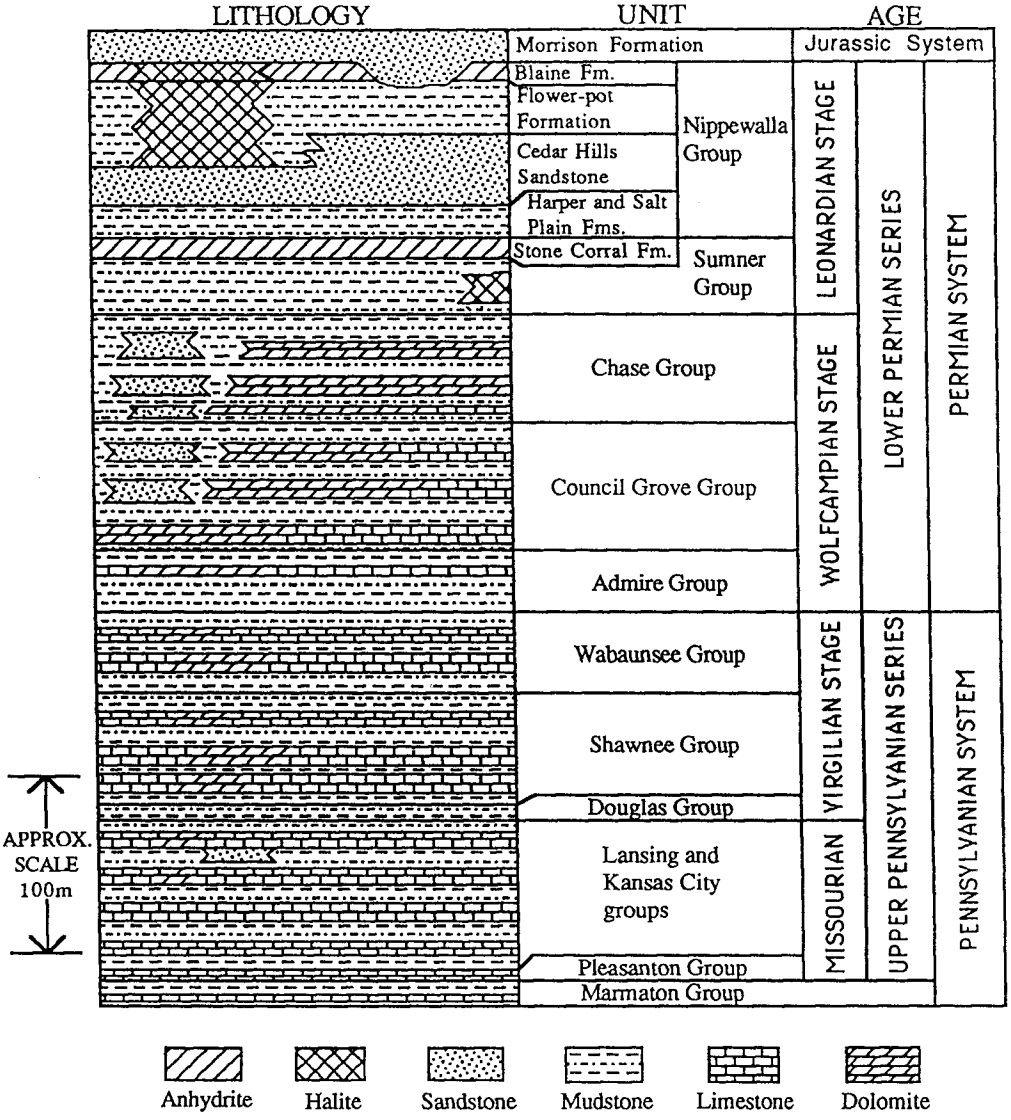

have a salinity of 22 weight-percent (282,000 mg/l) composed of 65 percent calcium chloride and 35 percent sodium chloride (0.65 Ca/Ca + Na molar ratio, Figure 36). The high salinity of these fluids suggests an evaporitic source. The Permian System in this area includes anhydrite and halite (Figure 37). The Stone Corral Formation (Figure 37) is composed of anhydrite and ranges in thickness from 7 to 12 m throughout the area of study (Figure IX-A, Appendix IX). The Blaine Formation of the Nippewalla Group (Figure 37) is commonly composed of anhydrite and is present in most of the area of study. For the southwestern part of the area of study, $\geq$25 percent of the Stone Corral Formation and Nippewalla Group interval is composed of anhydrite or halite (Figure 23). In this area, there is halite in the Flower-pot and Blaine formations (Figure 37). The stratigraphic interval between the top of the Lansing Group and the base of the Stone Corral Formation ranges from 300 to 500 m. The Nippewalla Group is 400 to 600 m above the top of the Lansing Group. The calculated overburden during precipitation of the #1 and #3 calcite cements and dolomite cements is within this depth range. Based on these comparable depths of overburden and the high salinity of the fluids, the brines causing precipitation of the calcite and dolomite cements could have been generated during deposition of Lower Permian evaporites from the Stone Corral Formation and the Nippewalla Group.

These brines were generated during the deposition of anhydrite and halite in evaporitic basins. The density of modern brines that

precipitate anhydrite and halite is approximately 1.2-1.3 grams/cm^3 (Zherebtsova and Volkova, 1966). Brines of such density might be capable of gravity-driven reflux to several kilometers of depth (Spencer, 1987). The brines that caused the precipitation of calcite and dolomite cements could have easily refluxed down 300 - 600 m to the Lansing and Kansas City groups.

A key factor that would control the composition of these brines is whether they were marine or nonmarine. The widespread distribution of the anhydrite beds in the Stone Corral and Blaine formations suggests they resulted from a marine transgression and are marine. Holdoway (1978) found possible evidence of a nonmarine origin for the halite of the Nippewalla Group, but ultimately concluded that the source of evaporitic minerals was the evaporation of marine-derived waters.

Because the source of the ions is interpreted to be seawater, the composition of brines generated from the deposition of these evaporites should be similar to the fluids from which modern marine evaporites precipitate. The composition of brines produced by evaporation of water from the Black Sea (Zherebtsova and Volkova, 1966) are:

Beginning of gypsum precipitation: 59,700 mg/l Na, 1,040 mg/l Ca, 7,590 mg/l Mg, 2,220 mg/l K, and 107,800 mg/l Cl.

Beginning of halite precipitation: 94,300 mg/l Na, 307 mg/l Ca, 19,600 mg/l Mg, 5,600 mg/l K, and 183,300 mg/l Cl.

During halite precipitation: 55,200 mg/l Na, 0 mg/l Ca, 50,500 mg/l Mg, 15,800 mg/l K, and 187,900 mg/l Cl.

These brines are rich in Na, Mg, and Cl. The brines from which the calcite and dolomite precipitated are rich in Ca. Some modern nonmarine saline lake systems are $CaCl_2$-rich (Hardie, 1984), but as the evaporites upsection have been interpreted as marine, the high Ca content of the brines of calcite and dolomite precipitation must be explained by other mechanisms. Listed below are several processes by which the calcium content of brines could be enhanced:

1. Reaction of potassium with low-potassium clay minerals to produce potassium-rich aluminosilicates that release H^+ which dissolves calcite and releases Ca^{2+} (Carpenter, 1978).

$2K^+ + CaCO_3 + K_9Al_3Si_3O_{10}(OH)_2 + 6SiO_2 = Ca^{2+} + 3KAlSi_3O_8 + CO_2$

2. Alteration of a calcium plagioclase to albite (Carpenter, 1978), $Na_{.80}Ca_{.20}Al_{1.20}Si_{2.80}O_8 + .2Na^- + .4SiO_2 + .1H_2O + 2H^+ = NaAlSi_3O_8 + .1Al_2Si_2O_5(OH_4) + .2Ca^{2+}$

3. Conversion of gypsum or anhydrite to polyhalite (Hite, 1983),

$CaSO_4 \cdot 2H_2O + K^+ + Mg^{2+} = Ca_2K_2Mg(SO_4)_4 \cdot 2H_2O + Ca^{2+}$

4. Substitution of Na^+ for Ca^{2+} in exchange sites of smectites could enhance the Ca^{2+} content of brines (Hite, 1983).

5. Dolomitization of limestone (Carpenter, 1978; Hite, 1983),

$CaCO_3 + Mg^{2+} = CaMg(CO_3)_2 + Ca^{2+}$

Carpenter (1978) and Hite (1983) stated that dolomitization is the most important mechanism for enhancing the Ca^{2+} content of

brines. Spencer (1987) interpreted albitization of feldspars to the most important mechanism for enhancing the Ca^2 content of calcium chloride brines in Devonian strata of western Canada.

The high Ca content of the brines from which calcite and dolomite precipitated may be explained by dolomitization, albitization of plagioclase in the sandstones, and the exchange of sodium for calcium in the smectite clays of the mudstones as these brines refluxed down through the Wolfcampian and Virgilian strata (Figure 37). The Wolfcampian and Virgilian strata in this area have been extensively dolomitized (Mudge, 1967), and the Wolfcampian strata are sand and shale rich (Rascoe and Baars, 1971; Mudge, 1967). This dolomitization may have resulted from the reflux of brines originating from the deposition of overlying evaporites. The sand and shale may have also been altered to release Ca.

If calcite and dolomite cement in units underlying the evaporites was precipitated from brines refluxing down from the deposition of the evaporites, one might predict that there would be a positive correlation between the abundance of evaporites upsection and the abundance of calcite cement downsection. The maps showing the mean abundance of the calcite and dolomite cements (Figure 23) are divided across the areas with <25 percent and $\geq$25 percent evaporites in the overlying Stone Corral Formation and Nippewalla Group interval. Table 5 tabulates the mean abundance of these cements for the area with <25 percent and $\geq$25 percent evaporites. There is higher calcite cement in the thin sections from areas with

≥25 percent evaporites (78.2 percent of "precementation porosity", Table 5) than in the thin sections from areas with <25 percent evaporites (61.9 percent of "precementation porosity", Table 5). For the individual calcite cements, all but the #2 calcite, are more common in the area with ≥25 percent evaporites. These data suggest that with increased evaporites in the overlying Lower Permian strata, there is increased calcite cementation in the underlying Lansing and Kansas City groups. This correlation supports the hypothesis that the brines from which calcite and dolomite precipitated originated from the deposition of the Lower Permian evaporites (Figure 38).

CONCLUSIONS

1. The carbonate lithologies most likely to be porous include the non-argillaceous carbonate wackestones, packstones, grainstones, and dolostones. Argillaceous carbonates and carbonates with clayey infill are generally nonporous.
2. Although some molds and vugs probably formed during subaerial exposure, apparently, other molds and vugs formed after significant burial.
3. Calcite cement is the most common cement in these strata. The calcite cement precipitated from calcium and sodium chloride brines with a salinity of approximately 21 to 23 weight-percent Ca-Na chloride. The initial calcite cement (#1 calcite cement) precipitated at less than 45°C. A later

Figure 38. Integrated diagenetic model for Upper Pennsylvanian and Lower Permian strata in northwestern Kansas and southwestern Nebraska. The model proposes that Na-Mg-Cl brines from the precipitation of Lower Permian evaporites sink into the Lower Permian carbonates, sandstones, and silty shales (Figure 37). Dolomitization of the carbonates exchanges Ca for Mg. Albitization of plagioclase grains and the exchange of Na for Ca in smectite may enhance the Ca and decrease the Na. Dolomitization is probably the primary means for enhancing Ca. With the enhancement of the calcium content of the brines, the brines continue to sink and precipitate calcite and minor dolomite cement in the Lansing and Kansas City groups.

The evaporites in the Stone Corral Formation and the Nippewalla Group range from 300 to 600 meters above the Lansing and Kansas City groups. The #1 calcite is interpreted to have precipitated at less than 45°C. The #3 calcite is interpreted to have precipitated at approximately 45° to 50°C. The model assumes a surface temperature of 30°C, and a geothermal gradient of 38°C. This geothermal gradient is within the range of the geothermal gradient estimated for a maximum temperature of 100°-110°C with a maximum burial of 1.5 to 2.0 km.

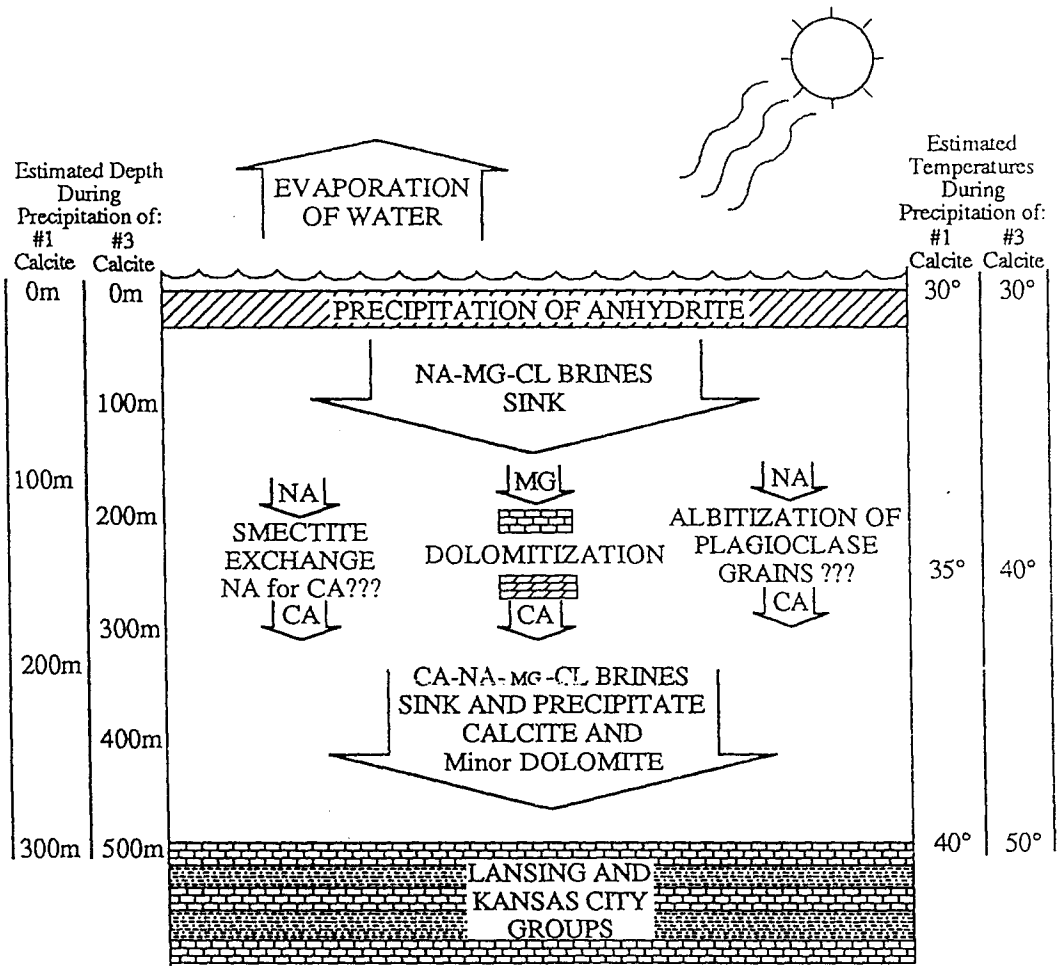
Estimated Depth During Precipitation of:
#1 Calcite
#3 Calcite
EVAPORATION OF WATER
Estimated Temperatures During Precipitation of:
#1 Calcite
#3 Calcite
0m
0m
PRECIPITATION OF ANHYDRITE
30°
30°
NA-MG-CL BRINES SINK
100m
100m
NA
SMECTITE EXCHANGE NA for CA???
CA
MG
DOLOMITIZATION
CA
NA
ALBITIZATION OF PLAGIOCLASE GRAINS ???
CA
35°
40°
200m
300m
CA-NA-MG-CL BRINES SINK AND PRECIPITATE CALCITE AND Minor DOLOMITE
300m
500m
LANSING AND KANSAS CITY GROUPS
40°
50°

generation of calcite cement (#3 calcite cement) precipitated at approximately 45° to 50°C.

4. The dolomite precipitated from calcium and sodium chloride brines with a salinity of approximately 21 to 23 weight-percent Ca-Na chloride. The temperature of dolomite precipitation is interpreted to be approximately 45° to 70°C.
5. The highly saline brines from which calcite and dolomite precipitated originated as brines generated during precipitation of Lower Permian anhydrite and possibly halite in the overlying Stone Corral Formation and Nippewalla Group. The dense brines refluxed down through the section and the calcium content was enhanced by dolomitization, possible albitization, and possible exchange of Na for Ca in smectites. After these Ca-enriching reactions, the brines precipitated calcite and dolomite cement in the Lansing and Kansas City groups.
6. Later fluids of higher temperature and lower salinity were present in these strata.
7. The maximum temperature in these strata was approximately 100°-110°C.

REFERENCES CITED

Bodnar, R.J., and P.M. Bethke, 1984, Systematics of stretching of fluid inclusions I: Fluorite and sphalerite at 1 atmosphere confining pressure: Economic Geology, v. 79, p. 141-161.

Burruss, R.C., 1981, Hydrocarbon fluid inclusions in studies of sedimentary diagenesis, *in* L.S. Hollister and M.L. Crawford, eds., Fluid inclusions: Applications to petrology: Mineralogical Association of Canada Short Course Handbook 6, p. 138-156.

Carpenter, A.B., 1978, Origin and chemical evolution of brines in sedimentary basins: Oklahoma Geological Survey Circular, v. 79, p. 60-77,

Choquette, P.W., and Pray, L.C., 1970, Geological nomenclature and classification of porosity in sedimentary carbonates: AAPG Bulletin, v. 54, p. 207-250.

Crawford, M.L., 1981, Phase equilibria in aqueous fluid inclusions, *in* L.S. Hollister and M.L. Crawford, eds., Fluid inclusions: Applications to petrology: Mineralogical Association of Canada Short Course Handbook 6, p. 75-100.

Dickson, J.A.D., 1965, A modified staining technique for carbonates in thin section : Nature, v. 205, p. 587.

Dubois, M.K., 1979, Factors controlling the development and distribution of porosity in the Lansing-Kansas City "E" zone, Hitchcock County, Nebraska: University of Kansas, M.S. thesis, 100 p.

Dubois, M.K., 1985, Application of cores in development of an exploration strategy for the Lansing-Kansas City "E" Zone, Hitchcock County, Nebraska;in W.L. Watney,et al., compilers, Core studies in Kansas, Sedimentology and diagenesis of economically important rock strata in Kansas, Subsurface geology series 6: Kansas Geological Survey, p.120-132.

Dunham, R.J., 1962, Classification of carbonate rocks according to depositional texture, in W.E. Ham, ed., Classification of carbonate rocks: AAPG Memoir 1, p. 108-121.

Ebanks, W.J., Jr.,and Watney, W.L., Geology of Upper Pennsylvanian carbonate oil reservoirs, Happy and Seberger Fields, Northwestern Kansas, in P.O. Roehl and P.W. Choquette (eds.), Carbonate Petroleum Reservoirs: Springer-Verlag (New York), p. 237-250.

Fife, J.L., 1973, Compilation of brine data for the state of Kansas (unpublished report): Operations Research Section, Kansas Geological Survey.

Frank, J.R., A.B. Carpenter, and T.W. Oglesby, 1982, Cathodoluminescence and composition of calcite cement in the Taum Sauk Limestone (Upper Cambrian), southeast Missouri: Journal of Sedimentary Petrology, v. 52, p. 631-638.

Goldstein, R.H., 1986, Reequilibration of fluid inclusions in low-temperature calcium-carbonate cement: Geology, v. 14, p. 792-795.

Goldstein, R.H., 1988, Cement stratigraphy of Pennsylvanian Holder Formation, Sacramento Mountains, New Mexico: AAPG Bulletin, v. 72, p. 425-438.

Grover, G., Jr., and J.F. Read, 1983, Paleoaquifer and deep burial related cements defined by regional cathodoluminescent patterns, Middle Ordovician carbonates, Virginia: AAPG Bulletin, v. 67, p. 1275-1303.

Hanor, J.S., 1980, Dissolved methane in sedimentary brines: Potential effect on the PVT properties of fluid inclusions: Economic Geology, v. 75, p. 603-609.

Hardie, L.A., 1984, Evaporites: Marine or non-marine?: American Journal of Science, v. 284, p. 193-240.

Haynes, F.M., 1985, Determination of fluid inclusion compositions by sequential freezing: Economic Geology, v. 80, p. 1436-1439.

Heckel, P.H., 1977, Origin of phosphatic black shale facies in Pennsylvanian cyclothems of the Mid-Continent, North America: AAPG Bulletin, v. 61, no. 2, p. 1045-1068.

Heckel, P.H., 1983, Diagenetic model for carbonate rocks in Mid-Continental Pennsylvanian eustatic cyclothems: Journal of Sedimentary Petrology, v. 54, No. 3, p. 733-759.

Hite, R.J., 1983, The sulfate problem in marine evaporites, in B.C. Schreiber and H.L. Harner, eds., Sixth international symposium on salt, Salt Institute, v.1, p. 217-230.

Holdoway, K.A., 1978, Deposition of evaporites and red beds of the Nippewalla Group, Permian, western Kansas: Kansas Geological Survey Bulletin 215, 43 p.

Hunt, J.A., 1981, Polyacrylamide polymer flow through carbonate rocks for enhanced oil recovery: An experimental study of polymer-brine stability, resistance factor and related geologic characteristics: University of Kansas, M.S. thesis, 119 p.

McNeice, B.T., 1987, Clay-rich zones in Upper Pennsylvanian (Missourian-Virgilian) shelf limestones, eastern Kansas: University of Kansas, M.S. thesis, 86 p.

Merriam, D.F., 1963, The geologic history of Kansas: Kansas Geological Survey Bulletin 162, 312 p.

Meyers, W.J., 1980, Compaction in Mississippian skeletal limestones, southwestern New Mexico: Journal of Sedimentary Petrology, v. 50, p. 457-474.

Moore, C.H., Jr., 1979, Porosity of carbonate rock sequences, in Geology of carbonate porosity: American Association of Petroleum Geologists Continuing Education Course Note Series #11, P. A1-A124.

Moore, R.C., 1936, Stratigraphic classification of the Pennsylvanian rocks of Kansas: Kansas Geological Survey Bulletin, v. 22, 256 p.

Moore, R.C., 1949, Divisions of the Pennsylvanian System in Kansas: Kansas Geological Survey Bulletin, v. 83, 203 p.

Morgan, J.V., 1952, Correlation of radioactive logs of the Lansing and Kansas City Groups in central Kansas: Journal of Petroleum Technology, v.4, p. 111-118.

Mudge, M.R., 1967, Central Midcontinent region, *in* E.D. McKee, S.S. Oriel, et al., Paleotectonic investigations of the Permian System in the United States: United States Geological Survey Professional Paper 515-A, Chapter F, p. 95-123.

Parkhurst, R.W., 1959, Surface to subsurface correlations and oil entrapment in the Lansing and Kansas City groups (Pennsylvanian) in northwest Kansas: University of Kansas M.S. thesis, 71 p.

Potter, R.W., II, 1977, Pressure corrections for fluid-inclusion homogenization temperatures based on the volumetric properties of the system NaCl-H_2O: USGS Journal of Research, v.5, p. 603-607.

Prather, B.E., 1981, Petrology and diagenesis of the D-zone megacyclothem of the Lansing-Kansas City groups, Hitchcock County, Nebraska: University of New Orleans, M.S. thesis, 97 p.

Prather, B.E., 1984, Deposition and diagenesis of an upper Pennsylvanian cyclothem from the Lansing-Kansas City Groups, Hitchcock County, Nebraska;in N. Hyne,ed., Limestones of the Midcontinent: Tulsa Geological Groups, Hitchcock County, Nebraska: in N. Hyne,ed., Limestones of the Midcontinent: Tulsa Geological Society Special Publication No. 2., p. 394-419.

Prather, B.E., 1985a, An Upper Pennsylvanian desert paleosol in the D- zone of the Lansing-Kansas City Groups, Hitchcock County, Nebraska: Journal of Sedimentary Petrology, v.55, p. 213-221.

Prather, B.E., 1985b, Depositional facies and diagenetic fabrics of the D-zone cyclothem Lansing-Kansas City Groups, Hitchcock County, Nebraska; in W.L. Watney et al., Core studies in Kansas, Subsurface geology series 6: Kansas Geological Survey, p. 133-144.

Prezbindowski, D.R., 1987, Experimental stretching of fluid inclusions in calcite--Implications for diagenetic studies: Geology, v. 15, p. 333-336.

Rascoe, Bailey, Jr., 1978, Late Paleozoic structural evolution the Las Animas Arch, in Rocky Mountain Association of Geologists-1978 Symposium, p. 113-127.

Rascoe, Bailey, Jr., and Adler, F.J., 1983, Permo-Carboniferous hydrocarbon accumulations, Mid-continent, U.S.A.: AAPG Bulletin, v. 67, p. 979- 1,001.

Rascoe, Bailey, Jr., and D.L. Baars, 1972, The Permian System, *in* Geologic Atlas of the Rocky Mountain Region: Denver, Colorado, Rocky Mountain Association of Geologists, p. 143-165.

Roedder, E., 1984, Fluid inclusions: Reviews in mineralogy, v. 12, 644 p.

Shinn, E.A., and D.M. Robbin, 1983, Mechanical and chemical compaction in fine-grained shallow-water limestones: Journal of Sedimentary Petrology, v. 53, p. 595-618.

Spencer, R.J., 1987, Origin of Ca-Cl brines in Devonian formations, western Canada sedimentary basin: Applied Geochemistry, v. 2, p. 373-384.

Stavnes, S.A., 1982, A preliminary study of the subsurface temperature distribution in Kansas and it relationship to the geology: University of Kansas, M.S. thesis, 169 p.

Stell, M.J., 1988, Chemical evolution of waters in the Lansing-Kansas City groups in western Kansas: Kansas State University, M.S. thesis, 97 p.

Wagner, P.D., and R.K. Matthews, 1982, Porosity preservation in the Upper Smackover (Jurassic) carbonate grainstone, Walker Creek Field, Arkansas: Response of paleophreatic lenses to burial processes--Reply: Journal of Sedimentary Petrology, v. 52, p. 24-25.

Wanless, H.R., and Shepard, F.P., 1936, Sea level and climatic changes related to late Paleozoic cycles: Geological Society of America, Bulletin, v. 47, p. 1177-1206.

Wanless, H.R., Jr., 1979, Limestone response to stress: pressure solution and dolomitization: Journal of Sedimentary Petrology, v. 49, p. 437-462.

Watney, W.L., 1980, Cyclic sedimentation of the Lansing-Kansas City Groups in northwestern Kansas and southwestern Nebraska: Kansas Geological Survey, Bulletin 220, 70 p.

Watney, W.L., 1985, Origin of cyclothems in the subsurface of western Kansas: Application to search for accumulation of petroleum: University of Kansas, Ph.D thesis, 506 p.

Watney, W.L., and W.J. Ebanks, Jr., 1978, Early subaerial exposure and freshwater diagenesis of Upper Pennsylvanian cyclic sediments in northern Kansas and southern Nebraska (abs.): AAPG Bulletin, v. 62, p. 570-571.

Yanatieva, O.K., 1946, Solubility polytherms in the systems $CaCl_2$-$MgCl_2$-H_2O and $CaCl_2$-NaCl-H_2O: Zhur. Prikladnoi Khimii, v. 19, p. 709-722 (in Russian).

Zherebtsova, I.K., and N.N. Volkova, 1966, Experimental study of behavior of trace elements in the process of natural solar evaporation of Black Sea water and Sasyk-Sivash brine: Geochemistry International, v. 3, p. 656-670.

APPENDIX I

UPPER SHALE LITHOLOGIES

Upper shales commonly are composed of red-brown (2.5YR 3/4) silty shales (Table I-A). Gray-green (5Y 5/2) silty shales are also present. Less common are non-silty shales, siltstones, and sandstone (Table I-A). Some of these lithologies include microcrystalline calcite nodules or tubes. These nodules or tubes range in color from tan to gray, in contrast to the red-brown or gray-green shale.

	Number of Beds	Thickness	Thickness of These Strata with Microcrystalline-Calcite Nodules
Red-Brown Silty Shale	87	433.5 ft.	194.6 ft.
Gray-Green Silty Shale	44	101.1 ft.	39.1 ft.
Red-Brown Shale	2	4.1 ft.	0 ft.
Gray-Green Shale	11	11.4 ft.	0.9 ft.
Siltstone	6	18.2 ft.	12.5 ft
Very-Fine Grained Sandstone	1	6.5 ft.	0 ft.

Table I-A. Lithologies and their thicknesses in the upper shales. The number of intervals with these lithologies and the thicknesses of these lithologies which include microcrystalline-calcite nodules or tubes are listed.

APPENDIX II

LOWER SHALE LITHOLOGIES

The lower shale lithology generally is a shale; silty shales are less common (Table II-A). Red-brown (2.5YR 3/4) shale, red-brown silty shales, and gray silty shales (Table II-A) are limited to the northern half of the area of study.

	Number of Beds	Thickness
Black Fissile Shale	5	9.4 ft.
Dark-Gray Shale	12	24.4 ft.
Gray-Green Shale	13	23.1 ft.
Red-Brown Shale	4	21.1 ft.
Gray-Green Silty Shale	4	10.4 ft.
Red-Brown Silty Shale	2	9.6 ft
Siltstone	2	2.0 ft.

Table II-A. The lithologies, the number of intervals with these lithologies, and their thicknesses in the lower shales.

APPENDIX III

DISTRIBUTION OF GRAIN-SUPPORTED CARBONATE LITHOLOGIES

In the upper carbonates, grain-supported packstones and grainstones commonly cap the upper carbonates. Packstones and grainstones occur in 67 of the 83 described upper carbonates. Including multiple occurrences, packstones are present at or near the top of the upper carbonates in 58 cases, in the middle of the upper carbonates in 8 cases, and at the base in 6 cases.

Packstones and grainstones occur in 16 of the 19 described lower carbonates. For 8 of these 16 lower carbonates, all of the interval is packstone or grainstone. For five lower carbonates, the packstone or grainstone is at the base and is overlain by mud-supported texture. For three lower carbonates, the base has mud-supported texture that is overlain by packstone or grainstone.

APPENDIX IV

VERTICAL DISTRIBUTION OF CLAYEY INFILL IN UPPER CARBONATES

Clayey infill is present in 48 of the 83 described upper carbonates. For these 48 upper carbonates, the average depth of strata with clayey infill is 6.8 feet (2.1 m). Generally, not all the beds within this average depth contains clayey infill. An average of 79% of the strata within this 6.8 feet (2.1 m) interval have clayey infill. 29.7% of the wackestones, 25.1% of the packstones, and 10.8% of the grainstones are altered by clayey infill (Table 3). Packstones and grainstones are less altered by clayey infill even though packstones and grainstones are commonly at the top of the upper carbonates (Appendix III). Of the 33 upper carbonates in which the total depth of clayey infill includes grainstones or packstones, there are 22 upper carbonates where at least part of the packstone or grainstone interval is not altered by clayey infill.

In 13 upper carbonates, the total depth of clayey infill exceeds 10 feet (3 m). The maximum depth of clayey infill is 42 feet (12.8 m) in the "J" L.S. of the Ladd Petr. DC Unit #2-3A core.

With only one exception, the 48 upper carbonates with clayey infill are directly overlain by silty shale. The exception is an interval of autoclastic breccia with minor clayey infill that is overlain by a red-brown shale. For the seven cases where the upper carbonate is overlain by gray-green shale, there is no clayey infill in the upper carbonate.

APPENDIX V

DISTRIBUTION OF GRAY-GREEN SHALES AND CLAYEY INFILL

In the upper shales, red-brown (2.5YR 3/4) silty shales are the most common lithology (Table I-A). The gray-green (5Y 5/2) silty shales generally are thin and occur at the top or bottom of the upper shales, above or below limestones. Of the 44 gray-green silty shale intervals, 38 are directly above or below limestones. All 11 intervals of gray-green shale are also directly above or below limestones.

Of the 238.1 feet of carbonate with clayey infill, 99.6 feet include clayey infill by green-colored shale and 113.8 feet include clayey infill by red-colored shale. The source of the clayey infill is the overlying upper shale. Generally, the upper shale is colored red-brown, but it is common for the clayey infill to be colored green. There are 29 cases in which the upper shale overlying a carbonate with clayey infill is all red-brown in color. In 20 of these 29 cases, the clayey infill is at least partially green colored.

The above data concerning the distribution of gray-green shales and clayey infill suggest that shales or clayey infill in proximity to limestones are more likely to to be colored green or gray-green. The cause of the green coloration could be that organics in the limestones hindered the oxidation of iron in nearby shales or that organics in the limestones promoted the reduction of iron in nearby shales.

APPENDIX VI

ABBREVIATIONS AND LOCATION OF CORE SAMPLES

ABBREVIATION	CORE NAME	SPOT LOCATION
ADELL	Continental Oil Co. Adell Unit #406	SE SW SW 2-T6S-R27W
BART	Skelly Oil Co. #1 Bartosovsky	SE SW SW 9-T1S-R34W
CITA	Conoco #1 Taylor	SW NW NW 35-T5S-R27W
CS1BA	Cities Service #1-A Bourquin	NE NW NE 18-T6S-R32W
CS1RB	Cities Service #1-B Ryan	NW SW NW 14-T5S-R32W
CSAIH	Cities Service #1-A Holmdahl	NE SW SW 29-T3S-31W
CSZIM	Cities Service #1-Z Miller	SE NE SE 31-T2S-R27W
E10P	Empire Drilling #10 Palmer	NE NE SE 6-T1S-R33W
E1W	Empire Drilling #1 Wicke	C NE NE 23-T2S-R33W
ELA1	Empire Drilling #1 Lankas	SE SE NW 13-T3S-R34W
ERA1	Empire Drillng #1 Rathe	C NW SW 9-T3N-R30W
G122H	Gulf Oil #1-22 Hughes	C SW SW 22-T9S-R29W
G1DE	Theodore Gore Co. #1 Denny	C NE SW 5-T5S-R34W
GUY MERCER	Sinclair Prairie #1 Guy Mercer	C NE NW 28-T10S-R40W
HB6	Husky Oil Co. #6 Brookes	C SW NW 18-T2N-R27W
HIDY	Geoson Oil Co. #2 Hidy	C SE NW 27-T3N-R33W
KA	Cities Service #1-A Knudson	NE SE NW 16-T7S-R32W
L23A	Ladd Petroleum DC Unit #A 2-3	C SW SE 21-T3N-R34W
L7	Continental Oil Co. #7 J.E. Leonard	SW NW SE 12-T6S-R27W
M124K	Murfin Drilling Co. #1-25 Kincaid	E/2 NW NW 24-T3S-R27W
M17S	Murfin Drilling Co. #1-7 Stroup	C SW SE 21-T2N-R37W
M1PR	Murfin Drilling Co. #1 Prentice	C NE NE 30-T2S-R35W
M2EL	Murfin Drilling Co. #2 Elvin	SE NW SE 14-T3S-R27W
MB2	Murfin Drilling Co. #2-B Messner	SE SE SW 10-T1N-R27W
ME3K	Midwest Energy #3 Kircher	C NW NE 4-T1N-R27W
N1	John Farmer Co. #1 Nicholson	C SW SW 12-T1N-R27W
N2	John Farmer Co. #2 Nicholson	C SW SE 11-T1N-R27W
N3	John Farmer Co. #3 Nicholson	C NE NE 14-T1N-R27W
N5	John Farmer Co. #5 Nicholson	C SW NE 14-T1N-R27W
PARKER B	Petroleum Producers #2-B Parker	C NW SW 10-T1N-27W
S7CGK	Skelly Oil Co. #7 C.G. Kisling	C NW NW 10-T1S-R34W
SCH2	Theodore Gore Co. #2 Schaffert	C SW SE 28-T3N-R32W
SOU1	Murfin Drilling Co. #1 Souchek	C SE NE 2-T1S-R34W
SRW	Shakespeare #2 Rudolph Walter	NE NE NE 2-T3S-R41W
W1	Theodore Gore Co. #1 Wertz	C SE SW 6-T2N-R32W

APPENDIX VII

POROSITY AND CEMENT-REDUCTION DATA FOR EACH THIN SECTION

Table VII-A. The porosity and cement-reduction data for each thin section. The first twelve columns ("precementation porosity" to open porosity) are the same type of data as used in Tables 3,4, and 5, in text. The thirteenth column (interval & carb. lithology) lists the stratigraphic interval of each sample (a letter system, A-L, as shown in Figure 4, in text; other terms are MARM. - Marmaton Group, FT.SC. - Fort Scott Limestone, CHRK. - Cherokee Group, TOR - Toronto Limestone, and L.LEC - Big Springs Limestone) and the carbonate lithology of each sample: WS-carbonate wackestone, PS-carbonate packstone, and GS-carbonate grainstone. The fourteenth column (core name & depth of T.S. in feet) lists the abbreviated name for each core (listed in Appendix VI) and the depth, in feet, of the thin-sectioned core sample.

This table is three pages long.

	% Pre-cementation Porosity	% Calcite Cement	% Calcite Cement #1	% Calcite Cement #2	% Calcite Cement #3	% Calcite Cement #4	% Calcite Cement #5	% Dolomite Cement	% Anhydrite Cement	% Pre-LSD Porosity	% Porosity from LSD	% Open Porosity	Interval & Carb. Lithology	Core name & Depth of T.S. in feet
	PRE-C...	CAL...	#1	#2	#3	#4	#5	Dol.	ANH	PRE-L...	LSD P...	OPEN P...	INTERVA...	CORE NAME-...
1	21.0	81.0	12.1	64.8	4.0	0	0	0	0	4.0	0	4.0	A GS	ADELL 3605
2	11.0	90.9	18.2	72.7	0	0	0	0	0	1.0	0	1.0	A WS	ADELL 3614
3	35.0	85.7	25.7	47.1	12.9	0	0	0	0	5.0	0	5.0	B PS	ADELL 3622
4	23.0	30.4	13.7	16.7	0	0	0	4.3	0	15.0	0	15.0	C PS	ADELL 3635.5
5	37.5	93.3	14.0	32.7	46.7	0	0	0	0	2.5	2.5	5.0	D PS	ADELL 3643.6
6	19.6	66.3	16.6	36.3	13.3	0	0	20.4	0	2.6	10.4	13.0	D WS	ADELL 3650.9
7	15.0	40.0	10.0	30.0	0	0	0	40.0	0	3.0	7.0	10.0	D WS	ADELL 3655
8	28.0	42.9	6.4	15.0	21.4	0	0	0	0	16.0	4.0	20.0	E PS	ADELL 3662
9	33.0	90.9	22.7	68.2	0	0	0	6.1	0	1.0	0	1.0	G GS	ADELL 3689.8
10	35.0	71.4	17.9	53.6	0	0	0	5.7	2.9	7.0	0	7.0	G GS	ADELL 3694
11	15.0	100.0	15.0	85.0	0	0	0	0	0	0	0	0	G WS	ADELL 3698
12	33.0	84.8	12.7	67.9	4.2	0	0	0	0	5.0	5.0	10.0	G WS	ADELL 3700.9
13	30.0	76.7	23.0	53.7	0	0	0	0	0	7.0	7.0	14.0	G WS	ADELL 3701.5
14	10.0	100.0	30.0	65.0	5.0	0	0	0	0	0	0	0	G WS	ADELL 3703
15	27.0	92.6	23.1	69.4	0	0	0	0	0	2.0	0	2.0	H GS	ADELL 3725.8
16	17.4	86.2	34.5	51.7	0	0	0	0	0	2.4	5.6	8.0	H WS	ADELL 3728.1
17	28.0	17.9	4.3	13.4	0	0	0	28.6	0	15.0	0	15.0	J GS	ADELL 3761
18	18.0	44.4	4.4	15.6	24.4	0	0	0	0	10.0	0	10.0	J WS	ADELL 3783.5
19	20.0	40.0	4.0	4.0	32.0	0	0	0	0	12.0	8.0	20.0	A WS	BART 3987.5
20	26.0	46.2	6.9	11.5	27.7	0	0	7.7	7.7	12.0	8.0	20.0	A WS	BART 3991
21	20.0	75.0	11.3	52.5	11.3	0	0	0	0	5.0	0	5.0	D PS	BART 4035
22	50.0	24.0	6.0	10.8	7.2	0	0	16.0	0	30.0	0	30.0	H PS	BART 4128
23	17.0	76.5	22.9	38.2	15.3	0	0	0	5.9	3.0	12.0	15.0	H WS	BART 4131
24	46.0	97.8	2.0	57.7	38.2	0	0	2.2	0	0	0	0	H' PS	BART 4143
25	31.0	48.4	14.5	14.5	19.4	0	0	3.2	6.5	14.0	6.0	20.0	J WS	BART 4174.5
26	26.0	26.9	8.1	10.8	8.1	0	0	3.8	0	18.0	12.0	30.0	J WS	BART 4184
27	47.0	42.6	6.4	27.7	8.5	0	0	4.3	0	25.0	0	25.0	K WS	BART 4219
28	32.0	93.8	14.1	65.6	14.1	0	0	6.3	0	0	0	0	K PS	BART 4222
29	30.0	33.3	10.0	23.3	0	0	0	0	0	20.0	0	20.0	B PS	CITA 3644
30	31.0	32.3	12.9	17.7	1.6	0	0	3.2	0	20.0	0	20.0	F GS	CITA 3699
31	32.0	93.8	9.4	18.8	28.1	9.4	28.1	6.3	0	0	0	0	B PS	CS1BA 3953.5
32	20.0	75.0	15.0	18.8	30.0	11.3	0	0	0	5.0	0	5.0	C PS	CS1BA 3966
33	20.0	100.0	20.0	15.0	50.0	15.0	0	0	0	0	0	0	D PS	CS1BA 3977.5
34	27.0	92.6	13.9	9.3	46.3	23.1	0	7.4	0	0	0	0	G PS	CS1BA 4023.1
35	25.0	60.0	9.0	15.0	33.0	3.0	0	40.0	0	0	0	0	G PS	CS1BA 4031.7
36	36.0	97.2	1.9	61.3	29.2	4.9	0	2.8	0	0	0	0	G' PS	CS1BA 4042.5
37	35.0	100.0	20.0	50.0	20.0	10.0	0	0	0	0	0	0	MARM. PS	CS1BA 4301
38	17.5	85.7	12.9	25.7	47.1	0	0	0	0	2.5	2.5	5.0	J PS	CS1RB 4173
39	8.0	100.0	25.0	65.0	10.0	0	0	0	0	0	0	0	J WS	CS1RB 4180.5
40	15.0	100.0	20.0	78.0	2.0	0	0	0	0	0	0	0	FT. SC PS	CS1RB 4363
41	25.0	100.0	10.0	75.0	10.0	5.0	0	0	0	0	0	0	FT. SC PS	CS1RB 4369.5
42	56.0	53.6	8.0	18.8	26.8	0	0	19.6	0	15.0	0	15.0	D PS	CSA1H 3967
43	30.0	100.0	10.0	90.0	0	0	0	0	0	0	0	0	D WS	CSA1H 3982
44	45.0	66.7	13.3	23.3	30.0	0	0	6.7	0	12.0	0	12.0	J PS	CSA1H 4091
45	17.0	88.2	17.6	44.1	26.5	0	0	11.8	0	0	0	0	J WS	CSA1H 4098.5
46	25.0	60.0	15.0	45.0	0	0	0	0	0	10.0	0	10.0	D PS	CSZ1M 3688
47	43.0	41.9	16.7	25.1	0	0	0	58.1	0	0	0	0	F PS	CSZ1M 3721.5
48	21.0	95.2	14.3	81.0	0	0	0	0	0	1.0	0	1.0	G' PS	CSZ1M 3743
49	15.2	78.9	11.8	63.2	3.9	0	0	13.2	0	1.2	.8	2.0	H WS	CSZ1M 3761

	PRE-C...	CAL...	#1	#2	#3	#4	#5	Dol.	ANH	PRE-L...	LSD P...	OPEN P...	INTERVA...	CORE NAME-...
50	17.5	74.3	7.4	63.1	3.7	0	0	0	0	4.5	4.5	9.0	J WS	E10P 4064
51	28.5	21.1	3.2	9.5	8.4	0	0	0	0	22.5	2.5	25.0	G WS	E1W 3954
52	36.0	97.2	14.6	19.4	0	63.2	0	0	0	1.0	0	1.0	D WS	ELA1 3915.5
53	43.0	81.4	12.2	12.2	4.1	52.9	0	0	0	8.0	0	8.0	D WS	ELA1 3921.9
54	40.0	100.0	15.0	10.0	30.0	45.0	0	0	0	0	0	0	D WS	ELA1 3935.8
55	45.0	77.8	3.9	46.7	27.2	0	0	0	0	10.0	0	10.0	G PS	ELA1 3969
56	30.0	100.0	20.0	30.0	50.0	0	0	0	0	0	0	0	G WS	ELA1 3980.5
57	33.0	30.3	4.5	16.7	4.5	4.5	0	0	9.1	20.0	0	20.0	H WS	ELA1 4023
58	11.0	90.9	13.6	72.7	4.5	0	0	0	0	1.0	0	1.0	K PS	ERA1 3813.2
59	16.5	90.9	18.2	54.5	18.2	0	0	0	0	1.5	1.5	3.0	CHRK WS	ERA1 4216.5
60	25.5	58.8	20.6	35.3	2.9	0	0	11.8	0	7.5	7.5	15.0	TOR PS	G122H 3969.5
61	36.0	97.2	29.2	29.2	4.9	0	0	2.8	0	0	0	0	A GS	G122H 3986.5
62	38.0	92.1	27.6	64.5	0	0	0	7.9	0	0	0	0	H PS	G122H 4119
63	41.0	85.4	29.9	42.7	12.8	0	0	2.4	0	5.0	0	5.0	H GS	G122H 4121
64	14.0	57.1	8.6	37.1	11.4	0	0	7.1	0	5.0	0	5.0	I PS	G122H 4151
65	15.0	33.3	1.7	21.7	10.0	0	0	33.3	0	5.0	0	5.0	J WS	G122H 4172
66	13.8	72.5	3.6	47.1	21.7	0	0	14.5	0	1.8	1.2	3.0	J WS	G122H 4172.8
67	10.0	50.0	0	42.5	7.5	0	0	50.0	0	0	0	0	K PS	G122H 4192
68	26.0	15.4	3.1	8.5	3.8	0	0	46.2	0	10.0	0	10.0	L PS	G122H 4223
69	46.0	76.1	38.0	0	38.0	0	0	2.2	0	10.0	0	10.0	L.LEC. PS	G1DE 3694
70	40.0	37.5	15.0	22.5	0	0	0	0	0	25.0	0	25.0	TOR PS	G1DE 4034
71	15.0	100.0	15.0	20.0	65.0	0	0	0	0	0	0	0	A WS	G1DE 4058
72	30.0	50.0	10.0	15.0	22.5	2.5	0	6.7	0	10.0	0	10.0	C PS	G1DE 4077.5
73	34.0	73.5	7.4	22.1	25.7	18.4	0	14.7	0	4.0	0	4.0	C PS	G1DE 4081
74	20.0	75.0	22.5	52.5	0	0	0	25.0	0	0	0	0	D WS	G1DE 4099
75	55.0	27.3	6.8	16.4	4.1	0	0	0	0	40.0	0	40.0	G PS	G1DE 4140
76	10.0	100.0	5.0	95.0	0	0	0	0	0	0	0	0	G PS	G1DE 4143
77	35.0	71.4	10.7	57.1	3.6	0	0	28.6	0	0	0	0	H PS	G1DE 4184.5
78	56.0	44.6	4.5	37.9	2.2	0	0	1.8	0	30.0	0	30.0	J PS	G1DE 4231
79	34.0	11.8	3.5	5.3	2.9	0	0	0	0	30.0	0	30.0	G PS	HB6 3384
80	38.3	44.4	2.2	28.9	13.3	0	0	0	0	21.2	3.8	25.0	G PS	HB6 3395
81	48.0	27.1	5.4	13.5	8.1	0	0	0	0	35.0	0	35.0	G PS	HB6 3398
82	28.5	70.2	14.0	35.1	21.1	0	0	0	0	8.4	4.6	13.0	G WS	HB6 3402
83	15.0	100.0	3.0	97.0	0	0	0	0	0	0	0	0	J WS	HIDY 3970.5
84	35.0	85.7	11.7	19.5	46.7	7.8	0	0	0	5.0	5.0	10.0	J PS	KA 4252
85	22.5	88.9	13.3	48.9	26.7	0	0	0	0	2.5	2.5	5.0	J PS	KA 4253
86	21.0	95.2	19.0	28.6	47.6	0	0	0	0	1.0	0	1.0	J WS	KA 4259
87	18.0	83.3	0	83.3	0	0	0	16.7	0	0	0	0	G PS	L23A 4085
88	31.0	48.4	9.7	16.9	21.8	0	0	25.8	0	8.0	0	8.0	H PS	L23A 4109.3
89	30.0	83.3	.8	80.8	1.7	0	0	0	0	0	0	0	H PS	L23A 4144
90	43.0	7.0	2.1	4.9	0	0	0	58.1	0	15.0	0	15.0	J PS	L23A 4151.5
91	39.0	51.3	7.7	17.9	25.6	0	0	25.6	0	8.0	0	8.0	J PS	L23A 4164
92	42.0	35.7	5.4	12.5	17.9	0	0	2.4	2.4	25.0	0	25.0	K PS	L23A 4216.5
93	28.0	28.6	10.0	18.6	0	0	0	35.7	0	10.0	0	10.0	TOR GS	L7 3620
94	35.0	28.6	7.1	21.4	0	0	0	28.6	0	15.0	0	15.0	TOR GS	L7 3621
95	30.0	33.3	10.0	23.3	0	0	0	0	0	20.0	0	20.0	C GS	L7 3668
96	25.0	80.0	28.0	52.0	0	0	0	0	0	5.0	0	5.0	G PS	L7 3734.5
97	32.0	37.5	15.0	22.5	0	0	0	0	0	20.0	0	20.0	C GS	M124K 3568.5
98	35.0	14.3	4.3	4.3	5.7	0	0	28.6	0	20.0	0	20.0	D GS	M124K 3580

	PRE-C...	CAL...	#1	#2	#3	#4	#5	Dol.	ANH	PRE-L...	LSD P...	OPEN P...	INTERVA...	CORE NAME-...
99	15.9	94.3	9.4	12.3	72.6	0	0	0	0	.9	2.1	3.0	D WS	M124K 3586.5
100	27.0	37.0	7.4	9.3	20.4	0	0	7.4	0	15.0	0	15.0	D PS	M17S 4254
101	18.4	54.3	10.9	12.5	21.7	5.4	3.8	32.6	0	2.4	5.6	8.0	D PS	M17S 4254.8
102	30.0	60.0	12.0	21.0	27.0	0	0	0	0	12.0	0	12.0	D PS	M1PR 4243
103	6.0	50.0	10.0	7.5	5.0	27.5	0	50.0	0	0	0	0	D WS	M1PR 4250.3
104	22.0	45.5	11.4	15.9	9.1	9.1	0	9.1	0	10.0	0	10.0	D WS	M1PR 4252
105	38.0	65.8	13.2	19.7	19.7	13.2	0	7.9	0	10.0	0	10.0	D WS	M1PR 4255
106	11.0	72.7	7.3	10.9	21.8	32.7	0	27.3	0	0	0	0	D WS	M1PR 4259.5
107	45.0	55.6	.6	16.7	2.8	35.6	0	11.1	0	15.0	0	15.0	E WS	M1PR 4269
108	30.0	83.3	25.0	58.3	0	0	0	16.7	0	0	0	0	E WS	M1PR 4271
109	22.0	45.5	6.8	11.4	25.0	2.3	0	9.1	0	10.0	10.0	20.0	G PS	M1PR 4303
110	55.0	18.2	1.8	4.5	2.7	2.7	6.4	27.3	0	30.0	0	30.0	G WS	M1PR 4319
111	22.0	90.9	9.1	13.6	64.5	1.8	1.8	9.1	0	0	0	0	G WS	M1PR 4321.5
112	40.0	25.0	12.5	12.5	0	0	0	37.5	0	15.0	0	15.0	TOR PS	M2EL 3561
113	32.0	31.3	9.4	18.8	3.1	0	0	21.9	0	15.0	0	15.0	TOR PS	M2EL 3564
114	23.4	64.1	12.8	41.7	9.6	0	0	0	0	8.4	3.6	12.0	A WS	M2EL 3578
115	27.0	81.5	16.3	32.6	32.6	0	0	0	0	5.0	0	5.0	A WS	M2EL 3581
116	17.4	86.2	17.2	38.8	30.2	0	0	0	0	2.4	9.6	12.0	A WS	M2EL 3585
117	38.0	21.1	9.5	8.4	3.2	0	0	0	0	30.0	0	30.0	C GS	M2EL 3595
118	43.0	46.5	23.3	22.3	.9	0	0	0	0	23.0	0	23.0	C PS	M2EL 3596
119	20.0	75.0	18.8	52.5	3.8	0	0	0	0	5.0	0	5.0	D PS	M2EL 3608
120	14.0	92.9	9.3	83.6	0	0	0	0	0	1.0	9.0	10.0	D WS	M2EL 3614
121	35.0	94.3	18.9	61.3	14.1	0	0	5.7	0	0	0	0	F GS	M2EL 3643
122	13.0	100.0	15.0	85.0	0	0	0	0	0	0	0	0	G WS	M2EL 3665
123	18.0	100.0	5.0	55.0	40.0	0	0	0	0	0	0	0	G PS	M2EL 3671
124	23.2	94.8	11.4	83.4	0	0	0	0	0	1.2	.8	2.0	H WS	M2EL 3692
125	21.0	61.9	12.4	43.3	6.2	0	0	0	0	8.0	0	8.0	D WS	MB2 3160
126	19.8	75.8	15.2	41.7	18.9	0	0	0	0	4.8	3.2	8.0	G WS	ME3K 3324
127	22.0	68.2	20.5	34.1	13.6	0	0	0	0	7.0	0	7.0	D PS	N1 3162.3
128	15.0	100.0	20.0	45.0	35.0	0	0	0	0	0	0	0	D WS	N1 3168.1
129	20.2	74.3	7.4	40.8	26.0	0	0	0	0	5.2	7.8	13.0	D WS	N1 3170
130	13.0	92.3	18.5	73.8	0	0	0	0	0	1.0	0	1.0	D WS	N2 3160
131	31.0	64.5	6.5	48.4	9.7	0	0	0	3.2	10.0	15.0	25.0	D WS	N2 3163.5
132	23.0	65.2	6.5	42.4	16.3	0	0	0	0	8.0	4.0	12.0	D WS	N3 3166
133	50.0	30.0	4.5	24.0	1.5	0	0	0	0	35.0	0	35.0	D PS	N5 3158
134	17.0	88.2	7.1	81.2	0	0	0	0	0	2.0	0	2.0	D WS	N5 3161
135	20.0	75.0	7.5	52.5	15.0	0	0	0	0	5.0	5.0	10.0	D WS	N5 3164
136	25.0	60.0	6.0	33.0	21.0	0	0	0	0	10.0	10.0	20.0	D WS	PARKER B
137	30.0	40.0	2.8	29.2	8.0	0	0	0	0	18.0	2.0	20.0	A WS	S7CGK 4005.1
138	34.5	29.0	7.2	8.7	13.0	0	0	0	5.8	22.5	2.5	25.0	A PS	S7CGK 4006.4
139	19.0	78.9	15.8	51.3	11.8	0	0	5.3	0	3.0	0	3.0	J PS	S7CGK 4198.5
140	26.0	96.2	4.8	81.7	9.6	0	0	3.8	0	0	0	0	G PS	SCH2 3683.9
141	36.0	27.8	2.8	20.8	4.2	0	0	2.8	0	25.0	0	25.0	K PS	SCH2 3816
142	30.0	100.0	15.0	80.0	5.0	0	0	0	0	0	0	0	K PS	SCH2 3833
143	31.0	25.8	9.0	9.0	7.7	0	0	3.2	0	22.0	0	22.0	D PS	SOU1 4006
144	21.0	57.1	1.7	49.7	5.7	0	0	0	0	9.0	0	9.0	D WS	SOU1 4007
145	20.0	40.0	.4	13.6	26.0	0	0	0	0	12.0	0	12.0	E PS	SOU1 4029
146	12.5	80.0	8.0	64.0	8.0	0	0	0	0	2.5	2.5	5.0	H WS	SOU1 4108
147	43.0	27.9	1.1	19.5	7.3	0	0	0	2.3	30.0	0	30.0	H' PS	SOU1 4121
148	27.0	22.2	8.9	8.9	4.4	0	0	3.7	0	20.0	0	20.0	J PS	SOU1 4145
149	21.0	38.1	13.3	13.3	11.4	0	0	4.8	0	12.0	18.0	30.0	J WS	SOU1 4150
150	58.0	25.9	9.1	16.8	0	0	0	13.8	0	33.0	0	33.0	J GS	SRW 4651.5
151	64.0	17.2	6.9	6.9	3.4	0	0	4.7	0	50.0	0	50.0	J PS	W1 3779
152	38.0	39.5	2.8	28.8	7.9	0	0	0	0	23.0	0	23.0	J PS	W1 3789.8
153	42.0	35.7	2.5	26.1	7.1	0	0	0	0	2.0	0	2.0	J PS	W1 3790.3

APPENDIX VIII

POROSITY FROM LATE-STAGE DISSOLUTION COMPARED TO PETROPHYSICAL DATA

Table VIII-A. The core-plug porosity and permeability data for intervals with evidence of late-stage dissolution (LSD) in thin sections. These data are used in Figure 18, in text, which is a crossplot of the estimated porosity from LSD and the measured permeability. The data from the Gulf Oil #1-22 Hughes, 3969.5, are not used in Figure 18 because this sample is a packstone; all other data are from wackestones. The thin section data include the estimated porosity of the thin section and the estimated percent of this porosity caused by LSD. The product of these two factors (i.e. 50% of 10% = 5%) is the estimated porosity from LSD plotted in Figure 18. The measured permeability data is used in Figure 18. Where there are multiple permeability data, the closest interval to that of the thin section was used.

The Murfin Drilling #1 Souchek petrophysical data are from Hunt (1981). The remaining petrophysical data were measured by Core Laboratories, Inc. and were obtained from the core files of the Kansas Geological Survey.

Well Name	Petrographic Observations				Petrophysical Data from Core-plug Measurements		
	Interval of Decribed Thin Section	Estimated Porosity of Thin Secton	Estimated Percent of Porosity caused by Late-Stage Dissolution	Lithology Type	Depth of Interval with Petrophysical Analyses	Measured Porosity	Measured Permeability
John O. Farmer #1 Nicholson	3170 ft.	13%	60%	Fossiliferous Wackestone			Hor. & Vertical
					3170 - 71 ft.	13.3%	20 & 15 md.
					3171 - 72 ft.	9.7%	27 & 43 md.
					3172 - 73 ft.	8.0%	4.4 & 6.0 md.
John O. Farmer #2 Nicholson	3163.5 ft.	25%	60%	Fossiliferous Wackestone			Hor. & Vertical
					3162 - 63 ft.	13.0%	4.0 & <0.1 md.
					3163 - 64 ft.	11.4%	4.9 & 3.0 md.
					3164 - 65 ft.	13.4%	31 & 6.4 md.
John O. Farmer #3 Nicholson	3166.6 ft.	12%	35%	Fossiliferous Wackestone			Hor. & Vertical
					3163 - 64 ft.	15.7%	17 & 15 md.
					3164 - 65 ft.	9.7%	6.1 & 5.6 md.
					3165 - 66 ft.	10.8%	1.1 & 3.3 md.
					3166 - 67 ft.	10.9%	1.7 & 0.4 md.
					3167 - 68 ft.	5.9%	3.0 & 1.1 md.
John O. Farmer #5 Nicholson	3164 ft.	10%	50%	Fossiliferous Wackestone			
					3164 - 65 ft.	6.7%	1.1 md.
					3165 - 66 ft.	10.5%	6.0 md.
					3166 - 67 ft.	8.1%	5.3 md.
					3167 - 68 ft.	9.3%	19.0 md.
					3168 - 69 ft.	11.3%	7.3 md.
Murfin Drilling #1 Souchek	4150 ft.	30%	60%	Fossiliferous Wackestone with Microstylolites			
					4148 ft.	18.5%	0 md.
					4148 ft.	17.6%	0 md.
					4148 ft.	17.1%	3.51 md.
					4148 ft.	25.8%	67.8 md.
					4148 ft.	38.0%	67.94 md.
					4148 ft.	30.2%	58.81 md.
					4153 ft.	18.1%	13.76 md.
Skelly Oil Co. #1 Bartosovsky	4131 ft.	15%	80%	Fossiliferous Wackestone			
					4130 - 31 ft.	22.1%	124 md.
					4131 - 32 ft.	22.0%	211 md.
					4132 - 33 ft.	15.9%	4.4 md.
					4133 - 34 ft.	15.4%	6.5 md.
					4134 - 35 ft.	14.9%	2.9 md.
	4174 ft.	20%	30%	Fossiliferous Wackestone			
					4174 - 75 ft.	20.4%	160 md.
					4175 - 76 ft.	17.0%	82 md.
					4176 - 77 ft.	18.6%	2200 md.
					4177 - 78 ft.	17.0%	38 md.
	4184 ft.	30 %	40%	Fossiliferous Wackestone			
					4180 - 81 ft.	12.2%	226 md.
					4181 - 82 ft.	10.7%	255 md.
					4182 - 83 ft.	15.5%	2150 md.
					4183 - 84 ft.	10.4%	0.6 md.
Murfin Drilling #2 Elvin	3578 ft.	12%	30%	Fossiliferous Wackestone	3579 ft.	10.24%	15.79 md.
Continental Oil Co. Adell Unit #406	3650.9 ft.	13%	80%	Fossiliferous Wackestone with Microstylolites			Max. & Vertical
					3650 -51.5 ft.	6.6%	<0.1 & <0.1 md.
					3651.5 - 53 ft.	6.0%	0.2 & <0.1 md.
	3655 ft.	10%	70%	Fossiliferous Wackestone with Microstylolites			
					3653 - 54.6 ft.	6.9%	0.1 & 0.1 md.
					3654.6 - 56 ft.	7.3%	0.4 & <0.1 md.
					3656 - 57 ft.	4.8%	0.2 & 0.1 md.
	3700.9 ft.	10%	50%	Fossiliferous Wackestone	3700.0 - 1.2 ft.	8.0%	9.3 & 7.7 md.
	3701.5 ft.	14%	50%	Fossiliferous Wackestone	3701.2 - 3.0 ft.	7.0%	0.9 & 0.5 md.
Gulf Oil Co. #1-22 Hughes	3969.5	15%	50%	Fossiliferous and Peloildal Packstone			Max. & Vertical
					3970.0 - 71 ft	5.7%	1.3 & 0.8 md.
					3969.0 - 70 ft.	13.7%	22.0 & 13.0 md.

APPENDIX IX

ISOPACH MAP OF THE ANHYDRITE IN THE STONE CORRAL FORMATION

Figure IX-A. Isopach map (in feet) of the anhydrite in the Stone Corral Formation for the area of study. The data used are 264 thicknesses of the anhydrite measured from well logs (approximately one well per township, for the area of study). The measured thickness is limited to anhydrite with both low gamma ray values and high density values or low neutron porosity. Excluded are some intervals with low gamma ray values and high neutron porosity.

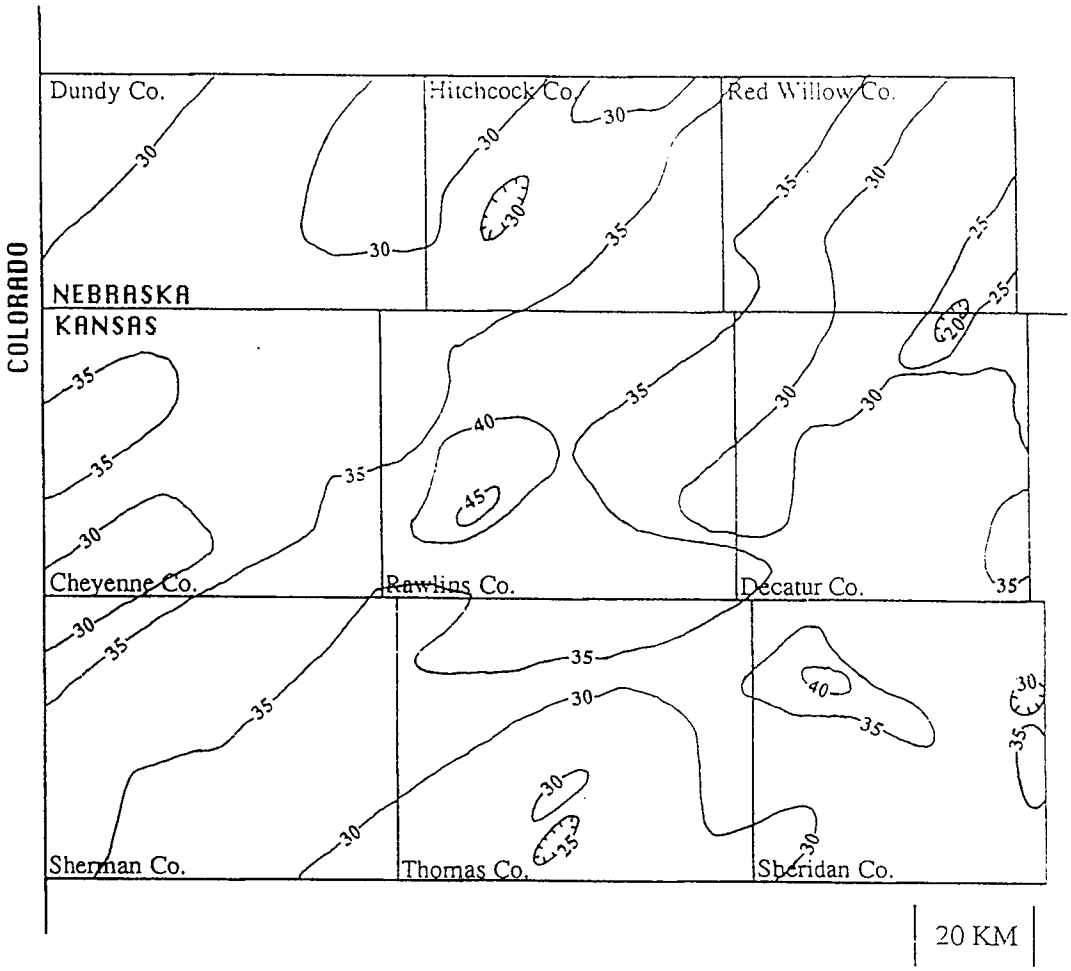
COLORADO
NEBRASKA
KANSAS
Dundy Co.
Hitchcock Co.
Red Willow Co.
Cheyenne Co.
Rawlins Co.
Decatur Co.
Sherman Co.
Thomas Co.
Sheridan Co.
20 KM

APPENDIX X

PREPARING THIN-SECTION CHIPS

1. Cut samples to 26 x 46 mm dimensions (size of the thin section)

IF POROUS:

2. Wrap the sample in aluminum foil with the top open to contain the impregnating epoxy. Place the front of the chip (the side to be thin sectioned) at the bottom the aluminum foil "pan". Leave the top open in order to pour the epoxy in. Along the bottom and sides of the sample, the aluminum foil should be rather tight; it is not necessary to have wide openings for the epoxy.
3. Mark the sample name on the aluminum foil in several places in case of overflow by the epoxy.
4. The epoxy used is Araldite Epoxy Resin (GY-506) and Hardener (GY-956) manufactured by Ciba-Geigy, Ph. (914) 347-4700. The epoxy and hardener are used at a 4:1 ratio.
5. Measure out the epoxy resin (do not add hardener, yet).
6. Mix in blue dye. Add blue dye until the epoxy is dark blue to black.
7. Mix in the hardener at a 1:4 ratio.
8. Add epoxy to each of the aluminum foil pans with samples.
9. Place samples in vacuum jar and apply vacuum.

The goal during vacuum impregnation is to remove all air from the sample and then to replace the air with epoxy. The first vacuum pump down should remove all air. When air is returned and pressure increased, epoxy is injected into the pores. The samples should be

pumped down to a vacuum at least three times with the air pressure reapplied. The purpose of the subsequent pump downs is not to remove air, but to inject epoxy when the air pressure is reapplied. Air pressure should be slowly applied to most efficiently push epoxy into the pores.

During vacuum pump downs, try to avoid boiling by the epoxy. When the epoxy boils, bubbles form in the epoxy and the epoxy overflows the aluminum foil pan.

10. After the addition of the hardener, the epoxy begins to harden. The quicker the impregnation can be completed, the more likely the epoxy will be injected. As epoxy hardens, its viscosity increases.
11. Allow the epoxy to harden for 20-24 hours.
12. If epoxy does not harden in this time, applying heat will complete the hardness. One means of applying heat is to set the samples in sun light.
13. When the epoxy has hardened, remove the aluminum foil.
14. The degree of impregnation may be judged by cutting into the sides of the sample.
15. With good impregnation, the bottom of the sample may be cut off. With poor impregnation, it may be necessary to grind into the base of the impregnated sample to avoid removing much of the impregnated rock. (When the sample was placed in the aluminum foil pan, the side intended to be thin sectioned was placed on the bottom.)

APPENDIX XI

POLISHING OF CHIPS AND THIN SECTIONS

1. All chips and thin sections were first ground at coarse grits (such as 400 or 600 grit) in a progression from coarse to fine. The final grit used in all cases was 1000 grit.
2. When the sample was complete at 1000 grit, it was thoroughly washed (such as in an ultrasonic cleaner) to remove all grit. Remaining grit would cause scratches during polishing.
3. The polishing compounds used are alumina powder with 1.0, 0.3, and 0.05 micron sizes. The 0.3 and 0.05 microns sizes produce the best polish.
4. The samples are polished on a rotating lap wheel with a nylon cloth. The chip is held by the hand and thin sections are held in a thin-section holder. The cloth is kept wet and polishing powder is occasionally added (this is best done with a mixture of water and polishing powder). The sample is most quickly polished when the wheel is turning at higher speed.
5. With thin sections, it may be necessary to grind the edges of the thin section to avoid tearing the cloth.

APPENDIX XII

CRUSHING ANALYSIS

For crushing analysis of fluid inclusions, a crushing device was made (Figure XII-A,B). This crushing device is made from two 5.0 x 7.5 cm thin section glasses, a 2.7 x 4.6 cm thin section glass, and duct tape. The 2.7 x 4.5 cm thin section glass is glued to a 5.0 x 7.5 cm thin section glass with epoxy. The second 5.0 x 7.5 cm thin section glass is attached with duct tape. The positioning of these thin section glasses is illustrated in Figure XII-A.

This crushing device is designed to be placed on a microscope stage. With a video camera and recorder, the process can be video taped to record the original size of the fluid-inclusion bubble and to record the changes in the bubble when it is crushed. Another aim of this device is to do crushing without excessive jostling or movement of the sample.

For crushing, the sample is placed at the point marked by the + in Figure XII-A. A medium, such as a drop of kerosene, should also be placed with the sample. Next, the top glass plate is brought down over the sample (Figure XII-B). Individual inclusions could now be selected and recorded on video tape. To crush the sample, the two large thin section glasses are pushed together (left side, Figure XII-B). As long as the two glass plates are properly taped together (right side, Figure XII-B), pressure is applied to the sample at the +.

Figure XII-A. The device for crushing analysis. It is composed of two 5.0 x 7.5 cm thin-section glasses, a 2.7 x 4.6 cm thin-section glass, and duct tape. The 2.7 x 4.6 cm (marked by the +) is glued to a 5.0 x 7.5 cm thin-section glass with epoxy. The second 5.0 x 7.5 cm thin-section glass (in a tilted position) is attached to the couplet of the other glasses by duct tape. The + marks the location where samples are placed for analysis.

Figure XII-B. For crushing analysis, the sample is placed at the point marked by the + on top of the 2.7 x 4.6 cm thin-section glass. A medium, such as a drop of kerosene, should also be placed with the sample at the +. For crushing the sample, the two large glass plates are pushed together on the left side. The duct tape on the right side (tape shown in A) holds the two glasses together and allows pressure to placed on the sample at the point marked by the +.

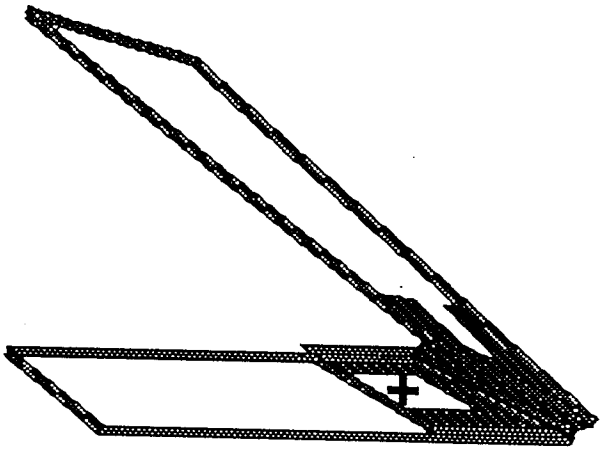

A

Duct Tape

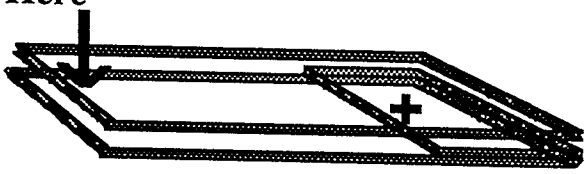

B

Table XII-A. The dimensions of fluid-inclusion bubbles before and after crushing and the calculated internal pressure of the bubbles before crushing. Based on Boyle's Law ($V_1/V_2 = P_2/P_1$), the pressure equals the change in the volume of the bubble before and after crushing. The inclusions were crushed using the device shown in Figures XII-A and XII-B, and the dimensions of the fluid-inclusion bubbles were measured by recording the inclusions on a VCR.

The volume of a fluid-inclusion bubble should be similar to a volume of an ellipsoid, V = 4/3(pi)abc, where a,b, and c are the three radii. The ratio V_1/V_2 = 4/3(pi)abc / 4/3(pi)def simplifies to abc/def. The dimensions of the bubbles listed in this table include only two diameters because only two dimensions can be measured from a television screen. The third diameter must be estimated. For these data, the third diameter is the mean of the two measured diameters.

The internal pressure of the fluid-inclusion bubble is the product of the two measured diameters after crushing (d3 and d4) and their mean divided by the product of the two measured diameters before crushing (d1 and d2) and their mean.

Pressure = d3 x d4 x (d3/2 + d4/2) / d1 x d2 x (d1/2 + d2/2)

All diameters were measured in cm from the television screen. 1 cm on the television screen equals 4.81 micrometers. All pressures are in atmospheres.

	Dimensions of Fluid-Inclusion Bubbles before and after Crushing Measured from television screen. All measurements are in cm. 1 cm = 4.81 micrometers		Pressure of the Bubble before Crushing, in Atmospheres
	Before Crushing	After Crushing	
#1 Calcite Cement			
Continental Oil #7 J.E. Leonard, 3620 Feet	0.2 x 0.2	0.7 x 0.7	40
	0.8 x 0.8	1.3 x 2.0	8
	0.2 x 0.2	0.5 x 0.5	20
#3 Calcite Cement			
Theodore Gore #1 Denny, 4058 Feet	0.7 x 0.7	2.0 x 1.7	18
	0.7 x 0.8	2.4 x 2.4	33
Murfin Drilling #2 Elvin, 3665 Feet	0.4 x 0.4	1.2 x 0.7	13
	0.6 x 0.6	1.6 x 0.8	7
	0.35 x 0.35	1.2 x 1.2	40
Cities Service #1-A Knudson, 4052 Feet	0.7 x 0.7	1.9 x 1.9	20
	0.7 x 0.7	1.8 x 2.2	23
Undifferentiated Calcite Cement			
Sinclair Prairie #1 Guy Mercer, 4728 Feet	0.3 x 0.3	1.0 x 1.0	37
Nonzoned Dolomite Cement			
Cities Service #1-A Bourquin, 3981 Feet	0.3 x 0.3	1.7 x 1.3	120
	0.3 x 0.3	1.5 x 2.4	260
	0.3 x 0.3	1.5 x 2.0	190
	0.2 x 0.2	0.6 x 0.6	27
Cities Service #1-A Bourquin, 3983 Feet	0.4 x 0.4	0.8 x 0.6	5
	0.5 x 0.8	1.5 x 1.1	8
	0.45 x 0.9	0.9 x 0.9	8
	0.6 x 0.9	3.0 x 1.8	32
Cities Service #1-A Bourquin, 4035 Feet	0.3 x 0.3	0.8 x 1.8	70
Theodore Gore #1 Denny, 3880 Feet	0.3 x 0.3	0.8 x 0.8	20
	0.4 x 0.4	0.8 x 0.8	8
Baroque Dolomite			
Sinclair Prairie #1 Guy Mercer, 4728 Feet	0.2 x 0.2	0.8 x 0.6	40
	0.2 x 0.2	0.6 x 0.6	30

APPENDIX XIII

AQUEOUS FLUID INCLUSION DATA

Table XIII. All fluid inclusion data from each sample. Th- temperature of homogenization. Tn- temperature of nucleation when the sample is frozen. Te-eutectic temperature, when the ice or hydrohalite begins to melt. Tm ice- the temperature of final melting of ice. Tm hydrohalite- the temperature of melting of hydrohalite. All measurements of the melting of hydrohalite are listed.

A. Continental Oil #7 J.E. Leonard, 3620 feet, #1 Calcite Cement, Fluid-Inclusion Data

	Th	Tn	Te	Tm ice	Tm hydrohalite
1	43.6	•	•	•	
2	51.9	-77.8	-47.0	-19.0	
3	53.8	•	•	•	
4	54.5	•	•	•	
5	57.4	•	•	•	
6	57.5	•	•	•	
7	59.1	•	•	•	
8	67.5	•	•	•	
9	68.7	•	•	•	
10	70.6	•	•	•	
11	70.9	•	•	•	
12	74.3	•	•	•	
13	75.1	•	•	•	
14	75.1	•	•	•	
15	79.3	•	•	•	
16	89	-75.0	-47.0	-17.1	
17	95.7	•	•	•	
18		•	-51.0	-21.8	
19		•	-47.0	-19.2	
20	one phase	-77.8	-42.0	-21.7	
21	one phase	•	•	-20.0	
22	one phase	-86.9	•	-19.1	
23		•	•	-19.0	
24	one phase	-79.0	•	-22.0	
25		-88.5	-50.0	-21.6	
26		-83.1	-45.5	-19.9	
27		•	-52.0	-21.6	-32.0

B. Cities Service #1-B Ryan, 4363 feet,
#1 Calcite Cement, Fluid-Inclusion Data

	Th	Tn	Te	Tm ice	Tm hydrohalite
1	52.8	-84.0	-45.0	-20.2	
2	73.7	•	•	•	
3	76.4	•	•	•	
4	•	-53.5	-45.0	-19.7	

C. Theodore Gore #1 Denny, 4058 feet,
#3 Calcite Cement, Fluid-Inclusion Data

	Th	Tn	Te	Tm ice	Tm hydrohalite
1	53.3	-84.2	-52.0	-21.8	-30.7,-30.4,-31.4,-31.8
2	60.6	•	-48.0	-22.1	
3	62.4	•	•	•	
4	63.4	•	•	•	
5	65.2	•	•	•	
6	66.2	•	•	•	
7	67.7	•	-48.0	-19.8	
8	69.7	•	-48.0	-21.9	
9	70.5	•	-52.0	-22.3	
10	73.2	•	-52.0	-22.4	-38.5,-37.4,-36.6
11	79.1	•	•	•	
12	81.5	•	•	•	
13	83.4	-84.0	-48.5	-22.1	
14	85.0	•	-50.0	-16.4	
15	88.8	•	-47.0	-21.6	
16	91.4	•	•	•	
17	93.1	-82.4	-49.0	-22.1	
18	94.0	-85.5	-52.0	-22.0	
19	97.5	•	•	•	
20	171.3	•	-46.0	-10.6	
21	217.1	•	•	•	
22	•	-78.4	-47.0	-20.3	

D. Murfin Drilling #2 Elvin, 3665 feet,
#3 Calcite Cement, Fluid-Inclusion Data

	Th	Tn	Te	Tm ice,	Tm hydrohalite
1	45.5	-88.8	-52.0	-22.2	-33 to -34.5
2	47.0	•	•	•	
3	47.3	•	•	•	
4	47.3	•	•	•	
5	47.5	-91.7	-52.0	-19.1	-30.8
6	48.5	•	•	•	
7	49.0	•	•	•	
8	49.5	•	•	•	
9	49.8	•	•	•	
10	50.8	•	•	•	
11	50.8	•	•	•	
12	51.5	•	•	•	
13	52.2	•	•	•	
14	52.6	•	•	•	
15	52.7	•	•	•	
16	53.0	•	•	•	
17	53.4	-68.0	-52.0	-22.1	-34.0,-33.0,-33.0
18	55.8	•	•	•	
19	56.5	•	•	•	
20	57.0	•	•	•	
21	58.1	•	•	•	
22	58.2	•	•	•	
23	59.1	•	•	•	
24	59.1	•	•	•	
25	59.1	•	•	-19.8	
26	60.5	•	•	•	
27	60.6	•	•	•	
28	65.6	-70.0	-46.0	•	
29	71.0	•	•	•	
30	72.5	•	•	•	
31	72.8	-64.6	-53.0	-12.8	
32	73.8	•	•	•	
33	74.0	•	•	•	
34	75.8	-84.0	-47.0	-17.0	
35	78.9	•	•	-12.2	
36	80.0	•	•	-10.8	
37	81.1	•	•	•	
38	81.1	•	•	•	
-39	•	-85.0	-47.6	-20.0	
40	•	•	-52.0	-17.0	-27.0
41	•	•	-52.0	-14.2	-27.0

E. Cities Service #1-A Knudson, 4052 feet,
#3 Calcite Cement, Fluid-Inclusion Data

	Th	Tn	Te	Tm ice	Tm hydrohalite
1	92.3	•	•	•	
2	98.9	•	-47.0	-14.1	
3	105.5	-72.0	-47.0	-11.8	
4	110.2	•	•	•	
5	112.4	•	•	•	
6	116.3	•	•	•	
7	121.9	•	•	•	
8	127.0	•	•	•	
9	155.0	•	•	•	
10	158.3	•	•	•	
11	178.0	•	-47.0	-13.9	
12	183.0	-71.0	-48.4	-14.1	
13	196.9	-70.2	-47.0	-15.9	
14	197.7	-69.2	-47.9	-19.8	
15	207.1	•	•	•	
16	208.6	-74.2	-48.9	-13.4	
17	•	•	•	-14.1	
18	•	•	•	-13.8	
19	•	•	-52.0	-12.0	
20	•	-75.6	-52.0	-14.3	-33.0,-37.2,-35.5,-36.8
21	•	•	-52.0	-14.1	
22	•	•	•	-12.5	
23	•	•	•	-12.6	

F. Cities Service #1-A Bourquin, 3981, 3983, 4015.8 feet, Dolomite Cement, Fluid-Inclusion Data

	Ti	Tn	Te	Tm ice	Tm hydrohalite	Depth
1	75.1	-82.0	-52.0	-18.9	-33.0	3983
2	81.5	•	•	•		3983
3	85.1	•	•	•		3983
4	85.3	•	•	•		3983
5	88.5	•	•	•		3983
6	88.5	-82.5	-52.0	-22.1	-33.3,-33.7	3983
7	91.1	•	•	•		3983
8	93.3	•	•	•		3983
9	97.9	•	•	•		3983
10	98.2	•	•	•		3981
11	98.9	-85.5	-49.0	-22.9		4015.8
12	99.5	•	•	•		3983
13	101.0	•	•	•		3981
14	101.3	-71.4	-48.0	-22.9		4015.8
15	102.8	-87.0	-49.4	-17.8		4015.8
16	103.0	•	•	•		3983
17	104.0	•	•	•		3981
18	104.6	•	•	•		3983
19	104.7	•	•	•		3983
20	104.8	•	•	•		4015.8
21	105.0	-80.0	-48.0	-22.4		4015.8
22	107.1	•	•	•		4015.8
23	107.1	•	•	•		4015.8
24	107.7	•	•	•		3981
25	108.3	•	•	-22.7		3983
26	111.0	•	-49.0	-18.4		3981
27	111.2	•	•	•		3983
28	112.9	•	•	•		3981
29	114.5	-85.2	-52.0	-22.8		3983
30	115.0	•	•	•		3981
31	128.7	•	•	•		3981
32	129.7	•	•	•		3983
33	130.4	•	-49.6	-20.1		3981
34	131.3	•	•	•		3981
35	136.5	•	-49.4	-21.2		3981
36	147.9	•	•	•		3983
37	171.8	•	-30.3	-15.8		3983
38	•	-109.0	-49.0	-18.0		4015.8
39	•	-78.0	-48.0	-22.4		4015.8
40	•	•	-50.0	-22.8		4015.8
41	•	•	-47.0	-15.8		3983
42	•	-72.9	-49.0	-16.0		3983

G. Murfin Drilling #1 Prentice, 4250.3 feet,
Baroque Dolomite Cement, Fluid-Inclusion Data

	Th	Tn	Te	Tm ice	Tm hydrohalite
1	66.2	•	•	•	
2	66.2	-70.2	-52.0	-22.7	
3	82.0	•	•	•	
4	82.3	•	•	•	
5	83.0	•	•	•	
6	83.4	•	•	•	
7	85.8	-71.0	-52.0	-20.5	
8	88.0	•	•	•	
9	94.0	•	•	•	
10	95.8	•	•	•	
11	96.8	-72.8	-48.0	-22.7	
12	101.3	•	•	•	
13	104.0	-78.1	-48.0	-21.1	
14	104.4	•	•	•	
15	109.6	•	•	•	
16	110.0	•	•	-22.9	
17	125.0	•	•	•	
18	•	-73.9	-52.2	-22.1	-32.2,-31.8,-33.0,-31.5,-31.0,-31.0
19	•	•	•	-22.9	
20	•	•	•	-22.5	
21	•	•	-52.0	-22.7	

APPENDIX XIV

PETROLEUM-FILLED FLUID-INCLUSION Th DATA

Table XIV. The Th (temperature of homogenization) of secondary petroleum-filled fluid inclusions from these samples.

A. Murfin Drilling #1 Prentice, 4029 feet,
Secondary Petroleum-Filled
Fluid-Inclusion Th Data

	Th
1	59.0
2	63.4
3	63.8
4	70.2
5	71.1
6	72.1
7	77.6
8	80.8
9	83.9
10	88.9
11	89.0
12	89.2
13	90.9

B. Murfin Drilling #2 Elvin, 3692 feet,
Secondary Petroleum-Filled
Fluid-Inclusion Th Data

	Th
1	68.4
2	75.8
3	77.6
4	81.8

D. Skelly Oil #1 Bartosovsky, 4035 feet,
Secondary Petroleum-Filled
Fluid-Inclusion Th Data

	Th
1	56.0
2	77.0

C. Empire Drilling #1 Rathe, 4216.5 feet,
Secondary Petroleum-Filled
Fluid-Inclusion Th Data

	Th
1	52.6
2	59.8
3	61.3
4	66.3
5	80.2
6	90.0
7	91.5
8	96.8
9	101.4

E. Cities Service #1-A Knudson, 4252 feet,
Secondary Petroleum-Filled
Fluid-Inclusion Th Data

	Th
1	80.8
2	80.8
3	80.8
4	81.3
5	81.6
6	117.3
7	130.2
8	140.5
9	140.9
10	197.2
11	283.0

APPENDIX XV

CORE DESCRIPTIONS

The lithologic descriptions of the cores analyzed for this study are presented in the following pages. All core descriptions are presented in the order that they are listed in Appendix VI. Three cores that were analyzed are not included with these core descriptions because they only included several core pieces and were not continuous cores. These three cores are the Continental Oil Co. #7 J.E. Leonard, Murfin Drilling Co. #2-B Messner, and the Petroleum Producers #2-B Parker.

The layout of the core descriptions and the terms and symbols used in these core descriptions are described on the first two pages. Some of the terms used in the core descriptions differ from the terms used in the thesis text. These differences are referred to in these first two pages.

Table XV-A
CORE NAMES AND LOCATIONS, AND THE PAGE NUMBER OF CORE DESCRIPTIONS

CORE NAME	SPOT LOCATION	PAGE # OF DESCRIPTION
Continental Oil Co. Adell Unit #406	SE SW SW 2-T6S-R27W	131
Skelly Oil Co. #1 Bartosovsky	SE SW SW 9-T1S-R34W	140
Conoco #1 Taylor	SW NW NW 35-T5S-R27W	155
Cities Service #1-A Bourquin	NE NW NE 18-T6S-R32W	156
Cities Service #1-B Ryan	NW SW NW 14-T5S-R32W	162
Cities Service #1-A Holmdahl	NE SW SW 29-T3S-31W	164
Cities Service #1-Z Miller	SE NE SE 31-T2S-R27W	168
Empire Drilling #10 Palmer	NE NE SE 6-T1S-R33W	173
Empire Drilling #1 Wicke	C NE NE 23-T2S-R33W	174
Empire Drilling #1 Lankas	SE SE NW 13-T3S-R34W	175
Empire Drillng #1 Rathe	C NW SW 9-T3N-R30W	181
Gulf Oil #1-22 Hughes	C SW SW 22-T9S-R29W	190
Theodore Gore Co. #1 Denny	C NE SW 5-T5S-R34W	199
Sinclair Prairie #1 Guy Mercer	C NE NW 28-T10S-R40W	210
Husky Oil Co. #6 Brookes	C SW NW 18-T2N-R27W	211
Geoson Oil Co. #2 Hidy	C SE NW 27-T3N-R33W	213
Cities Service #1-A Knudson	NE SE NW 16-T7S-R32W	215
Ladd Petroleum DC Unit #A 2-3	C SW SE 21-T3N-R34W	217
Continental Oil Co. #7 J.E. Leonard	SW NW SE 12-T6S-R27W	n.a.
Murfin Drilling Co. #1-25 Kincaid	E/2 NW NW 24-T3S-R27W	226
Murfin Drilling Co. #1-7 Stroup	C SW SE 21-T2N-R37W	228
Murfin Drilling Co. #1 Prentice	C NE NE 30-T2S-R35W	231
Murfin Drilling Co. #2 Elvin	SE NW SE 14-T3S-R27W	236
Murfin Drilling Co. #2-B Messner	SE SE SW 10-T1N-R27W	n.a.
Midwest Energy #3 Kircher	C NW NE 4-T1N-R27W	243
John Farmer Co. #1 Nicholson	C SW SW 12-T1N-R27W	244
John Farmer Co. #2 Nicholson	C SW SE 11-T1N-R27W	245
John Farmer Co. #3 Nicholson	C NE NE 14-T1N-R27W	246
John Farmer Co. #5 Nicholson	C SW NE 14-T1N-R27W	247
Petroleum Producers #2-B Parker	C NW SW 10-T1N-27W	n.a.
Skelly Oil Co. #7 C.G. Kisling	C NW NW 10-T1S-R34W	248
Theodore Gore Co. #2 Schaffert	C SW SE 28-T3N-R32W	250
Murfin Drilling Co. #1 Souchek	C SE NE 2-T1S-R34W	252
Shakespeare #2 Rudolph Walter	NE NE NE 2-T3S-R41W	256
Theodore Gore Co. #1 Wertz	C SE SW 6-T2N-R32W	257

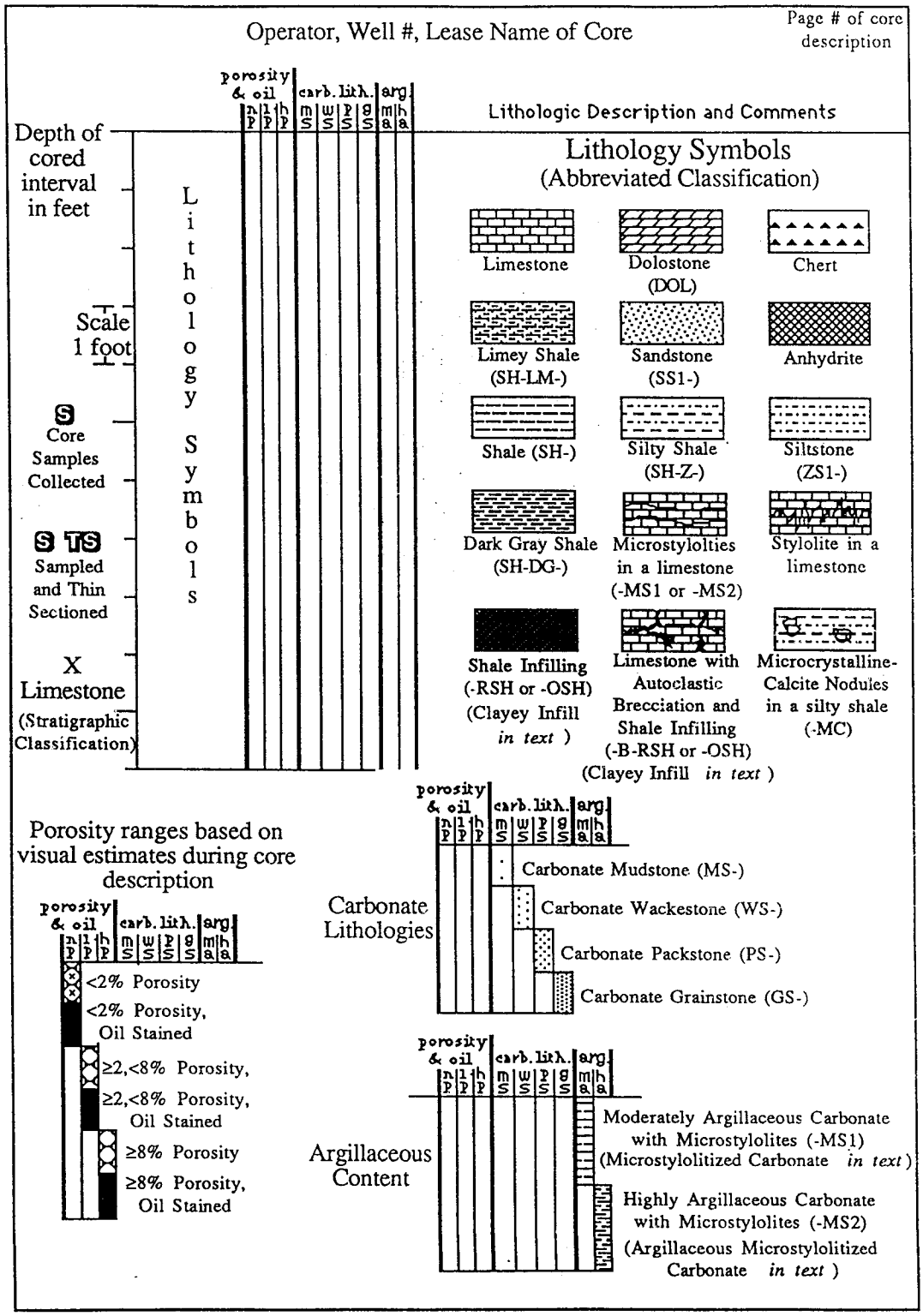
Operator, Well #, Lease Name of Core
Page # of core description
porosity & oil
carb. lith.
arg.
Lithologic Description and Comments
Depth of cored interval in feet
Lithology Symbols
Scale 1 foot
Core Samples Collected
Sampled and Thin Sectioned
X Limestone (Stratigraphic Classification)
Lithology Symbols (Abbreviated Classification)
Limestone
Dolostone (DOL)
Chert
Limey Shale (SH-LM-)
Sandstone (SS1-)
Anhydrite
Shale (SH-)
Silty Shale (SH-Z-)
Siltstone (ZS1-)
Dark Gray Shale (SH-DG-)
Microstylolties in a limestone (-MS1 or -MS2)
Stylolite in a limestone
Shale Infilling (-RSH or -OSH) (Clayey Infill in text)
Limestone with Autoclastic Brecciation and Shale Infilling (-B-RSH or -OSH) (Clayey Infill in text)
Microcrystalline-Calcite Nodules in a silty shale (-MC)
Porosity ranges based on visual estimates during core description
<2% Porosity
<2% Porosity, Oil Stained
≥2,<8% Porosity,
≥2,<8% Porosity, Oil Stained
≥8% Porosity
≥8% Porosity, Oil Stained
Carbonate Lithologies
Carbonate Mudstone (MS-)
Carbonate Wackestone (WS-)
Carbonate Packstone (PS-)
Carbonate Grainstone (GS-)
Argillaceous Content
Moderately Argillaceous Carbonate with Microstylolites (-MS1) (Microstylolitized Carbonate in text)
Highly Argillaceous Carbonate with Microstylolites (-MS2) (Argillaceous Microstylolitized Carbonate in text)

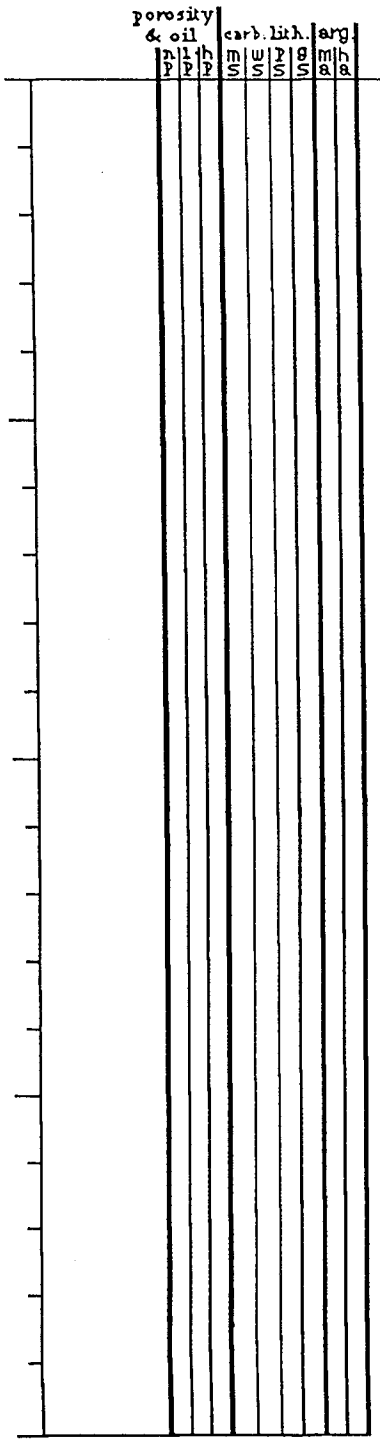

LITHOLOGY CLASSIFICATION

After the written description of each stratum, the lithology is classified by an abbreviated classification in parenthesis.

Carbonate Lithologies

(MS-) Carbonate Mudstone
(PS-) Carbonate Packstone
(WS-) Carbonate Wackestone
(GS-) Carbonate Grainstone
(DOL-) Dolostone
(LM-SH-) Limey Shale (Highly-argillaceous microstylolitized carbonate *in text*)

Modifiers to Carbonate Lithologies

(-F) Fossiliferous
(-P) Peloidal
(-LM) Laminated
(-O) Oolitic
(-ONC) Oncolitic
(-FR) Fractured

(-MS1) Microstylolites (less argillaceous) (microstylolitized carbonate *in text*)
(-MS2) Microstylolites (more argillaceous) (argillaceous microstylolitized carbonate *in text*)

(-B) Autoclastic Brecciation
(-RSH) Infilling by Gray-Colored Shale } Clayey infill *in text*
(-OSH) Infilling by Red-Colored Shale

Shales

(SH-) Shale

Modifiers to Shales

(-Z) Silty
(-F) Fossiliferous
(-RB) Red-Brown
(-GG) Gray-Green
(-DG) Dark Gray
(-BL) Black
(-MC) Contains Microcrystalline-Calcite Nodules

Other Lithologies

(SS1-) Very-fine grained Sandstone

(ZS-) Siltstone

CONTINENTAL OIL COMPANY #406 ADELL

SE SW SW, Sec. 2- T6S-R27W
Sheridan Co., Kansas

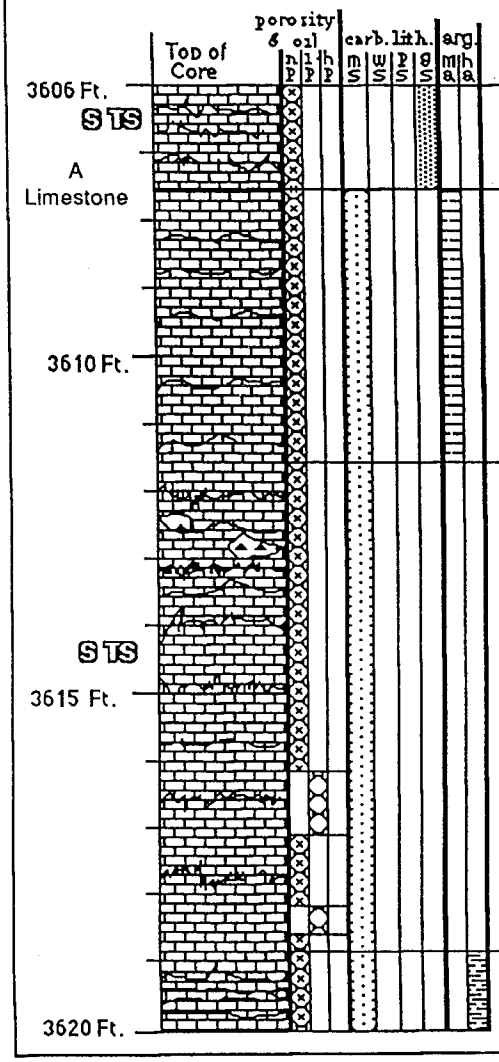

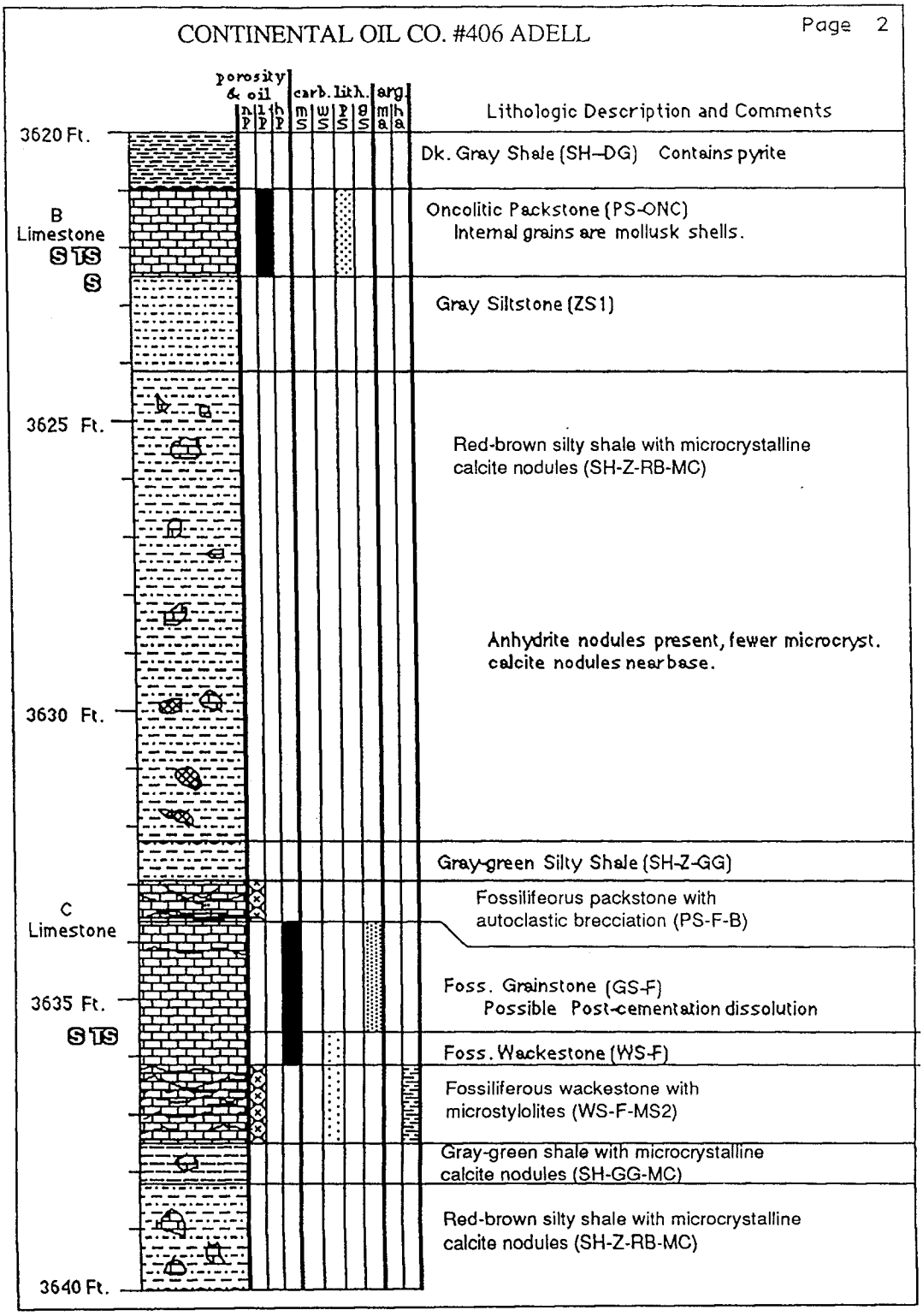
CONTINENTAL OIL CO. #406 ADELL
porosity & oil
carb. lith.
arg.
Lithologic Description and Comments
3620 Ft.
Dk. Gray Shale (SH–DG) Contains pyrite
B Limestone
Oncolitic Packstone (PS-ONC)
Internal grains are mollusk shells.
Gray Siltstone (ZS1)
3625 Ft.
Red-brown silty shale with microcrystalline calcite nodules (SH-Z-RB-MC)
Anhydrite nodules present, fewer microcryst. calcite nodules near base.
3630 Ft.
Gray-green Silty Shale (SH-Z-GG)
C Limestone
Fossilifeorus packstone with autoclastic brecciation (PS-F-B)
Foss. Grainstone (GS-F)
Possible Post-cementation dissolution
3635 Ft.
Foss. Wackestone (WS-F)
Fossiliferous wackestone with microstylolites (WS-F-MS2)
Gray-green shale with microcrystalline calcite nodules (SH-GG-MC)
Red-brown silty shale with microcrystalline calcite nodules (SH-Z-RB-MC)
3640 Ft.

CONTINENTAL OIL CO. #406 ADELL

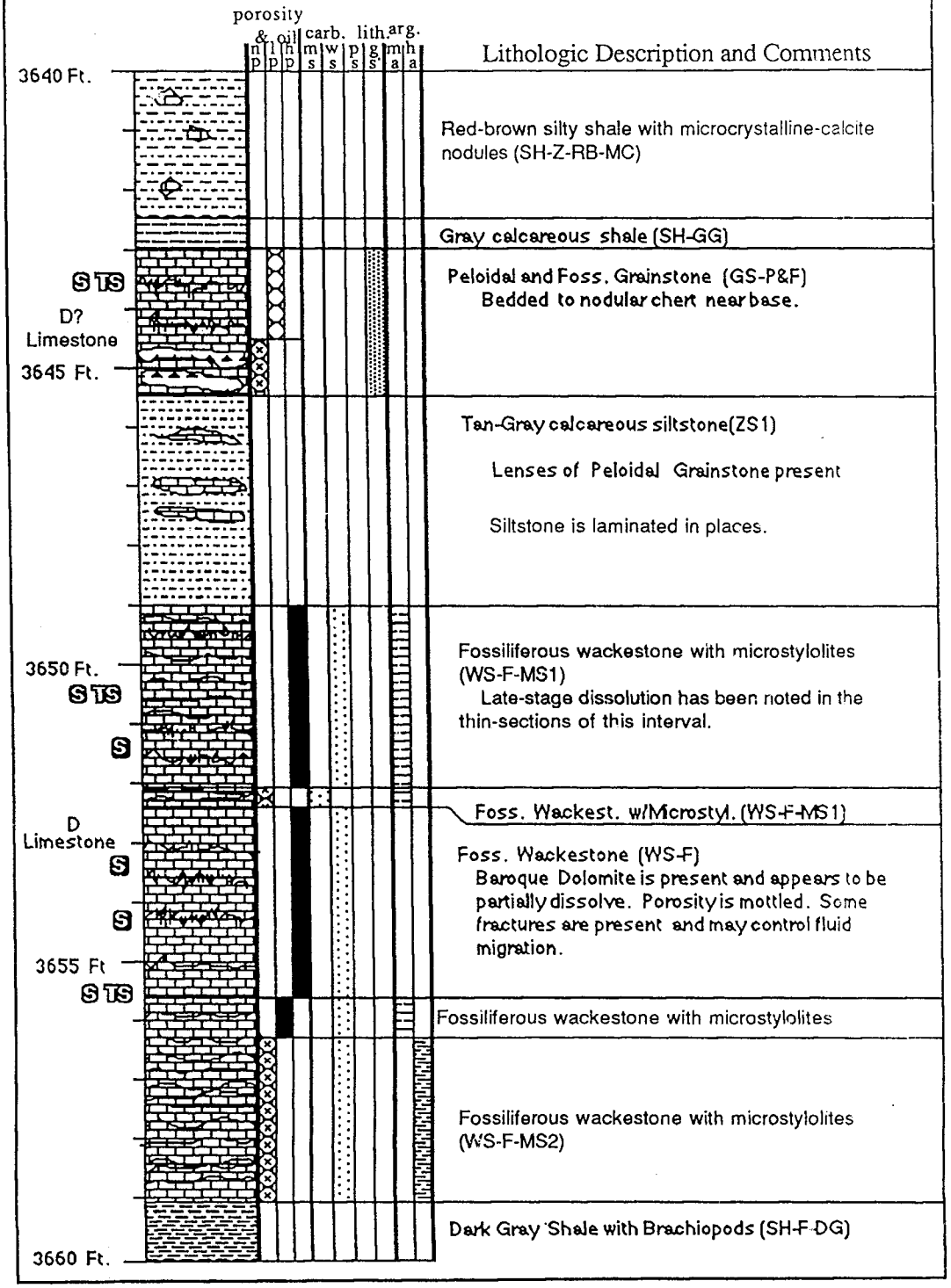

CONTINENTAL OIL CO. #406 ADELL

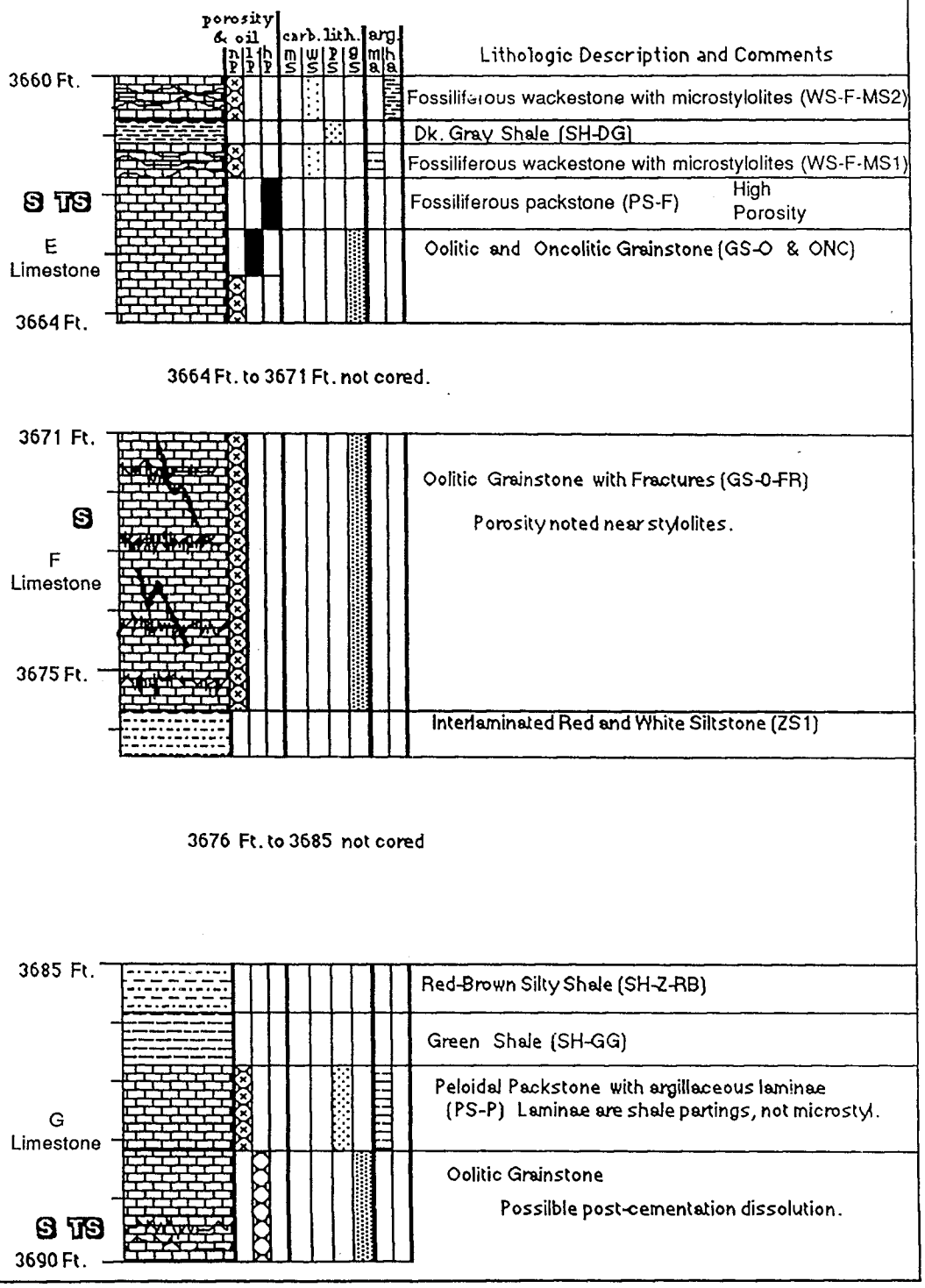

CONTINENTAL OIL CO. #406 ADELL

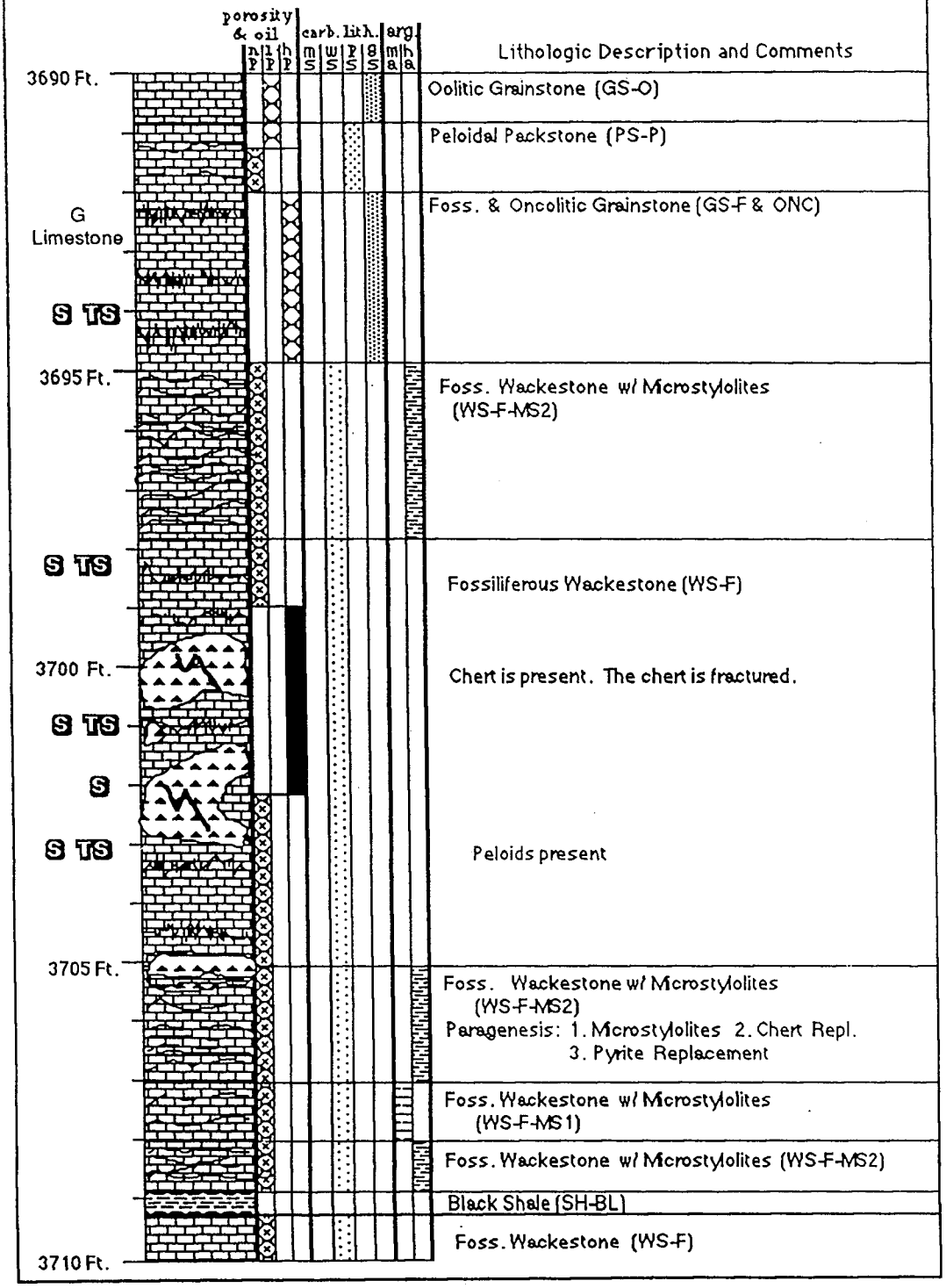

CONTINENTAL OIL CO. #406 ADELL

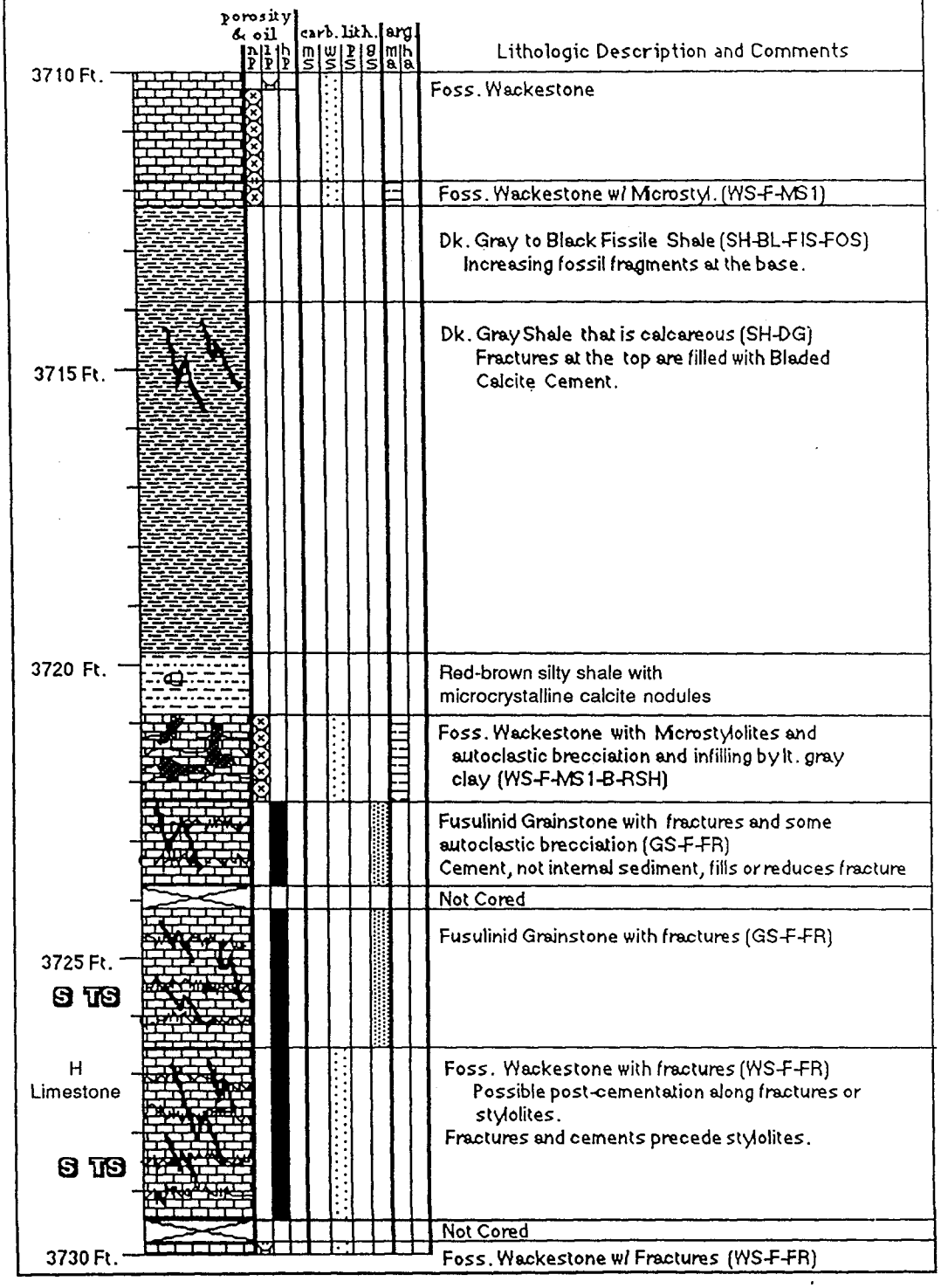

CONTINENTAL OIL CO. #406 ADELL

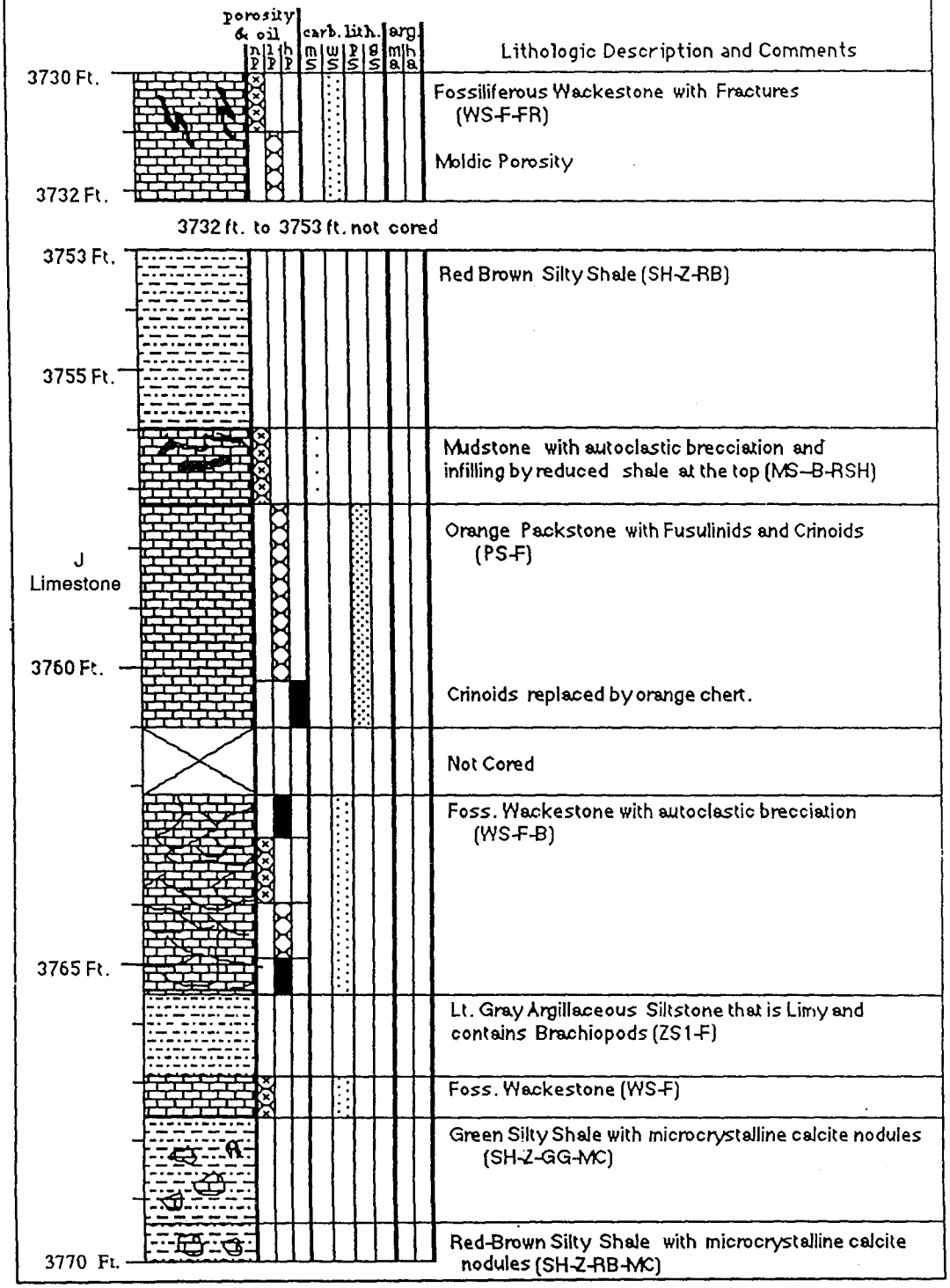

CONTINENTAL OIL COMPANY #406 ADELL

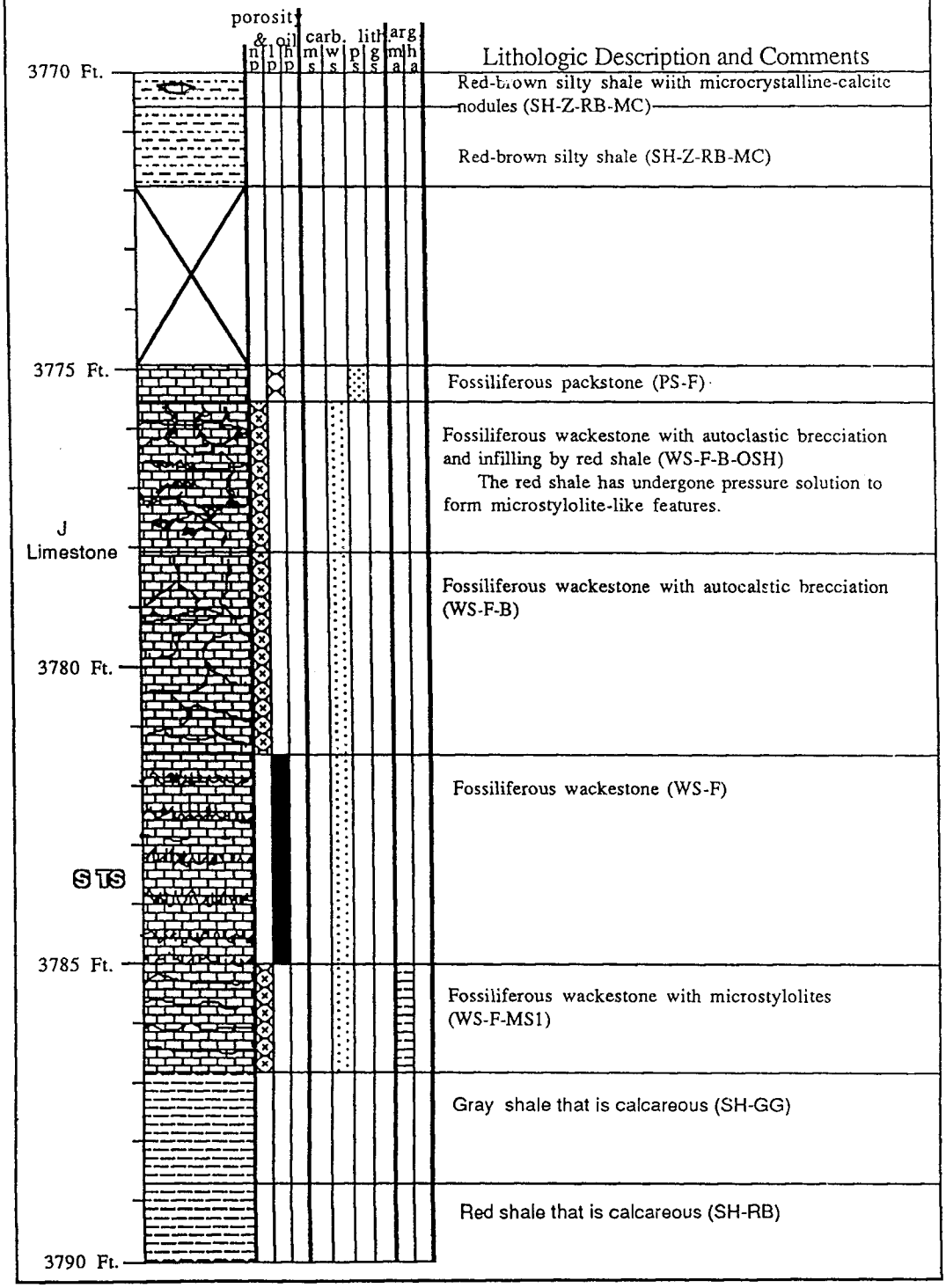

CONTINENTAL OIL COMPANY #406 ADELL

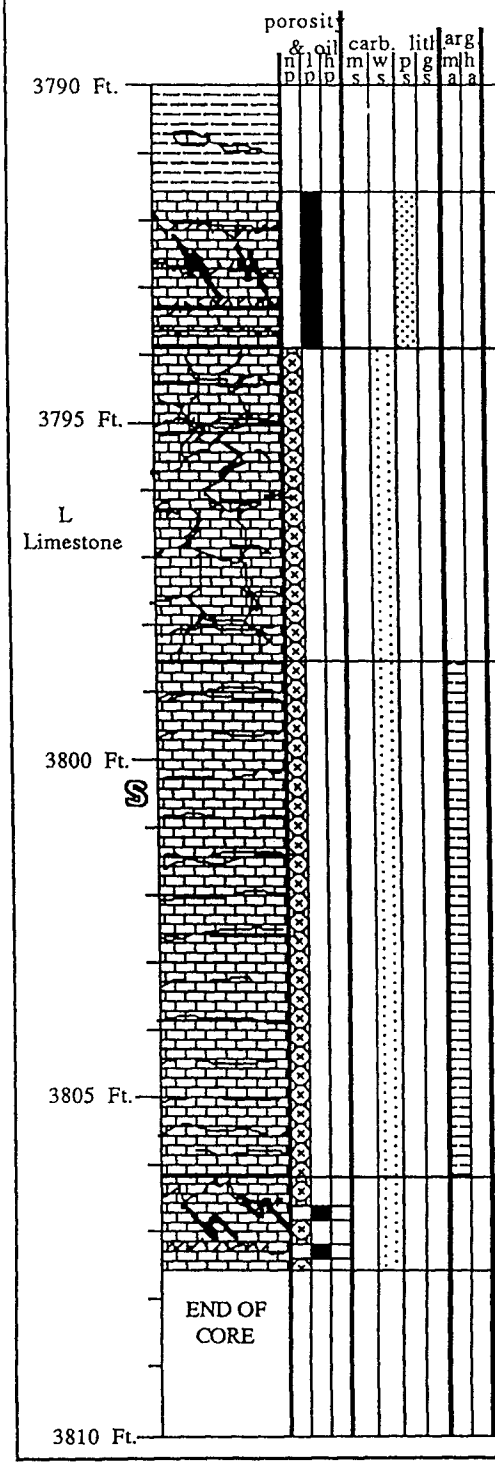

Lithologic Description and Comments

Red shale with microcrystalline-calcite nodules (SH-RB-MC)

Fossiliferous packstone (PS-F-FR)
Fractures are present.

Fossiliferous wackestone with autoclastic brecciaion (WS-F-B)
Brecciation is significant, microstylolites have formed from pressure solution of these features.

Fossiliferous wackestone with microstylolites (WS-F-MS1)

MOcf is common.

Fossiliferous wackestone (WS-F)
Fractures noted

SKELLY OIL CO. #1 BARTOSOVSKY

SE SW SW, Sec. 9-T1S-R34W
Cahoj Field, Rawlins County, Kansas
IPP 3702 BOPD, Drilled1959.

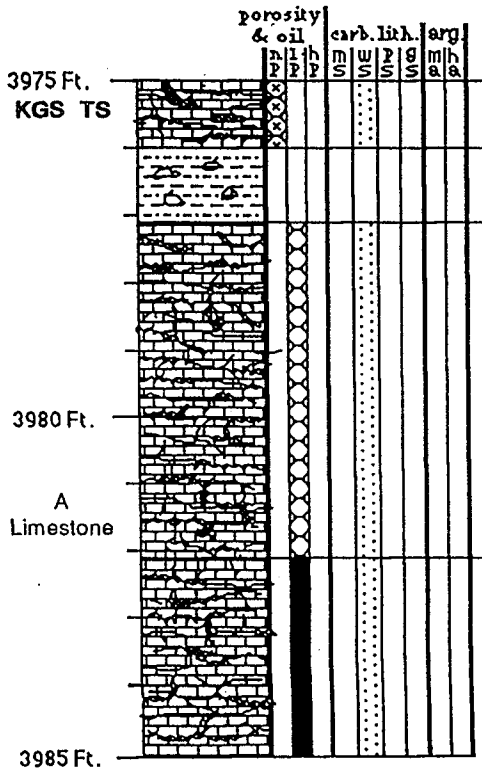

Lithologic Description and Comments
Fossiliferous wackestone with autoclastic brecciation and infilling by green shale (WS-F-B-RSH)
Red-brown silty shale with microcrystalline-calcite nodules (SH-Z-RB-MC)
Fossiliferous wackestone with autoclastic brecciation and infilling by green shale (WS-F-B-RSH) The autoclastic brecciation and shale infilling in these intervals is major. The infilling green shale has undergone pressure solution to form microstylolite seams. Post-microstylolite fractures may also be present. Oil staining is present in the fractures from brecciation.
Fossiliferous wackestone with autoclastic brecciation and infilling by green shale (WS-F-B-RSH) Fusulinids common, some may be moldic. Oil staining is more apparent in this interval than the above stratum.

SKELLY OIL CO. #1 BARTOSOVSKY

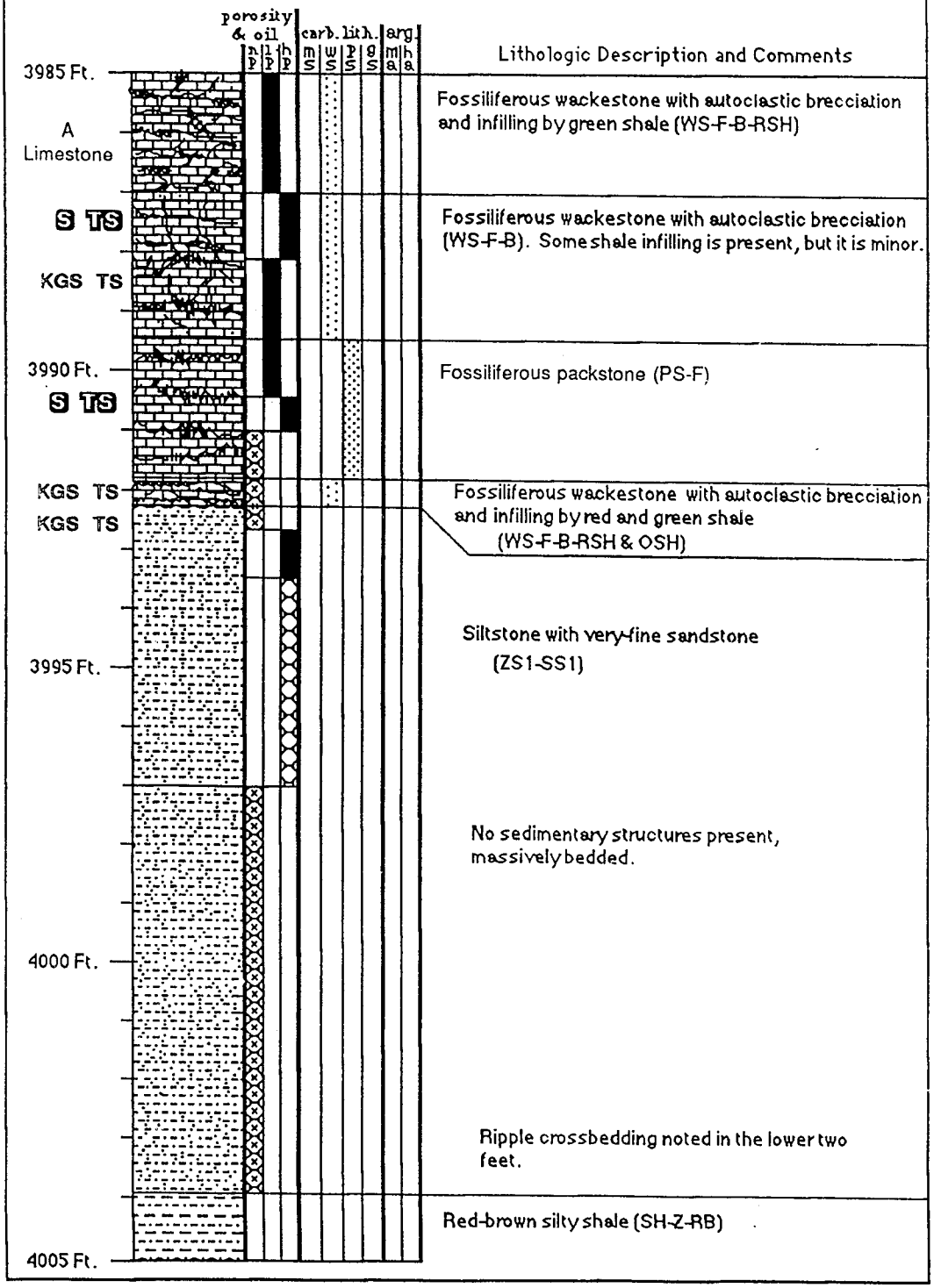

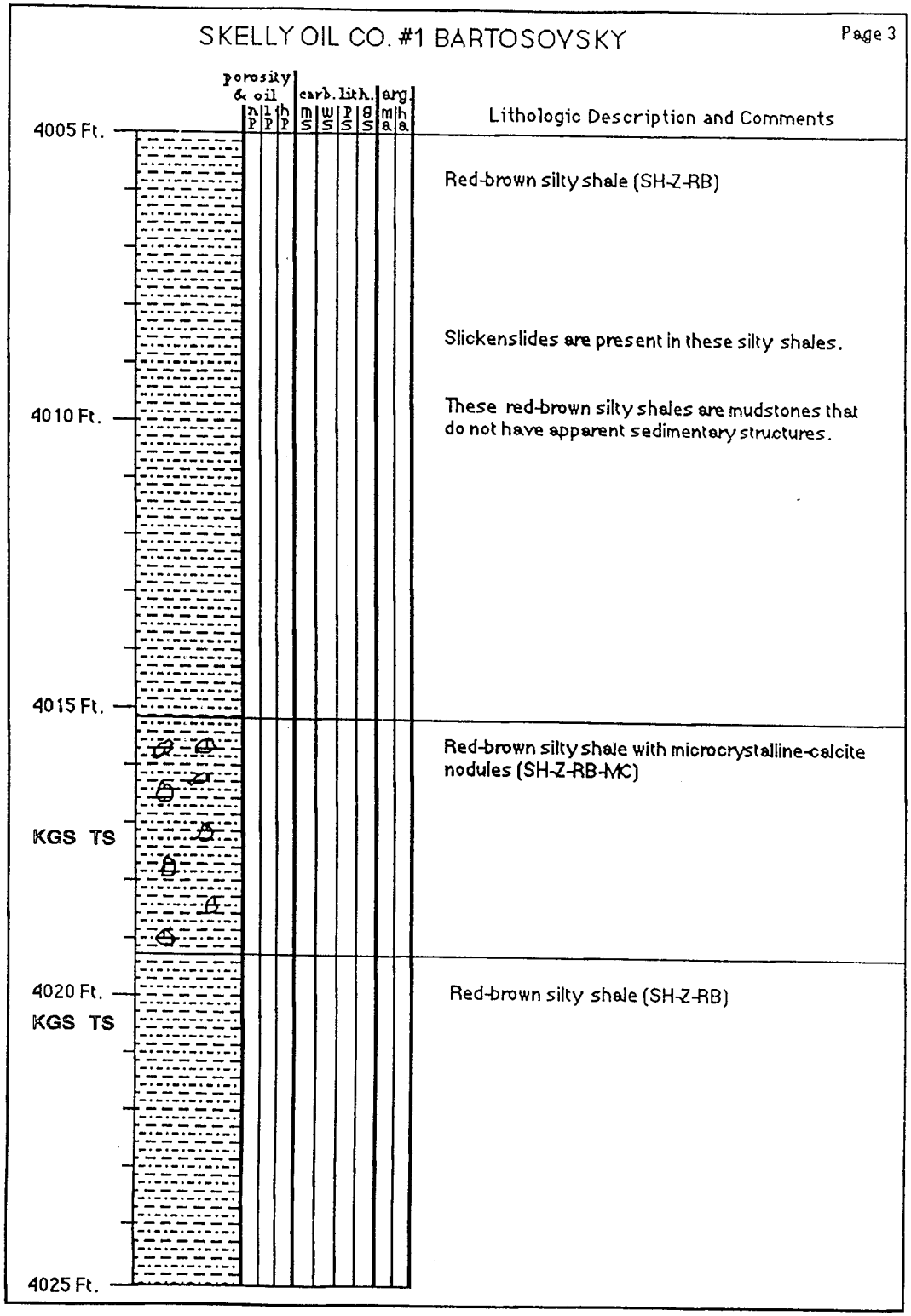
SKELLY OIL CO. #1 BARTOSOVSKY
Page 3
porosity & oil
carb. lith.
arg.
Lithologic Description and Comments
4005 Ft.
Red-brown silty shale (SH-Z-RB)
Slickenslides are present in these silty shales.
4010 Ft.
These red-brown silty shales are mudstones that do not have apparent sedimentary structures.
4015 Ft.
Red-brown silty shale with microcrystalline-calcite nodules (SH-Z-RB-MC)
KGS TS
4020 Ft.
KGS TS
Red-brown silty shale (SH-Z-RB)
4025 Ft.

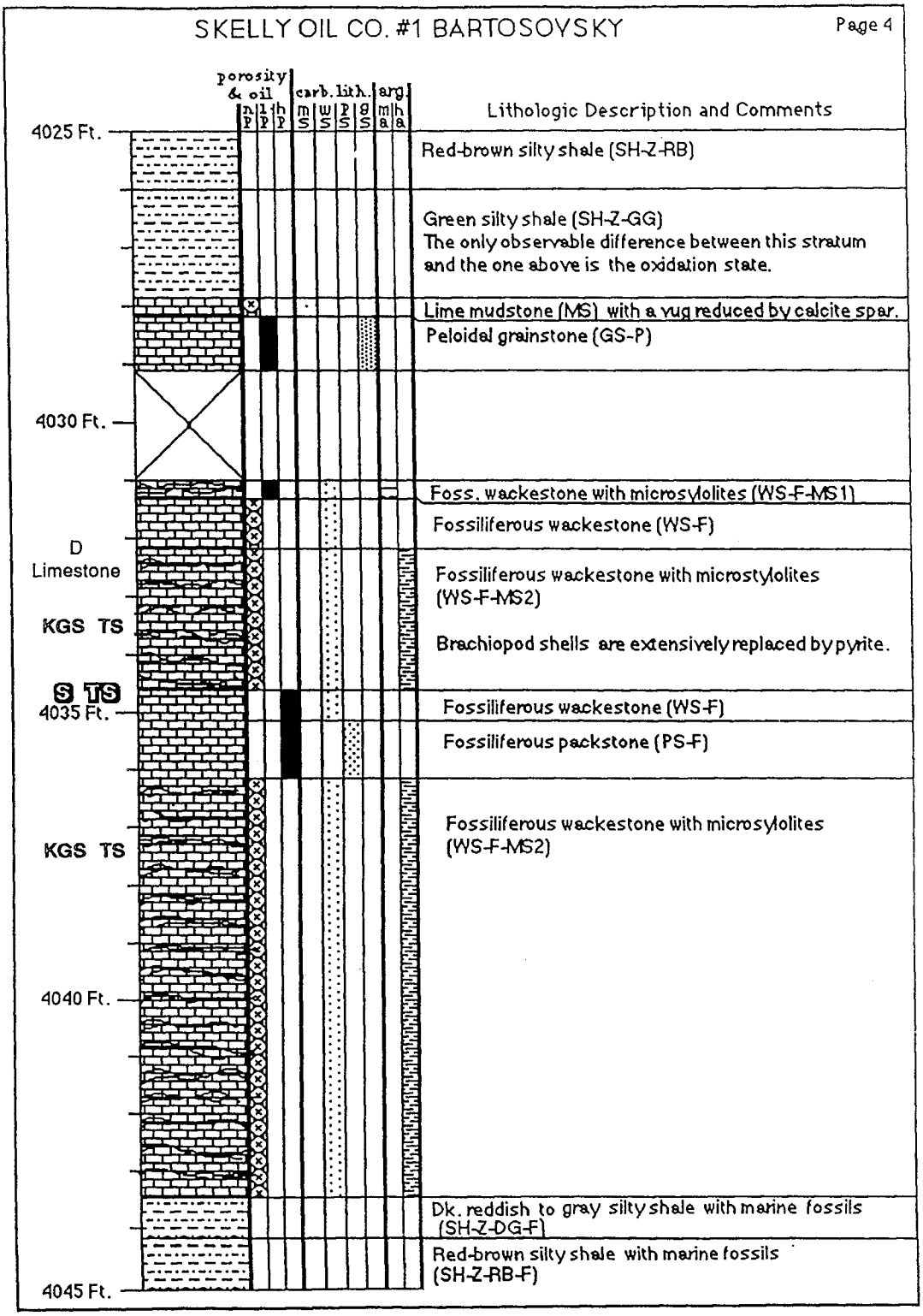
SKELLY OIL CO. #1 BARTOSOVSKY
Page 4
porosity & oil
carb. lith.
arg.
Lithologic Description and Comments
4025 Ft.
Red-brown silty shale (SH-Z-RB)
Green silty shale (SH-Z-GG)
The only observable difference between this stratum and the one above is the oxidation state.
Lime mudstone (MS) with a vug reduced by calcite spar.
Peloidal grainstone (GS-P)
4030 Ft.
Foss. wackestone with microsylolites (WS-F-MS1)
Fossiliferous wackestone (WS-F)
D Limestone
Fossiliferous wackestone with microstylolites (WS-F-MS2)
KGS TS
Brachiopod shells are extensively replaced by pyrite.
S TS
4035 Ft.
Fossiliferous wackestone (WS-F)
Fossiliferous packstone (PS-F)
KGS TS
Fossiliferous wackestone with microsylolites (WS-F-MS2)
4040 Ft.
Dk. reddish to gray silty shale with marine fossils (SH-Z-DG-F)
Red-brown silty shale with marine fossils (SH-Z-RB-F)
4045 Ft.

SKELLY OIL CO. #1 BARTOSOYSKY

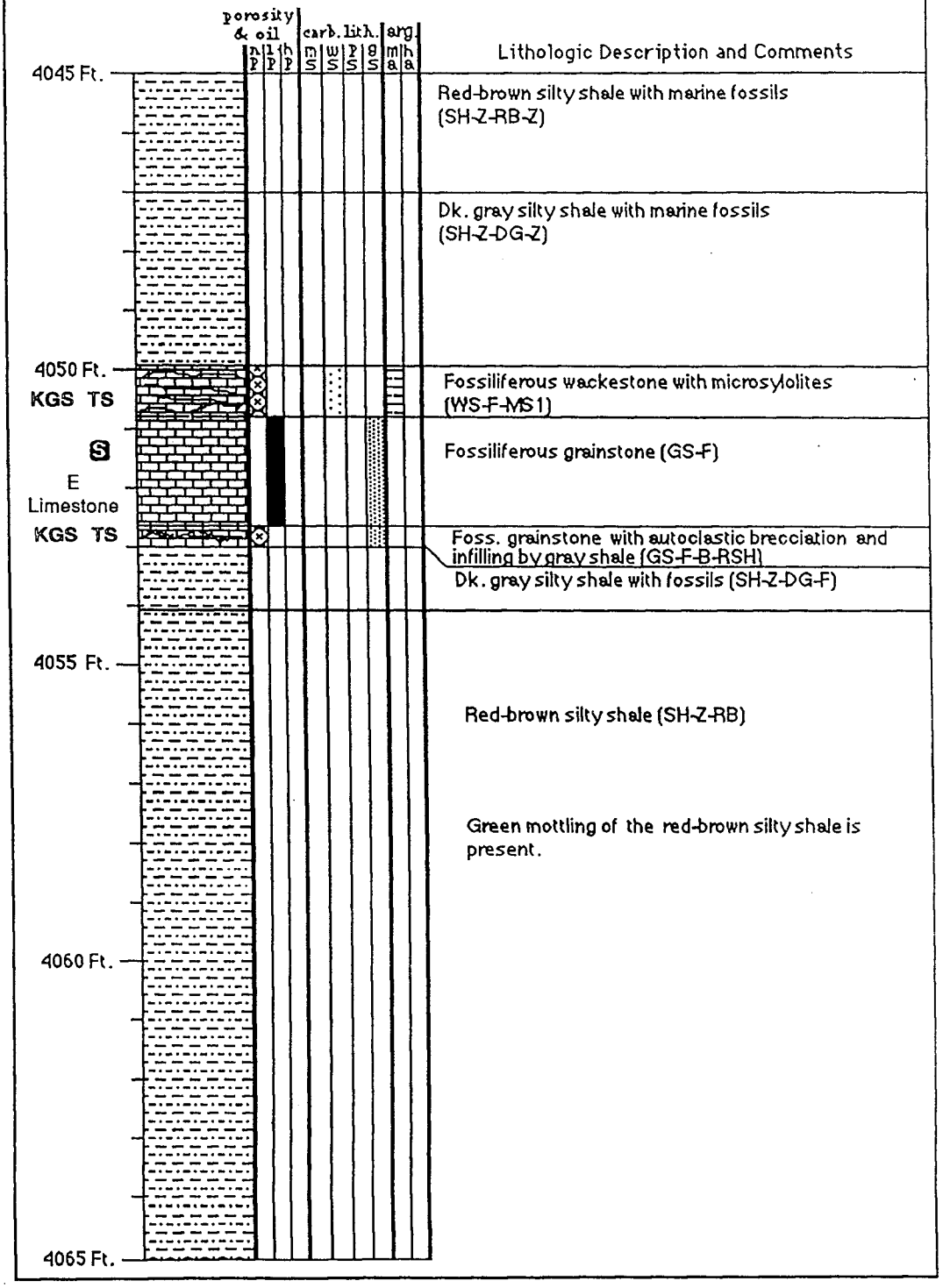

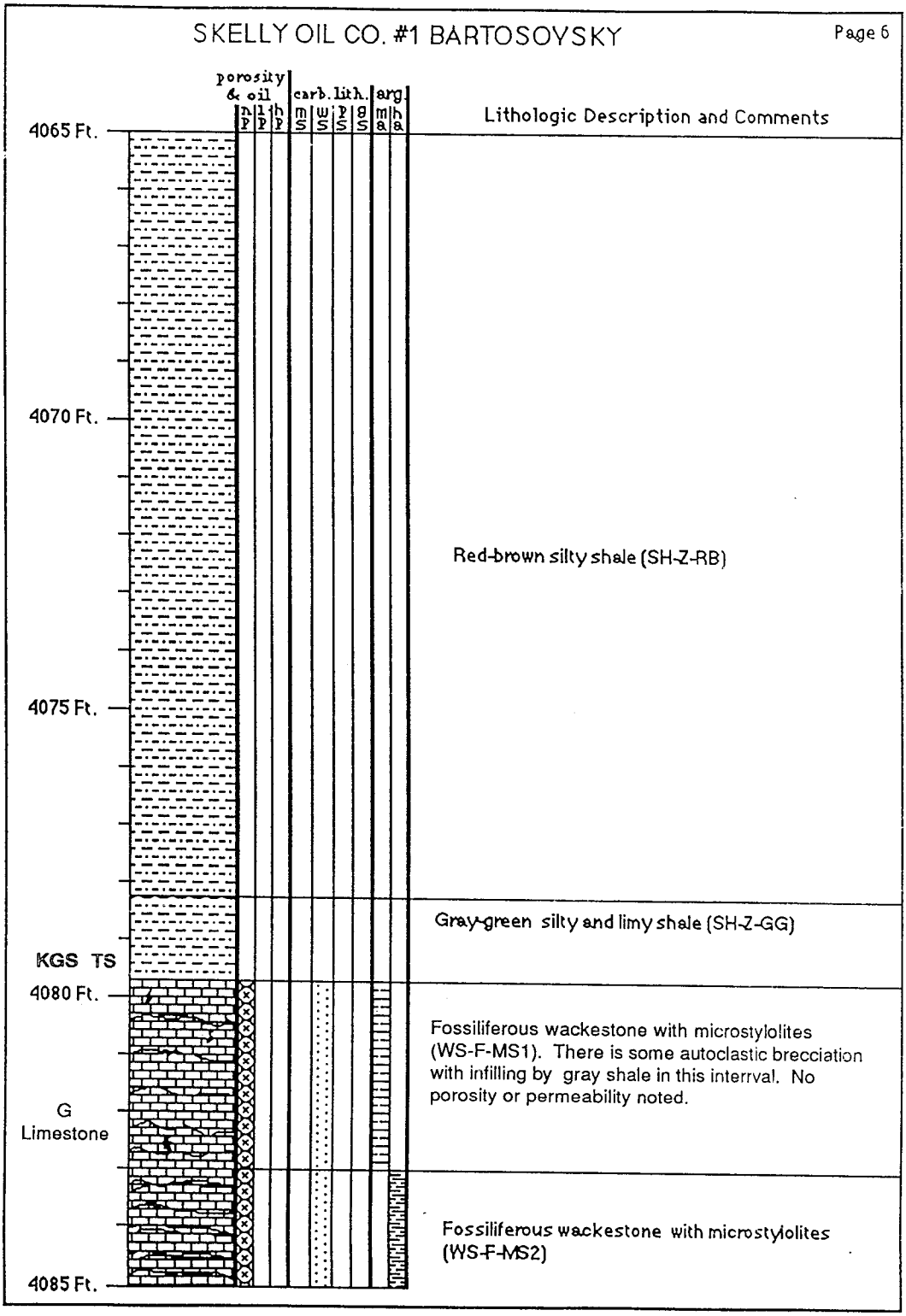
SKELLY OIL CO. #1 BARTOSOYSKY
Page 6
porosity & oil
carb. lith.
arg.
Lithologic Description and Comments
4065 Ft.
4070 Ft.
4075 Ft.
KGS TS
4080 Ft.
G Limestone
4085 Ft.
Red-brown silty shale (SH-Z-RB)
Gray-green silty and limy shale (SH-Z-GG)
Fossiliferous wackestone with microstylolites (WS-F-MS1). There is some autoclastic brecciation with infilling by gray shale in this interval. No porosity or permeability noted.
Fossiliferous wackestone with microstylolites (WS-F-MS2)

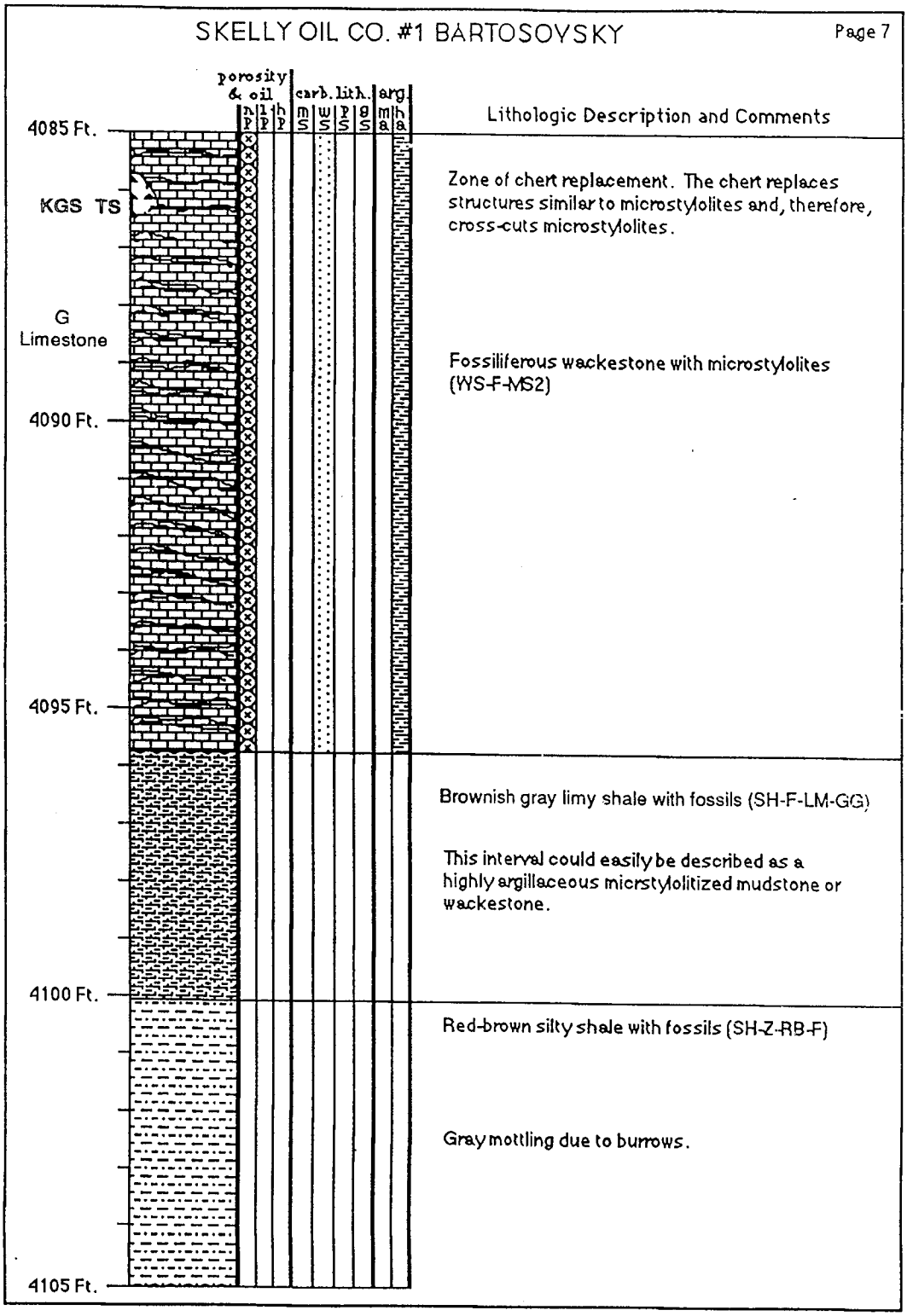
SKELLY OIL CO. #1 BARTOSOVSKY
Page 7
porosity & oil
carb. lith.
arg.
Lithologic Description and Comments
4085 Ft.
KGS TS
G Limestone
4090 Ft.
4095 Ft.
4100 Ft.
4105 Ft.
Zone of chert replacement. The chert replaces structures similar to microstylolites and, therefore, cross-cuts microstylolites.
Fossiliferous wackestone with microstylolites (WS-F-MS2)
Brownish gray limy shale with fossils (SH-F-LM-GG)
This interval could easily be described as a highly argillaceous micrstylolitized mudstone or wackestone.
Red-brown silty shale with fossils (SH-Z-RB-F)
Gray mottling due to burrows.

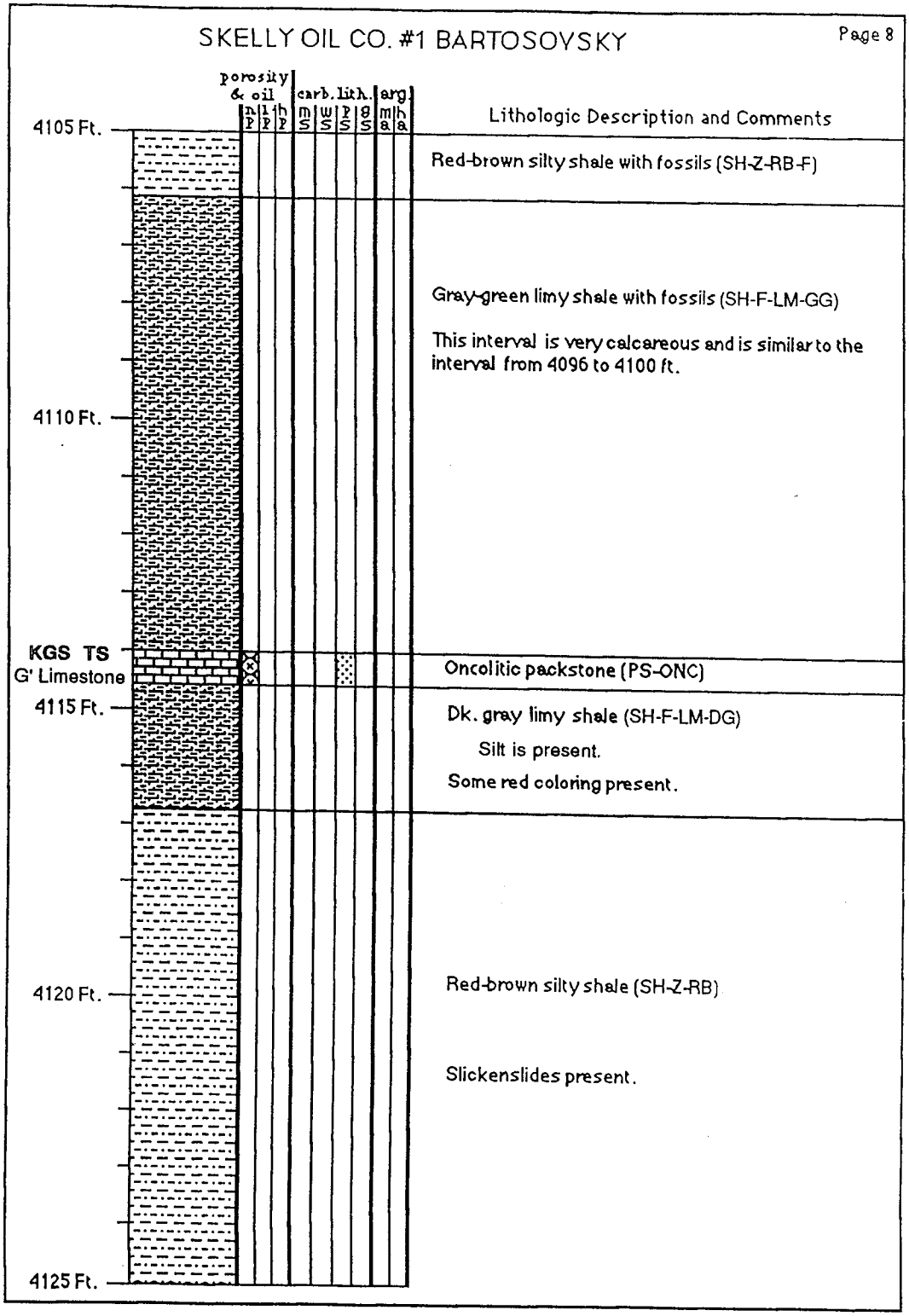
SKELLY OIL CO. #1 BARTOSOYSKY
Page 8
porosity & oil
carb. lith.
arg
Lithologic Description and Comments
4105 Ft.
Red-brown silty shale with fossils (SH-Z-RB-F)
Gray-green limy shale with fossils (SH-F-LM-GG)
This interval is very calcareous and is similar to the interval from 4096 to 4100 ft.
4110 Ft.
KGS TS
G' Limestone
Oncolitic packstone (PS-ONC)
4115 Ft.
Dk. gray limy shale (SH-F-LM-DG)
Silt is present.
Some red coloring present.
4120 Ft.
Red-brown silty shale (SH-Z-RB)
Slickenslides present.
4125 Ft.

SKELLY OIL CO. #1 BARTOSOVSKY

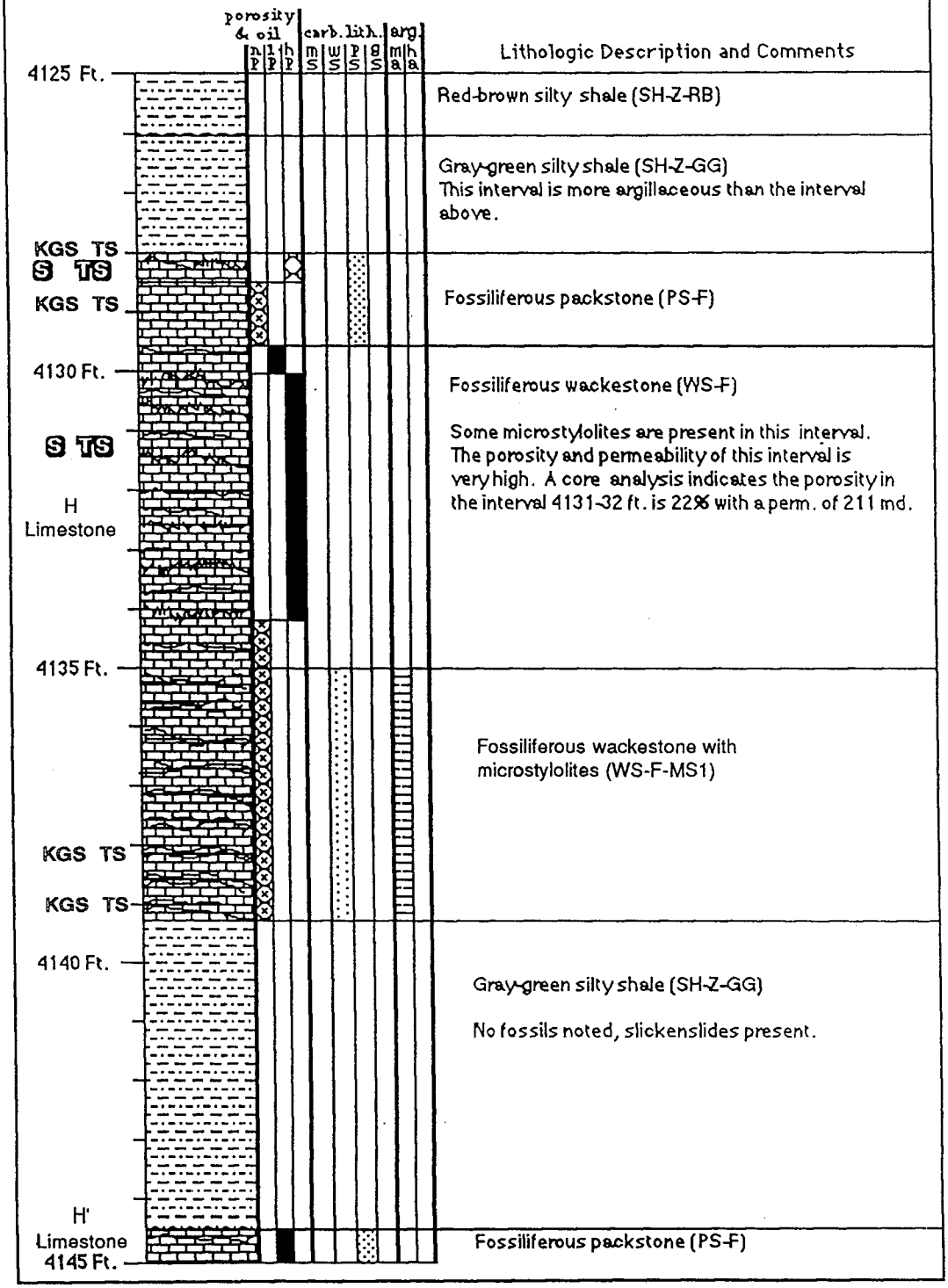

SKELLY OIL CO. #1 BARTOSOYSKY

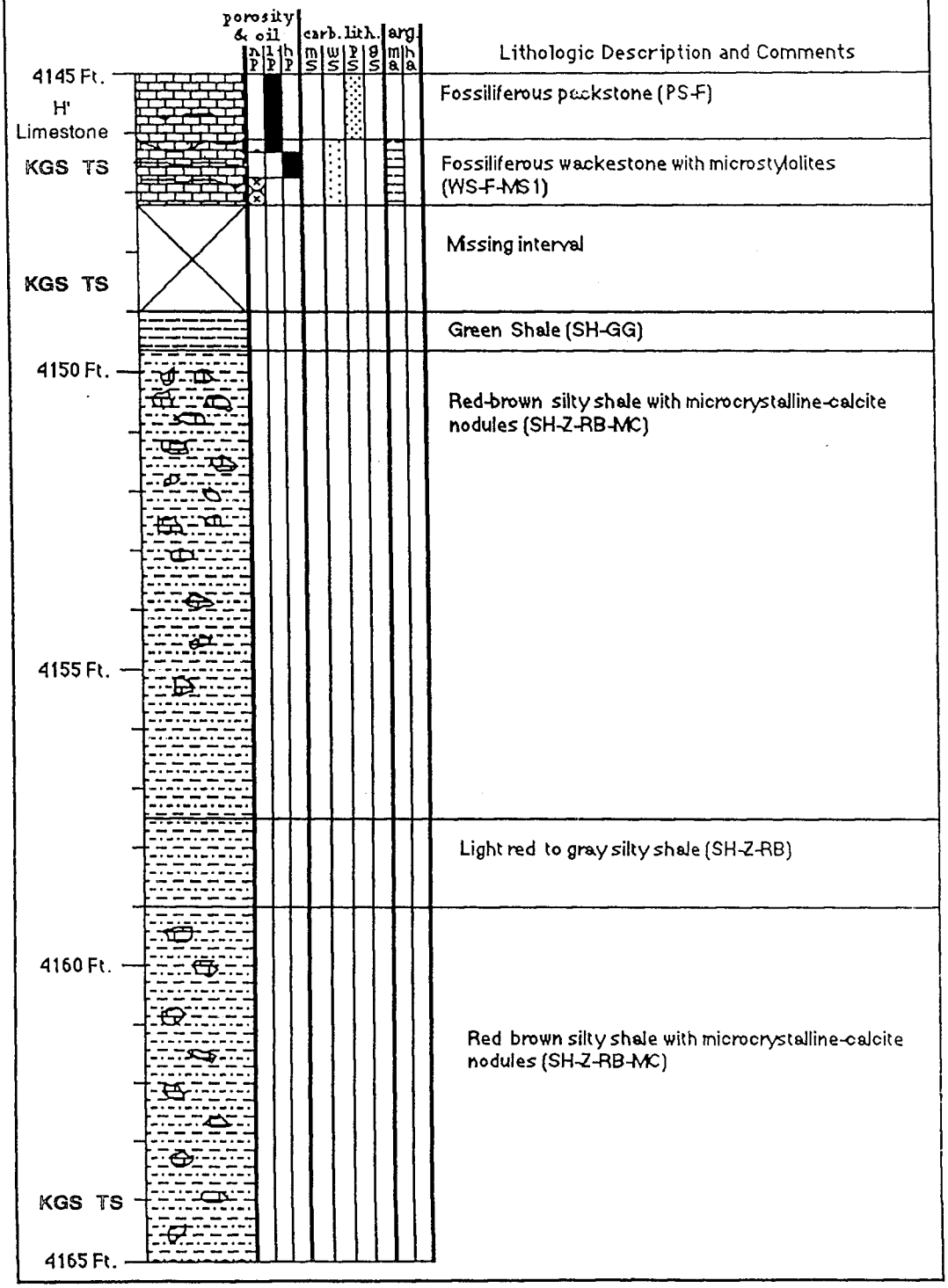

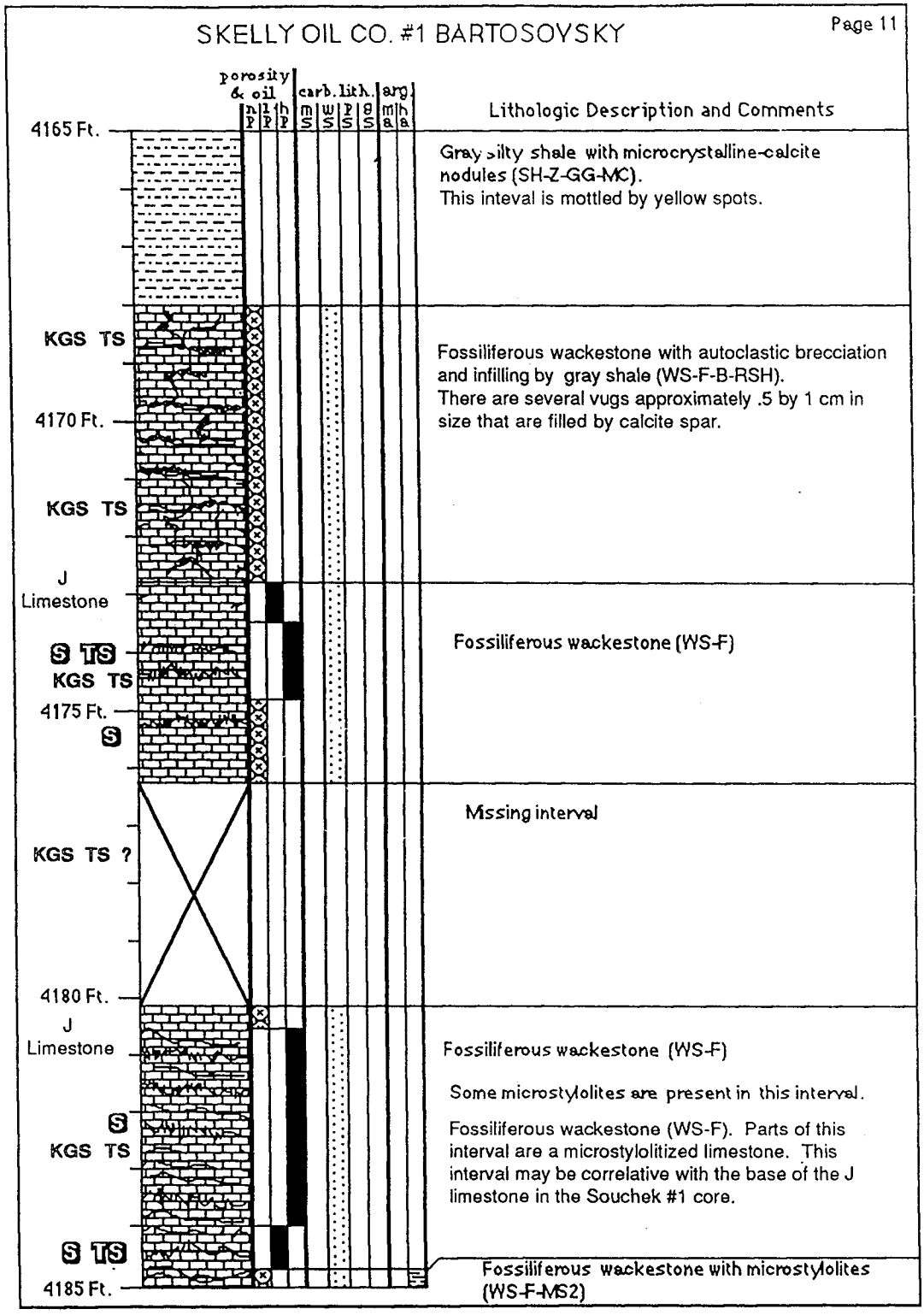
SKELLY OIL CO. #1 BARTOSOYSKY
Page 11
porosity & oil
carb. lith.
arg
Lithologic Description and Comments
4165 Ft.
Gray silty shale with microcrystalline-calcite nodules (SH-Z-GG-MC).
This inteval is mottled by yellow spots.
KGS TS
4170 Ft.
Fossiliferous wackestone with autoclastic brecciation and infilling by gray shale (WS-F-B-RSH).
There are several vugs approximately .5 by 1 cm in size that are filled by calcite spar.
KGS TS
J Limestone
S TS
KGS TS
4175 Ft.
S
Fossiliferous wackestone (WS-F)
Missing interval
KGS TS ?
4180 Ft.
J Limestone
Fossiliferous wackestone (WS-F)
Some microstylolites are present in this interval.
S
KGS TS
Fossiliferous wackestone (WS-F). Parts of this interval are a microstylolitized limestone. This interval may be correlative with the base of the J limestone in the Souchek #1 core.
S TS
4185 Ft.
Fossiliferous wackestone with microstylolites (WS-F-MS2)

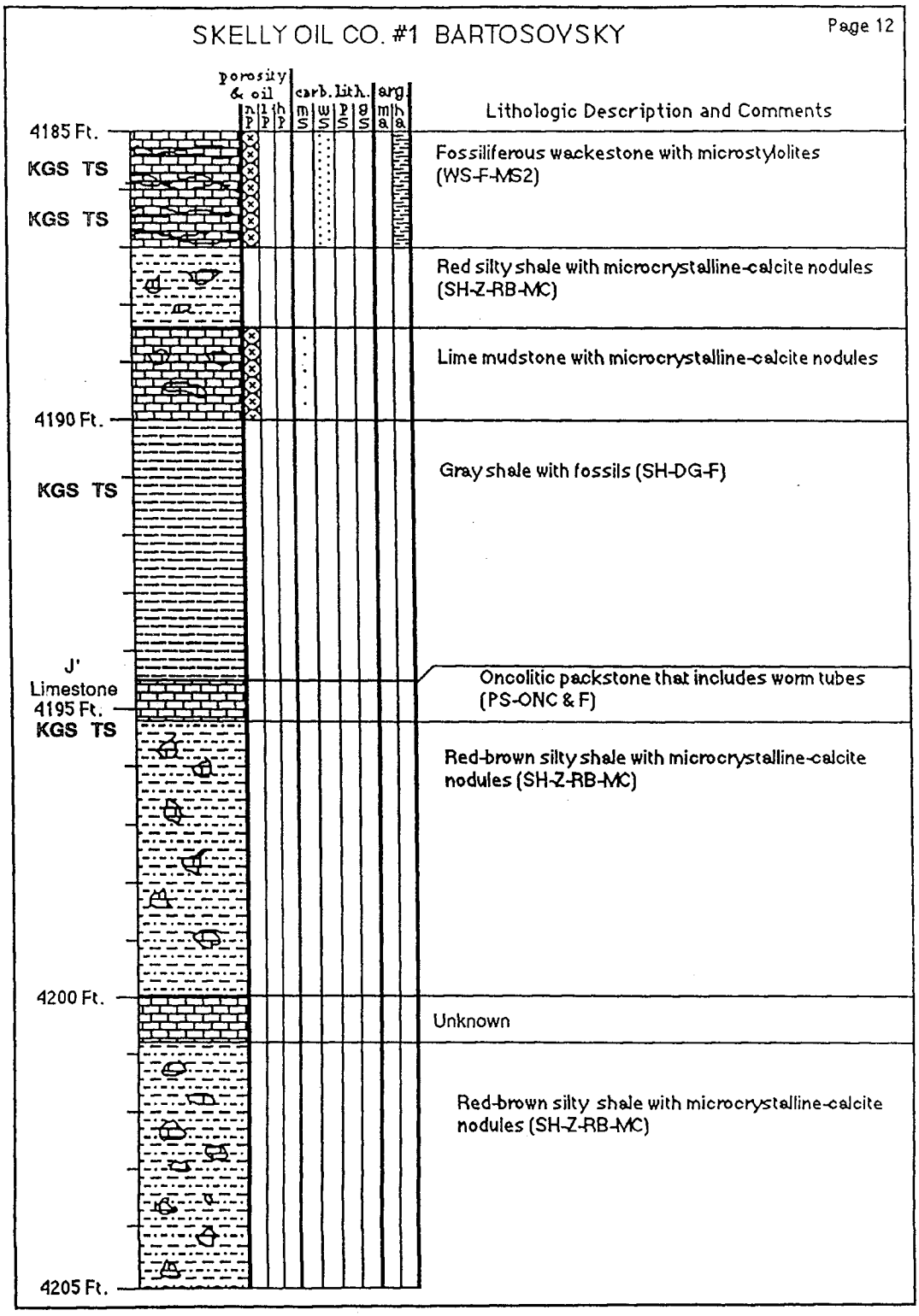
SKELLY OIL CO. #1 BARTOSOVSKY
Page 12
porosity & oil
carb. lith.
arg.
Lithologic Description and Comments
4185 Ft.
KGS TS
KGS TS
Fossiliferous wackestone with microstylolites (WS-F-MS2)
Red silty shale with microcrystalline-calcite nodules (SH-Z-RB-MC)
Lime mudstone with microcrystalline-calcite nodules
4190 Ft.
KGS TS
Gray shale with fossils (SH-DG-F)
J' Limestone
4195 Ft.
KGS TS
Oncolitic packstone that includes worm tubes (PS-ONC & F)
Red-brown silty shale with microcrystalline-calcite nodules (SH-Z-RB-MC)
4200 Ft.
Unknown
Red-brown silty shale with microcrystalline-calcite nodules (SH-Z-RB-MC)
4205 Ft.

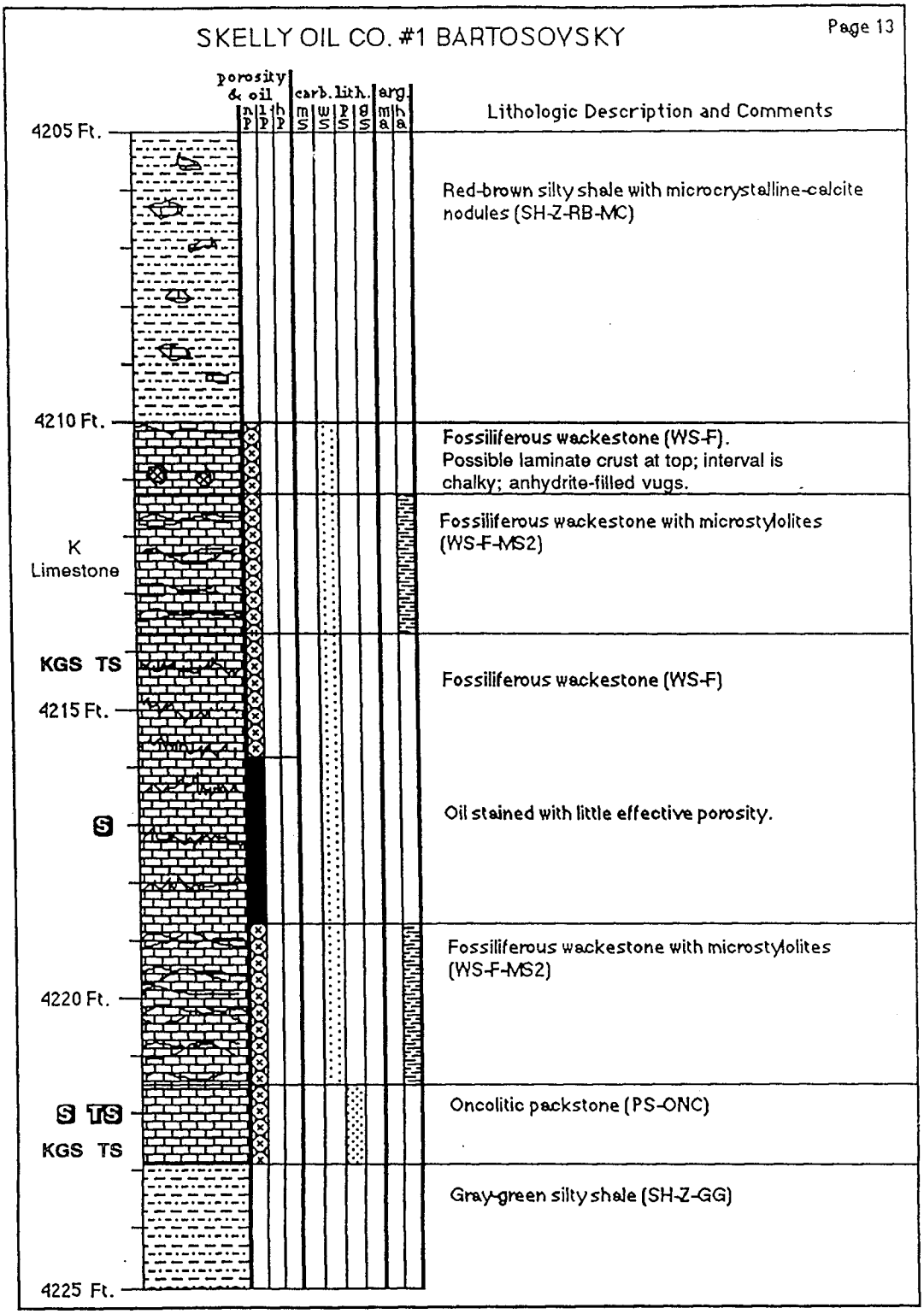
SKELLY OIL CO. #1 BARTOSOVSKY
porosity & oil
n p
l p
h p
carb. lith.
m s
w s
p s
g s
arg.
m a
h a
Lithologic Description and Comments
4205 Ft.
Red-brown silty shale with microcrystalline-calcite nodules (SH-Z-RB-MC)
4210 Ft.
Fossiliferous wackestone (WS-F). Possible laminate crust at top; interval is chalky; anhydrite-filled vugs.
Fossiliferous wackestone with microstylolites (WS-F-MS2)
K Limestone
KGS TS
Fossiliferous wackestone (WS-F)
4215 Ft.
S
Oil stained with little effective porosity.
Fossiliferous wackestone with microstylolites (WS-F-MS2)
4220 Ft.
S TS
Oncolitic packstone (PS-ONC)
KGS TS
Gray-green silty shale (SH-Z-GG)
4225 Ft.

SKELLY OIL CO. #1 BARTOSOVSKY

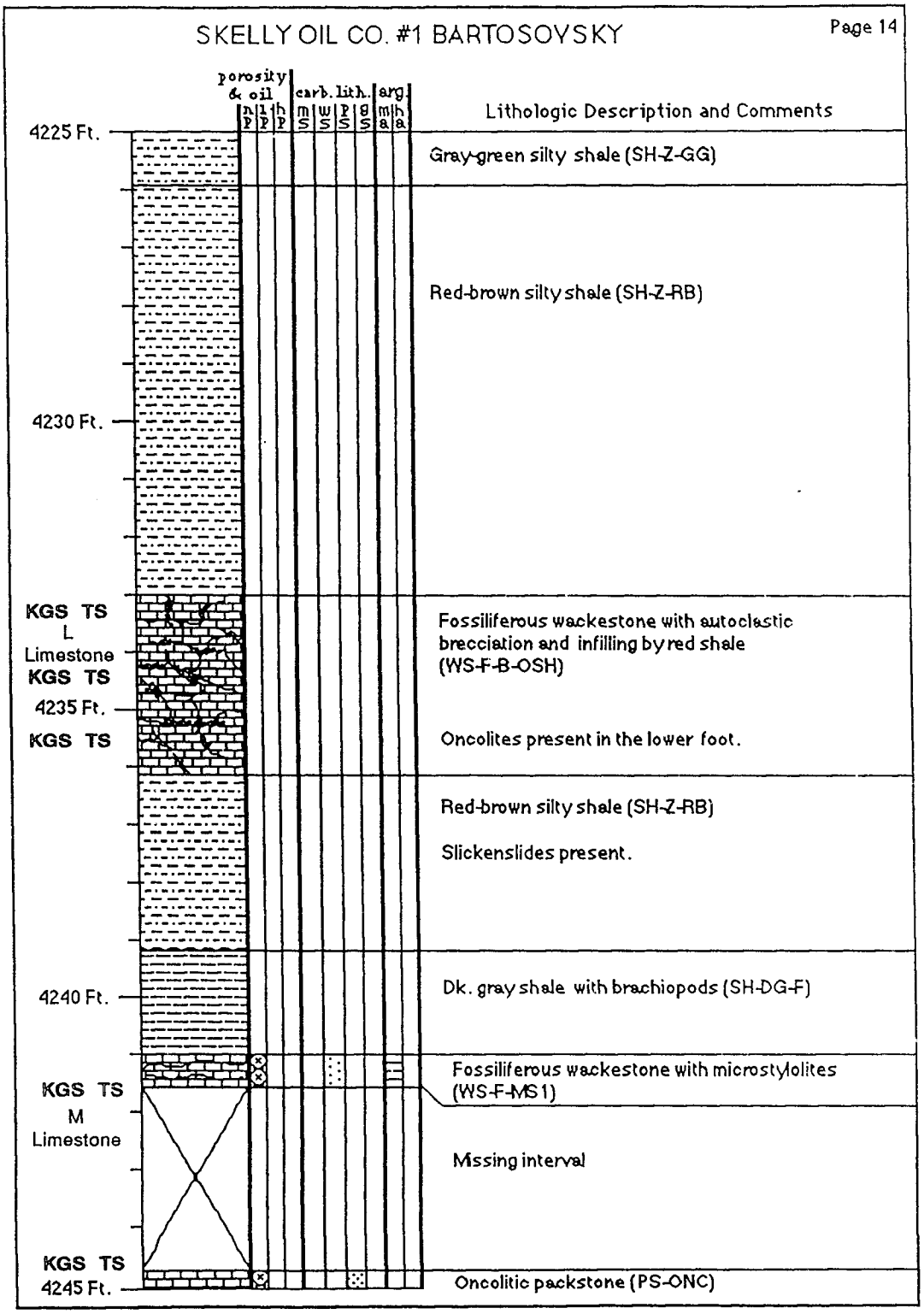

SKELLY OIL CO. #1 BARTOSOVSKY

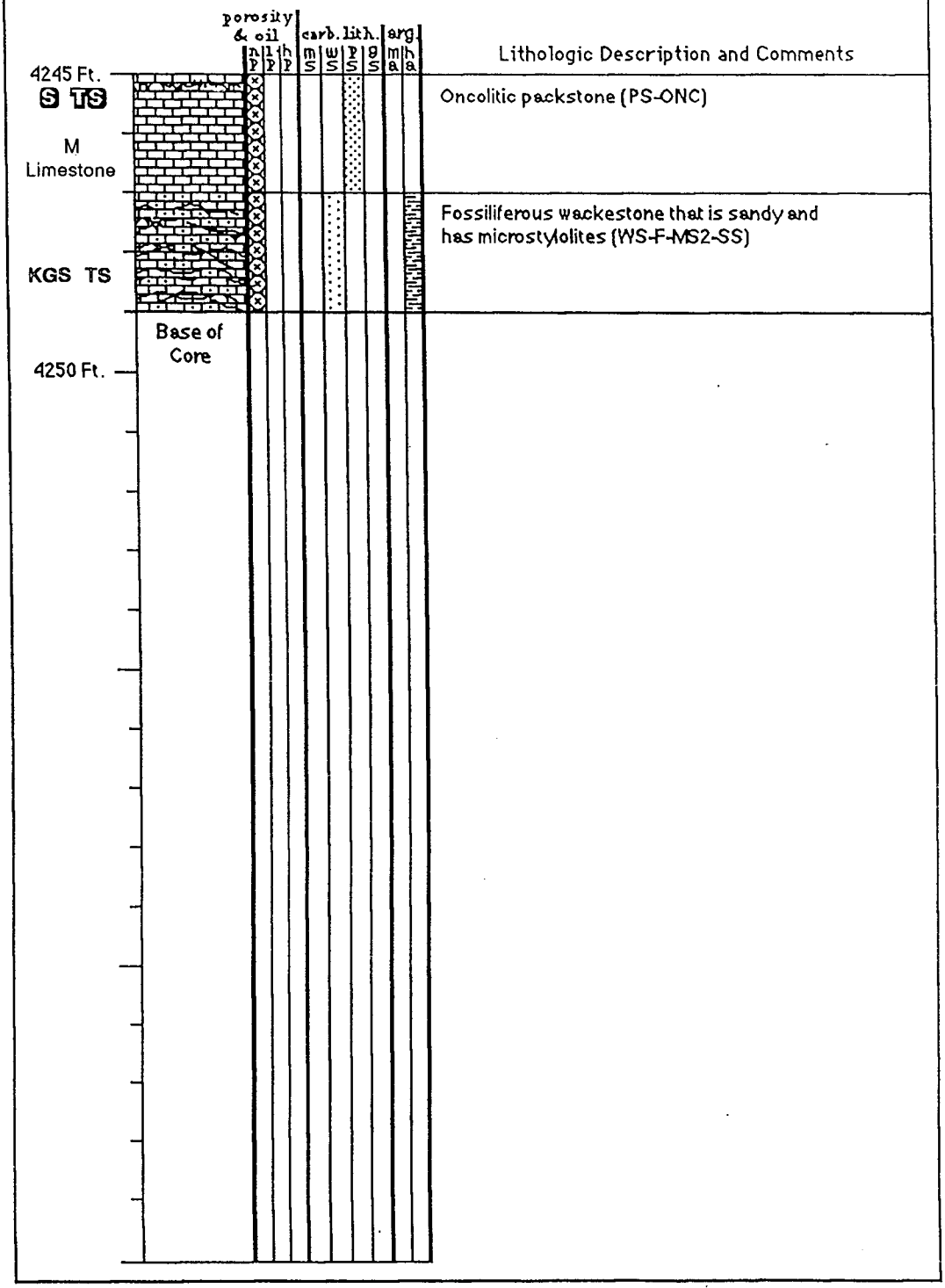

CONTINENTAL OIL CO. #1 MARY A. TAYLOR

SW SW NW, Section 35-T5S-R27W
Decatur County, Kansas

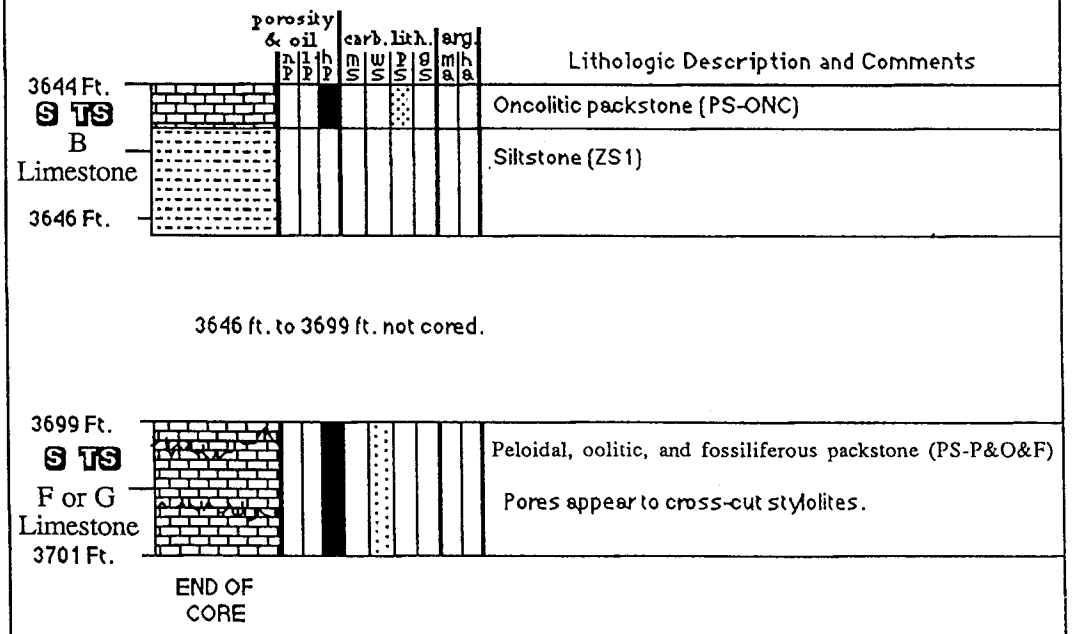

CITIES SERVICE #1 BOURQUIN "A"

NE NW NE, Sec. 18-T6S-R32W
Thomas County, Kansas

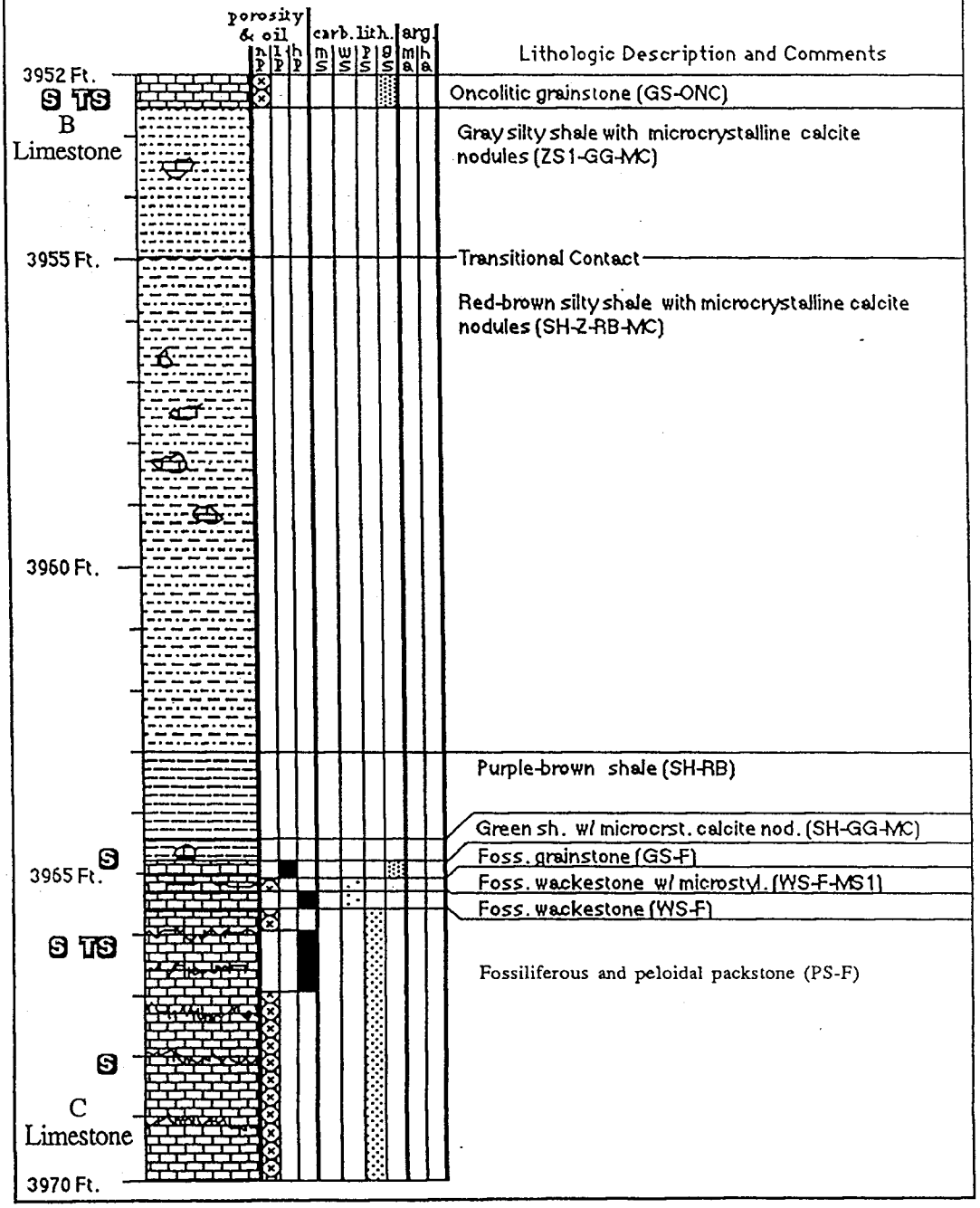

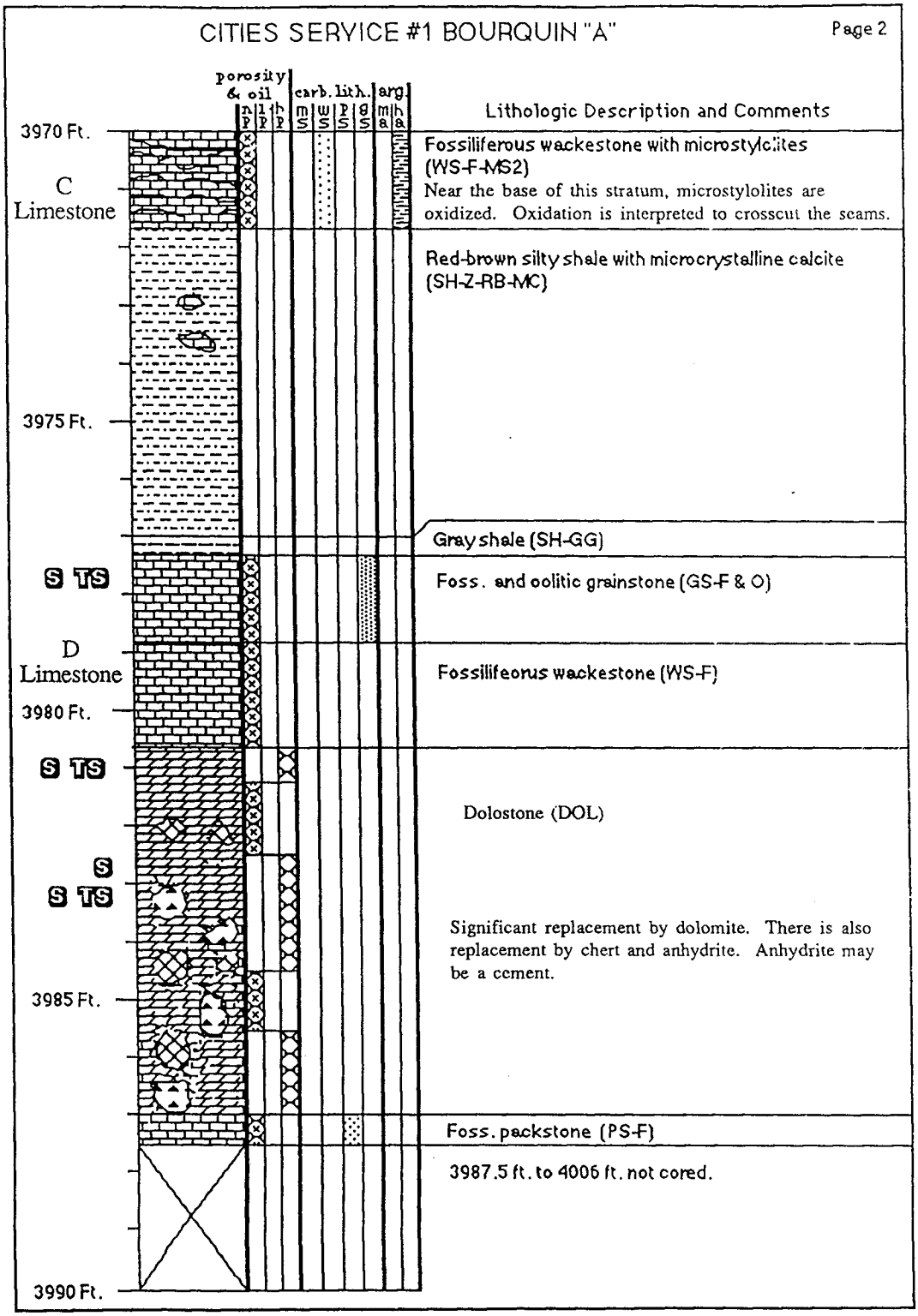
CITIES SERVICE #1 BOURQUIN "A"
Page 2
porosity & oil
carb. lith.
arg.
Lithologic Description and Comments
3970 Ft.
C Limestone
Fossiliferous wackestone with microstylolites (WS-F-MS2)
Near the base of this stratum, microstylolites are oxidized. Oxidation is interpreted to crosscut the seams.
Red-brown silty shale with microcrystalline calcite (SH-Z-RB-MC)
3975 Ft.
Gray shale (SH-GG)
S TS
Foss. and oolitic grainstone (GS-F & O)
D Limestone
Fossilifeorus wackestone (WS-F)
3980 Ft.
S TS
Dolostone (DOL)
S
S TS
Significant replacement by dolomite. There is also replacement by chert and anhydrite. Anhydrite may be a cement.
3985 Ft.
Foss. packstone (PS-F)
3987.5 ft. to 4006 ft. not cored.
3990 Ft.

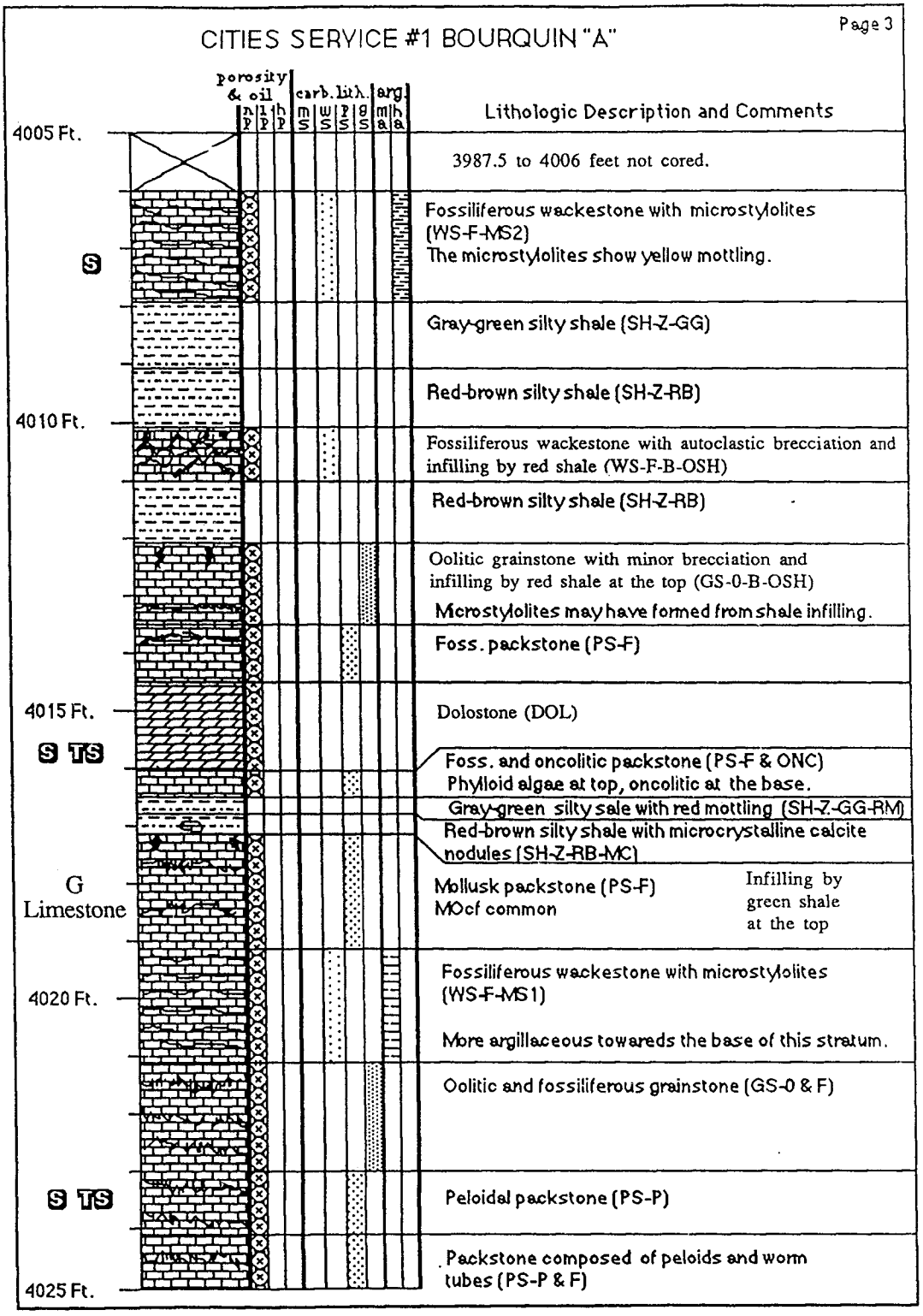
CITIES SERVICE #1 BOURQUIN "A"
porosity & oil
carb. lith.
arg.
Lithologic Description and Comments
4005 Ft.
3987.5 to 4006 feet not cored.
S
Fossiliferous wackestone with microstylolites (WS-F-MS2)
The microstylolites show yellow mottling.
Gray-green silty shale (SH-Z-GG)
Red-brown silty shale (SH-Z-RB)
4010 Ft.
Fossiliferous wackestone with autoclastic brecciation and infilling by red shale (WS-F-B-OSH)
Red-brown silty shale (SH-Z-RB)
Oolitic grainstone with minor brecciation and infilling by red shale at the top (GS-0-B-OSH)
Microstylolites may have formed from shale infilling.
Foss. packstone (PS-F)
4015 Ft.
Dolostone (DOL)
S TS
Foss. and oncolitic packstone (PS-F & ONC)
Phylloid algae at top, oncolitic at the base.
Gray-green silty sale with red mottling (SH-Z-GG-RM)
Red-brown silty shale with microcrystalline calcite nodules (SH-Z-RB-MC)
G Limestone
Mollusk packstone (PS-F)
MOcf common
Infilling by green shale at the top
Fossiliferous wackestone with microstylolites (WS-F-MS1)
4020 Ft.
More argillaceous towareds the base of this stratum.
Oolitic and fossiliferous grainstone (GS-0 & F)
S TS
Peloidal packstone (PS-P)
Packstone composed of peloids and worm tubes (PS-P & F)
4025 Ft.

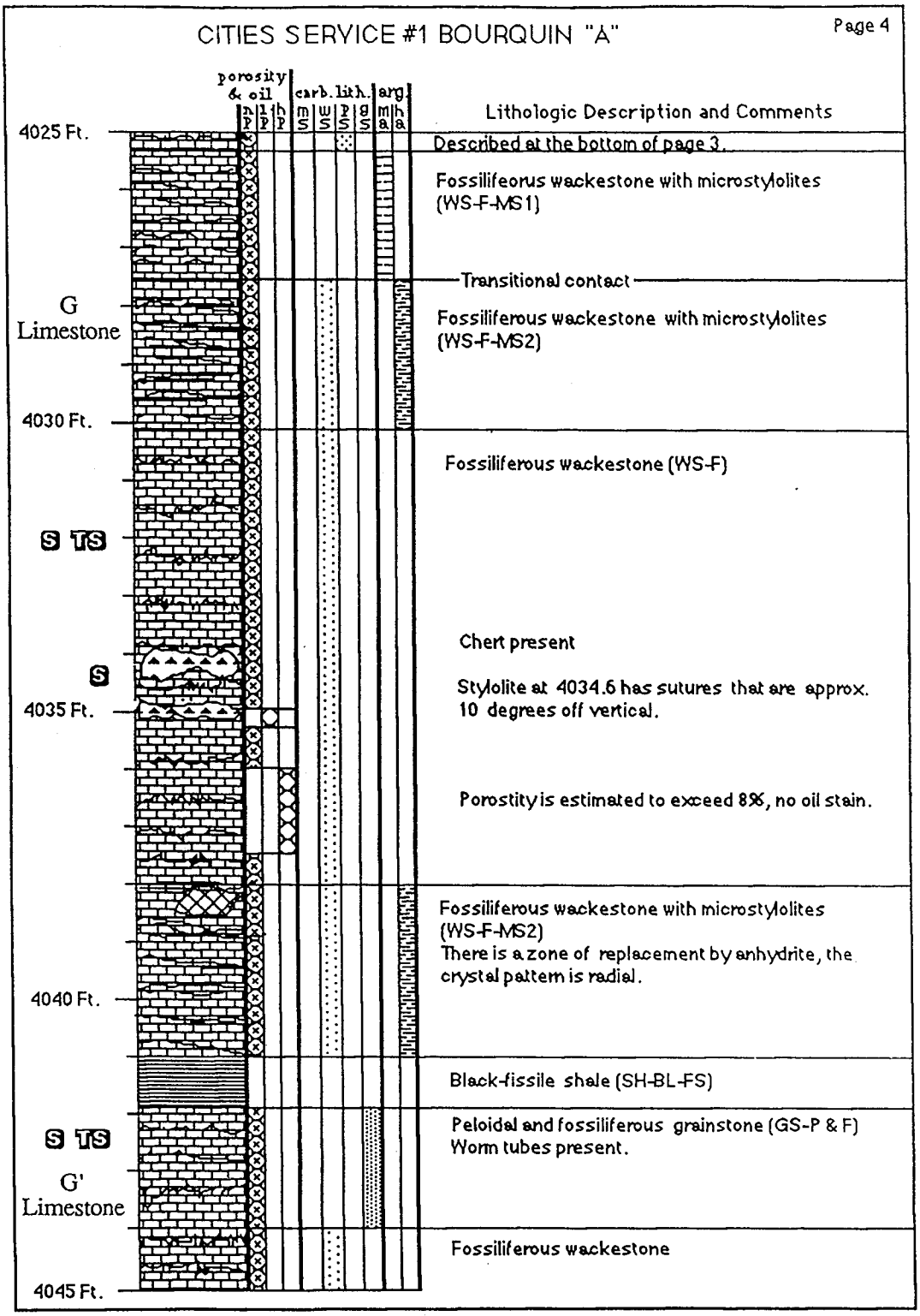
CITIES SERVICE #1 BOURQUIN "A"
Page 4
porosity & oil
carb. lith.
arg.
Lithologic Description and Comments
4025 Ft.
Described at the bottom of page 3.
Fossilifeorus wackestone with microstylolites (WS-F-MS1)
Transitional contact
G Limestone
Fossiliferous wackestone with microstylolites (WS-F-MS2)
4030 Ft.
Fossiliferous wackestone (WS-F)
S TS
Chert present
S
Stylolite at 4034.6 has sutures that are approx. 10 degrees off vertical.
4035 Ft.
Porostity is estimated to exceed 8%, no oil stain.
Fossiliferous wackestone with microstylolites (WS-F-MS2)
There is a zone of replacement by anhydrite, the crystal pattern is radial.
4040 Ft.
Black-fissile shale (SH-BL-FS)
S TS
Peloidal and fossiliferous grainstone (GS-P & F)
Worm tubes present.
G' Limestone
Fossiliferous wackestone
4045 Ft.

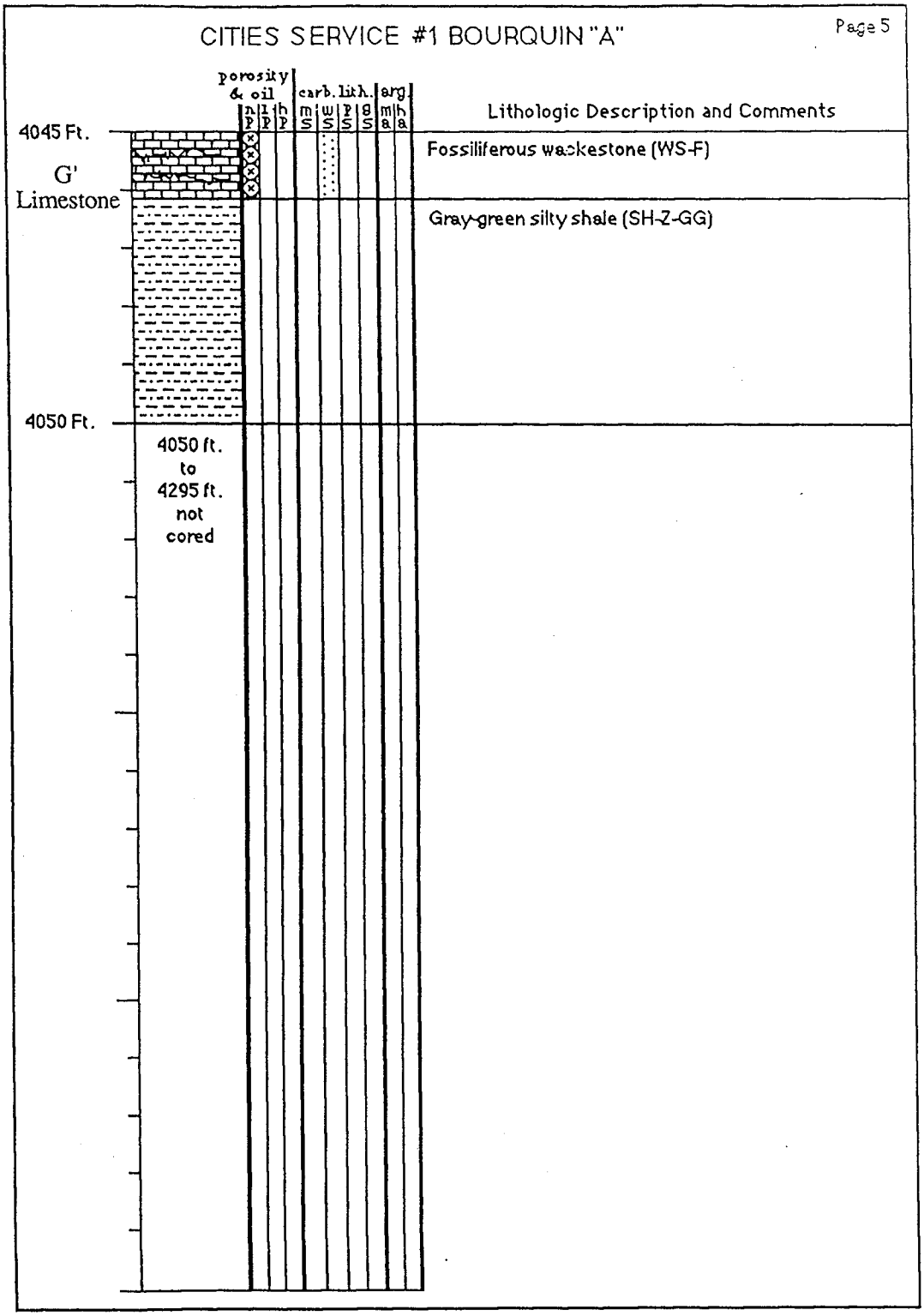
CITIES SERVICE #1 BOURQUIN "A"
Page 5
porosity & oil
carb. lith.
arg
Lithologic Description and Comments
4045 Ft.
G'
Limestone
Fossiliferous wackestone (WS-F)
Gray-green silty shale (SH-Z-GG)
4050 Ft.
4050 ft.
to
4295 ft.
not
cored

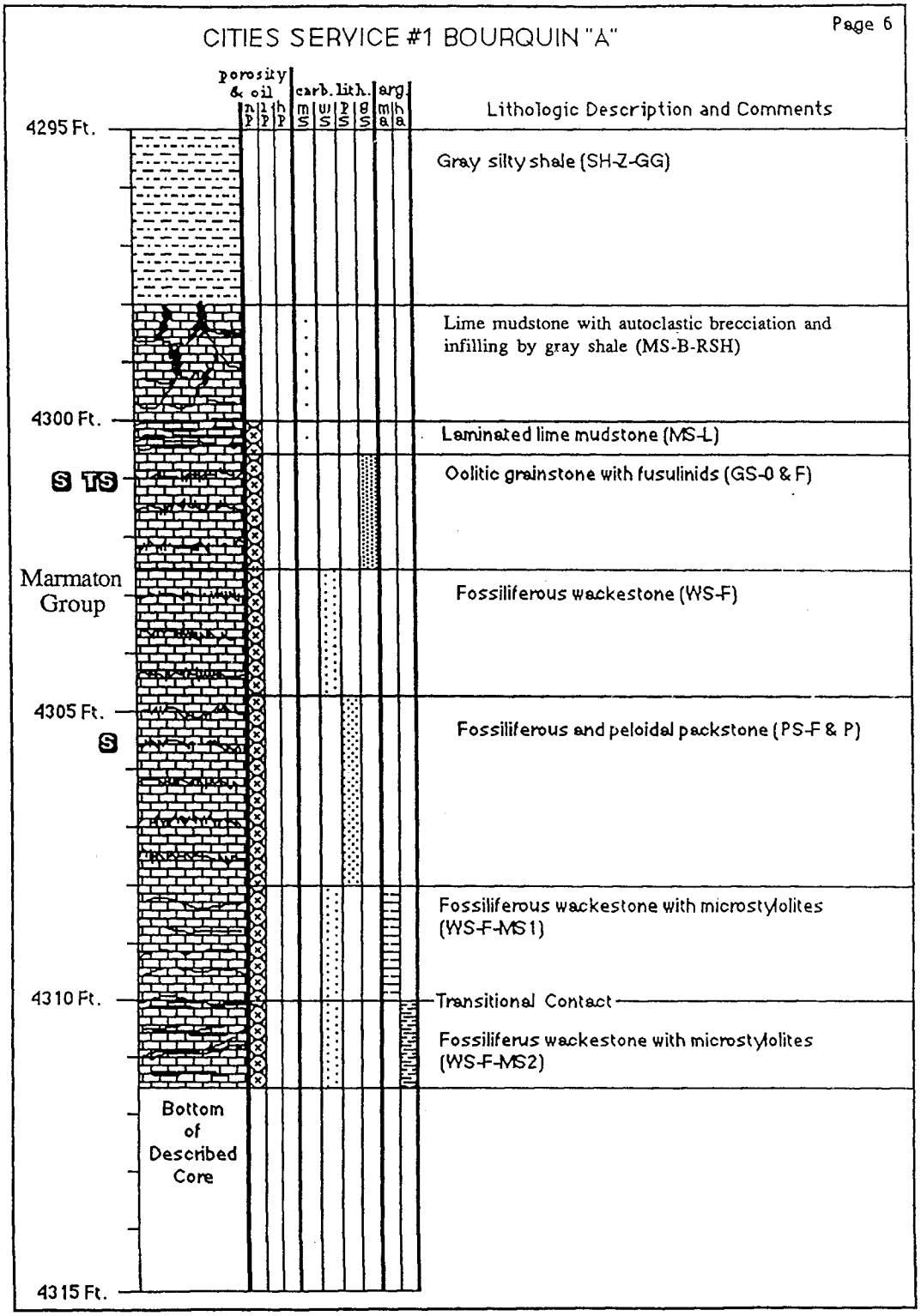
CITIES SERVICE #1 BOURQUIN "A"
porosity & oil
carb. lith.
arg
Lithologic Description and Comments
4295 Ft.
Gray silty shale (SH-Z-GG)
Lime mudstone with autoclastic brecciation and infilling by gray shale (MS-B-RSH)
4300 Ft.
Laminated lime mudstone (MS-L)
S TS
Oolitic grainstone with fusulinids (GS-O & F)
Marmaton Group
Fossiliferous wackestone (WS-F)
4305 Ft.
S
Fossiliferous and peloidal packstone (PS-F & P)
Fossiliferous wackestone with microstylolites (WS-F-MS1)
4310 Ft.
Transitional Contact
Fossiliferus wackestone with microstylolites (WS-F-MS2)
Bottom of Described Core
4315 Ft.

CITIES SERVICE #1 RYAN B

NW SW NW,
Sec.14-T5S-R32W

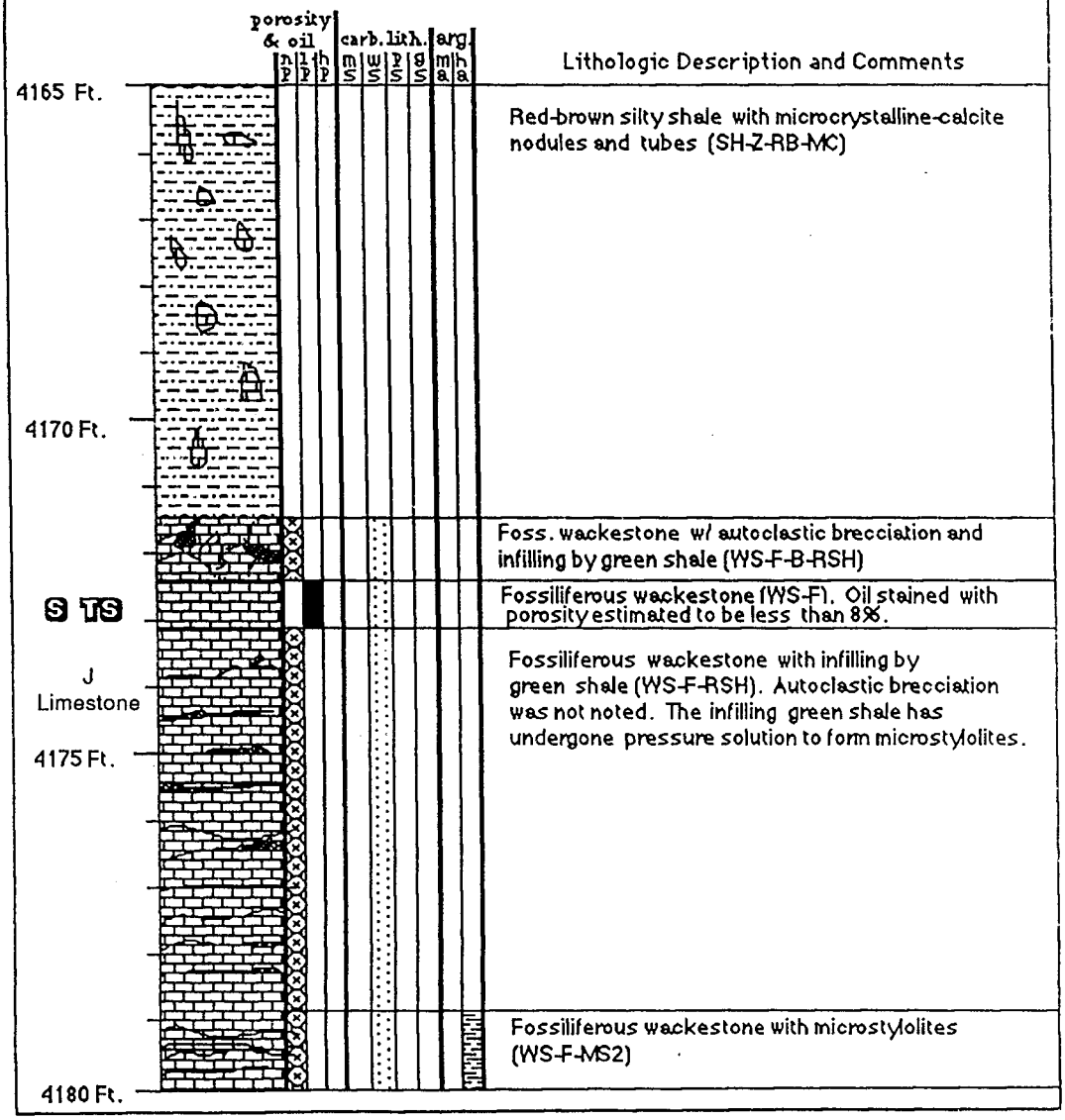

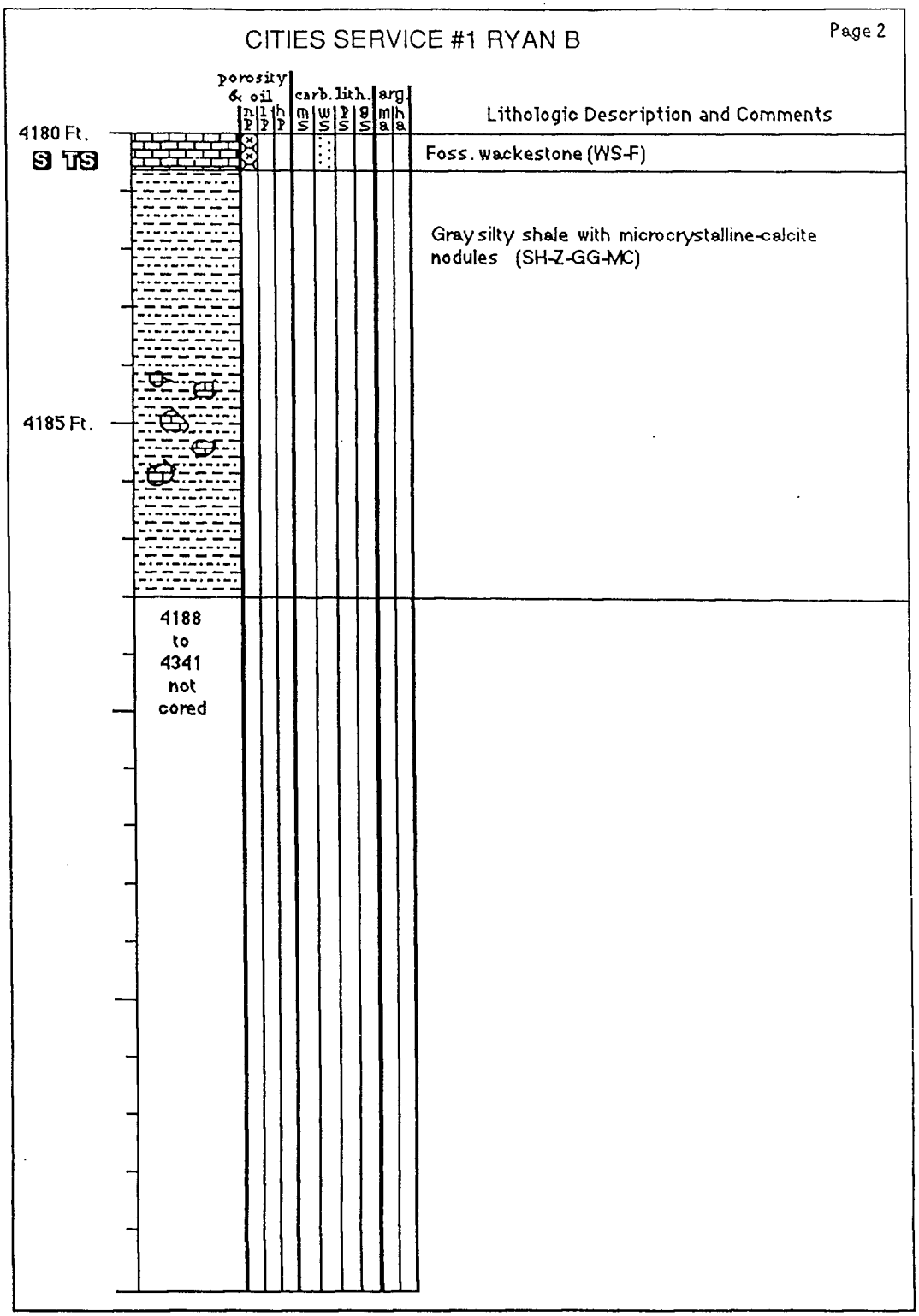
CITIES SERVICE #1 RYAN B
Page 2
porosity & oil
carb. lith.
arg.
Lithologic Description and Comments
4180 Ft.
S TS
Foss. wackestone (WS-F)
Gray silty shale with microcrystalline-calcite nodules (SH-Z-GG-MC)
4185 Ft.
4188 to 4341 not cored

CITIES SERVICES #1 HOLMDAHL A

NE SW SW, Sec. 29-T3S-R31W
Rawlins Co., Kansas
D&A, 1977

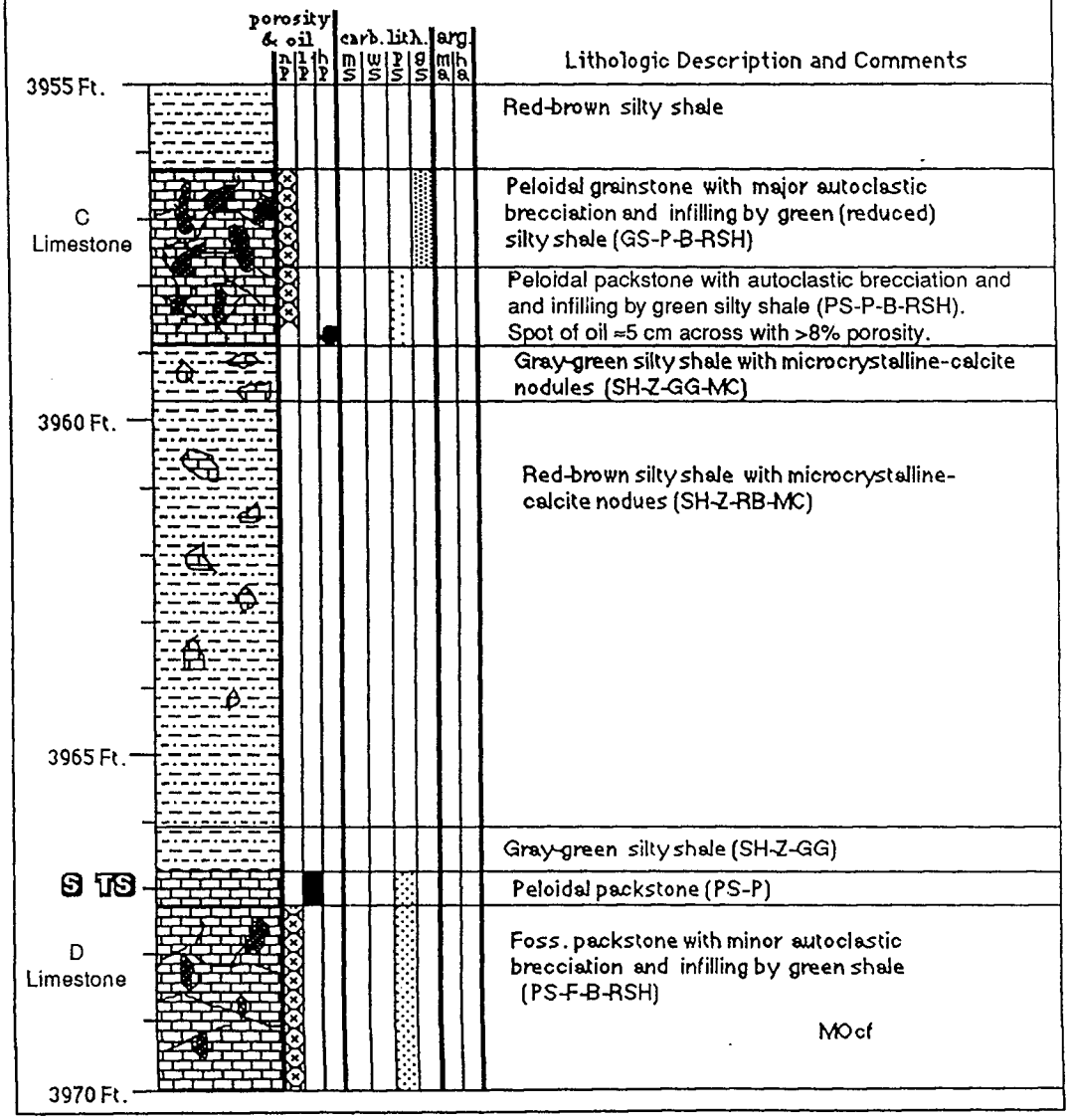

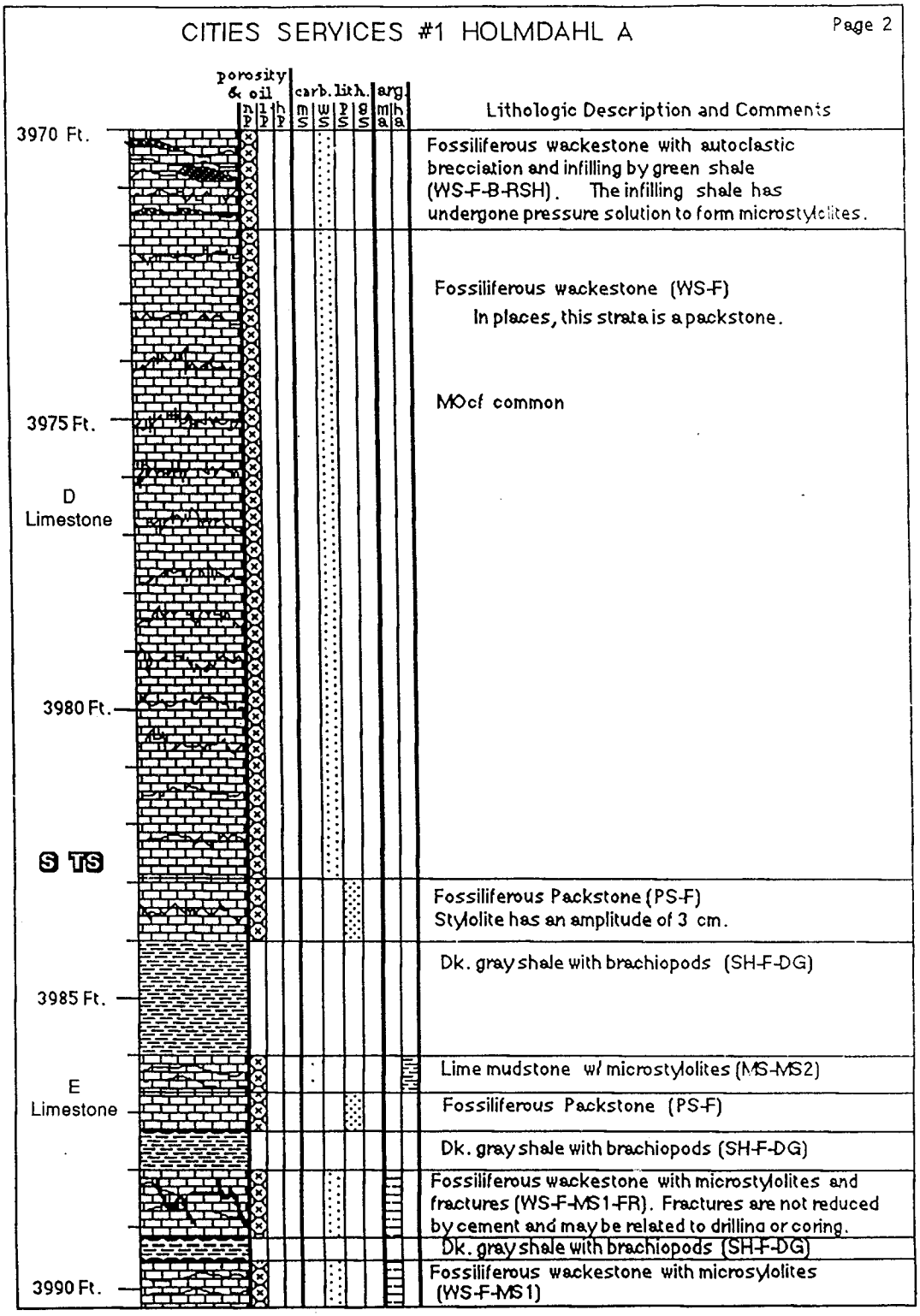
CITIES SERVICES #1 HOLMDAHL A
Page 2
porosity & oil
carb. lith.
arg
Lithologic Description and Comments
3970 Ft.
Fossiliferous wackestone with autoclastic brecciation and infilling by green shale (WS-F-B-RSH). The infilling shale has undergone pressure solution to form microstylolites.
Fossiliferous wackestone (WS-F)
In places, this strata is a packstone.
MOcf common
3975 Ft.
D Limestone
3980 Ft.
S TS
Fossiliferous Packstone (PS-F)
Stylolite has an amplitude of 3 cm.
Dk. gray shale with brachiopods (SH-F-DG)
3985 Ft.
Lime mudstone w/ microstylolites (MS-MS2)
E Limestone
Fossiliferous Packstone (PS-F)
Dk. gray shale with brachiopods (SH-F-DG)
Fossiliferous wackestone with microstylolites and fractures (WS-F-MS1-FR). Fractures are not reduced by cement and may be related to drilling or coring.
Dk. gray shale with brachiopods (SH-F-DG)
Fossiliferous wackestone with microsylolites (WS-F-MS1)
3990 Ft.

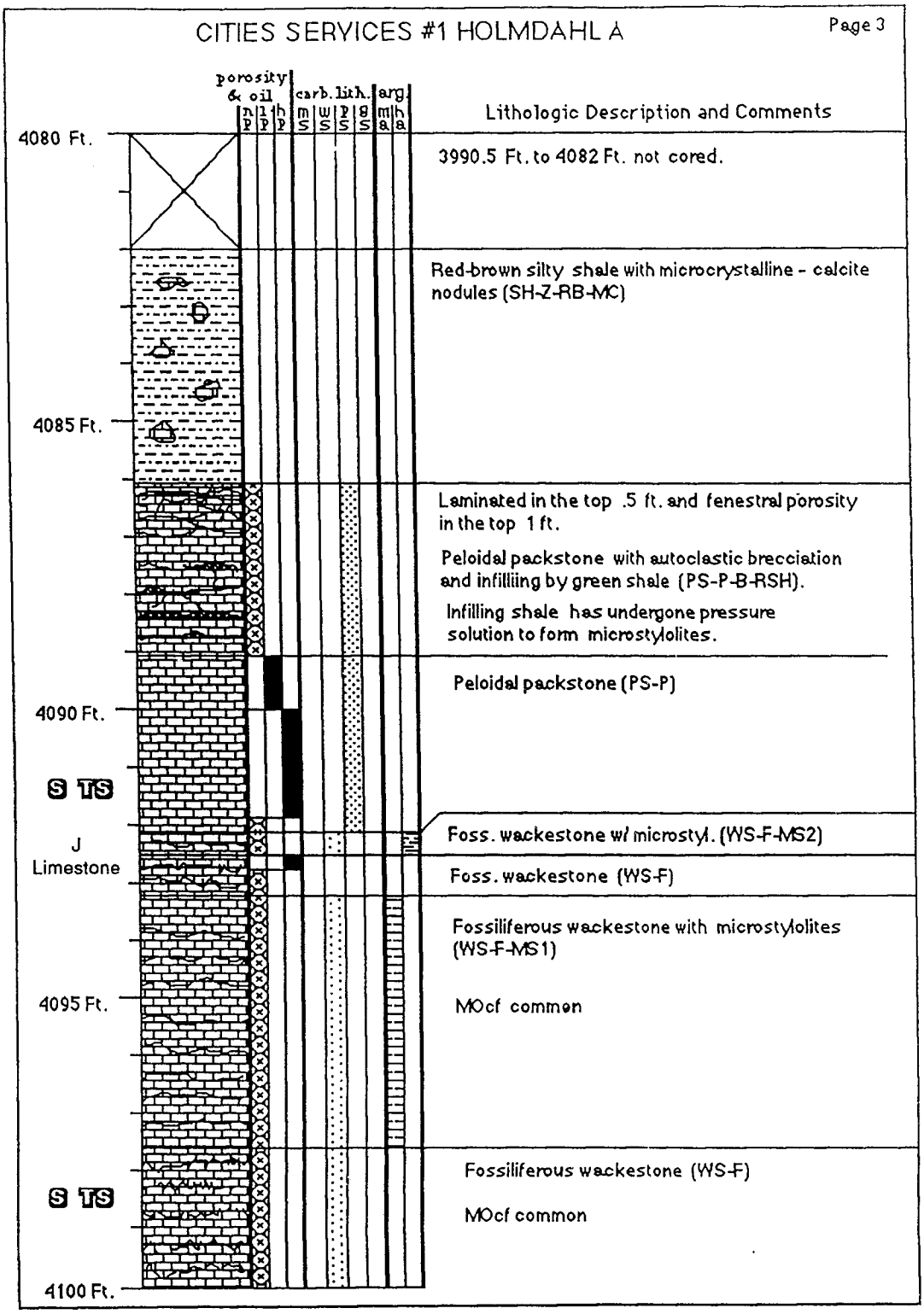
CITIES SERVICES #1 HOLMDAHL A
Page 3
porosity & oil
carb. lith.
arg.
Lithologic Description and Comments
4080 Ft.
3990.5 Ft. to 4082 Ft. not cored.
Red-brown silty shale with microcrystalline - calcite nodules (SH-Z-RB-MC)
4085 Ft.
Laminated in the top .5 ft. and fenestral porosity in the top 1 ft.
Peloidal packstone with autoclastic brecciation and infilliing by green shale (PS-P-B-RSH).
Infilling shale has undergone pressure solution to form microstylolites.
Peloidal packstone (PS-P)
4090 Ft.
S TS
J Limestone
Foss. wackestone w/ microstyl. (WS-F-MS2)
Foss. wackestone (WS-F)
Fossiliferous wackestone with microstylolites (WS-F-MS1)
4095 Ft.
MOcf common
Fossiliferous wackestone (WS-F)
S TS
MOcf common
4100 Ft.

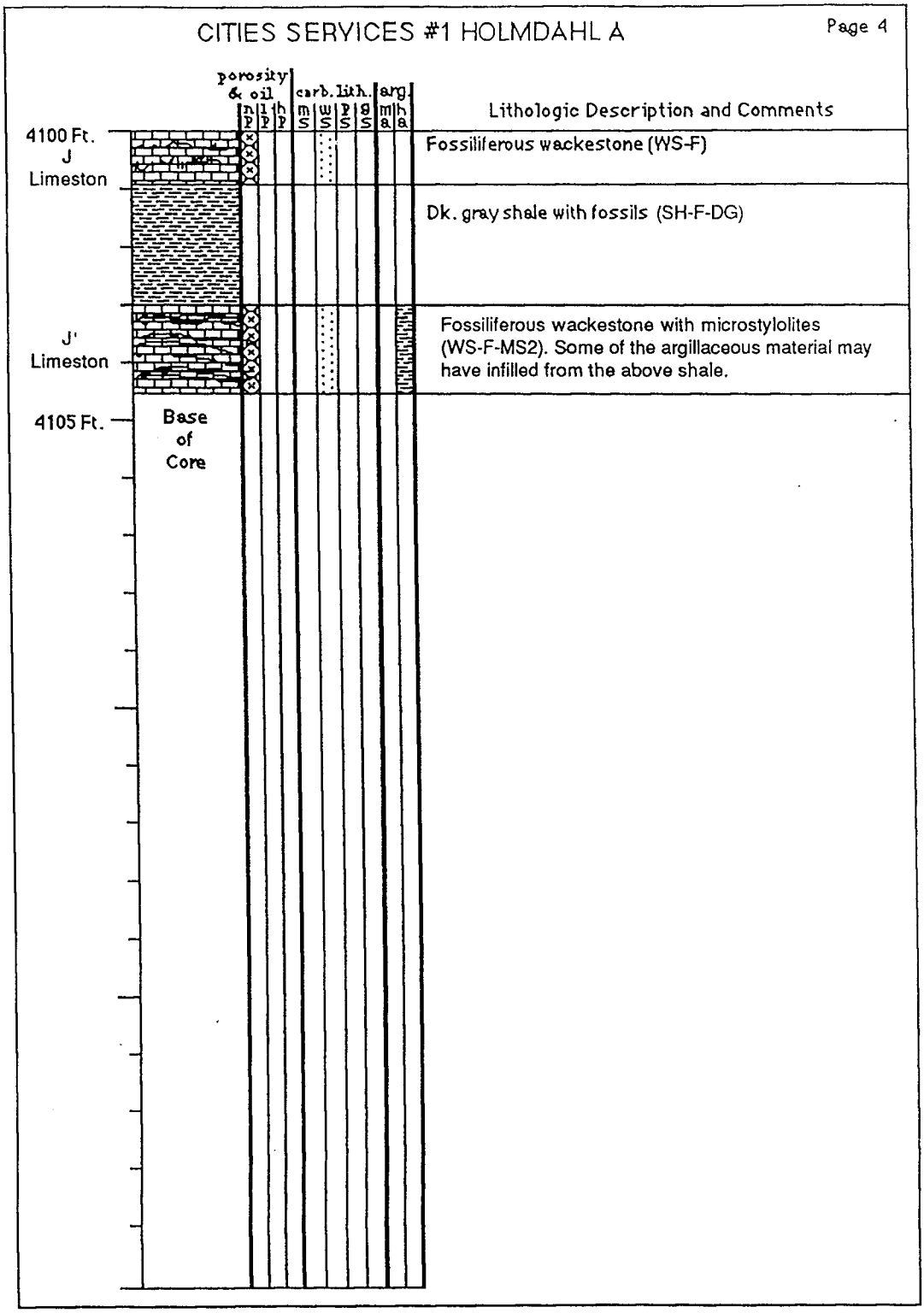
CITIES SERVICES #1 HOLMDAHL A
Page 4
porosity & oil
carb. lith.
arg.
Lithologic Description and Comments
4100 Ft.
J
Limeston
Fossiliferous wackestone (WS-F)
Dk. gray shale with fossils (SH-F-DG)
J'
Limeston
Fossiliferous wackestone with microstylolites (WS-F-MS2). Some of the argillaceous material may have infilled from the above shale.
4105 Ft.
Base of Core

CITIES SERVICE #1 MILLER Z
SE NE SE, Sec. 31-T2S-R27W
Decatur Co., Kansas

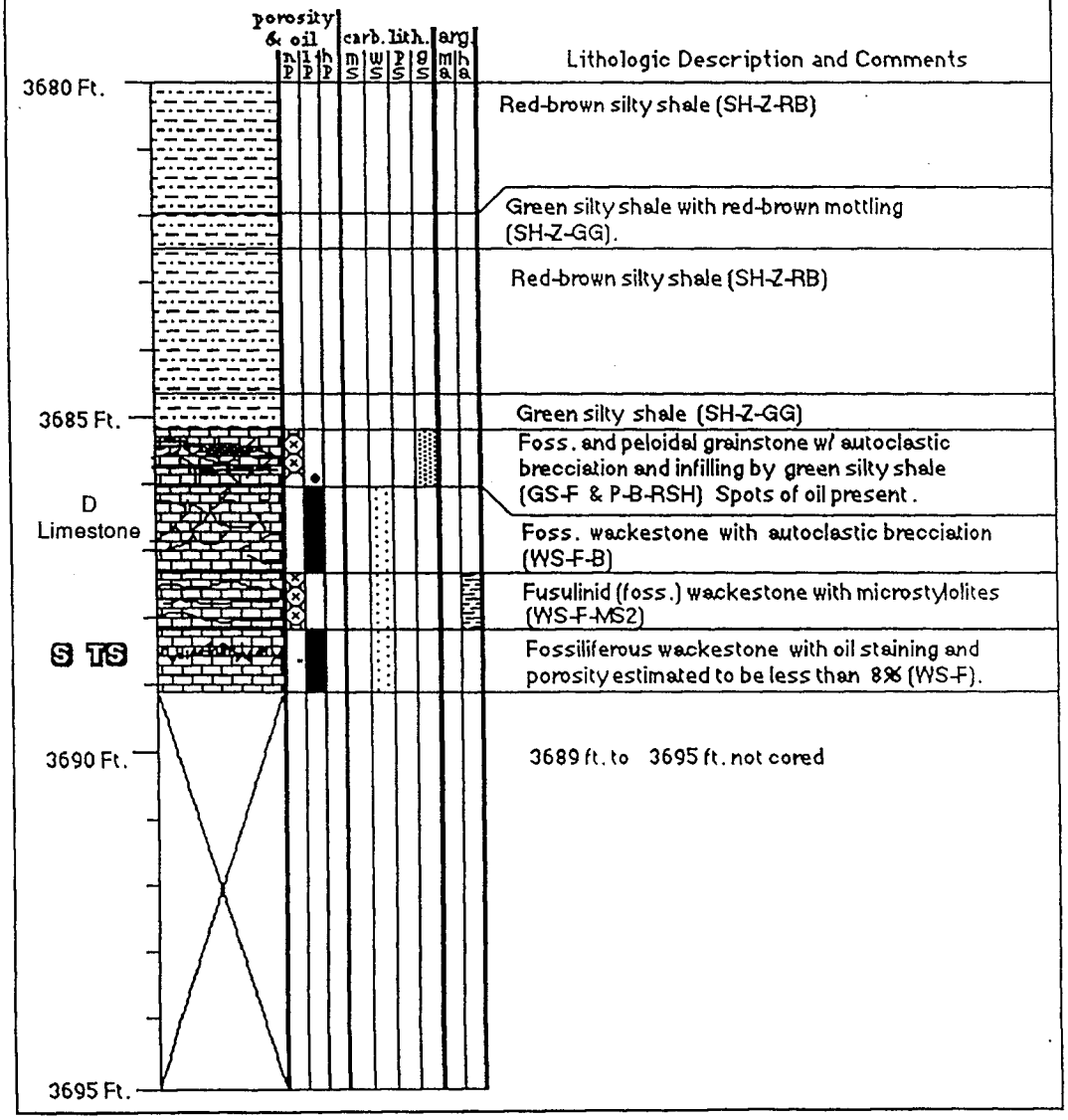

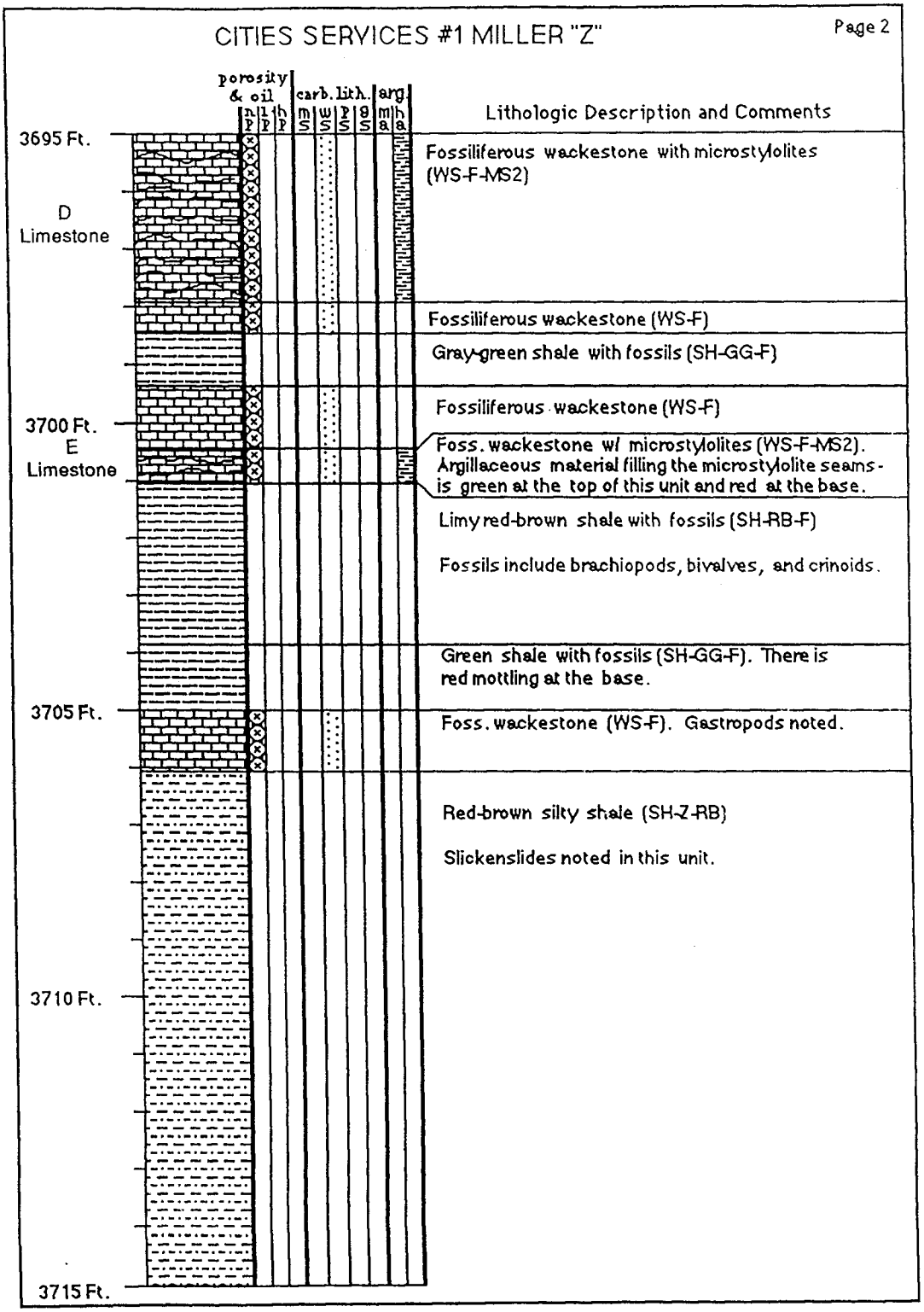
CITIES SERVICES #1 MILLER "Z"
Page 2
porosity & oil
carb. lith.
arg.
Lithologic Description and Comments
3695 Ft.
D Limestone
Fossiliferous wackestone with microstylolites (WS-F-MS2)
Fossiliferous wackestone (WS-F)
Gray-green shale with fossils (SH-GG-F)
Fossiliferous wackestone (WS-F)
3700 Ft.
E Limestone
Foss. wackestone w/ microstylolites (WS-F-MS2). Argillaceous material filling the microstylolite seams - is green at the top of this unit and red at the base.
Limy red-brown shale with fossils (SH-RB-F)
Fossils include brachiopods, bivalves, and crinoids.
Green shale with fossils (SH-GG-F). There is red mottling at the base.
3705 Ft.
Foss. wackestone (WS-F). Gastropods noted.
Red-brown silty shale (SH-Z-RB)
Slickenslides noted in this unit.
3710 Ft.
3715 Ft.

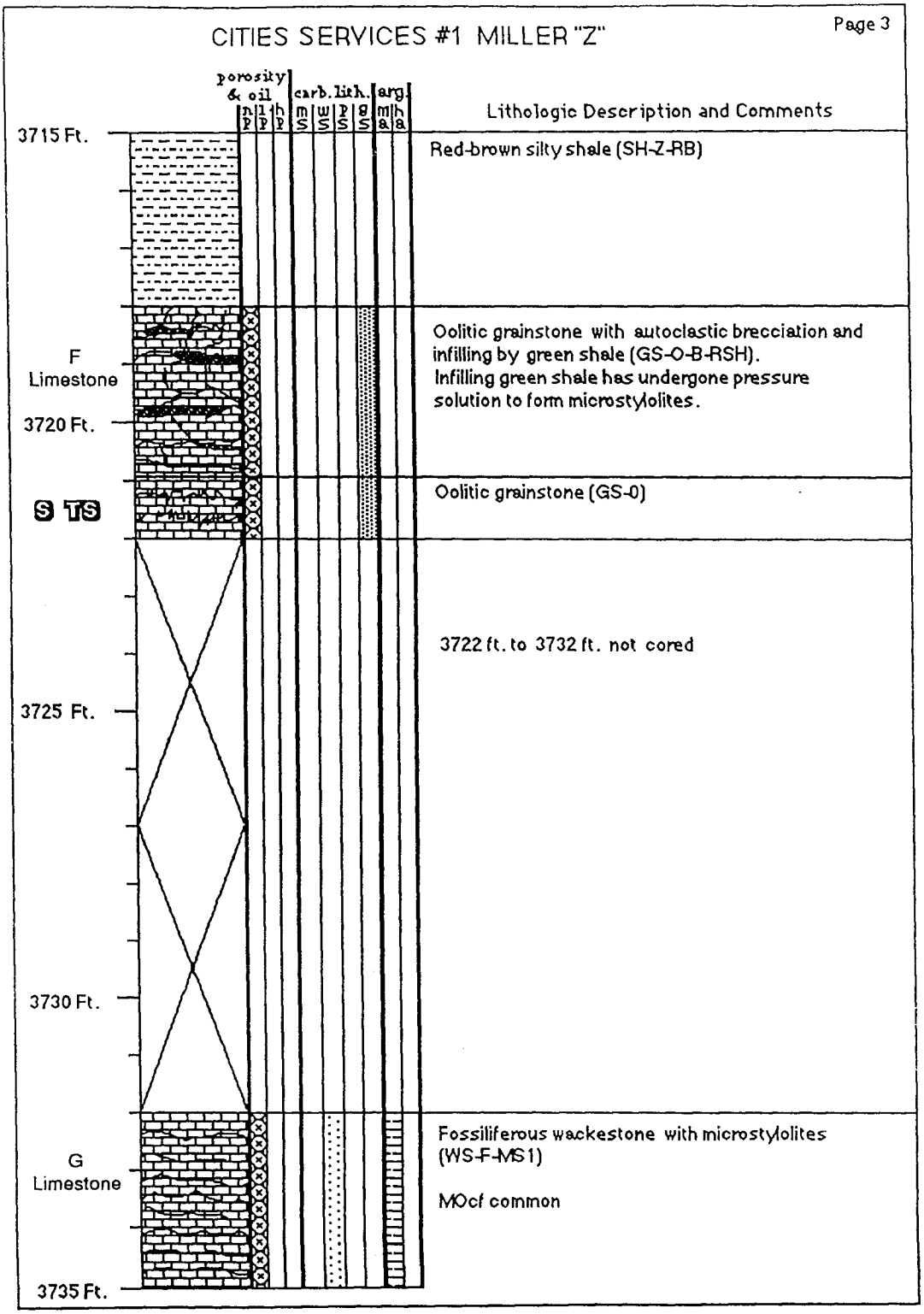
CITIES SERVICES #1 MILLER "Z"
Page 3
porosity & oil
carb. lith.
arg.
Lithologic Description and Comments
3715 Ft.
Red-brown silty shale (SH-Z-RB)
F Limestone
3720 Ft.
Oolitic grainstone with autoclastic brecciation and infilling by green shale (GS-O-B-RSH). Infilling green shale has undergone pressure solution to form microstylolites.
S TS
Oolitic grainstone (GS-O)
3722 ft. to 3732 ft. not cored
3725 Ft.
3730 Ft.
G Limestone
Fossiliferous wackestone with microstylolites (WS-F-MS1)
MOcf common
3735 Ft.

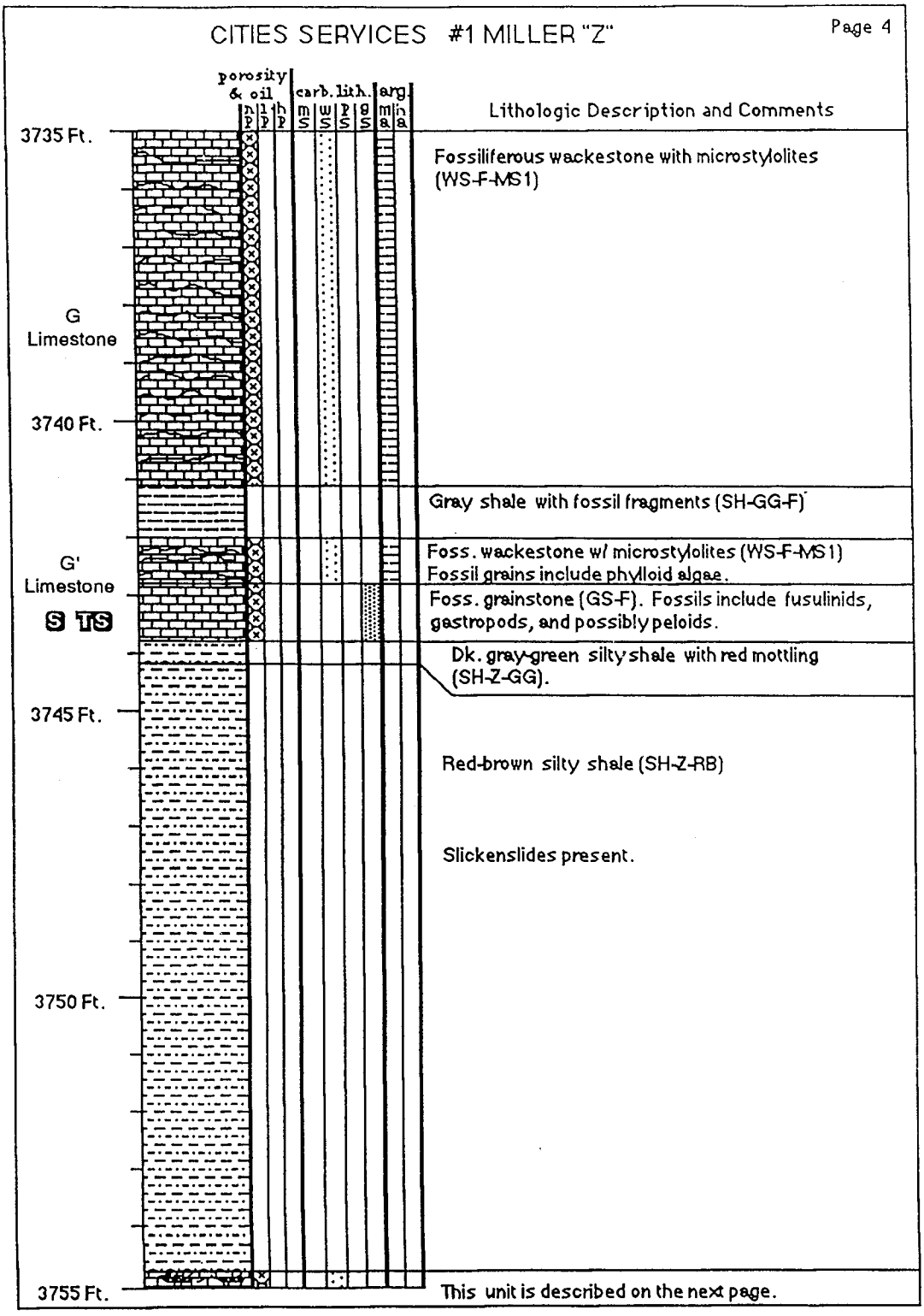
CITIES SERVICES #1 MILLER "Z"
Page 4
porosity & oil
carb. lith.
arg.
Lithologic Description and Comments
3735 Ft.
Fossiliferous wackestone with microstylolites (WS-F-MS1)
G Limestone
3740 Ft.
Gray shale with fossil fragments (SH-GG-F)
Foss. wackestone w/ microstylolites (WS-F-MS1) Fossil grains include phylloid algae.
G' Limestone
S TS
Foss. grainstone (GS-F). Fossils include fusulinids, gastropods, and possibly peloids.
Dk. gray-green silty shale with red mottling (SH-Z-GG).
3745 Ft.
Red-brown silty shale (SH-Z-RB)
Slickenslides present.
3750 Ft.
3755 Ft.
This unit is described on the next page.

CITIES SERVICES #1 MILLER "Z"

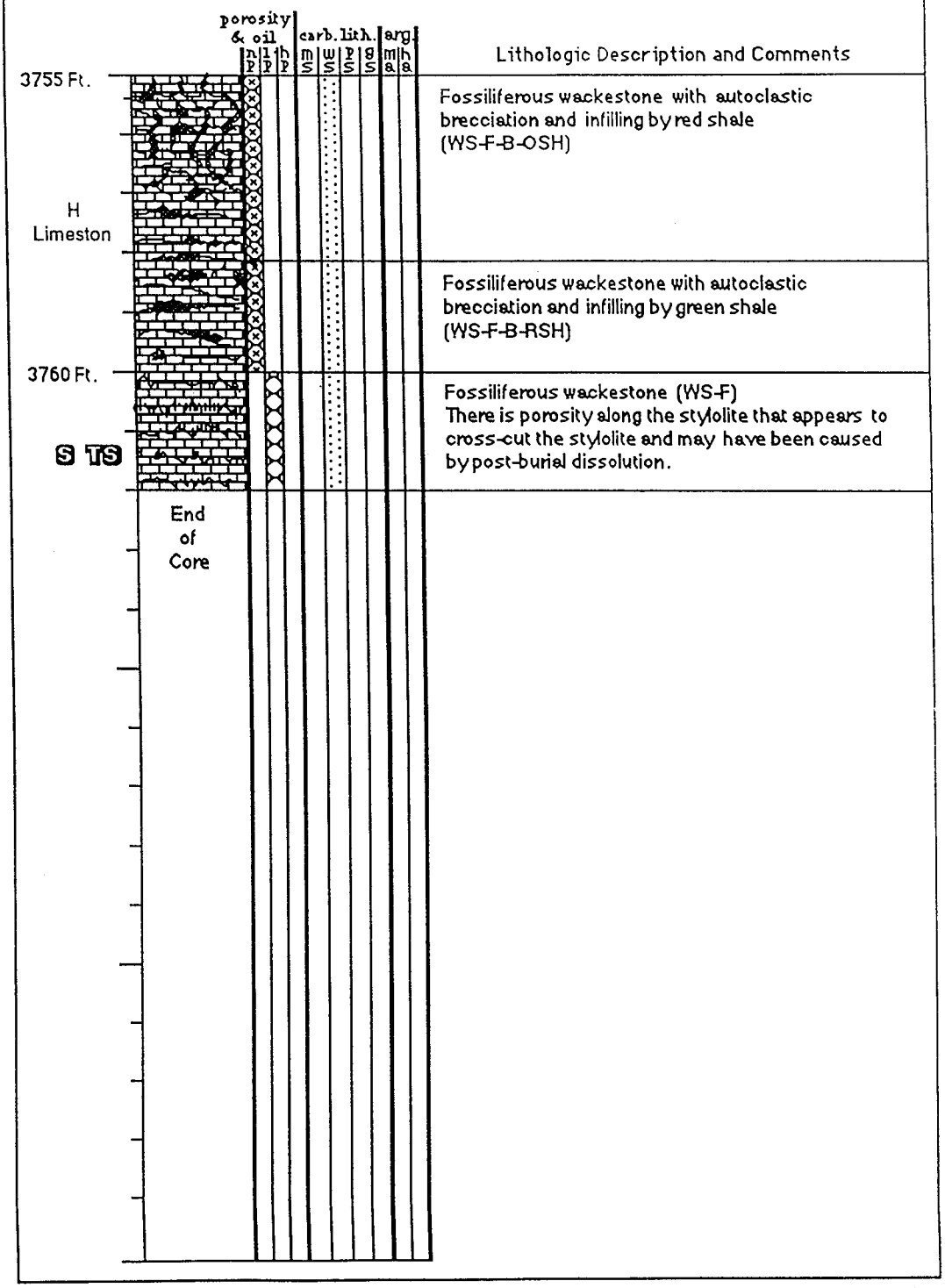

EMPIRE DRILLING CO. #10 PALMER
NE NE SE, Sec. 6-T1S-R33W
Rawlins Co., Kansas

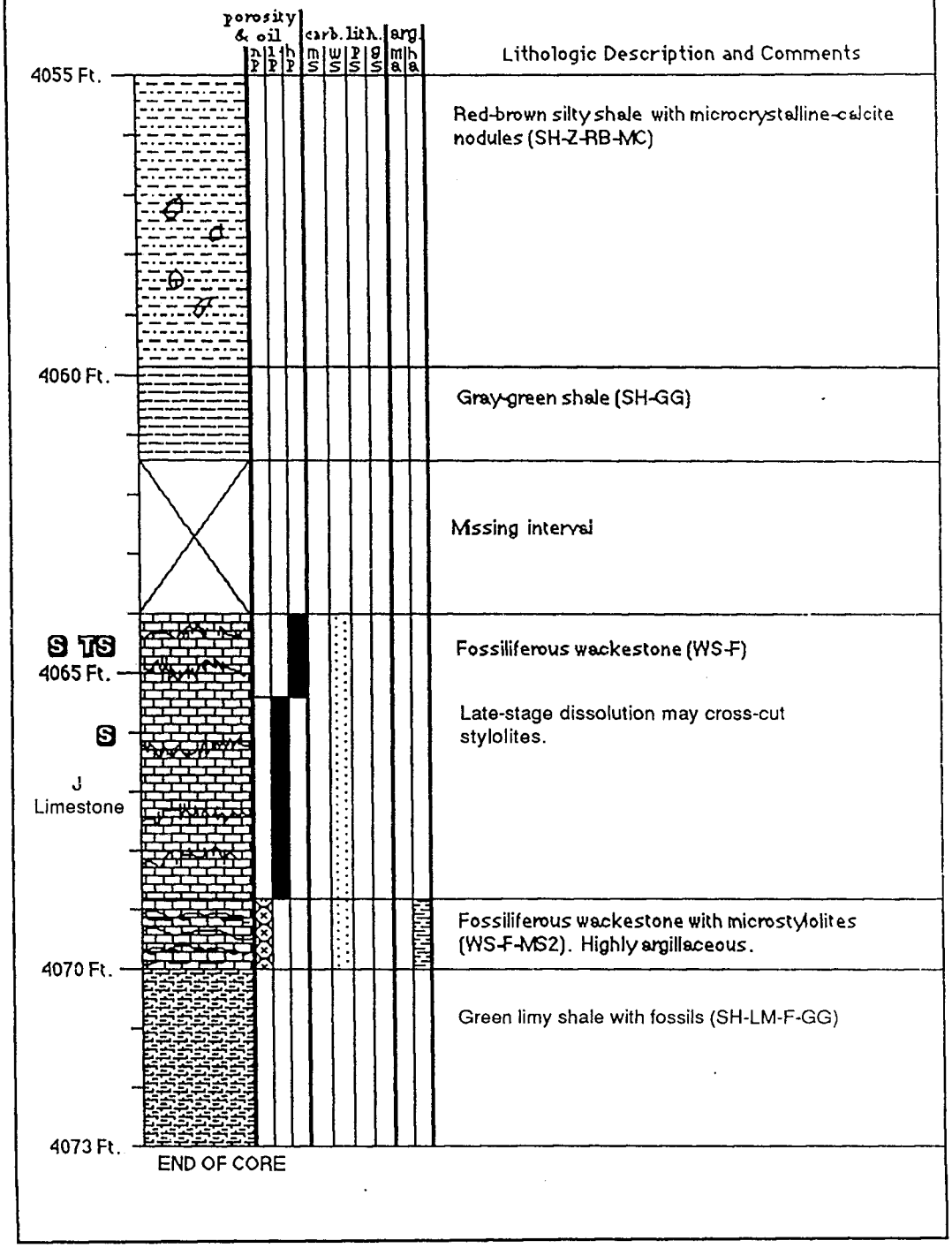

EMPIRE DRILLING CO. #1 WICKE

C NE NE, Sec.23-T2S-R33W
Rawlins Co., Kansas
D&A, 3.75 miles northeast of Atwood
North Field.

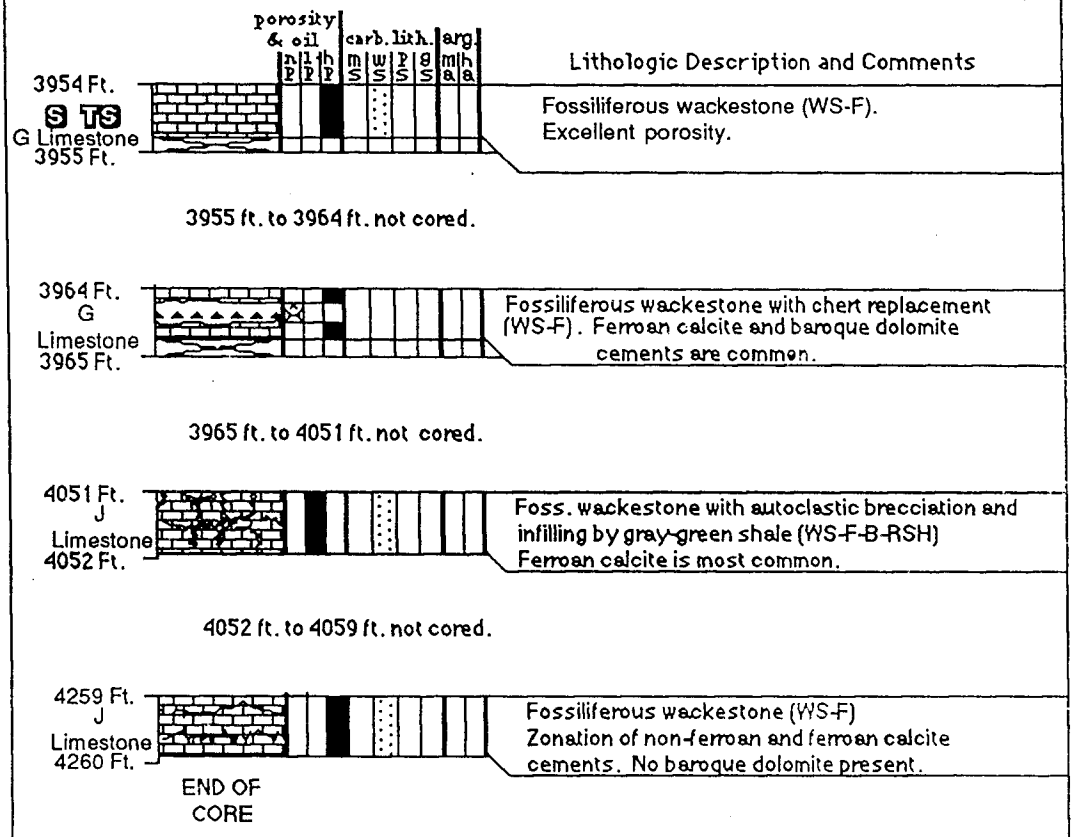

EMPIRE DRILLING CO. #1 LANKAS

SE SE NW, Sec. 13-T3S-R34W
Rawlins Co., Kansas
4 miles southwest of Atwood North Field
Drilled January, 1981

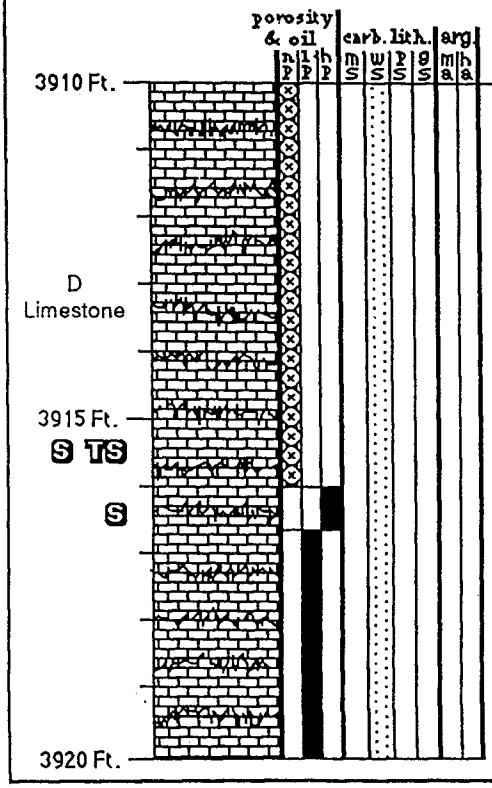

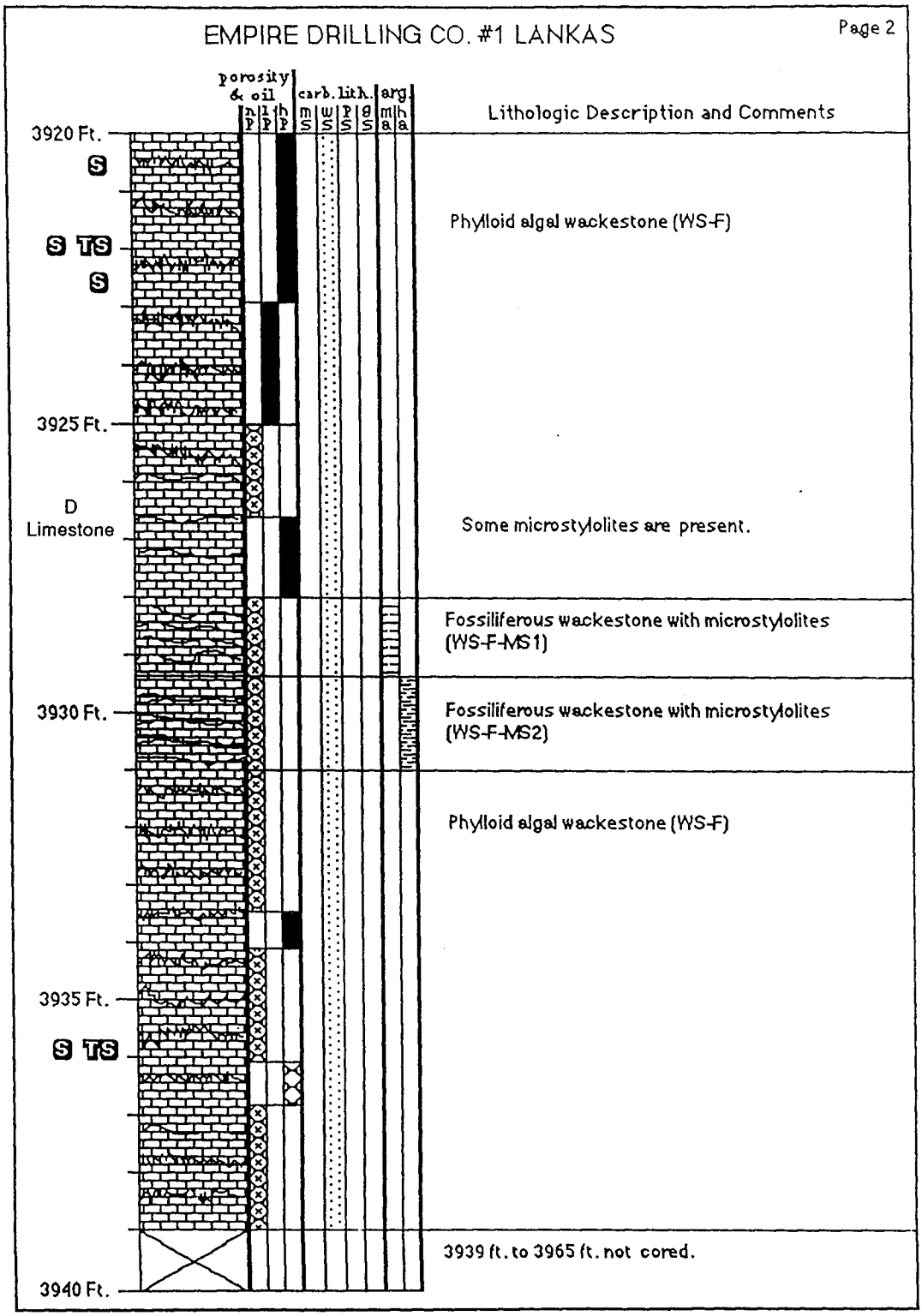
EMPIRE DRILLING CO. #1 LANKAS
Page 2
porosity & oil
carb. lith.
arg.
Lithologic Description and Comments
3920 Ft.
S
S TS
S
Phylloid algal wackestone (WS-F)
3925 Ft.
D
Limestone
Some microstylolites are present.
Fossiliferous wackestone with microstylolites (WS-F-MS1)
3930 Ft.
Fossiliferous wackestone with microstylolites (WS-F-MS2)
Phylloid algal wackestone (WS-F)
3935 Ft.
S TS
3939 ft. to 3965 ft. not cored.
3940 Ft.

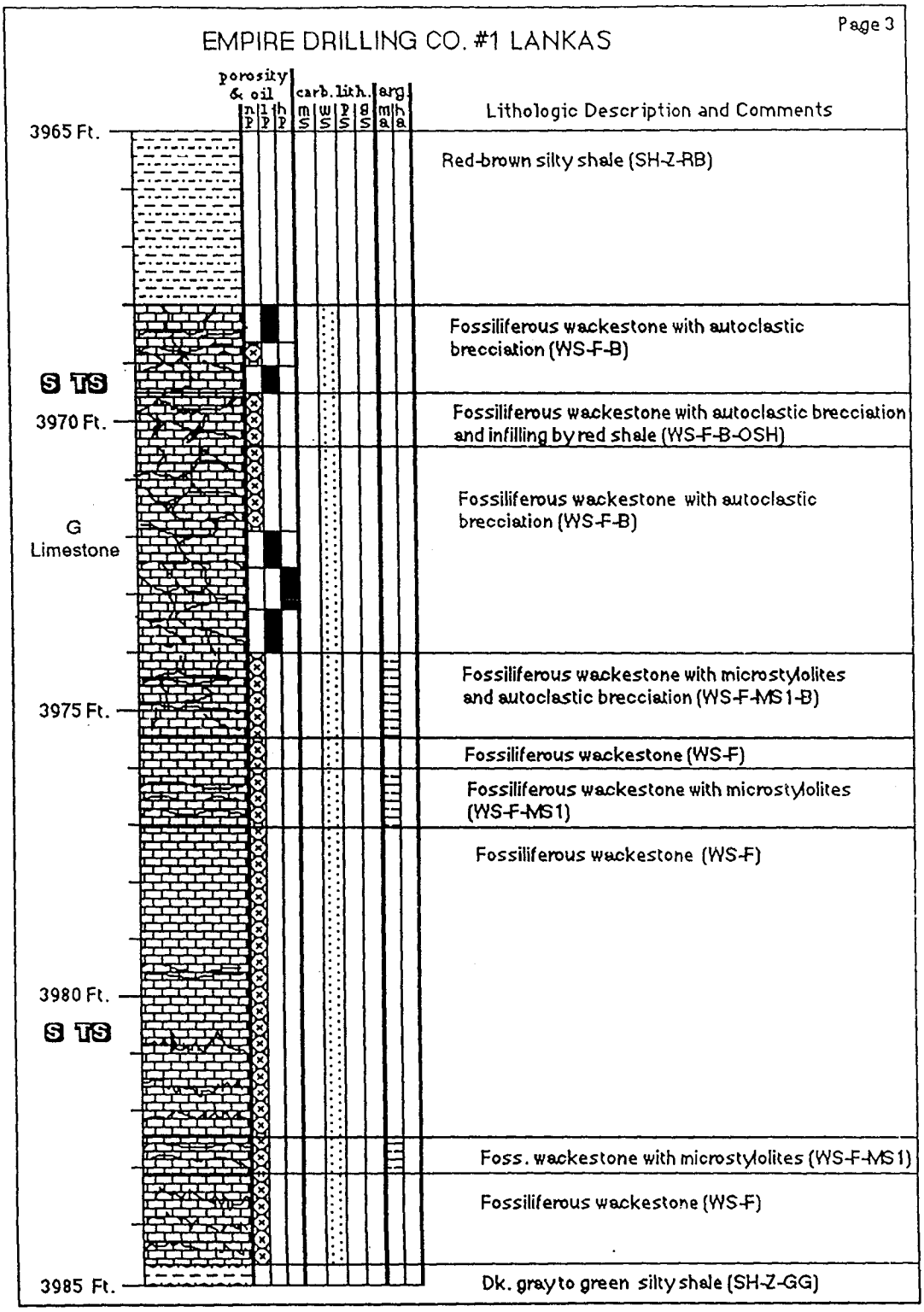
EMPIRE DRILLING CO. #1 LANKAS
porosity & oil
carb. lith.
arg.
Lithologic Description and Comments
3965 Ft.
Red-brown silty shale (SH-Z-RB)
Fossiliferous wackestone with autoclastic brecciation (WS-F-B)
S TS
3970 Ft.
Fossiliferous wackestone with autoclastic brecciation and infilling by red shale (WS-F-B-OSH)
Fossiliferous wackestone with autoclastic brecciation (WS-F-B)
G Limestone
Fossiliferous wackestone with microstylolites and autoclastic brecciation (WS-F-MS1-B)
3975 Ft.
Fossiliferous wackestone (WS-F)
Fossiliferous wackestone with microstylolites (WS-F-MS1)
Fossiliferous wackestone (WS-F)
3980 Ft.
S TS
Foss. wackestone with microstylolites (WS-F-MS1)
Fossiliferous wackestone (WS-F)
3985 Ft.
Dk. gray to green silty shale (SH-Z-GG)

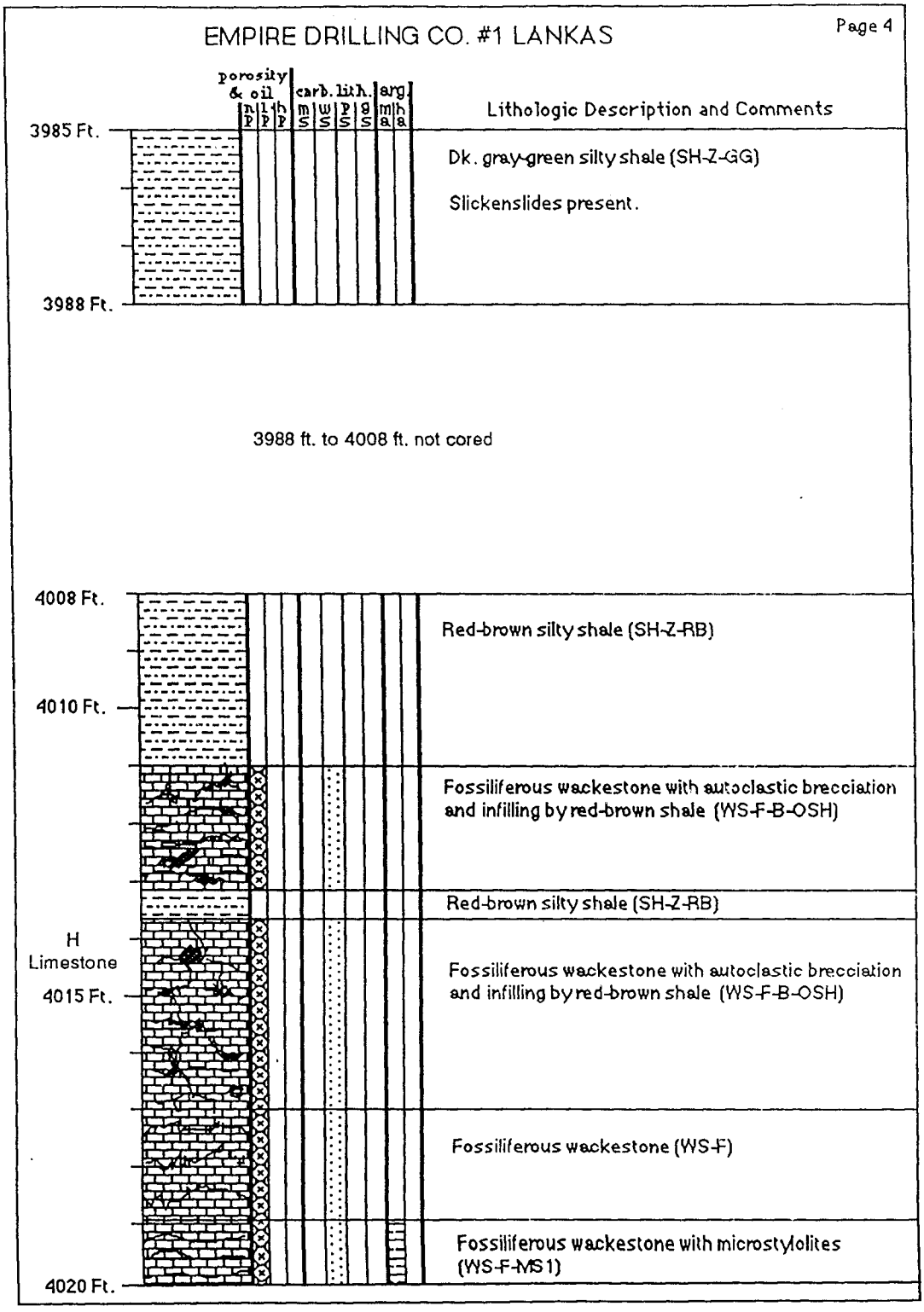
EMPIRE DRILLING CO. #1 LANKAS
porosity & oil
carb. lith.
arg.
Lithologic Description and Comments
3985 Ft.
Dk. gray-green silty shale (SH-Z-GG)
Slickenslides present.
3988 Ft.
3988 ft. to 4008 ft. not cored
4008 Ft.
Red-brown silty shale (SH-Z-RB)
4010 Ft.
Fossiliferous wackestone with autoclastic brecciation and infilling by red-brown shale (WS-F-B-OSH)
Red-brown silty shale (SH-Z-RB)
H Limestone
4015 Ft.
Fossiliferous wackestone with autoclastic brecciation and infilling by red-brown shale (WS-F-B-OSH)
Fossiliferous wackestone (WS-F)
Fossiliferous wackestone with microstylolites (WS-F-MS1)
4020 Ft.

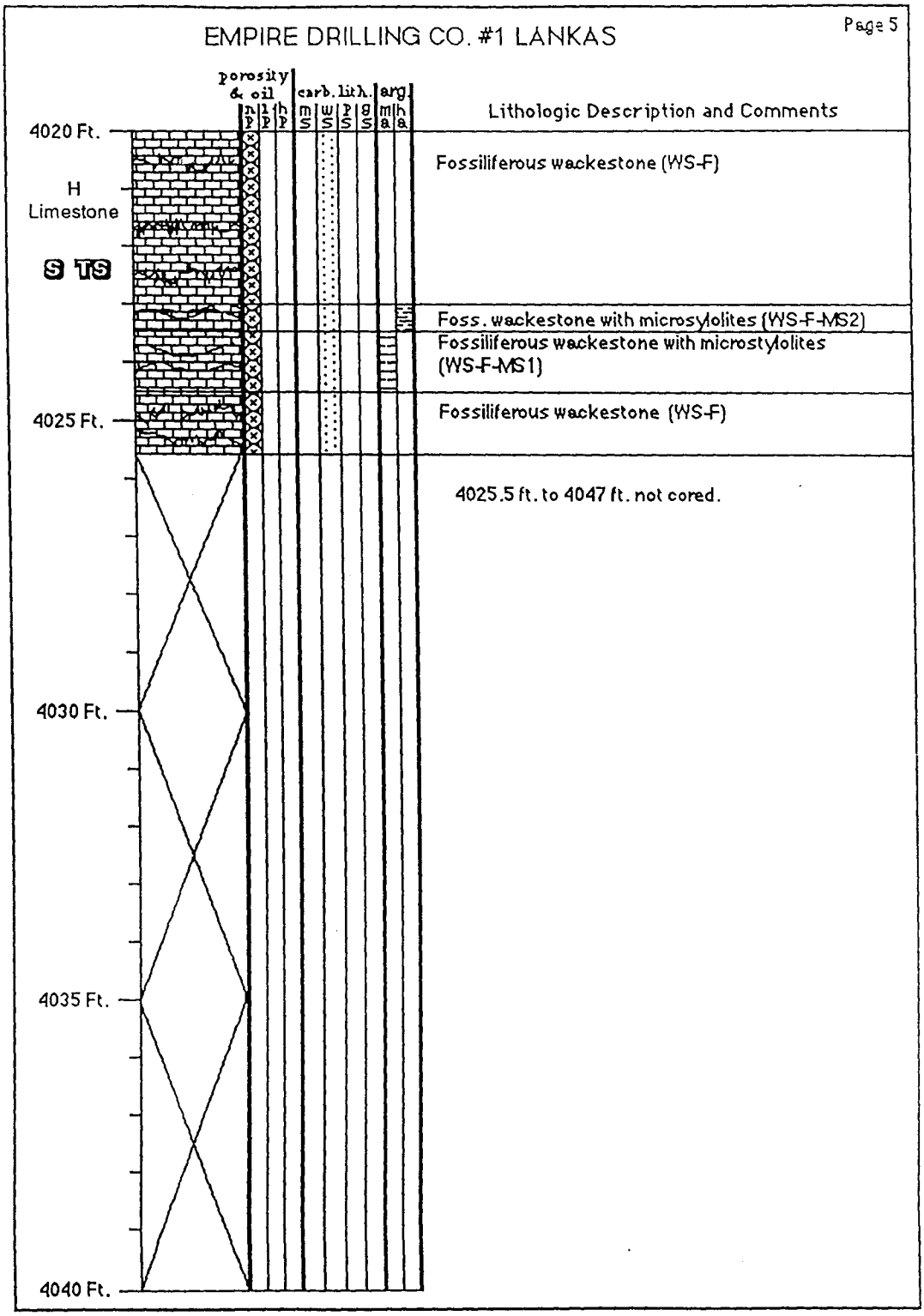
EMPIRE DRILLING CO. #1 LANKAS
Page 5
porosity & oil
carb. lith.
arg.
Lithologic Description and Comments
4020 Ft.
H Limestone
S TS
Fossiliferous wackestone (WS-F)
Foss. wackestone with microsylolites (WS-F-MS2)
Fossiliferous wackestone with microstylolites (WS-F-MS1)
4025 Ft.
Fossiliferous wackestone (WS-F)
4025.5 ft. to 4047 ft. not cored.
4030 Ft.
4035 Ft.
4040 Ft.

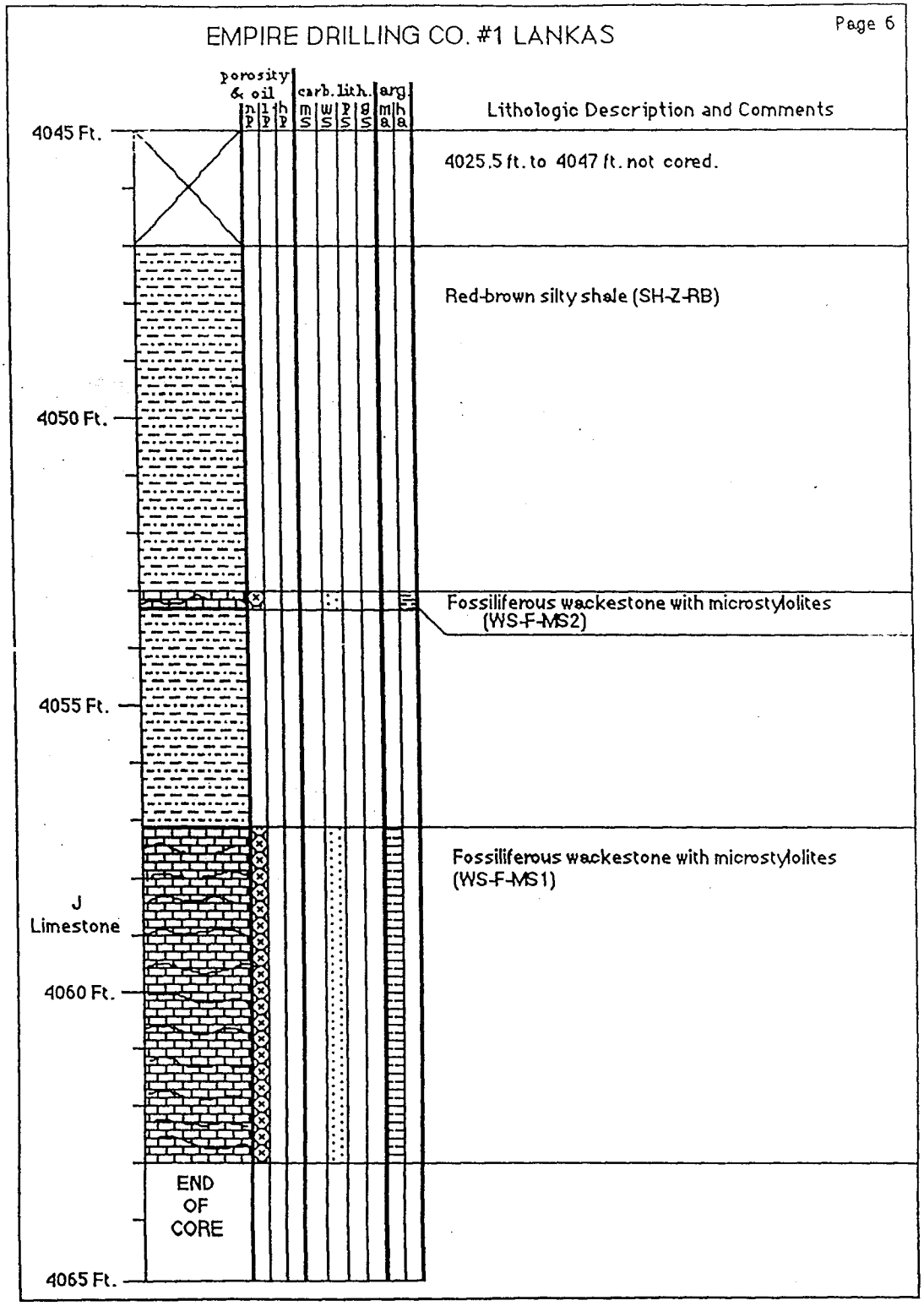
EMPIRE DRILLING CO. #1 LANKAS
Page 6
porosity & oil
carb. lith.
arg
Lithologic Description and Comments
4045 Ft.
4025.5 ft. to 4047 ft. not cored.
Red-brown silty shale (SH-Z-RB)
4050 Ft.
Fossiliferous wackestone with microstylolites (WS-F-MS2)
4055 Ft.
Fossiliferous wackestone with microstylolites (WS-F-MS1)
J Limestone
4060 Ft.
END OF CORE
4065 Ft.

EMPIRE DRILLING CO. #1 RATHE

NW SW, Sec. 9-T3N-R30W
Red Willow County, Nebraska
Drilled April, 1976

No intervals in this core look good for petroleum production with the possible exception of the interval at 4062 feet.

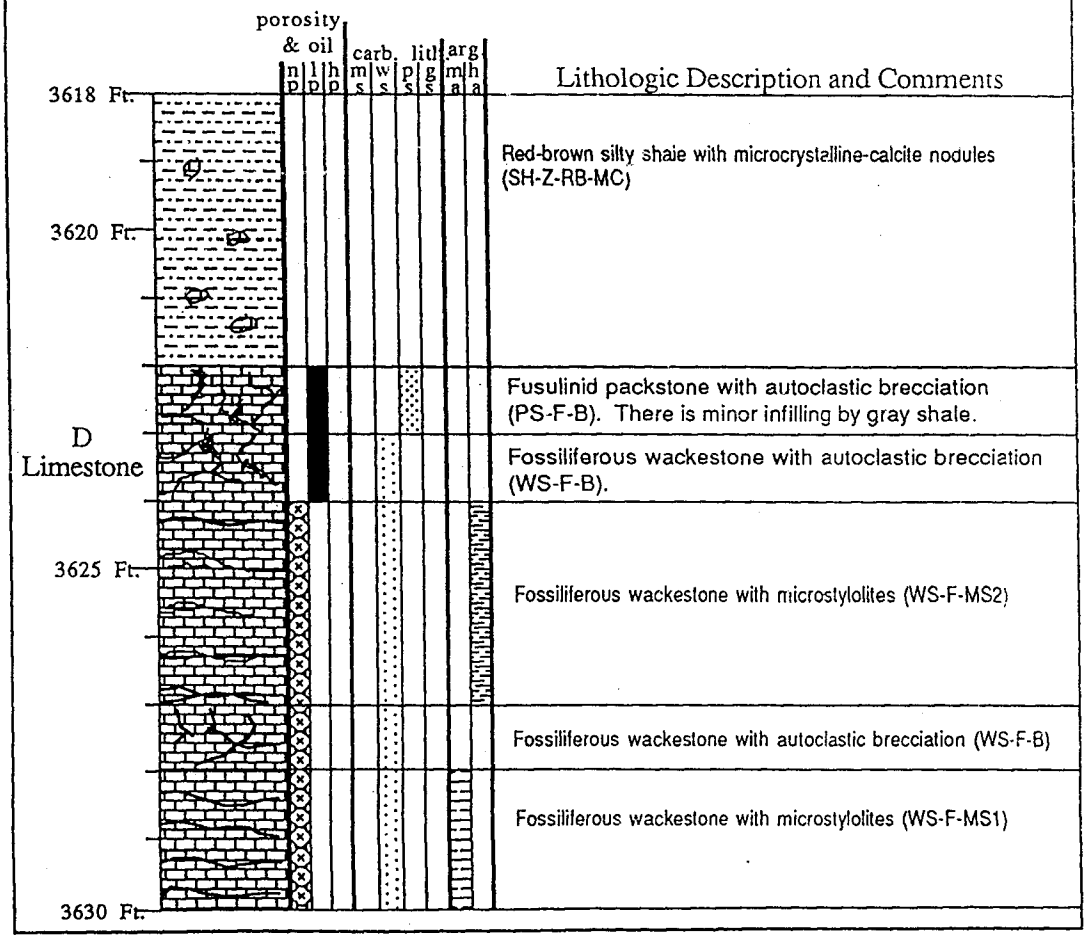

EMPIRE DRILLING CO. #1 RATHE

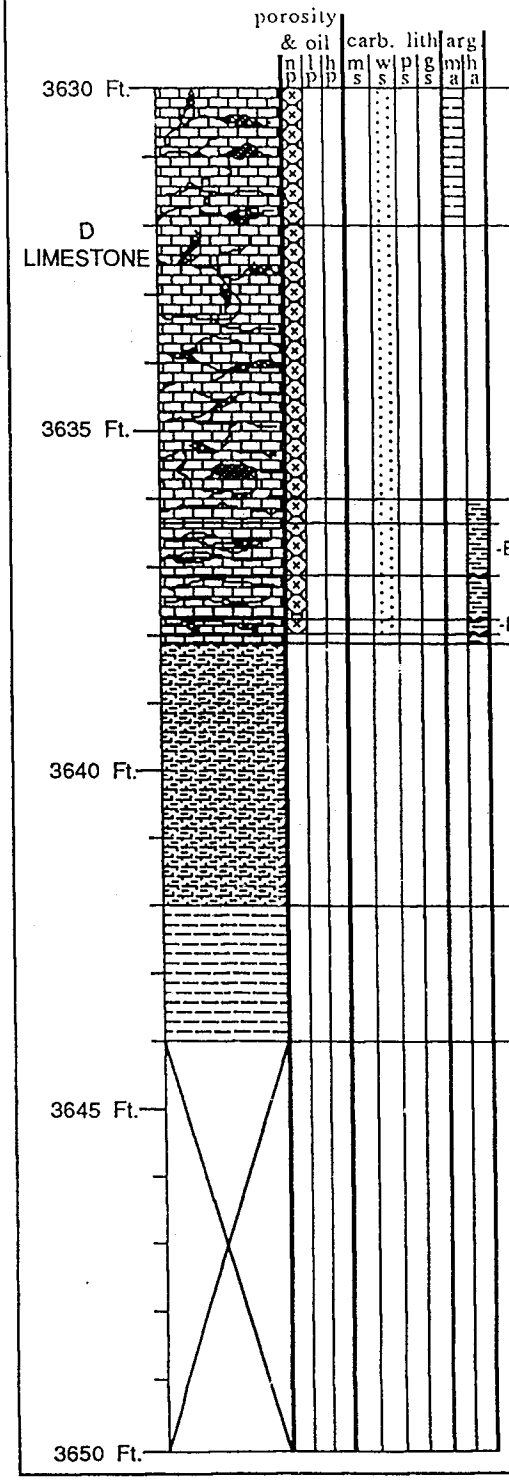

Lithologic Description and Comments

Fossiliferous wackestone with microstylolites, autoclasitic brecciation, and infilling by green shale (WS-F-MS1-B-RSH)

Fossiliferous wackestone with autoclastic brecciation and infilling by red-silty shale (WS-F-B-OSH)

The brecciation is more developed in this stratum than in the above stratum.

Fossiliferous wackestone with microtylolites (WS-F-MS2). There are two zones of autoclastic brecciation with infilling by red shale (-B-OSH) in this stratum.

Limy, dark red to gray, shale with fossils (SH-RB-F-LM). This lithology is similar to a highly argillaceous microstylolitzed limestone (-MS2) with less carbonate matrix and more shale.

Red-brown shale with fossils (SH-RB-F)

Not cored

EMPIRE DRILLING CO. #1 RATHE

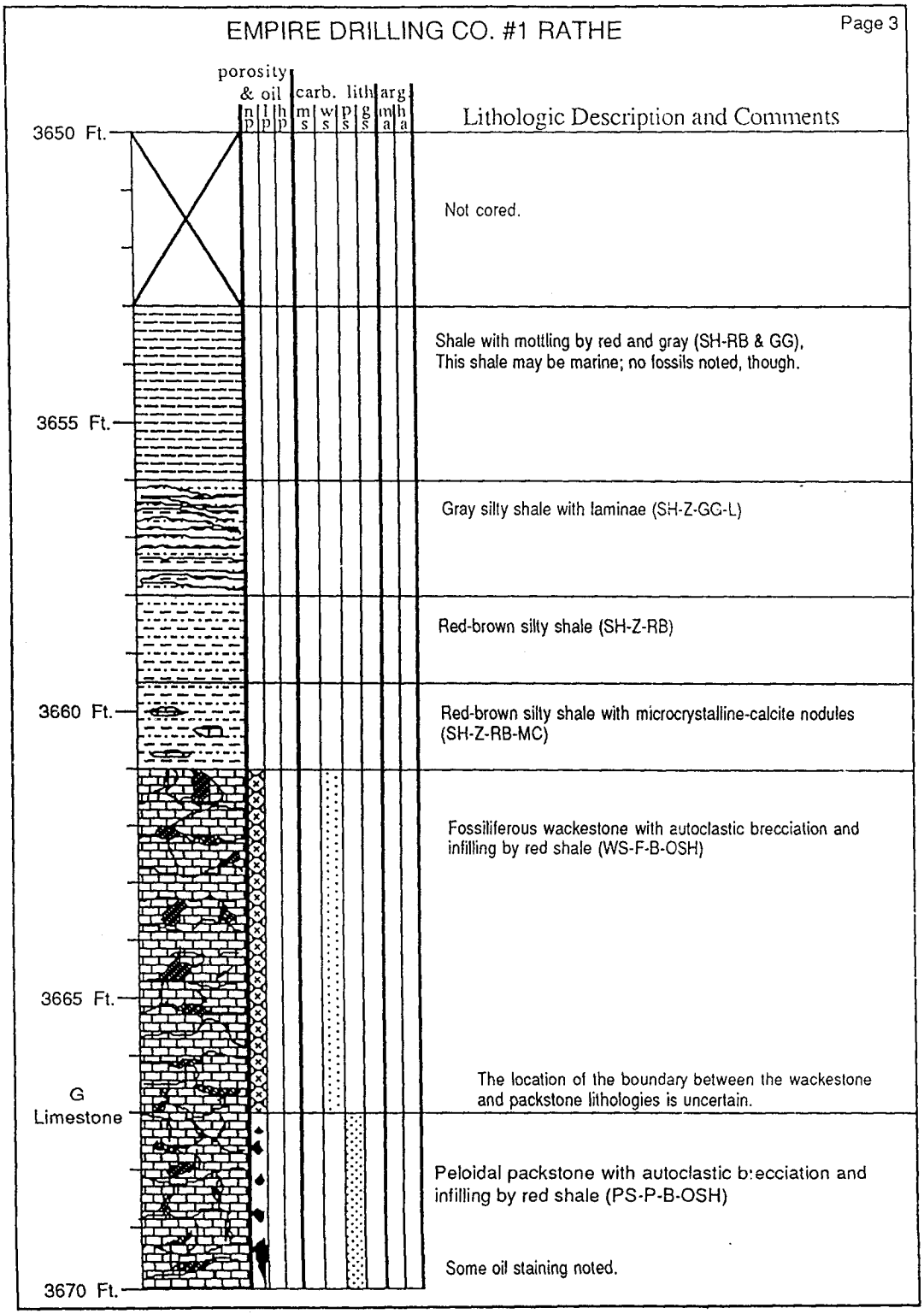

EMPIRE DRILLING CO. #1 RATHE

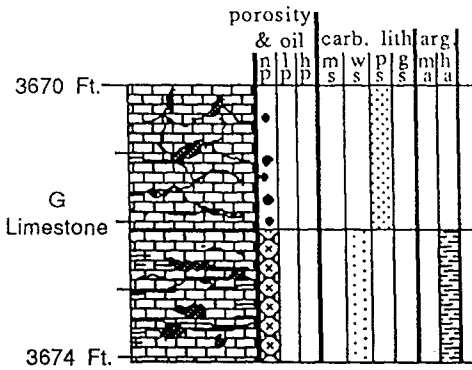

Peloidal packstone with autoclastic brecciation and infilling by red shale (PS-P-B-OSH).
Some oil staining noted.

Fossiliferous wackestone with microstylolites, autoclastic brecciation, and infilling by red shale (WS-F-MS2-B-OSH).
Shale infilling is cross-cut by pressure solution.

3674 ft. to 3712 ft. not cored.

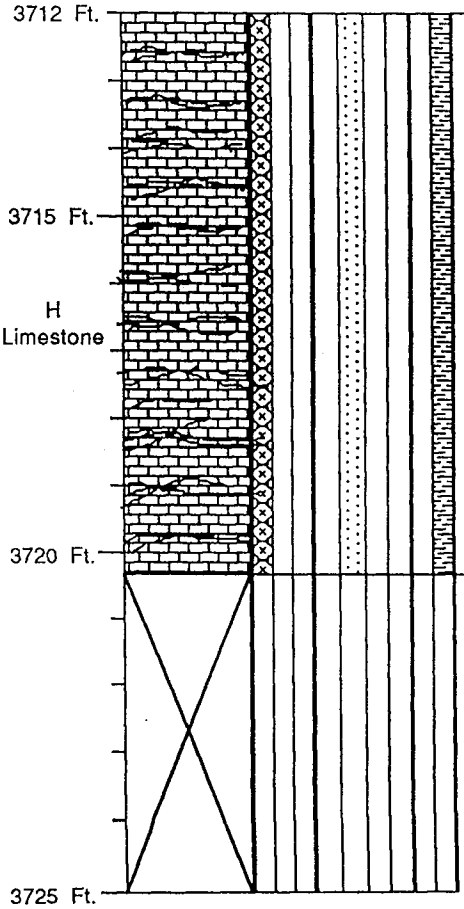

Fossiliferous wackestone with microstylolites (WS-F-MS2)

Many of the shale seams or microstylolites appear to be red in color.

3720 ft. to 3737 ft. not cored.

EMPIRE DRILLING CO. #1 RATHE

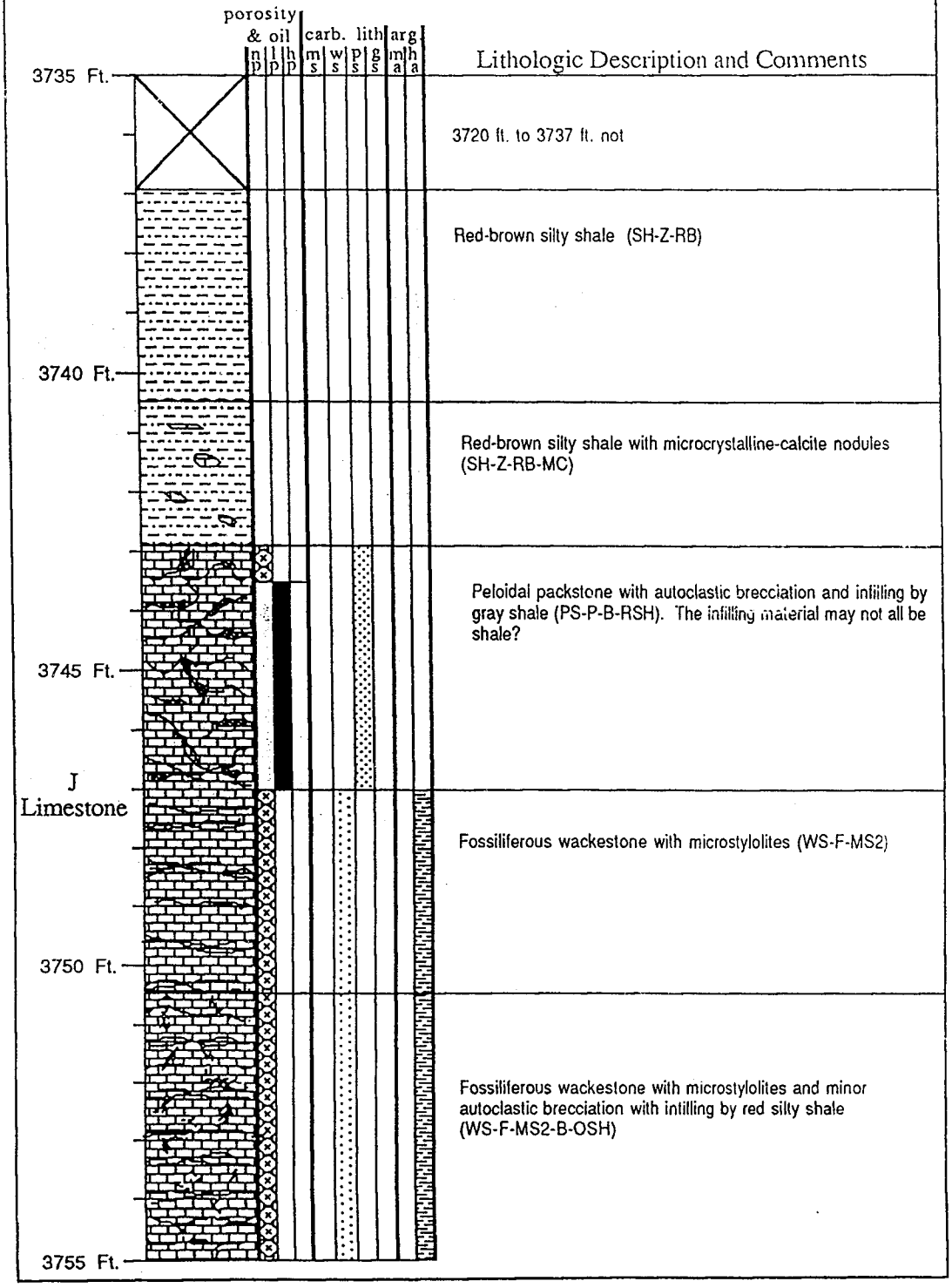

EMPIRE DRILLING CO. #1 RATHE

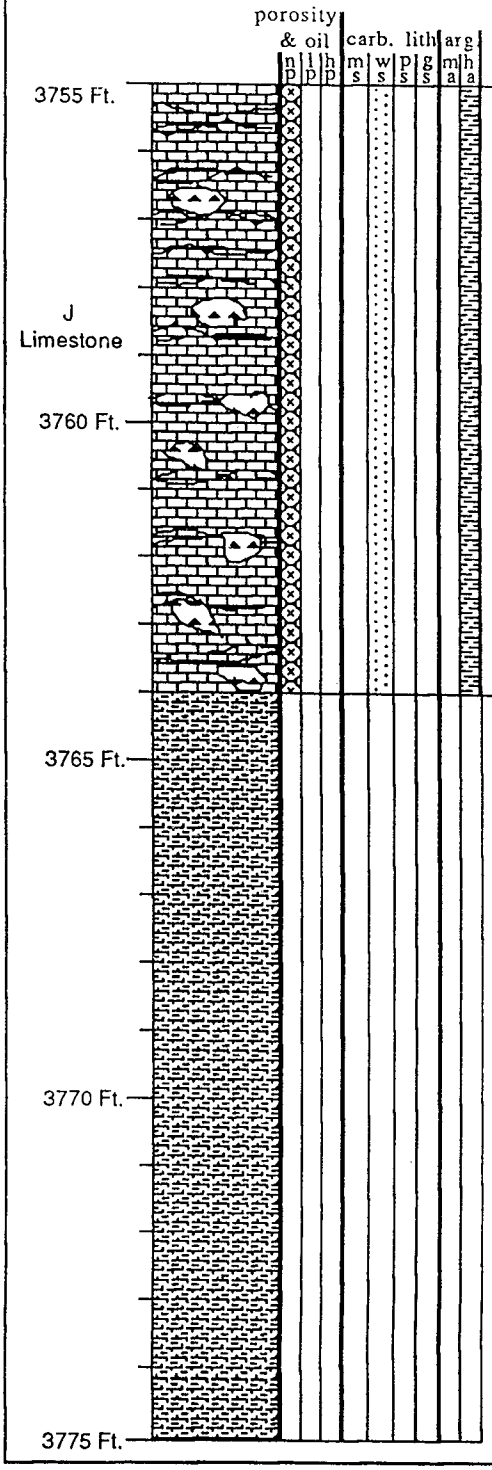

Lithologic Description and Comments

Fossiliferous wackestone with microstylolites (WS-F-MS2). There is replacement of the carbonate by orange chert.

Green to dark gray limy shale with fossils (SH-F-GG-LM). This lithology is more argillaceous than microstylolitized limestones..

EMPIRE DRILLING CO. #1 RATHE

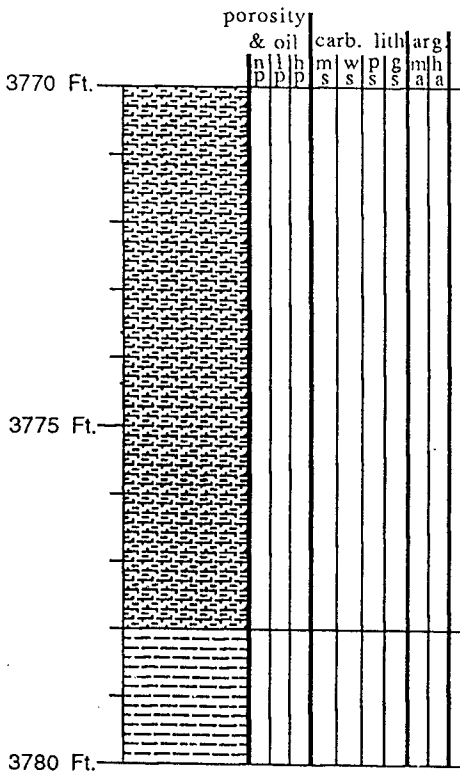

Lithologic Description and Comments

Green to dark-gray limy shale with fossils (SH-F-GG-LM).

At the base of this stratum, there is more carbonate.

Green to gray shale (SH-GG)

3780 ft. to 3795 ft. not cored.

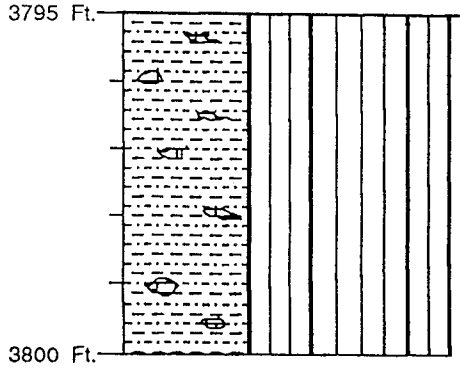

Red-brown silty shale with microcrystalline-calcite nodules (SH-Z-RB-MC)

EMPIRE DRILLING CO. #1 RATHE

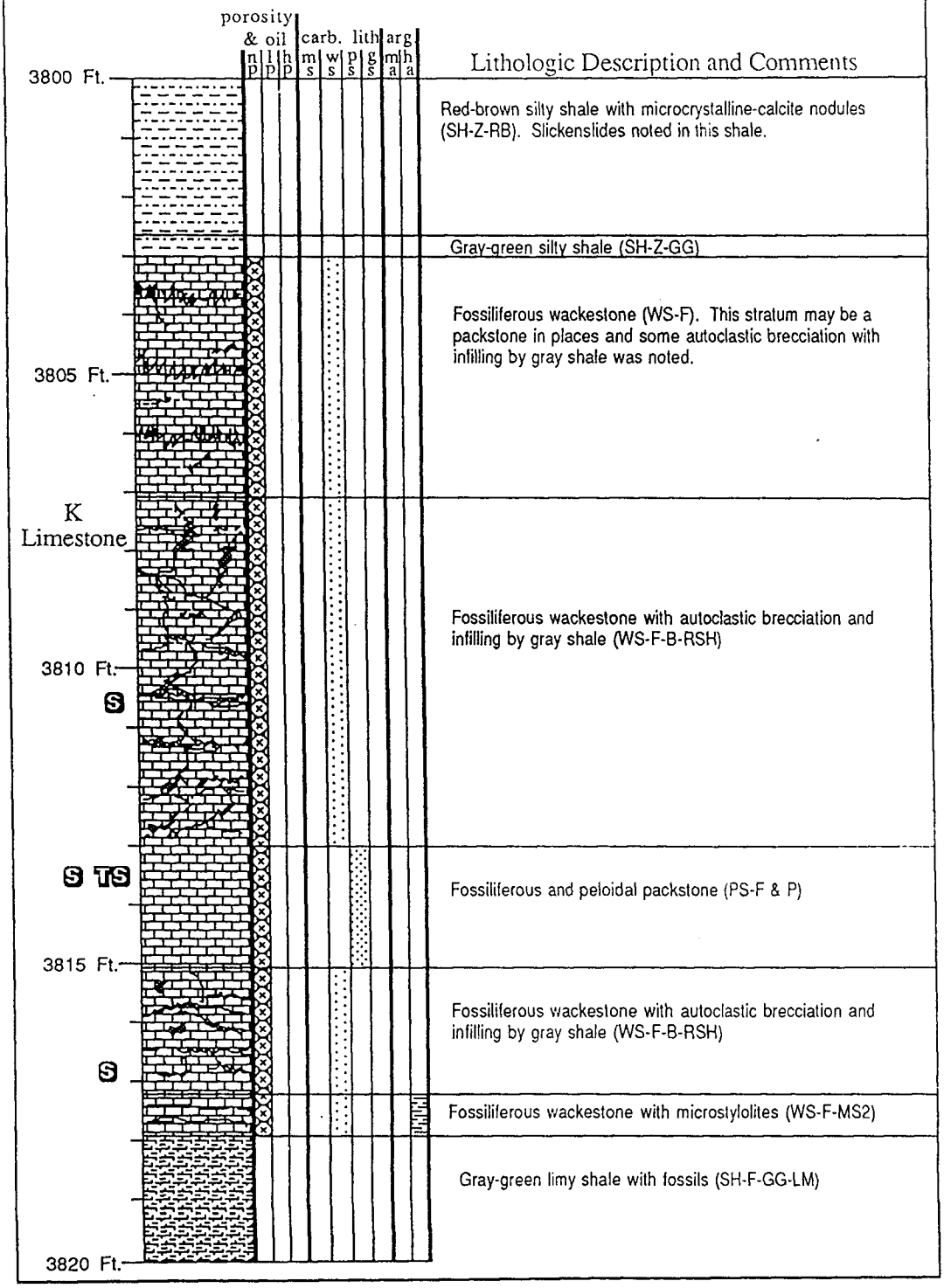

EMPIRE DRILLING CO. #1 RATHE

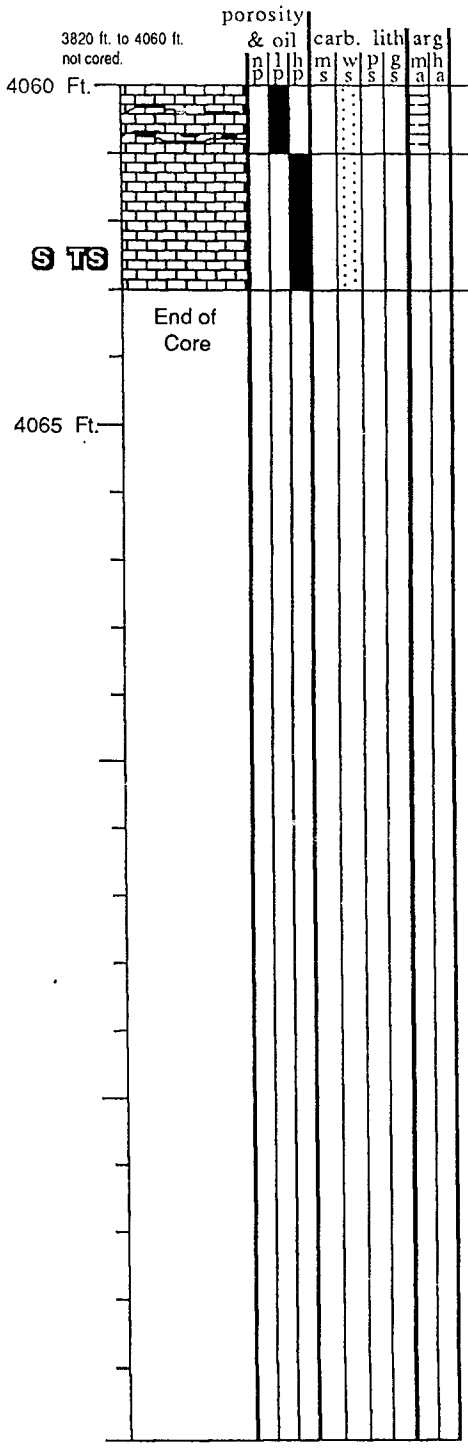

GULF #1-22 HUGHES

Page 1

C SW SW, Sec. 22-T9S-R29W
Sheridan County, Kansas
Drilled March, 1978

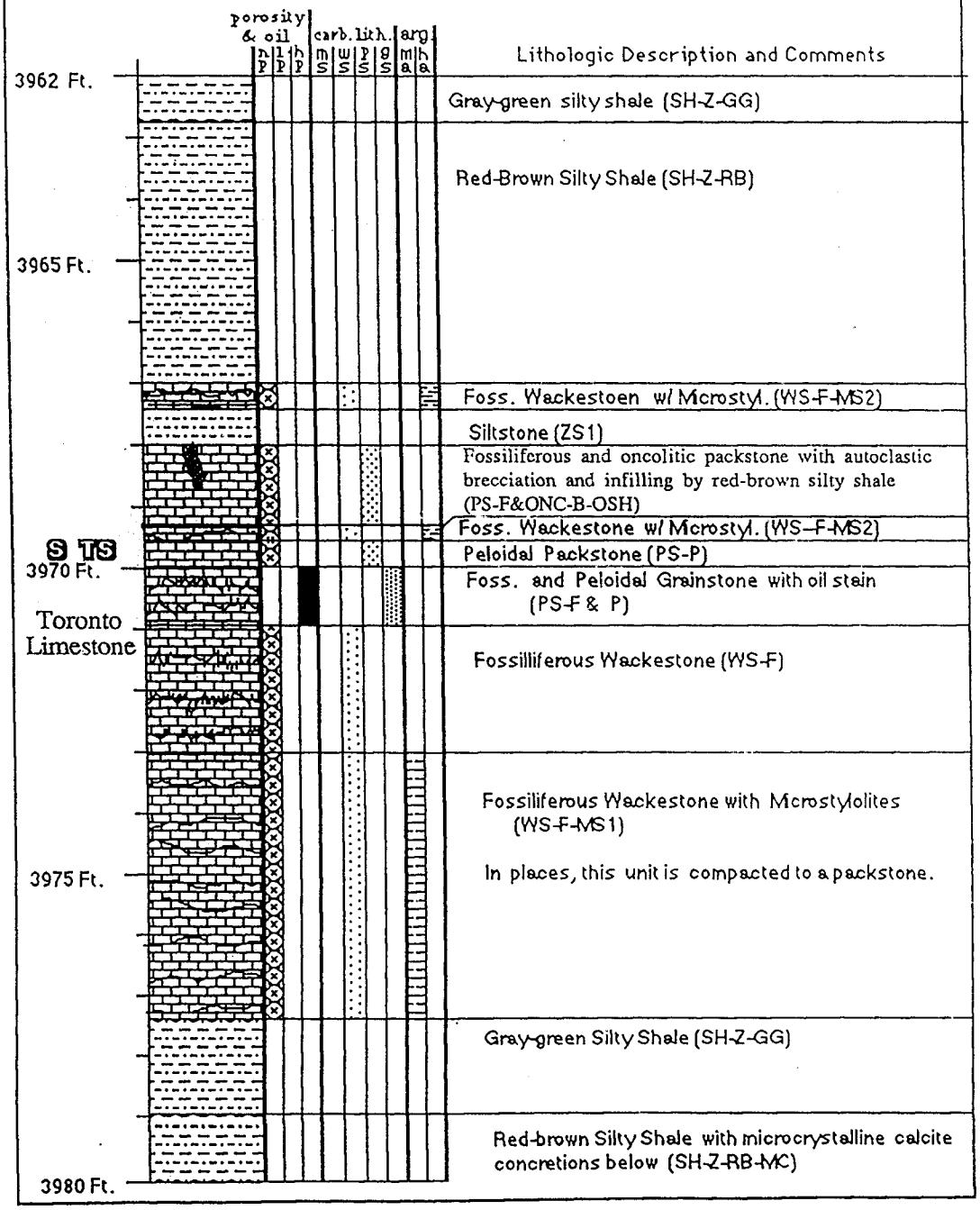

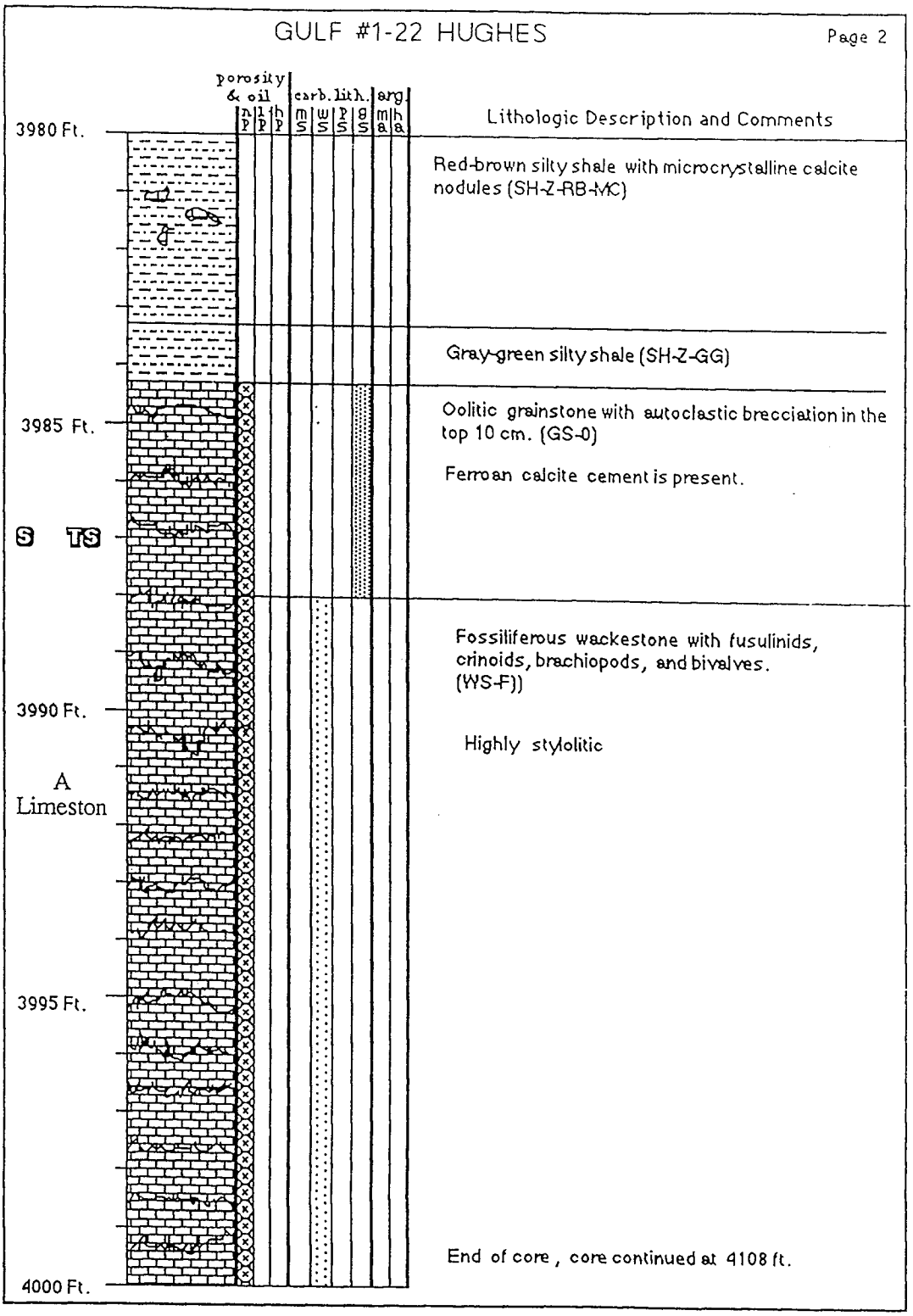
GULF #1-22 HUGHES
Page 2
porosity & oil
carb. lith.
arg.
Lithologic Description and Comments
3980 Ft.
Red-brown silty shale with microcrystalline calcite nodules (SH-Z-RB-MC)
Gray-green silty shale (SH-Z-GG)
3985 Ft.
Oolitic grainstone with autoclastic brecciation in the top 10 cm. (GS-O)
Ferroan calcite cement is present.
S
TS
Fossiliferous wackestone with fusulinids, crinoids, brachiopods, and bivalves. (WS-F))
3990 Ft.
Highly stylolitic
A Limeston
3995 Ft.
End of core, core continued at 4108 ft.
4000 Ft.

GULF #1-22 HUGHES

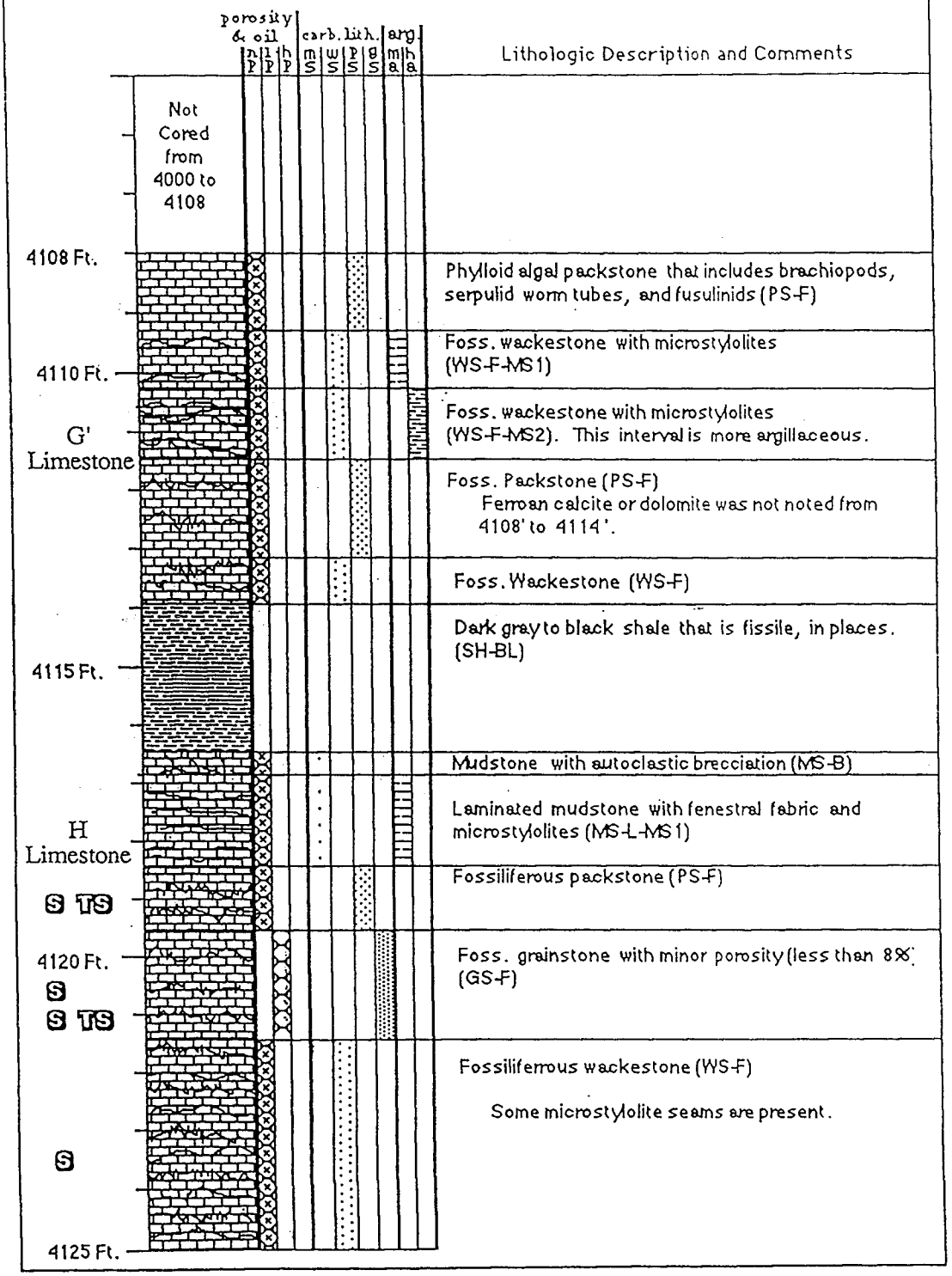

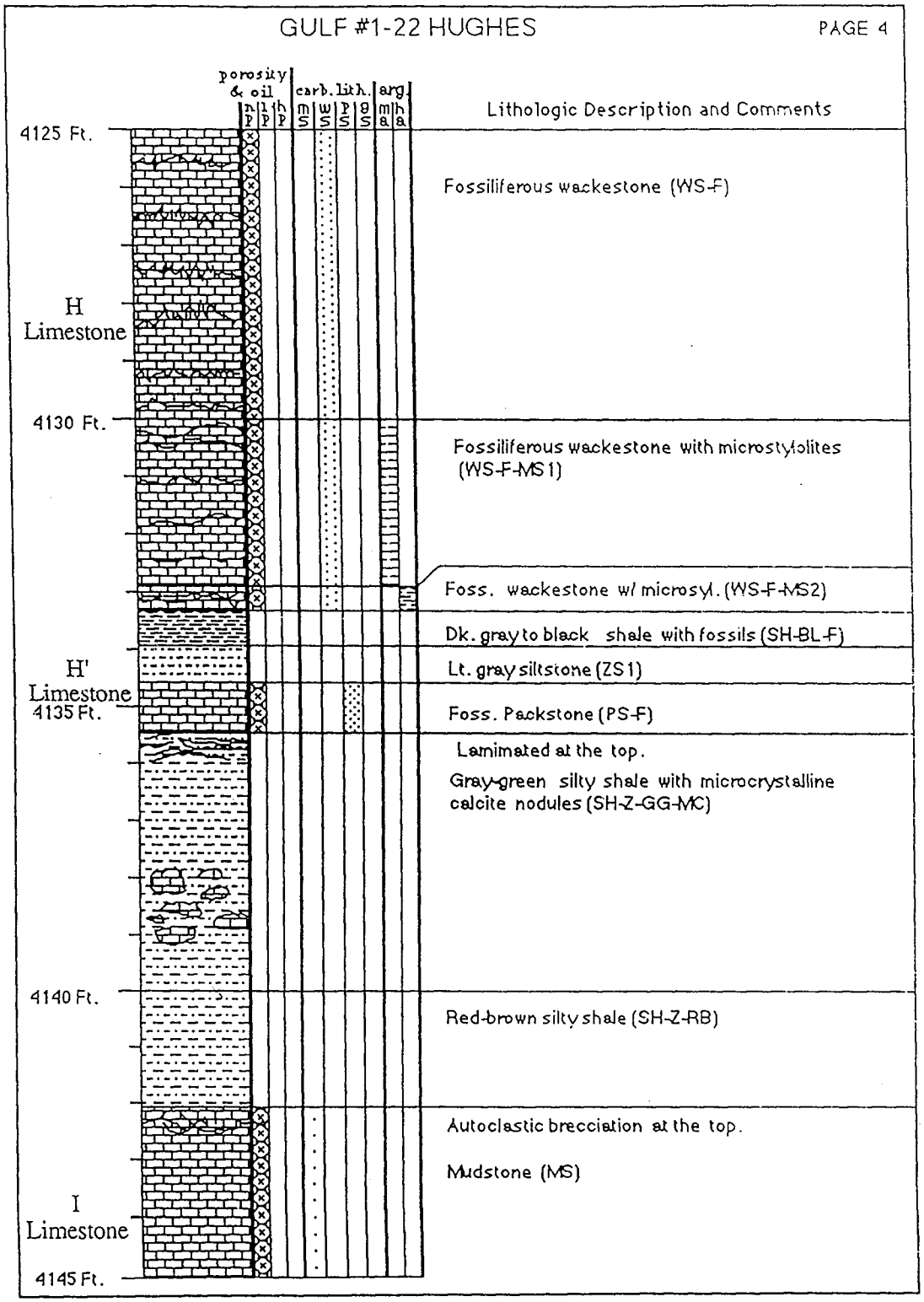
GULF #1-22 HUGHES
PAGE 4
porosity & oil
carb.
lith.
arg.
Lithologic Description and Comments
4125 Ft.
Fossiliferous wackestone (WS-F)
H Limestone
4130 Ft.
Fossiliferous wackestone with microstylolites (WS-F-MS1)
Foss. wackestone w/ microsyl. (WS-F-MS2)
Dk. gray to black shale with fossils (SH-BL-F)
Lt. gray siltstone (ZS1)
H' Limestone
4135 Ft.
Foss. Packstone (PS-F)
Laminated at the top.
Gray-green silty shale with microcrystalline calcite nodules (SH-Z-GG-MC)
4140 Ft.
Red-brown silty shale (SH-Z-RB)
Autoclastic brecciation at the top.
Mudstone (MS)
I Limestone
4145 Ft.

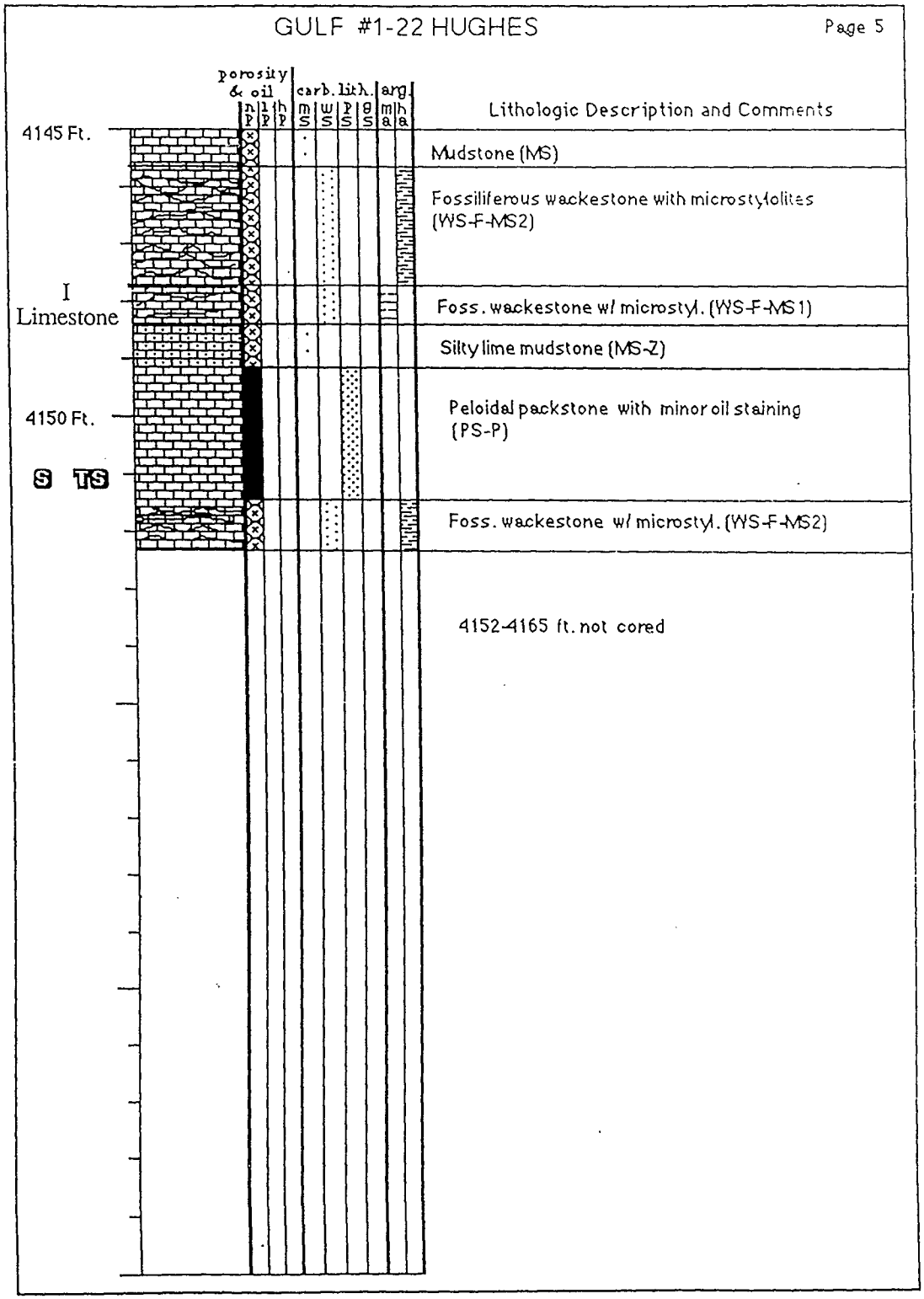
GULF #1-22 HUGHES
Page 5
porosity & oil
carb. lith.
arg.
Lithologic Description and Comments
4145 Ft.
Mudstone (MS)
Fossiliferous wackestone with microstylolites (WS-F-MS2)
I Limestone
Foss. wackestone w/ microstyl. (WS-F-MS1)
Silty lime mudstone (MS-Z)
4150 Ft.
Peloidal packstone with minor oil staining (PS-P)
S TS
Foss. wackestone w/ microstyl. (WS-F-MS2)
4152-4165 ft. not cored

GULF HUGHES #1-22

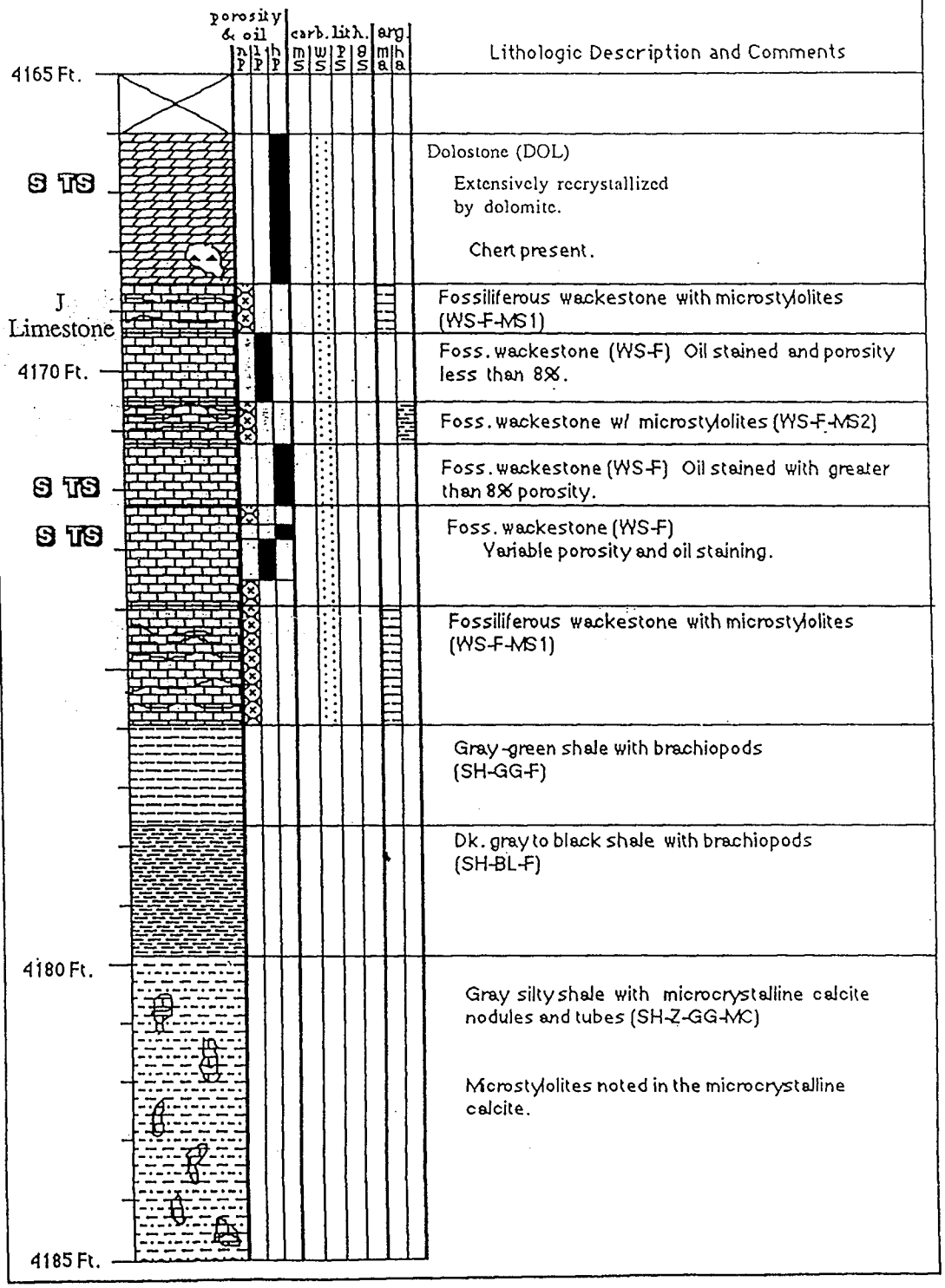

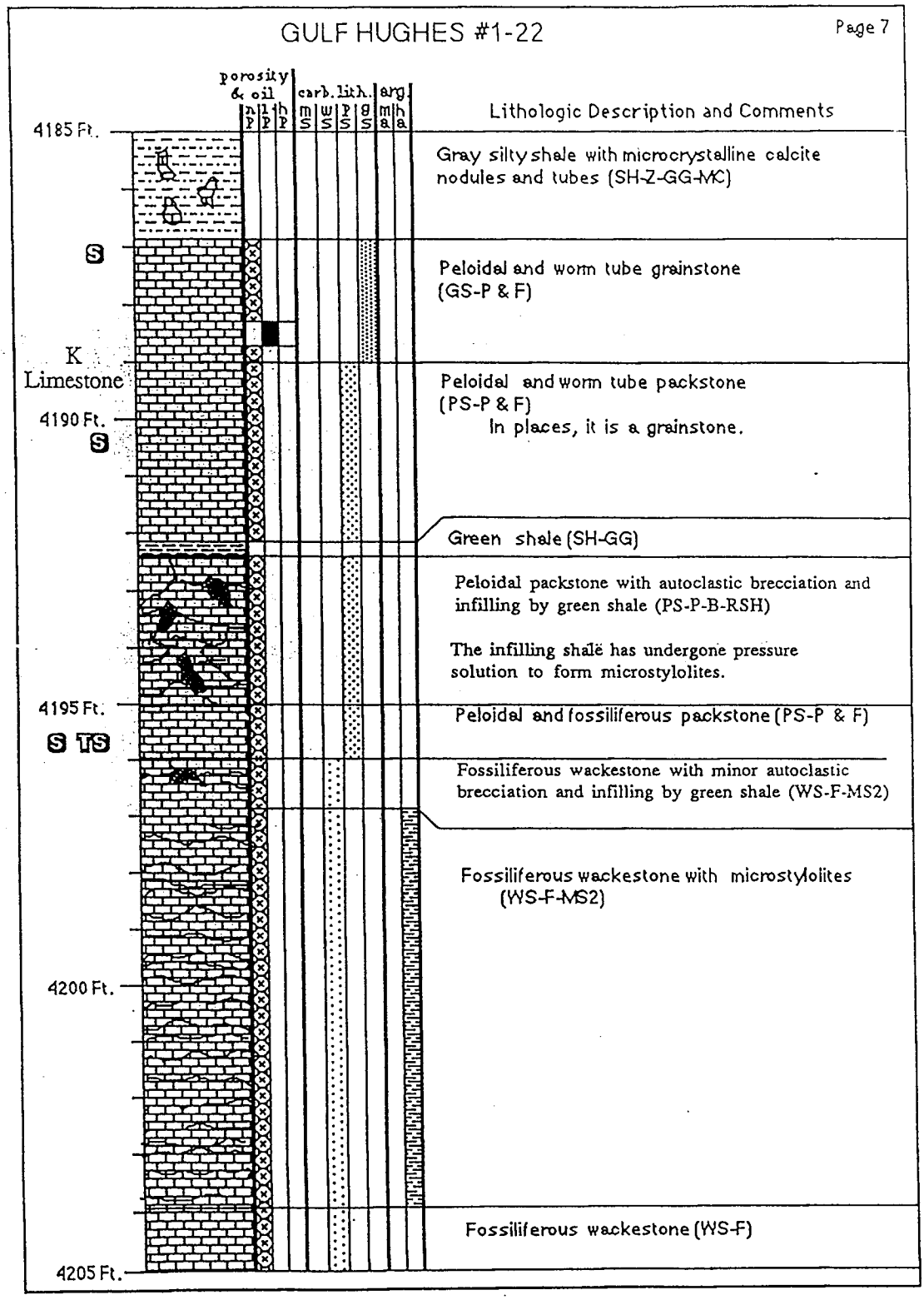
GULF HUGHES #1-22
Page 7
porosity & oil
carb. lith.
arg.
Lithologic Description and Comments
4185 Ft.
Gray silty shale with microcrystalline calcite nodules and tubes (SH-Z-GG-MC)
S
Peloidal and worm tube grainstone (GS-P & F)
K Limestone
Peloidal and worm tube packstone (PS-P & F)
In places, it is a grainstone.
4190 Ft.
S
Green shale (SH-GG)
Peloidal packstone with autoclastic brecciation and infilling by green shale (PS-P-B-RSH)
The infilling shale has undergone pressure solution to form microstylolites.
4195 Ft.
Peloidal and fossiliferous packstone (PS-P & F)
S TS
Fossiliferous wackestone with minor autoclastic brecciation and infilling by green shale (WS-F-MS2)
Fossiliferous wackestone with microstylolites (WS-F-MS2)
4200 Ft.
Fossiliferous wackestone (WS-F)
4205 Ft.

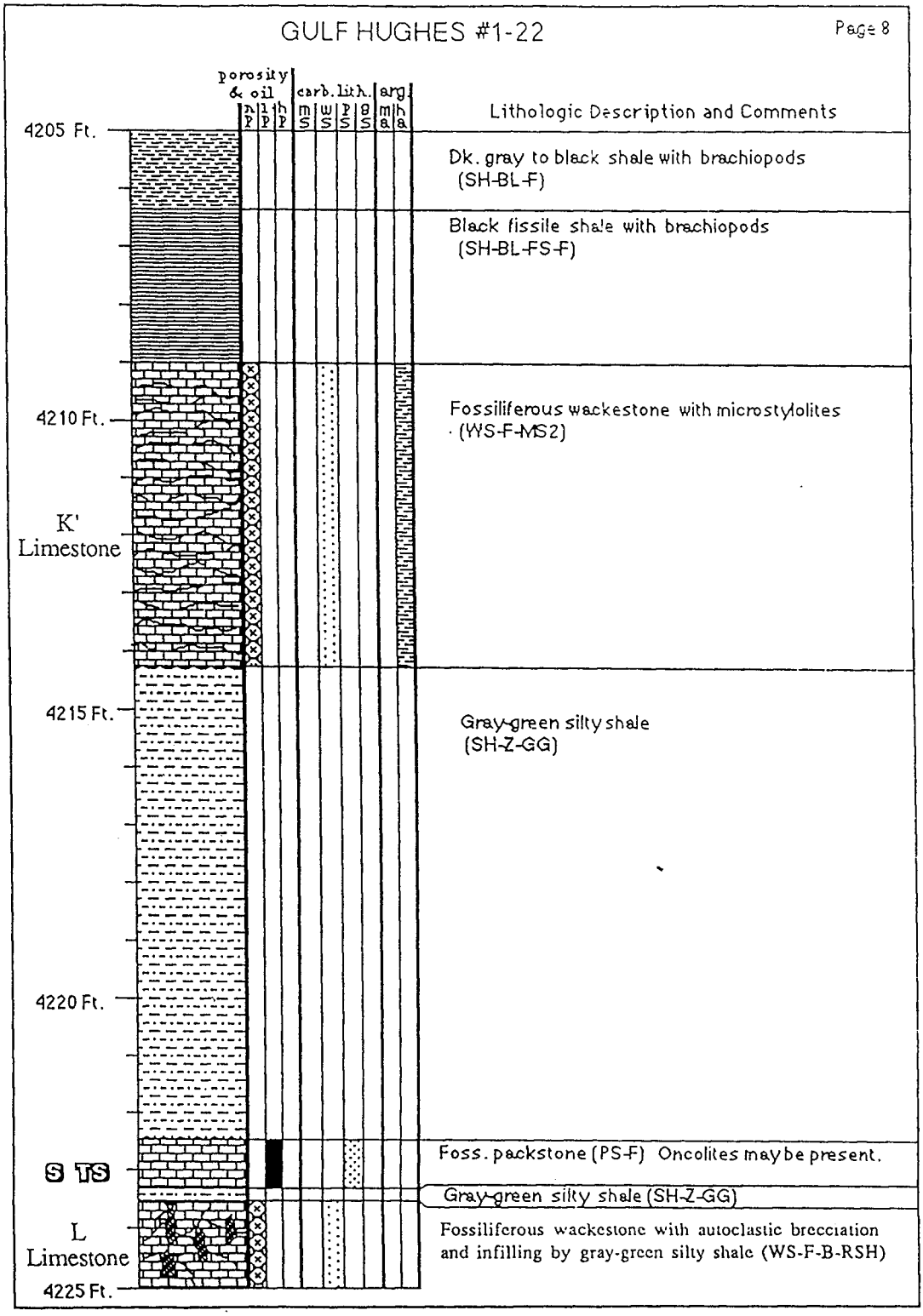
GULF HUGHES #1-22
Page 8
porosity & oil
carb. lith.
arg.
Lithologic Description and Comments
4205 Ft.
Dk. gray to black shale with brachiopods (SH-BL-F)
Black fissile shale with brachiopods (SH-BL-FS-F)
4210 Ft.
Fossiliferous wackestone with microstylolites (WS-F-MS2)
K' Limestone
4215 Ft.
Gray-green silty shale (SH-Z-GG)
4220 Ft.
S TS
Foss. packstone (PS-F) Oncolites may be present.
Gray-green silty shale (SH-Z-GG)
L Limestone
Fossiliferous wackestone with autoclastic brecciation and infilling by gray-green silty shale (WS-F-B-RSH)
4225 Ft.

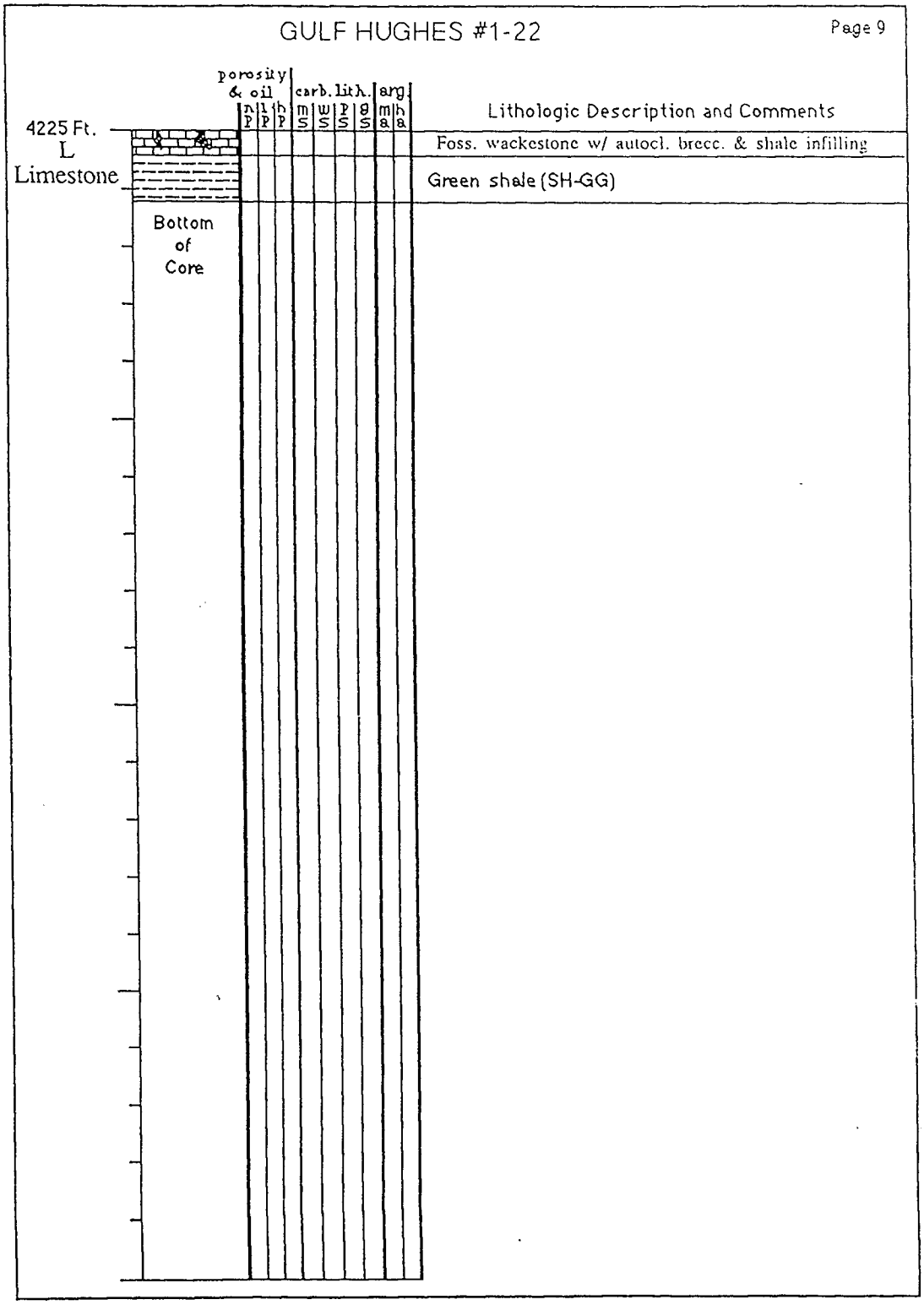
GULF HUGHES #1-22
Page 9
porosity & oil
carb. lith.
arg.
Lithologic Description and Comments
4225 Ft.
L
Limestone
Foss. wackestone w/ autocl. brecc. & shale infilling
Green shale (SH-GG)
Bottom of Core

Theodore Gore Co. #1 Denny
C NE SW, Sec. 5-T5S-R34W
Rawlins County, Kansas

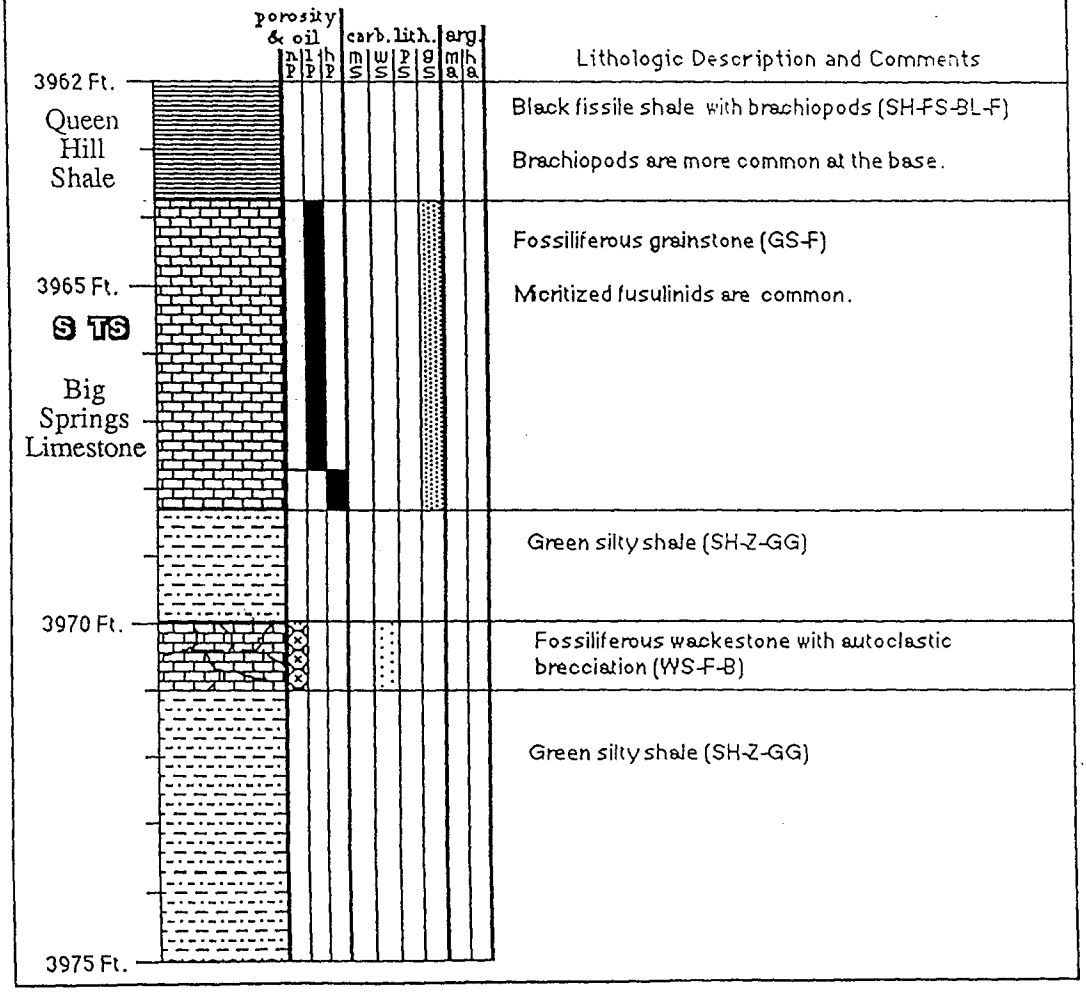

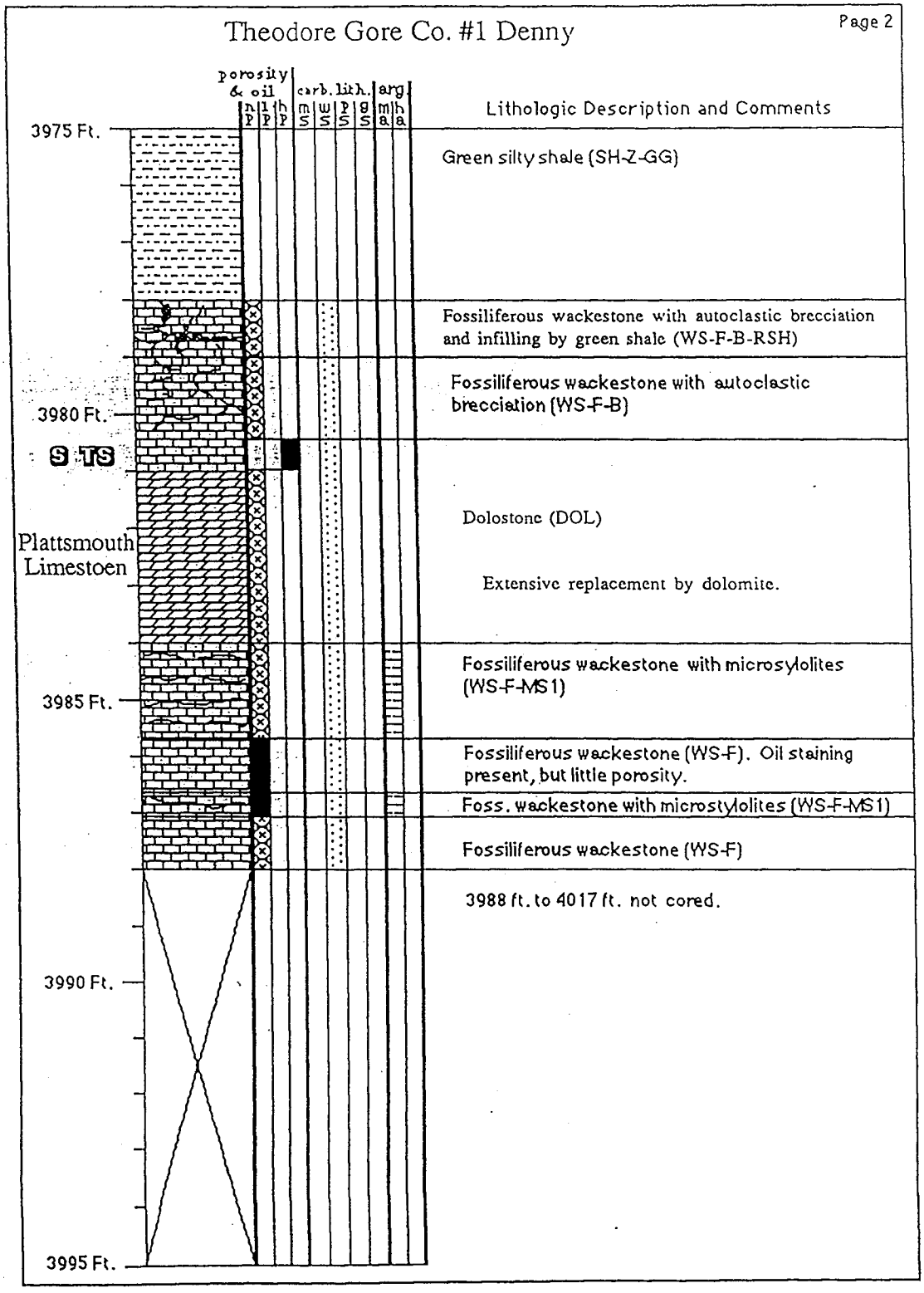
Theodore Gore Co. #1 Denny
Page 2
porosity & oil
carb. lith.
arg.
Lithologic Description and Comments
3975 Ft.
Green silty shale (SH-Z-GG)
Fossiliferous wackestone with autoclastic brecciation and infilling by green shale (WS-F-B-RSH)
Fossiliferous wackestone with autoclastic brecciation (WS-F-B)
3980 Ft.
S TS
Dolostone (DOL)
Plattsmouth Limestoen
Extensive replacement by dolomite.
Fossiliferous wackestone with microsylolites (WS-F-MS1)
3985 Ft.
Fossiliferous wackestone (WS-F). Oil staining present, but little porosity.
Foss. wackestone with microstylolites (WS-F-MS1)
Fossiliferous wackestone (WS-F)
3988 ft. to 4017 ft. not cored.
3990 Ft.
3995 Ft.

Theodore Gore Co. #1 Denny

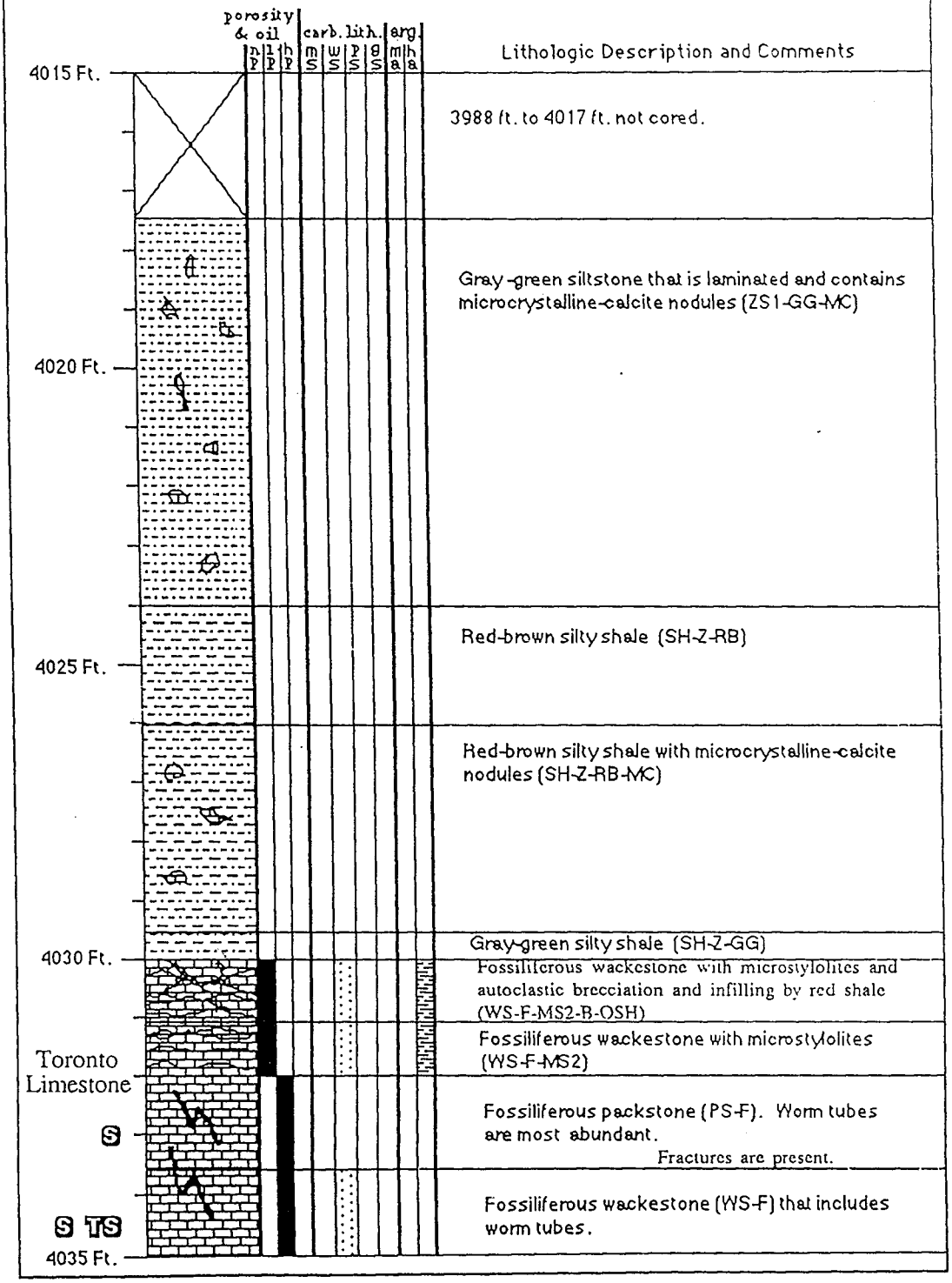

Theodore Gore Co. #1 Denny

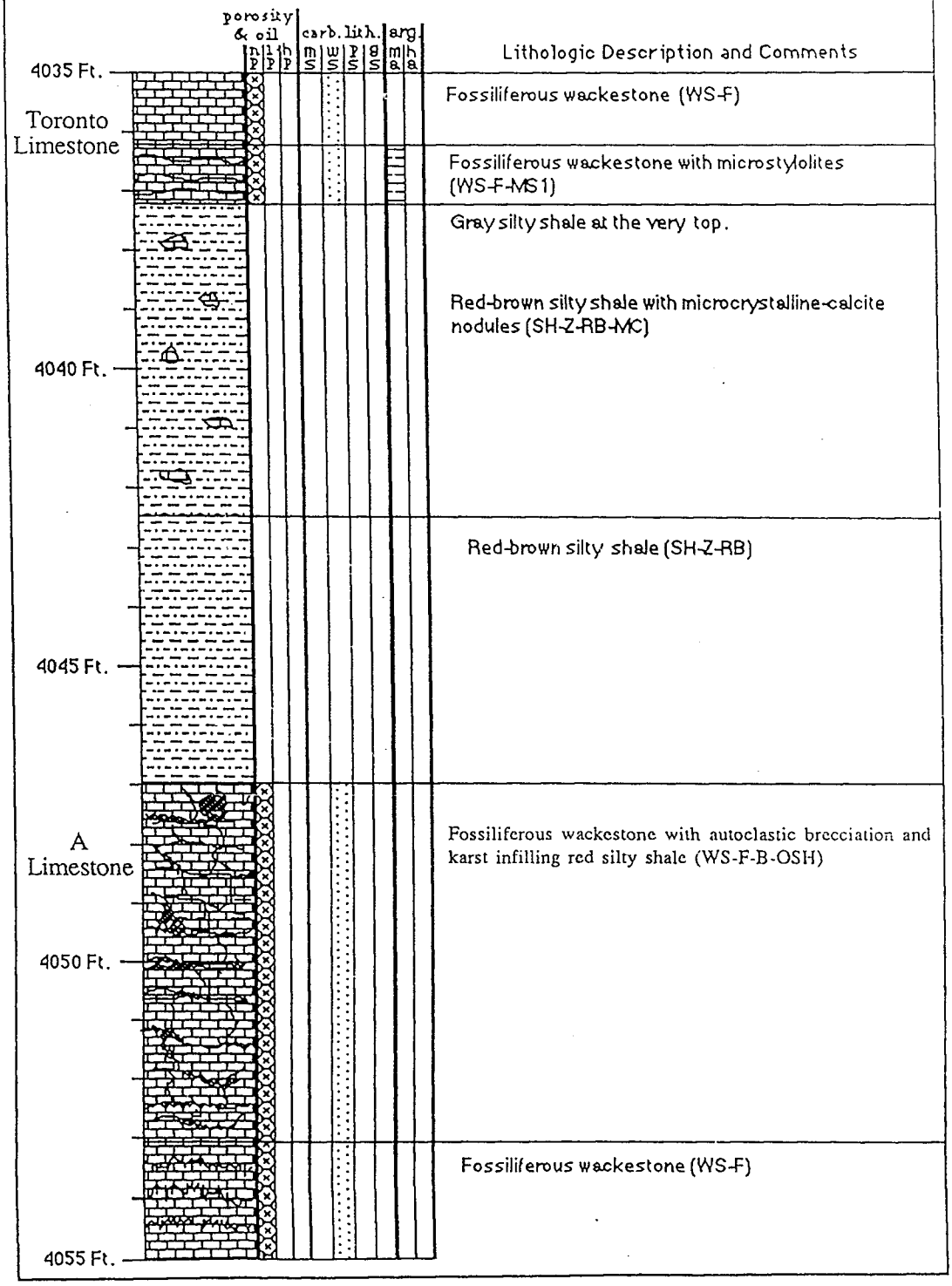

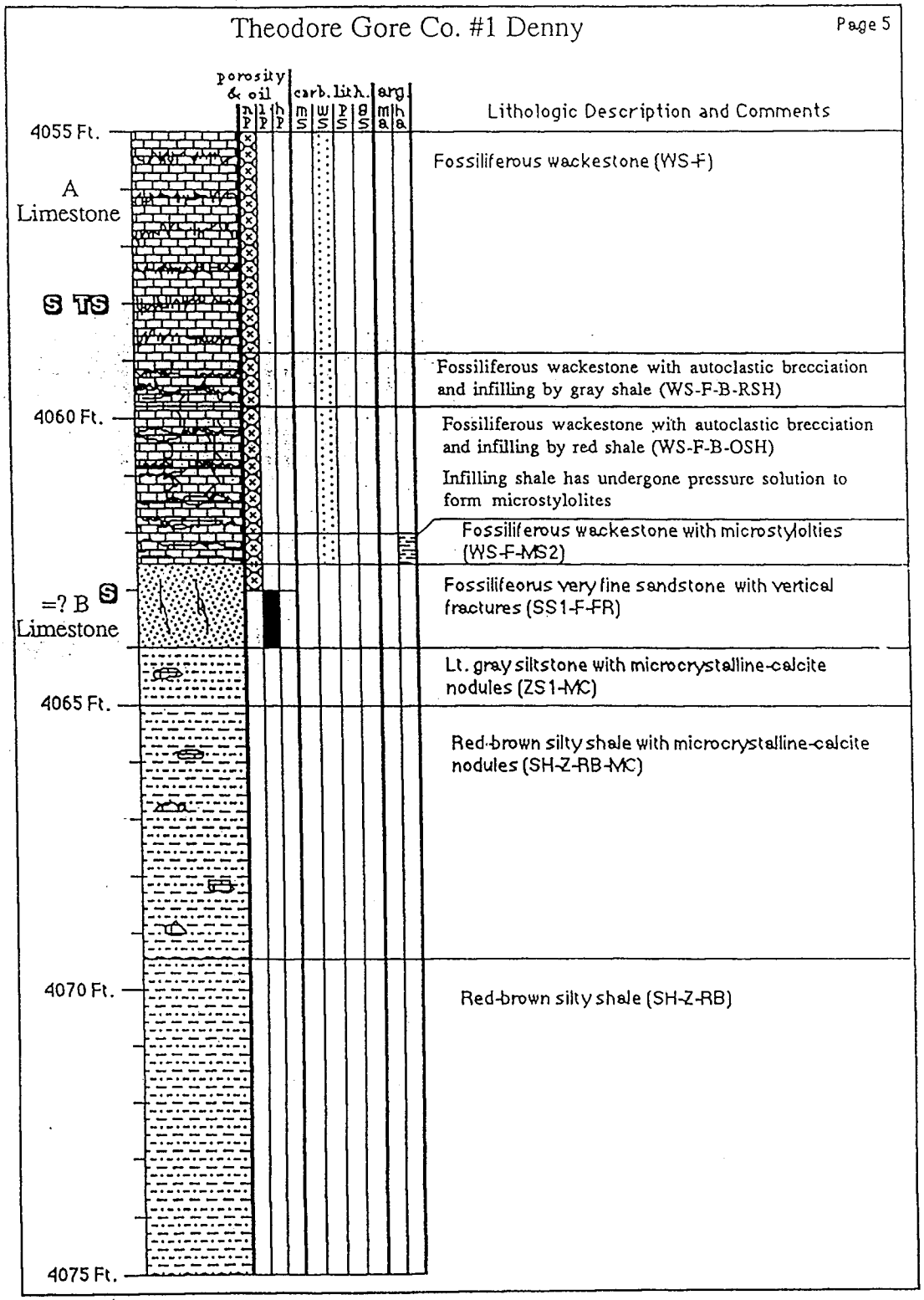
Theodore Gore Co. #1 Denny
Page 5
porosity & oil
carb. lith.
arg.
Lithologic Description and Comments
4055 Ft.
A Limestone
S TS
Fossiliferous wackestone (WS-F)
Fossiliferous wackestone with autoclastic brecciation and infilling by gray shale (WS-F-B-RSH)
4060 Ft.
Fossiliferous wackestone with autoclastic brecciation and infilling by red shale (WS-F-B-OSH)
Infilling shale has undergone pressure solution to form microstylolites
Fossiliferous wackestone with microstylolties (WS-F-MS2)
=? B Limestone
S
Fossilifeorus very fine sandstone with vertical fractures (SS1-F-FR)
Lt. gray siltstone with microcrystalline-calcite nodules (ZS1-MC)
4065 Ft.
Red-brown silty shale with microcrystalline-calcite nodules (SH-Z-RB-MC)
4070 Ft.
Red-brown silty shale (SH-Z-RB)
4075 Ft.

Theodore Gore Co. #1 Denny

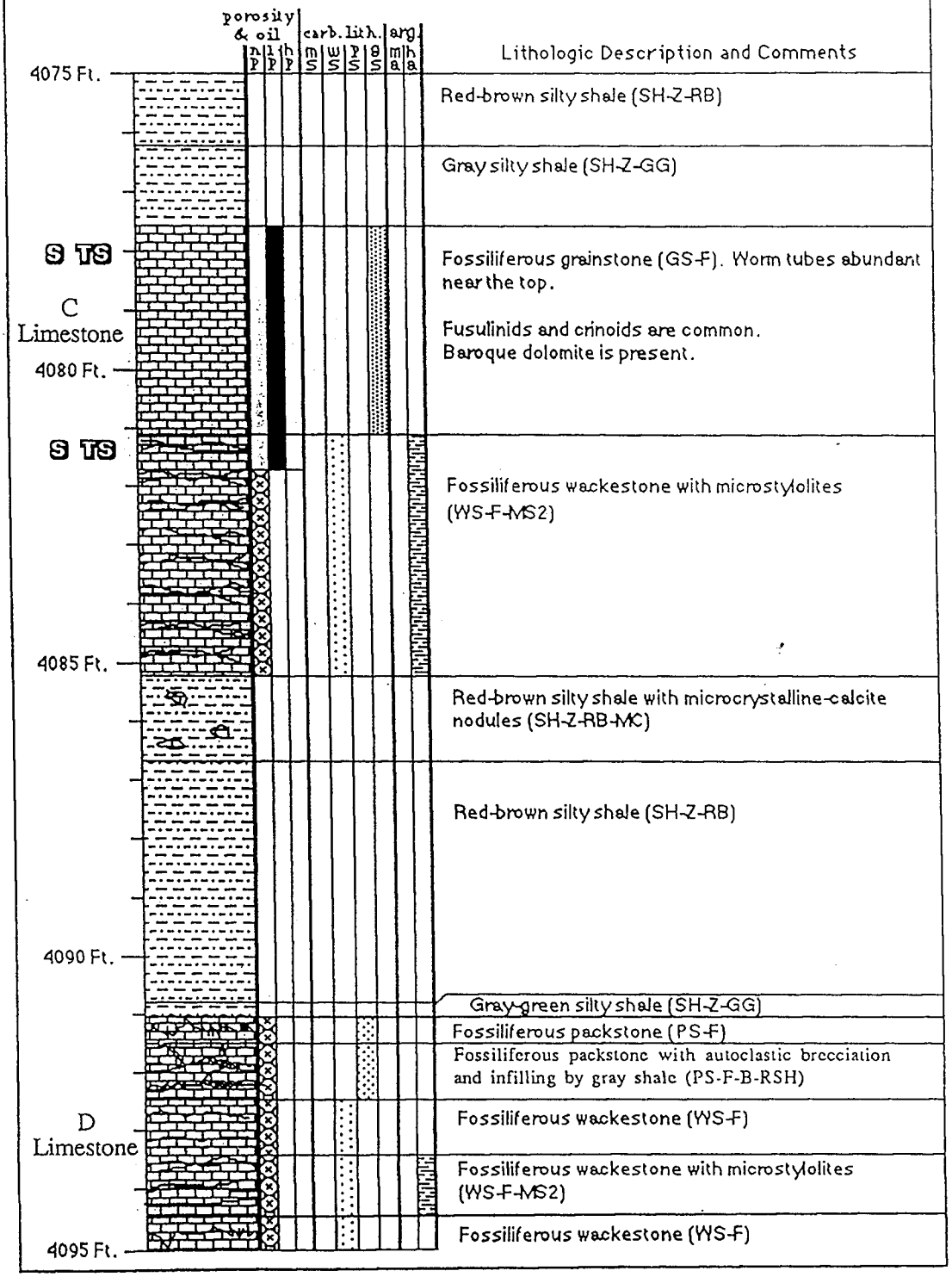

Theodore Gore Co. #1 Denny

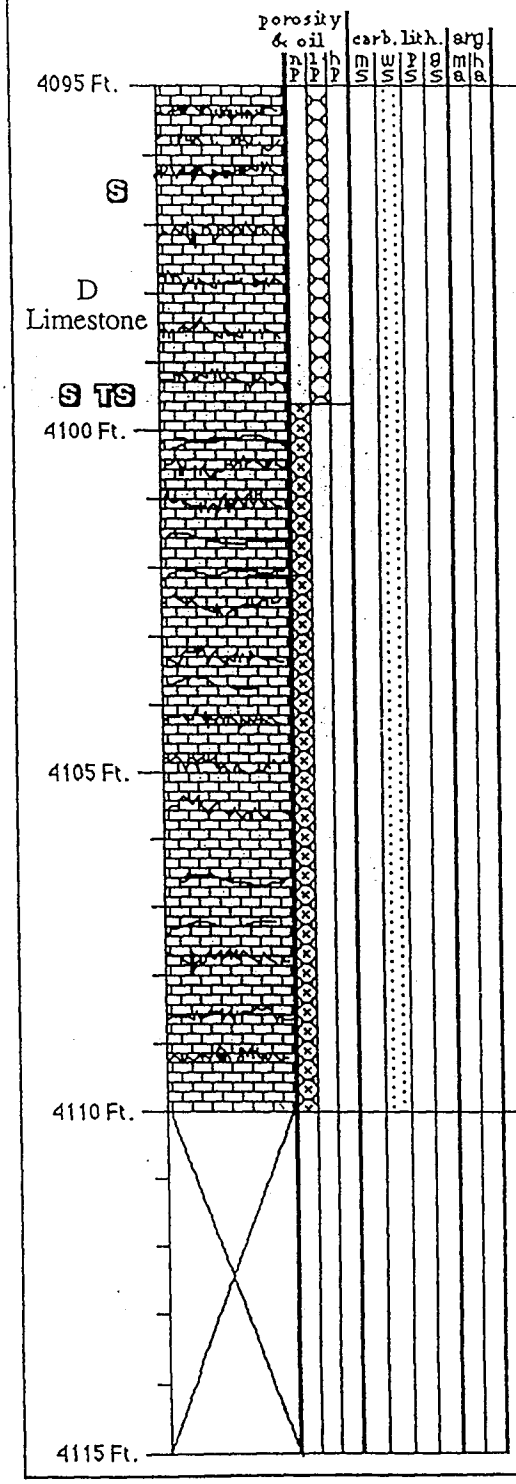

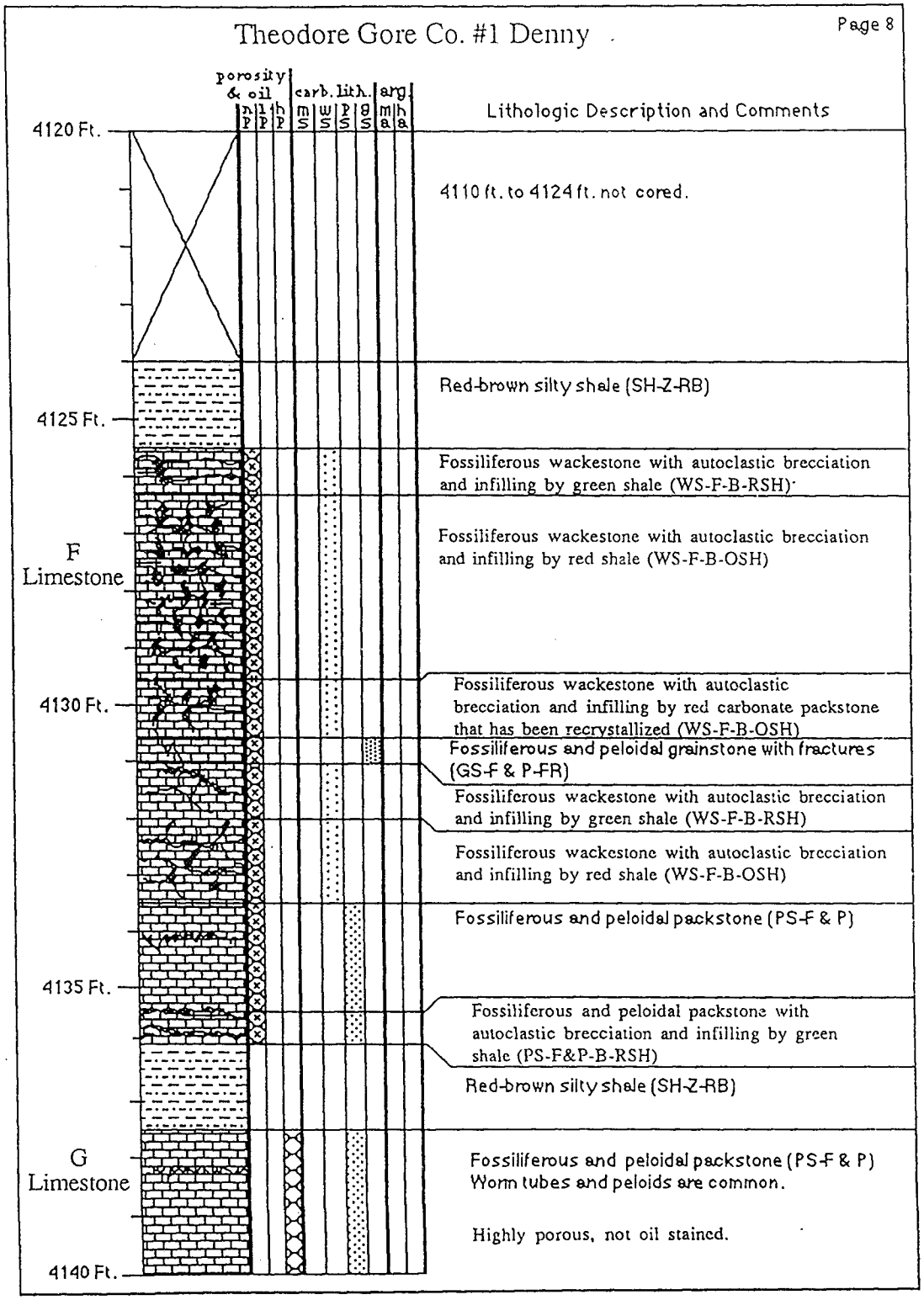
Theodore Gore Co. #1 Denny
porosity & oil
carb. lith.
arg.
Lithologic Description and Comments
4120 Ft.
4110 ft. to 4124 ft. not cored.
Red-brown silty shale (SH-Z-RB)
4125 Ft.
Fossiliferous wackestone with autoclastic brecciation and infilling by green shale (WS-F-B-RSH)
Fossiliferous wackestone with autoclastic brecciation and infilling by red shale (WS-F-B-OSH)
F Limestone
Fossiliferous wackestone with autoclastic brecciation and infilling by red carbonate packstone that has been recrystallized (WS-F-B-OSH)
4130 Ft.
Fossiliferous and peloidal grainstone with fractures (GS-F & P-FR)
Fossiliferous wackestone with autoclastic brecciation and infilling by green shale (WS-F-B-RSH)
Fossiliferous wackestone with autoclastic brecciation and infilling by red shale (WS-F-B-OSH)
Fossiliferous and peloidal packstone (PS-F & P)
4135 Ft.
Fossiliferous and peloidal packstone with autoclastic brecciation and infilling by green shale (PS-F&P-B-RSH)
Red-brown silty shale (SH-Z-RB)
G Limestone
Fossiliferous and peloidal packstone (PS-F & P)
Worm tubes and peloids are common.
Highly porous, not oil stained.
4140 Ft.

Theodore Gore Co. #1 Denny

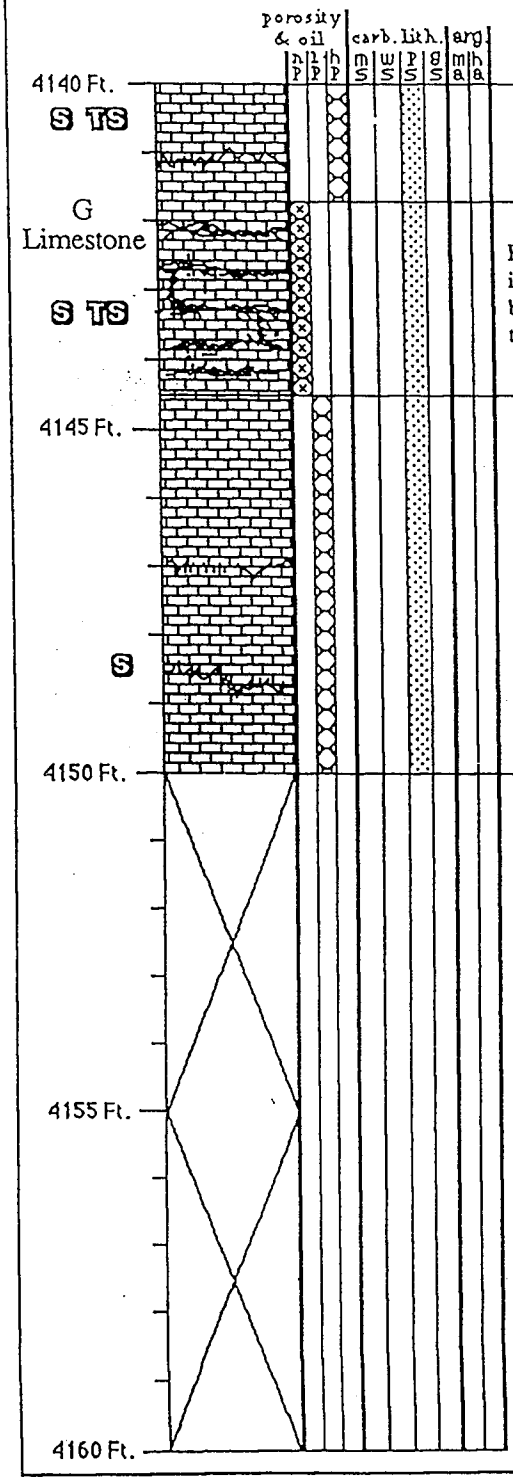

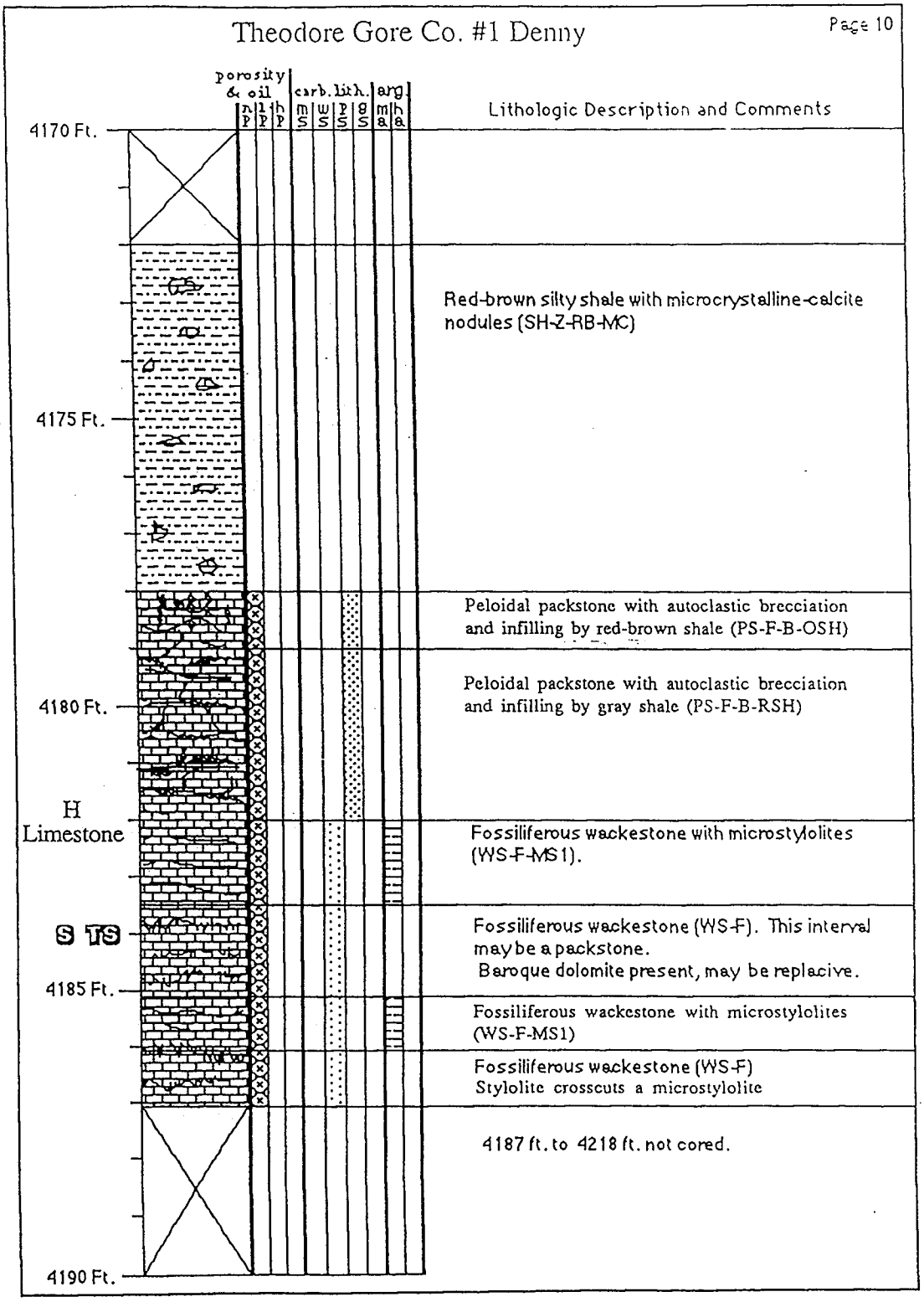
Theodore Gore Co. #1 Denny
porosity & oil
carb. lith.
arg
Lithologic Description and Comments
4170 Ft.
4175 Ft.
4180 Ft.
H Limestone
S TS
4185 Ft.
4190 Ft.
Red-brown silty shale with microcrystalline-calcite nodules (SH-Z-RB-MC)
Peloidal packstone with autoclastic brecciation and infilling by red-brown shale (PS-F-B-OSH)
Peloidal packstone with autoclastic brecciation and infilling by gray shale (PS-F-B-RSH)
Fossiliferous wackestone with microstylolites (WS-F-MS1).
Fossiliferous wackestone (WS-F). This interval may be a packstone.
Baroque dolomite present, may be replacive.
Fossiliferous wackestone with microstylolites (WS-F-MS1)
Fossiliferous wackestone (WS-F)
Stylolite crosscuts a microstylolite
4187 ft. to 4218 ft. not cored.

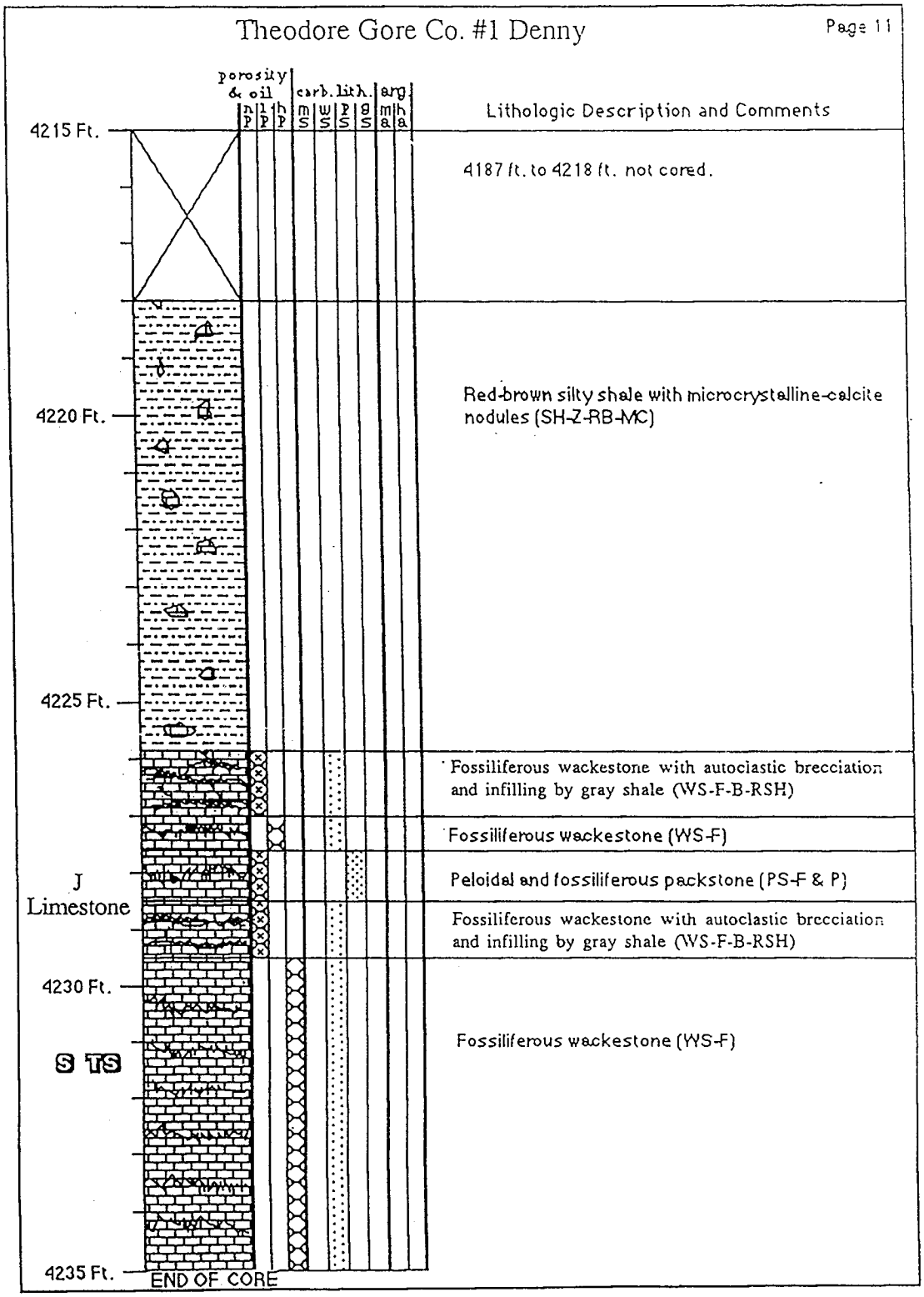
Theodore Gore Co. #1 Denny
Page 11
porosity & oil
carb. lith.
arg.
Lithologic Description and Comments
4215 Ft.
4187 ft. to 4218 ft. not cored.
4220 Ft.
Red-brown silty shale with microcrystalline-calcite nodules (SH-Z-RB-MC)
4225 Ft.
Fossiliferous wackestone with autoclastic brecciation and infilling by gray shale (WS-F-B-RSH)
Fossiliferous wackestone (WS-F)
Peloidal and fossiliferous packstone (PS-F & P)
J Limestone
Fossiliferous wackestone with autoclastic brecciation and infilling by gray shale (WS-F-B-RSH)
4230 Ft.
Fossiliferous wackestone (WS-F)
S TS
4235 Ft.
END OF CORE

SINCLAIR PRAIRIE #1 GUY MERCER

NE NE NW, Section 28-T10S-R40W
Sherman County, Kansas

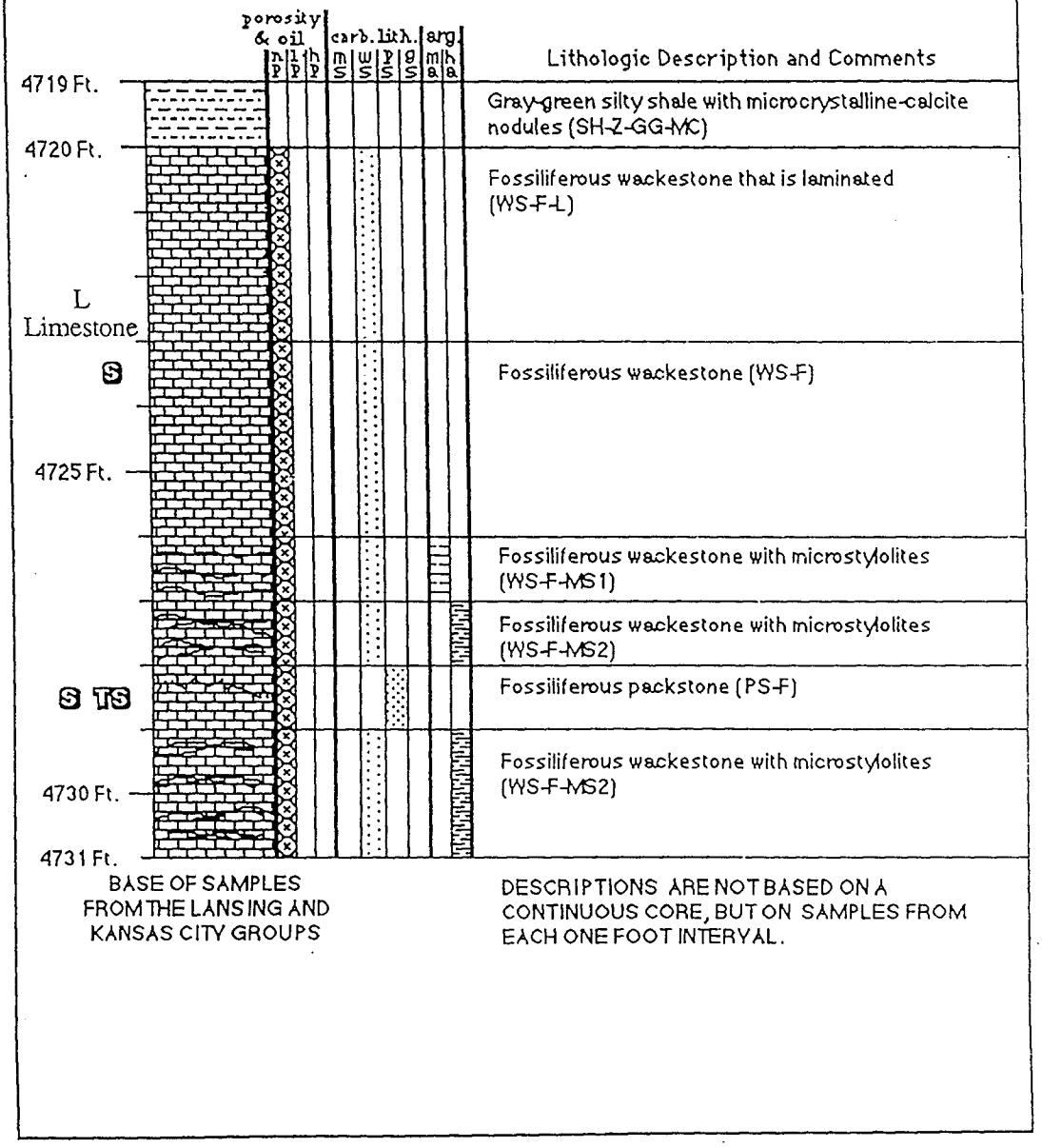

HUSKY OIL CO. #6 BROOKS

SW NW, Section 18-T2N-R27W
Red Willow County, Nebraska
Ackman Field

Latitude: 40.141437 N
Longitude: 100.416501 W

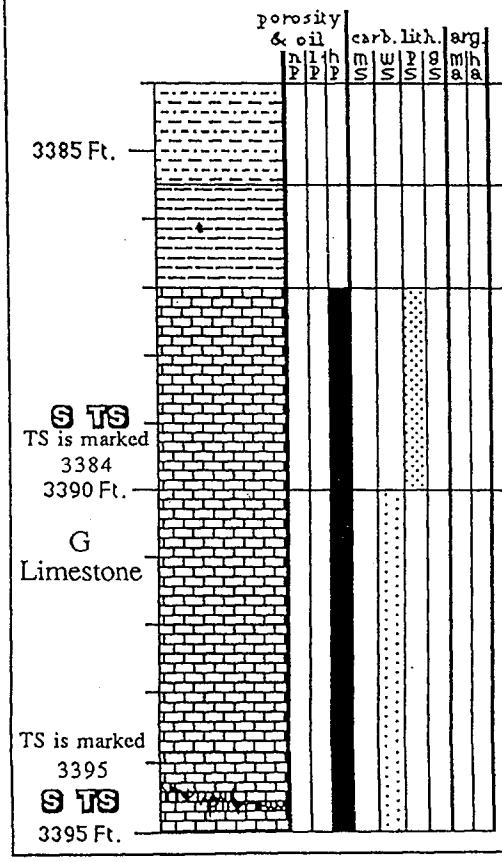

HUSKY OIL CO. #6 BROOKS

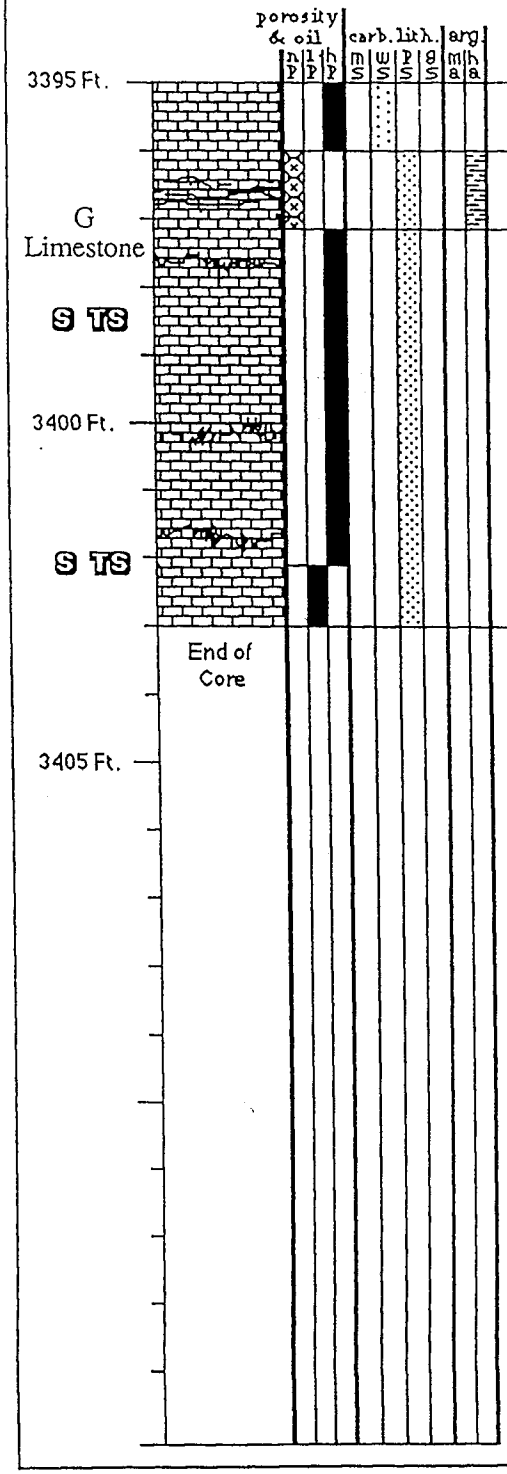

Porosity and Permeability data from Hunt (1981) for the Brooks #6 core.

Depth	Sample #	Porosity	Permeability
3390 ft.	H6A	*	6.44 md
3390 ft.	H6B	47.4%	6.44 md
3387 ft.	H2	24.9%	1.15 md
3389 ft.	H1	8.5%	.38 md
3394 ft.	H9	*	2.80 md
3396 ft.	H3	*	7.68 md
3400 ft.	H5	9.1%	0.00 md

*porosity values not obtained

GEOSON OIL COMPANY, INC. #2 HIDY

C SE NW, Sec. 27-T3N-33W
Drilled in 1981 and produced 23 IBOPD from
4065-76 ft. of which 4 ft. were perforated.
Bush Creek Field

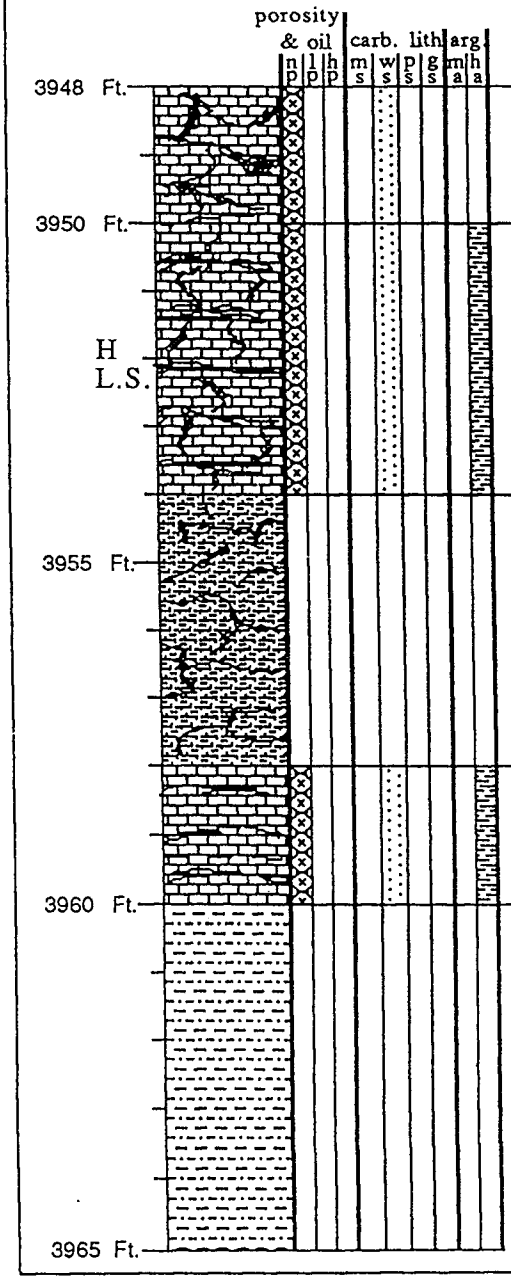

GEOSON OIL COMPANY, INC. #2 HIDY

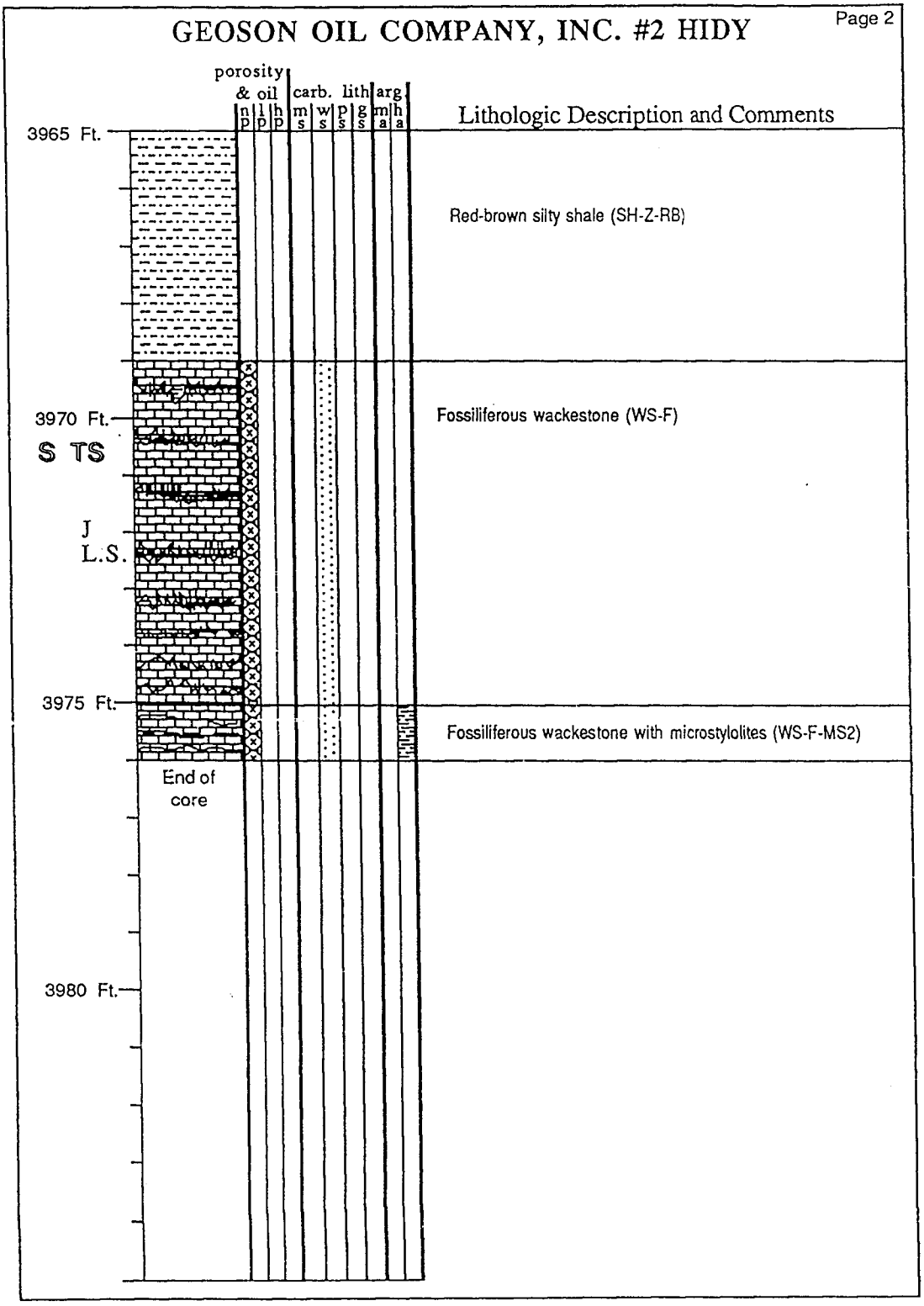

CITIES SERVICE # 1 KNUDSON "A"

NE SE NW, Section 16-T7S-R32W
Thomas County, Kansas

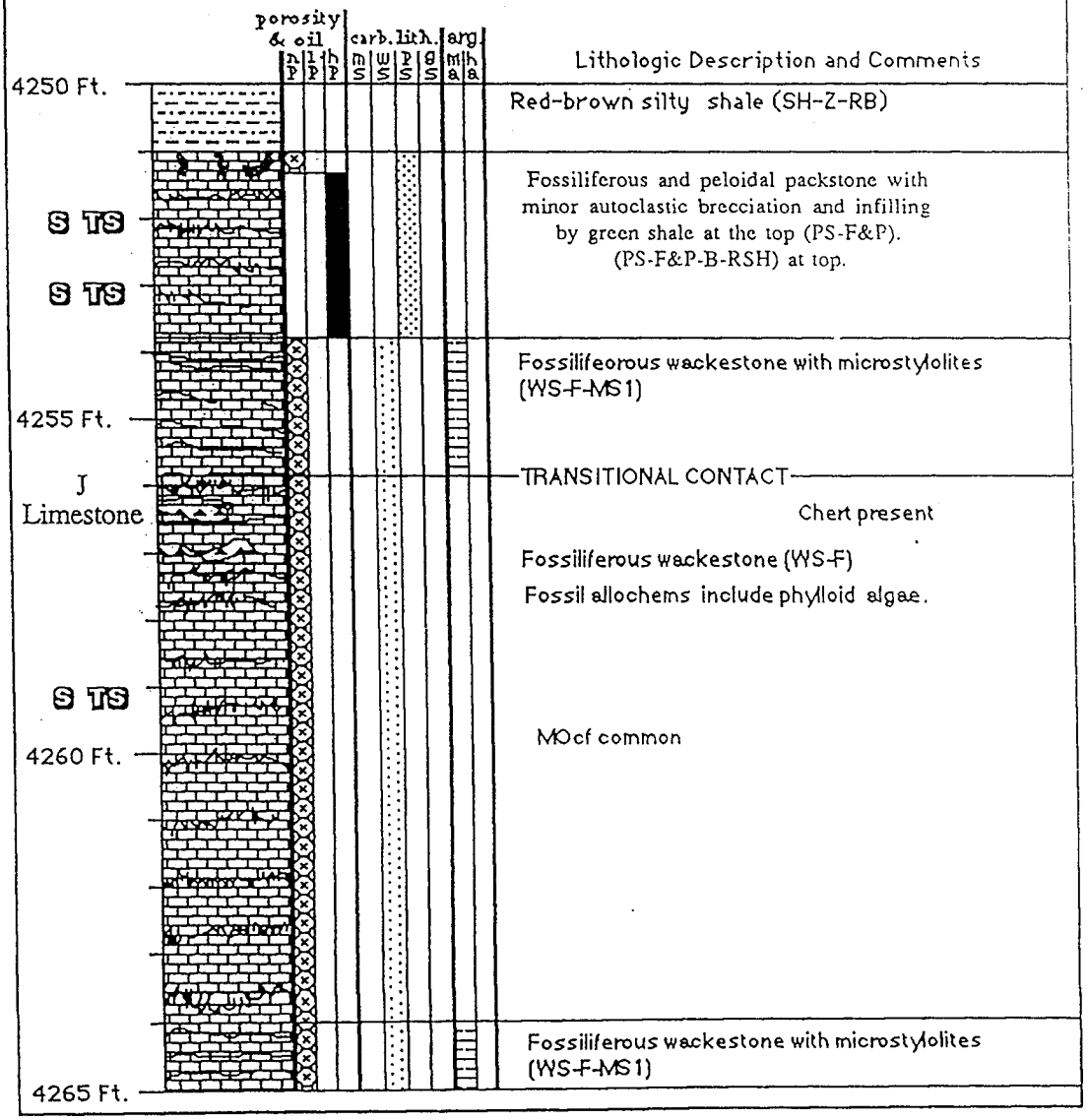

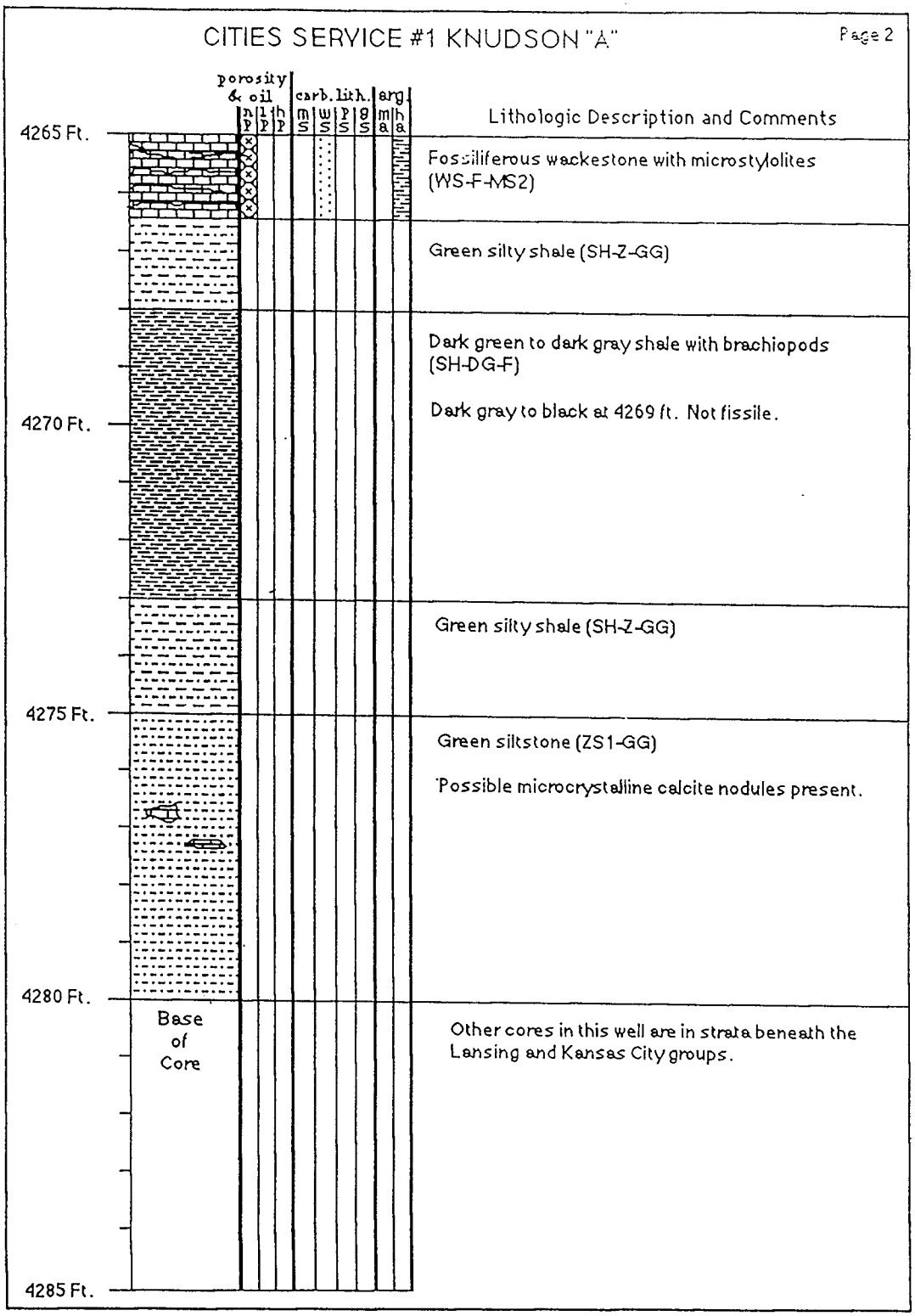
CITIES SERVICE #1 KNUDSON "A"
Page 2
porosity & oil
carb. lith.
arg.
n p
l p
h p
m s
w s
p s
g s
m a
h a
Lithologic Description and Comments
4265 Ft.
Fossiliferous wackestone with microstylolites (WS-F-MS2)
Green silty shale (SH-Z-GG)
Dark green to dark gray shale with brachiopods (SH-DG-F)
Dark gray to black at 4269 ft. Not fissile.
4270 Ft.
Green silty shale (SH-Z-GG)
4275 Ft.
Green siltstone (ZS1-GG)
Possible microcrystalline calcite nodules present.
4280 Ft.
Base of Core
Other cores in this well are in strata beneath the Lansing and Kansas City groups.
4285 Ft.

LADD PETROLEUM DC UNIT 2-3 A

C-SW-SE, Sec. 21-T3N-R34W
Hitchcock County, Nebraska
Drilled June, 1977

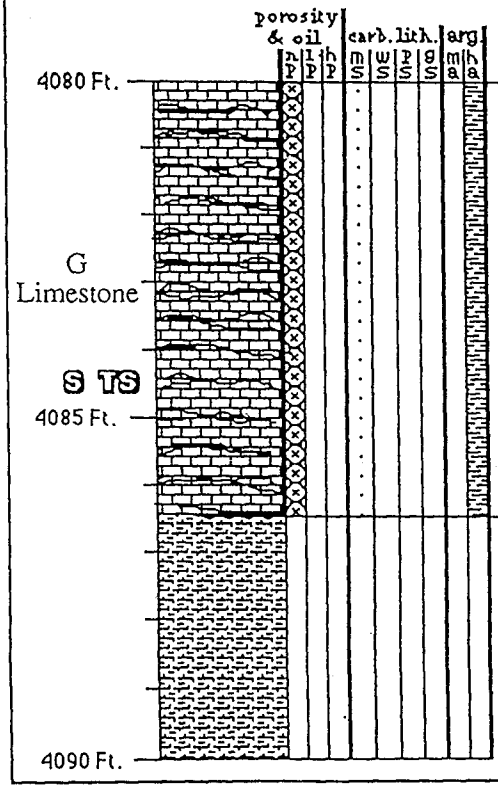

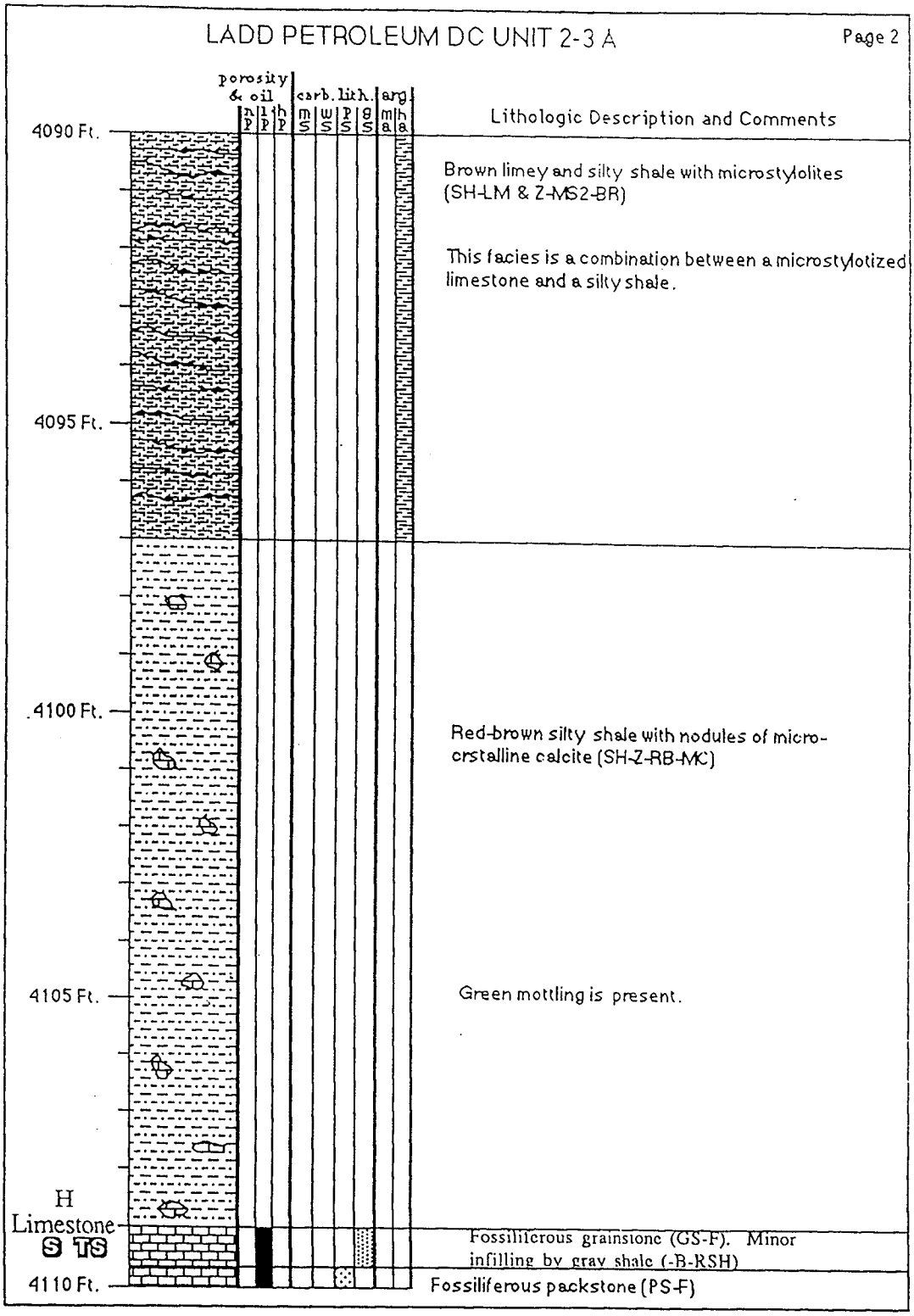
LADD PETROLEUM DC UNIT 2-3 A
Page 2
porosity & oil
carb. lith.
arg.
n p
l p
h p
m s
w s
p s
g s
m a
h a
Lithologic Description and Comments
4090 Ft.
4095 Ft.
4100 Ft.
4105 Ft.
4110 Ft.
H Limestone
S TS
Brown limey and silty shale with microstylolites (SH-LM & Z-MS2-BR)
This facies is a combination between a microstylolized limestone and a silty shale.
Red-brown silty shale with nodules of micro-crystalline calcite (SH-Z-RB-MC)
Green mottling is present.
Fossiliferous grainstone (GS-F). Minor infilling by gray shale (-B-RSH)
Fossiliferous packstone (PS-F)

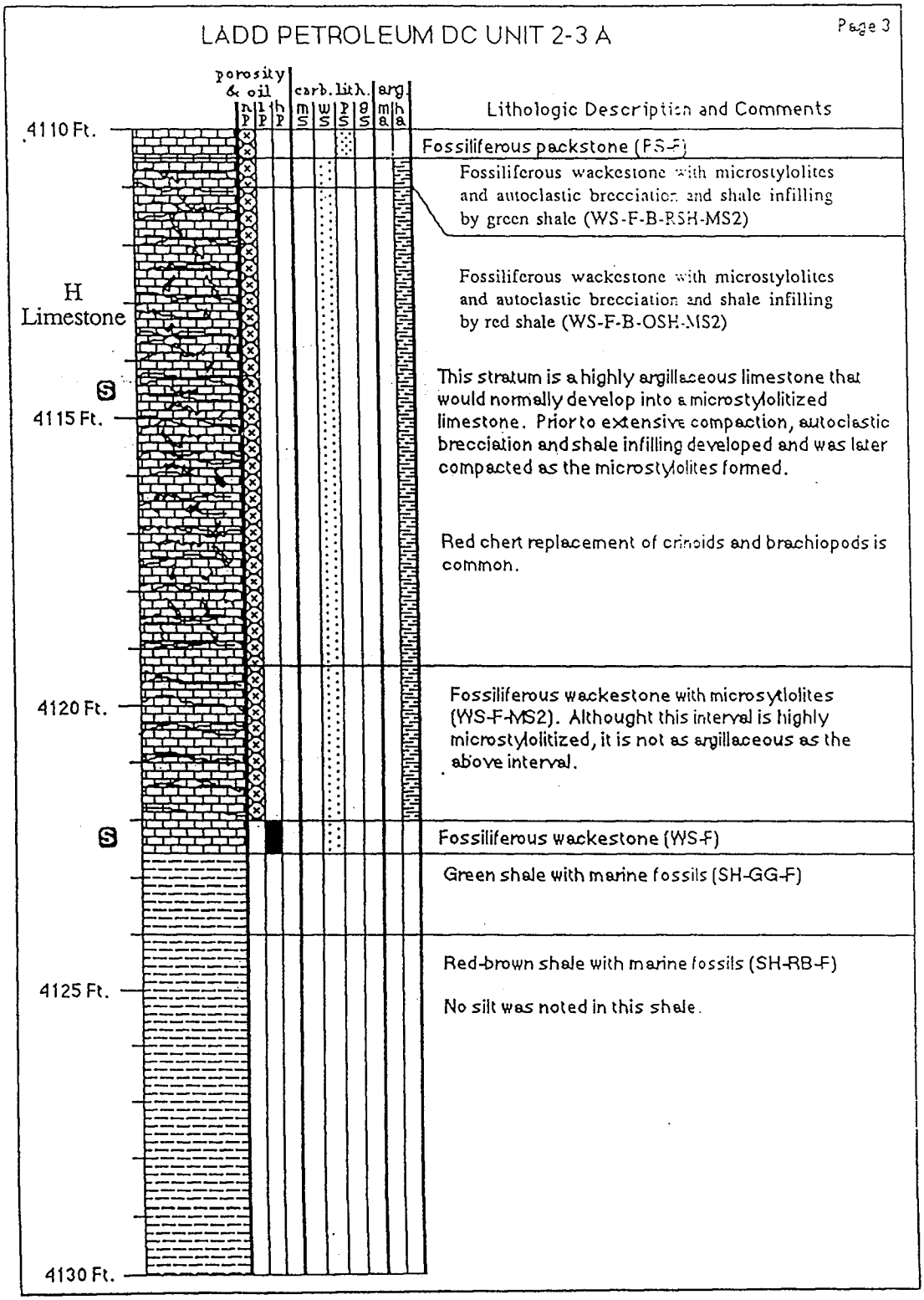
LADD PETROLEUM DC UNIT 2-3 A
Page 3
porosity & oil
carb. lith.
arg.
Lithologic Description and Comments
4110 Ft.
Fossiliferous packstone (FS-F)
Fossiliferous wackestone with microstylolites and autoclastic brecciation and shale infilling by green shale (WS-F-B-RSH-MS2)
H Limestone
Fossiliferous wackestone with microstylolites and autoclastic brecciation and shale infilling by red shale (WS-F-B-OSH-MS2)
S
4115 Ft.
This stratum is a highly argillaceous limestone that would normally develop into a microstylolitized limestone. Prior to extensive compaction, autoclastic brecciation and shale infilling developed and was later compacted as the microstylolites formed.
Red chert replacement of crinoids and brachiopods is common.
4120 Ft.
Fossiliferous wackestone with microsytlolites (WS-F-MS2). Althought this interval is highly microstylolitized, it is not as argillaceous as the above interval.
S
Fossiliferous wackestone (WS-F)
Green shale with marine fossils (SH-GG-F)
Red-brown shale with marine fossils (SH-RB-F)
4125 Ft.
No silt was noted in this shale.
4130 Ft.

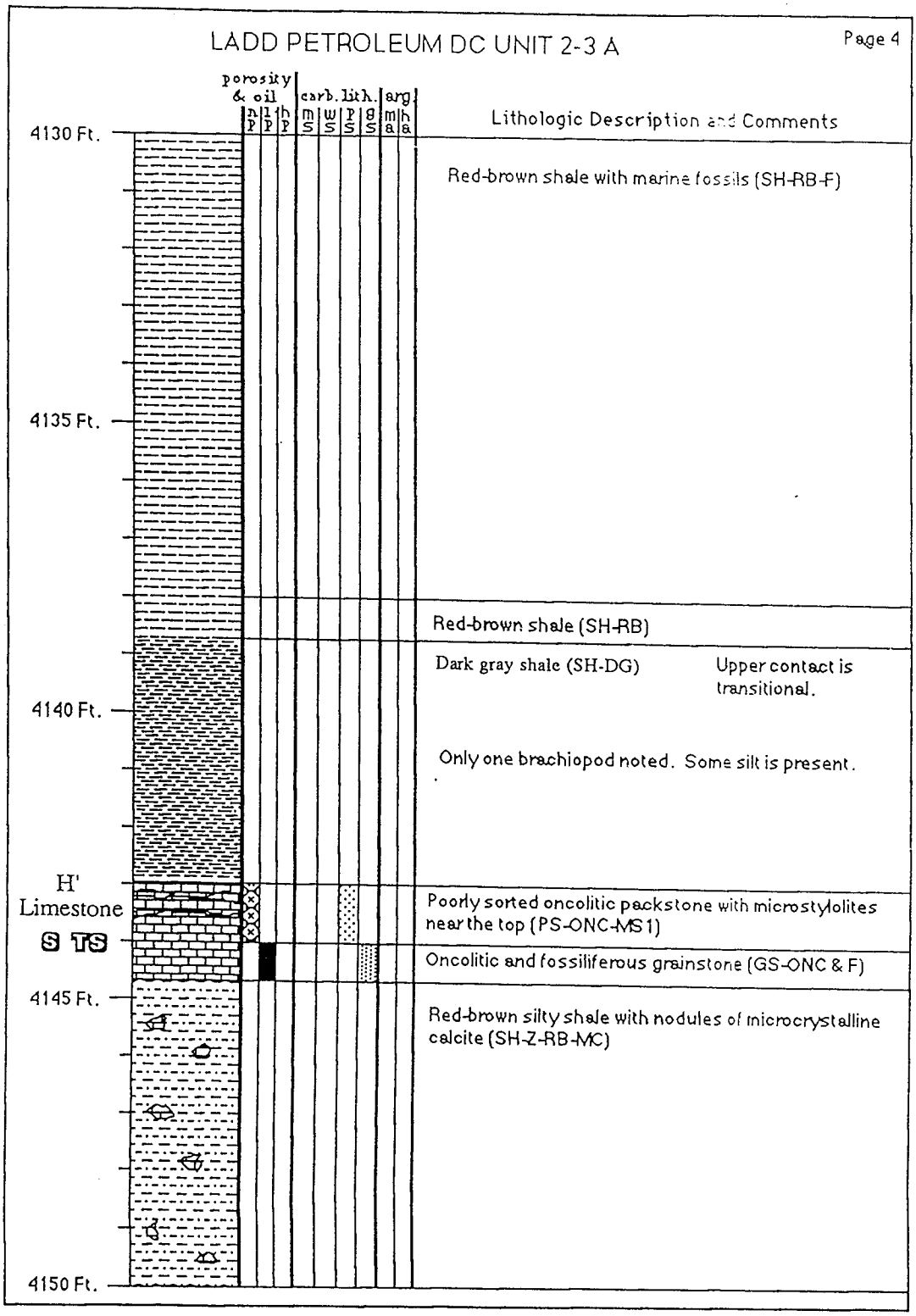
LADD PETROLEUM DC UNIT 2-3 A
Page 4
porosity & oil
carb. lith.
arg.
Lithologic Description and Comments
4130 Ft.
4135 Ft.
4140 Ft.
4145 Ft.
4150 Ft.
H' Limestone
S TS
Red-brown shale with marine fossils (SH-RB-F)
Red-brown shale (SH-RB)
Dark gray shale (SH-DG)
Upper contact is transitional.
Only one brachiopod noted. Some silt is present.
Poorly sorted oncolitic packstone with microstylolites near the top (PS-ONC-MS1)
Oncolitic and fossiliferous grainstone (GS-ONC & F)
Red-brown silty shale with nodules of microcrystalline calcite (SH-Z-RB-MC)

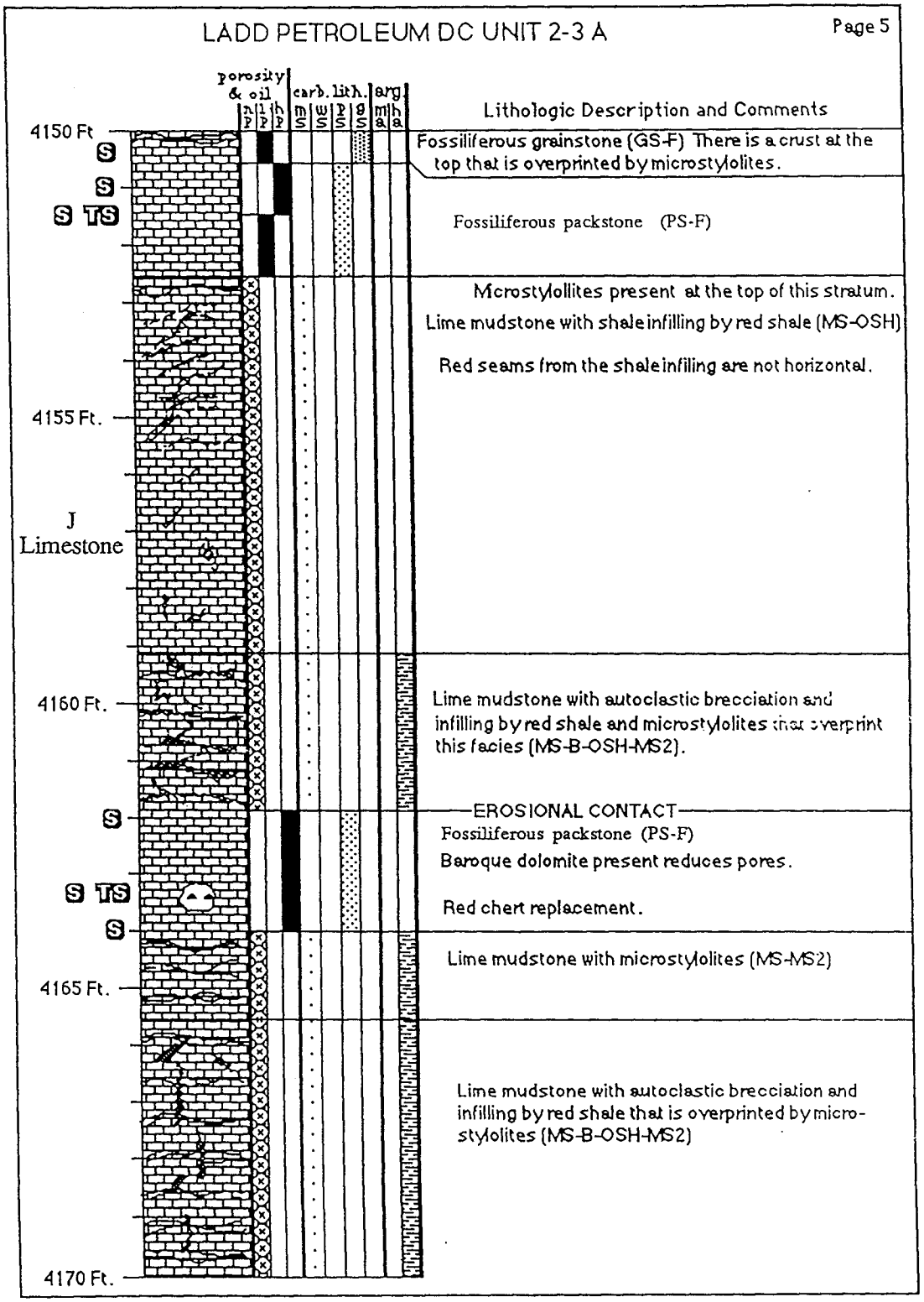
LADD PETROLEUM DC UNIT 2-3 A
Page 5
porosity & oil
carb. lith.
arg
Lithologic Description and Comments
4150 Ft
S
S
S TS
Fossiliferous grainstone (GS-F) There is a crust at the top that is overprinted by microstylolites.
Fossiliferous packstone (PS-F)
Microstylollites present at the top of this stratum.
Lime mudstone with shale infilling by red shale (MS-OSH)
Red seams from the shale infiling are not horizontal.
4155 Ft.
J
Limestone
4160 Ft.
Lime mudstone with autoclastic brecciation and infilling by red shale and microstylolites that overprint this facies (MS-B-OSH-MS2).
EROSIONAL CONTACT
S
Fossiliferous packstone (PS-F)
Baroque dolomite present reduces pores.
S TS
Red chert replacement.
S
Lime mudstone with microstylolites (MS-MS2)
4165 Ft.
Lime mudstone with autoclastic brecciation and infilling by red shale that is overprinted by micro-stylolites (MS-B-OSH-MS2)
4170 Ft.

LADD PETROLEUM DC UNITY 2-3 A

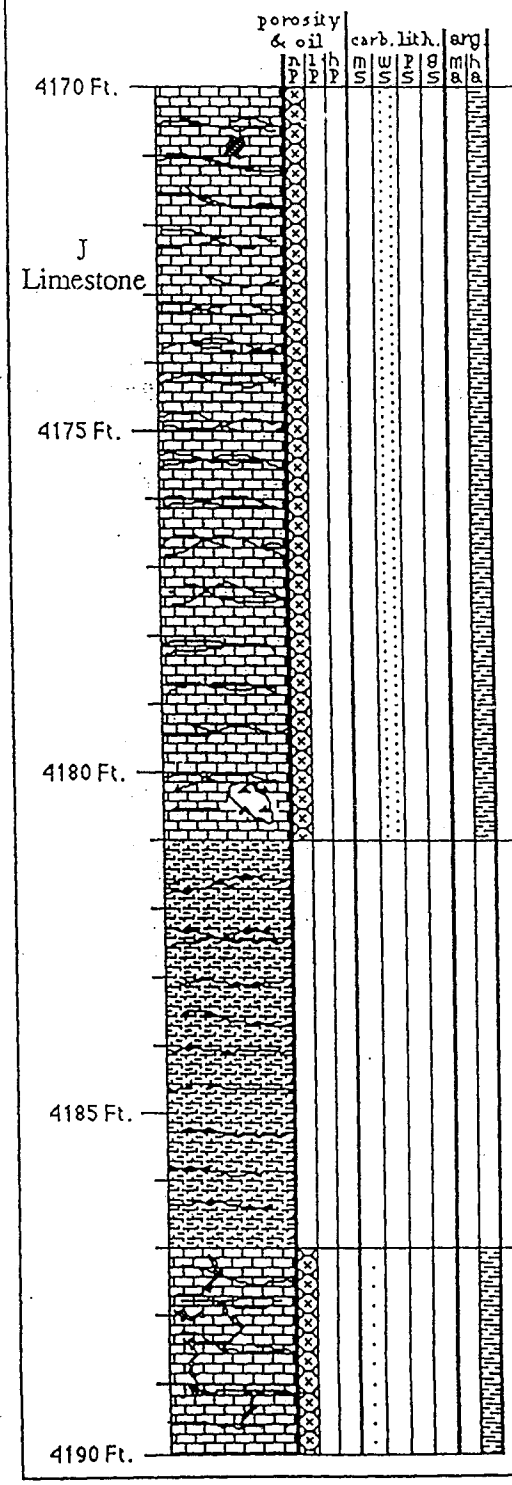

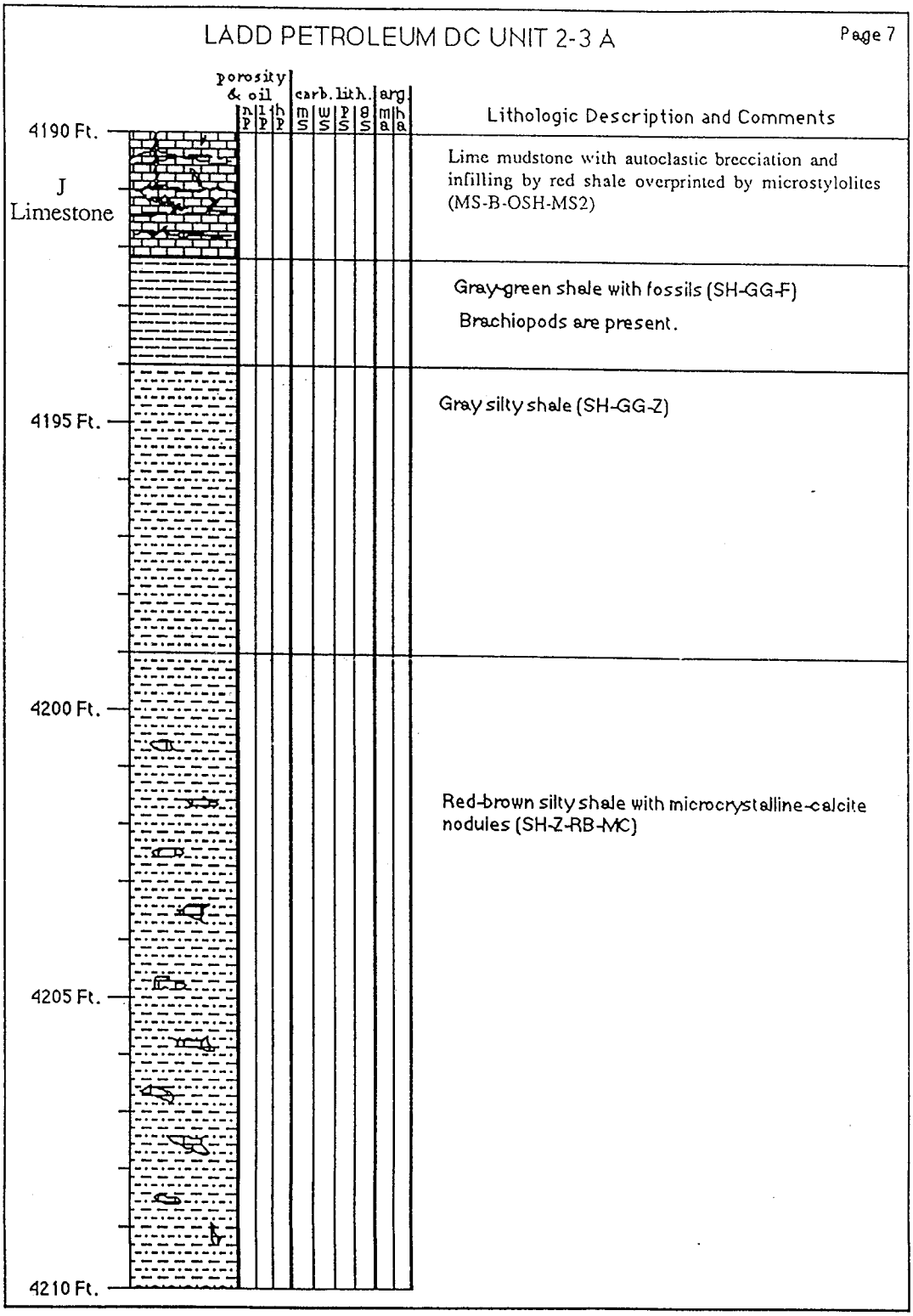
LADD PETROLEUM DC UNIT 2-3 A
Page 7
porosity & oil
carb. lith.
arg.
Lithologic Description and Comments
4190 Ft.
J Limestone
Lime mudstone with autoclastic brecciation and infilling by red shale overprinted by microstylolites (MS-B-OSH-MS2)
Gray-green shale with fossils (SH-GG-F)
Brachiopods are present.
4195 Ft.
Gray silty shale (SH-GG-Z)
4200 Ft.
Red-brown silty shale with microcrystalline-calcite nodules (SH-Z-RB-MC)
4205 Ft.
4210 Ft.

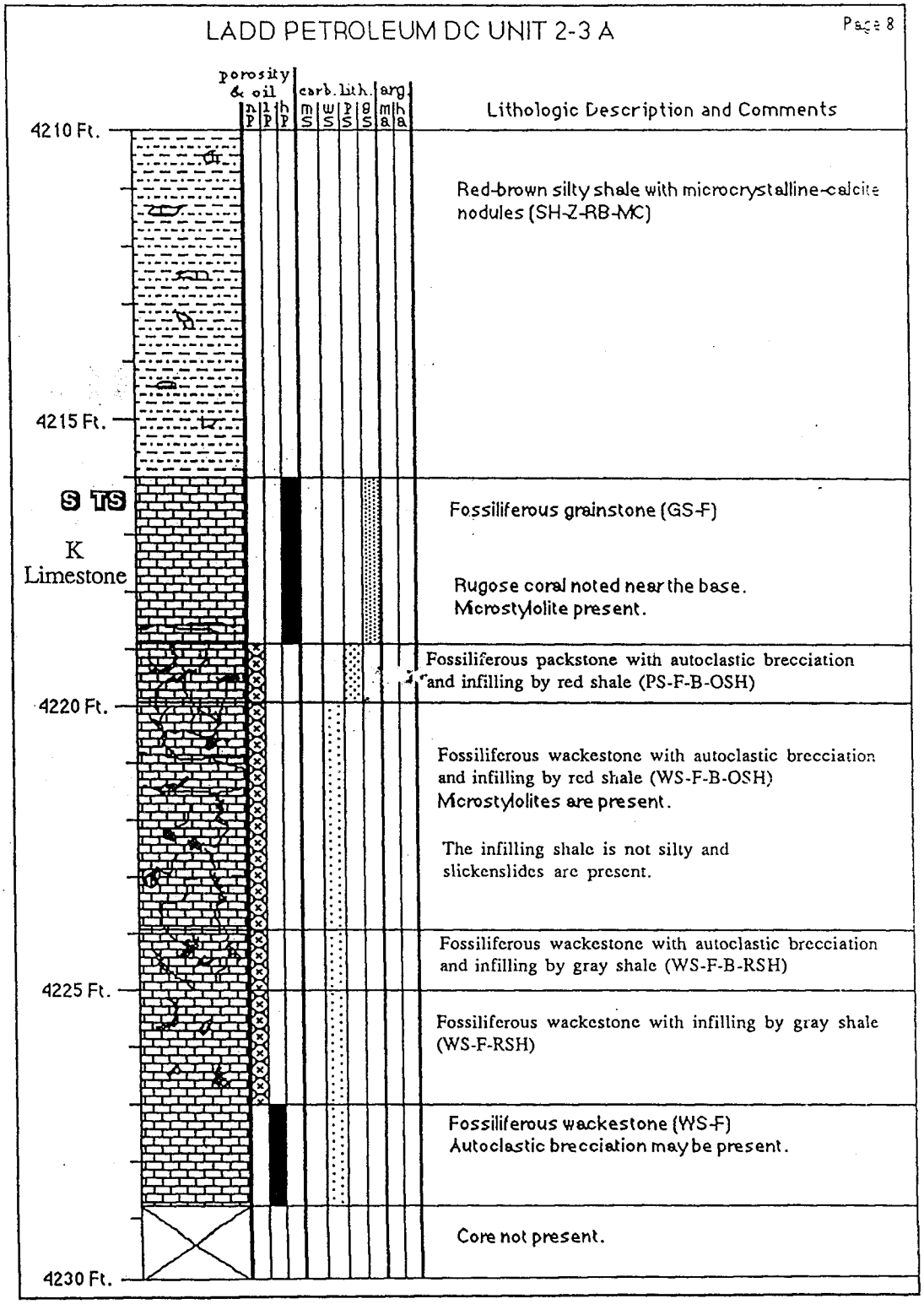
LADD PETROLEUM DC UNIT 2-3 A
Page 8
porosity & oil
carb. lith.
arg.
Lithologic Description and Comments
4210 Ft.
4215 Ft.
S TS
K Limestone
4220 Ft.
4225 Ft.
4230 Ft.
Red-brown silty shale with microcrystalline-calcite nodules (SH-Z-RB-MC)
Fossiliferous grainstone (GS-F)
Rugose coral noted near the base.
Microstylolite present.
Fossiliferous packstone with autoclastic brecciation and infilling by red shale (PS-F-B-OSH)
Fossiliferous wackestone with autoclastic brecciation and infilling by red shale (WS-F-B-OSH)
Microstylolites are present.
The infilling shale is not silty and slickenslides are present.
Fossiliferous wackestone with autoclastic brecciation and infilling by gray shale (WS-F-B-RSH)
Fossiliferous wackestone with infilling by gray shale (WS-F-RSH)
Fossiliferous wackestone (WS-F)
Autoclastic brecciation may be present.
Core not present.

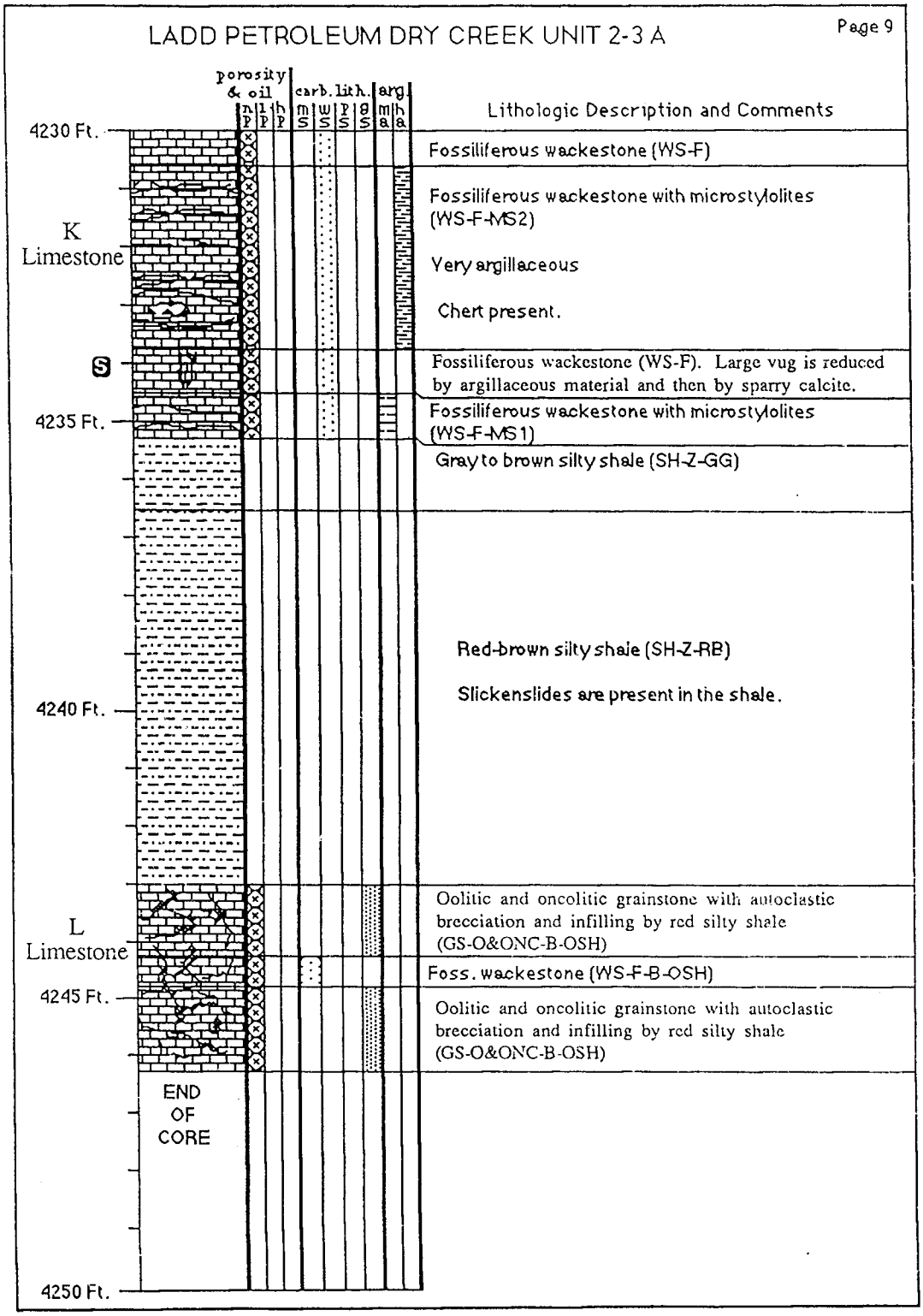
LADD PETROLEUM DRY CREEK UNIT 2-3 A
Page 9
porosity & oil
carb. lith.
arg
Lithologic Description and Comments
4230 Ft.
Fossiliferous wackestone (WS-F)
K Limestone
Fossiliferous wackestone with microstylolites (WS-F-MS2)
Very argillaceous
Chert present.
S
Fossiliferous wackestone (WS-F). Large vug is reduced by argillaceous material and then by sparry calcite.
4235 Ft.
Fossiliferous wackestone with microstylolites (WS-F-MS1)
Gray to brown silty shale (SH-Z-GG)
Red-brown silty shale (SH-Z-RB)
Slickenslides are present in the shale.
4240 Ft.
L Limestone
Oolitic and oncolitic grainstone with autoclastic brecciation and infilling by red silty shale (GS-O&ONC-B-OSH)
Foss. wackestone (WS-F-B-OSH)
4245 Ft.
Oolitic and oncolitic grainstone with autoclastic brecciation and infilling by red silty shale (GS-O&ONC-B-OSH)
END OF CORE
4250 Ft.

MURFIN DRILLING CO. #1-24 KINCAID

E/2 NW NW, Section 24-T3S-R27W
Gillespie SE Field, Decatur County, Kansas
Drilled September, 1982
Perforated: 3567.5-69 ft., 3580.5-81.5 ft., 3583-87 ft.,
and 3714-16 ft.
Initial Production: 86 BOPD + 10%

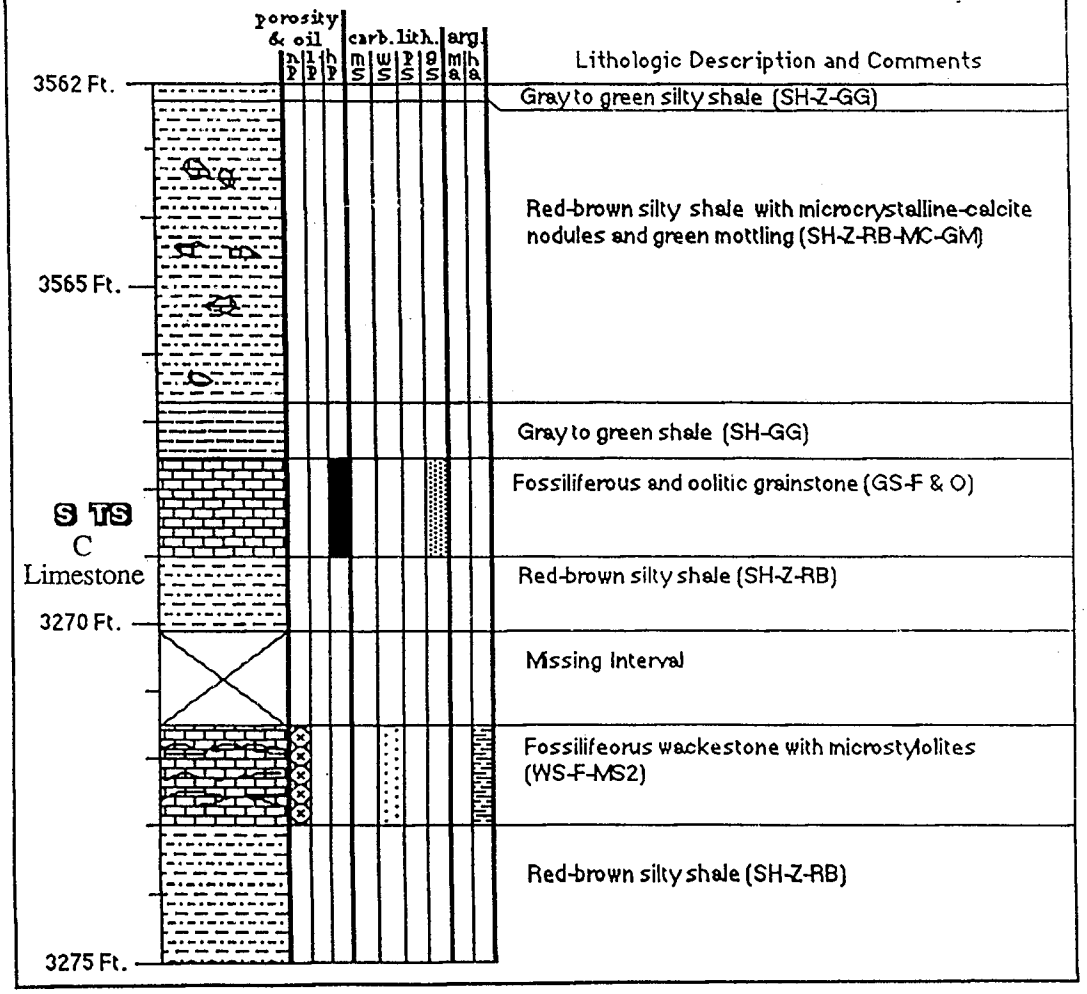

MURFING DRILLING CO. #1-24 KINCAID

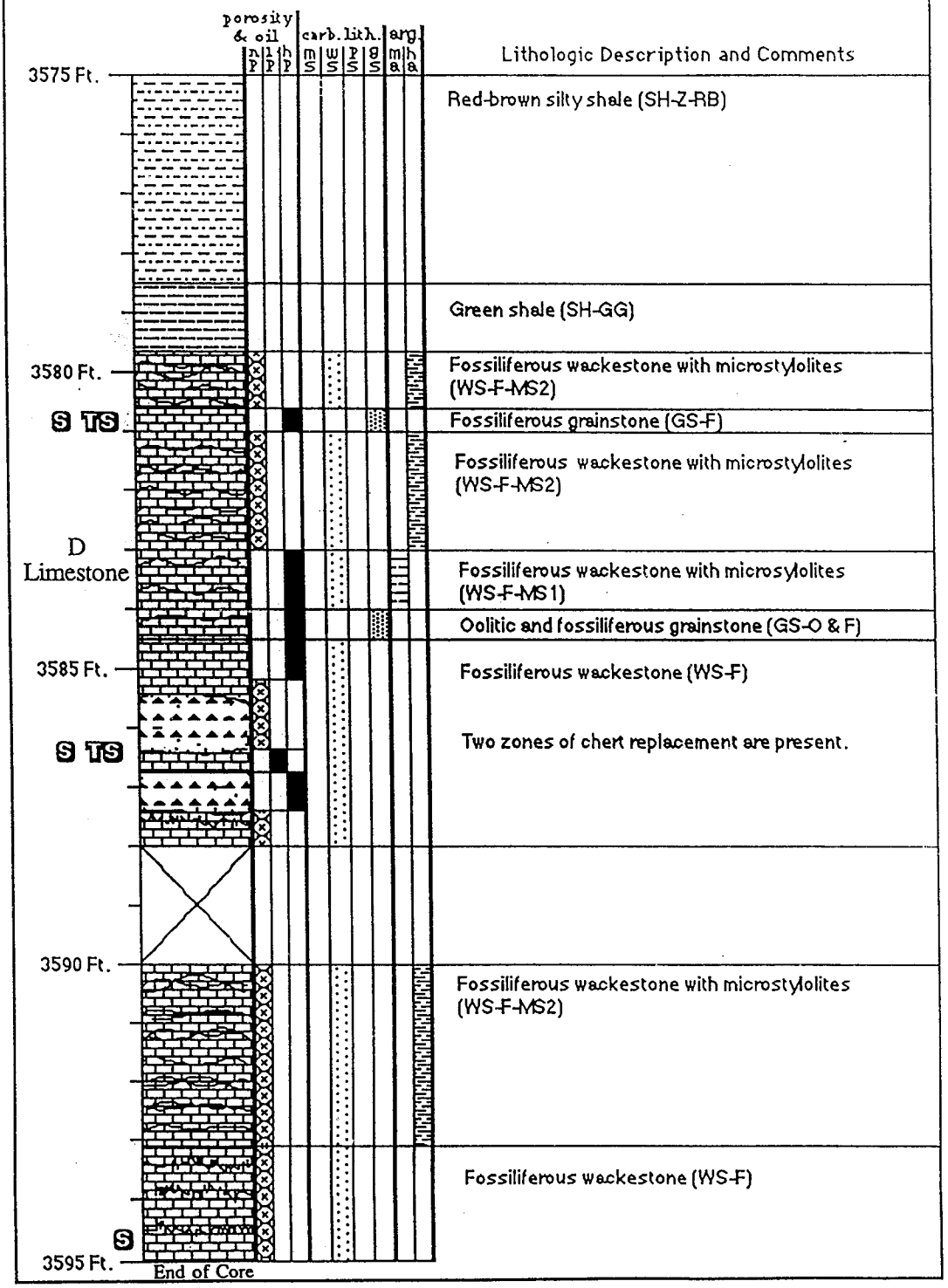

MURFIN DRILLING CO. #1-7 STROUP

150 Feet NW of C NE NE, Section 7-T2N-R37W
Dundy County, Nebraska
Drilled August, 1978

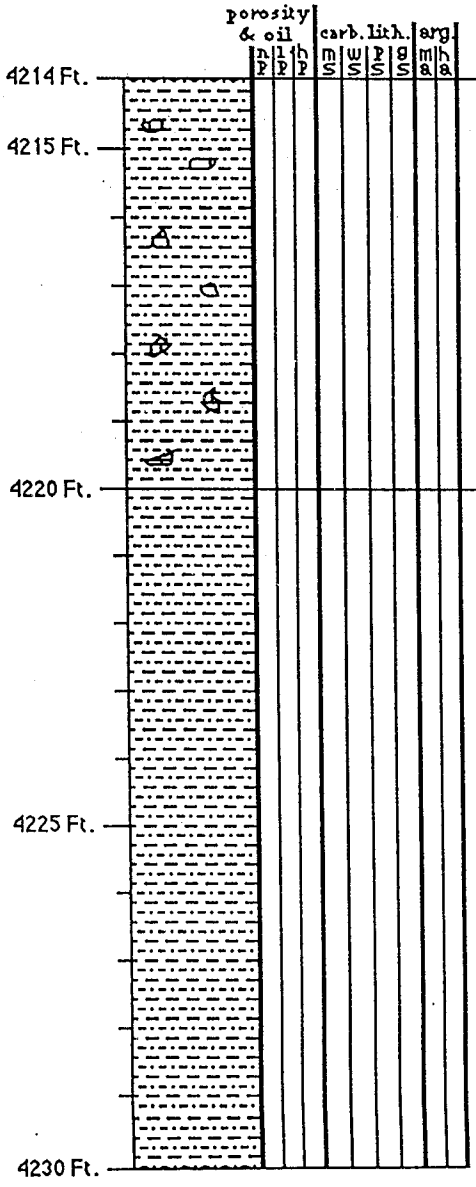

MURFIN DRILLING CO. #1-7 STROUP

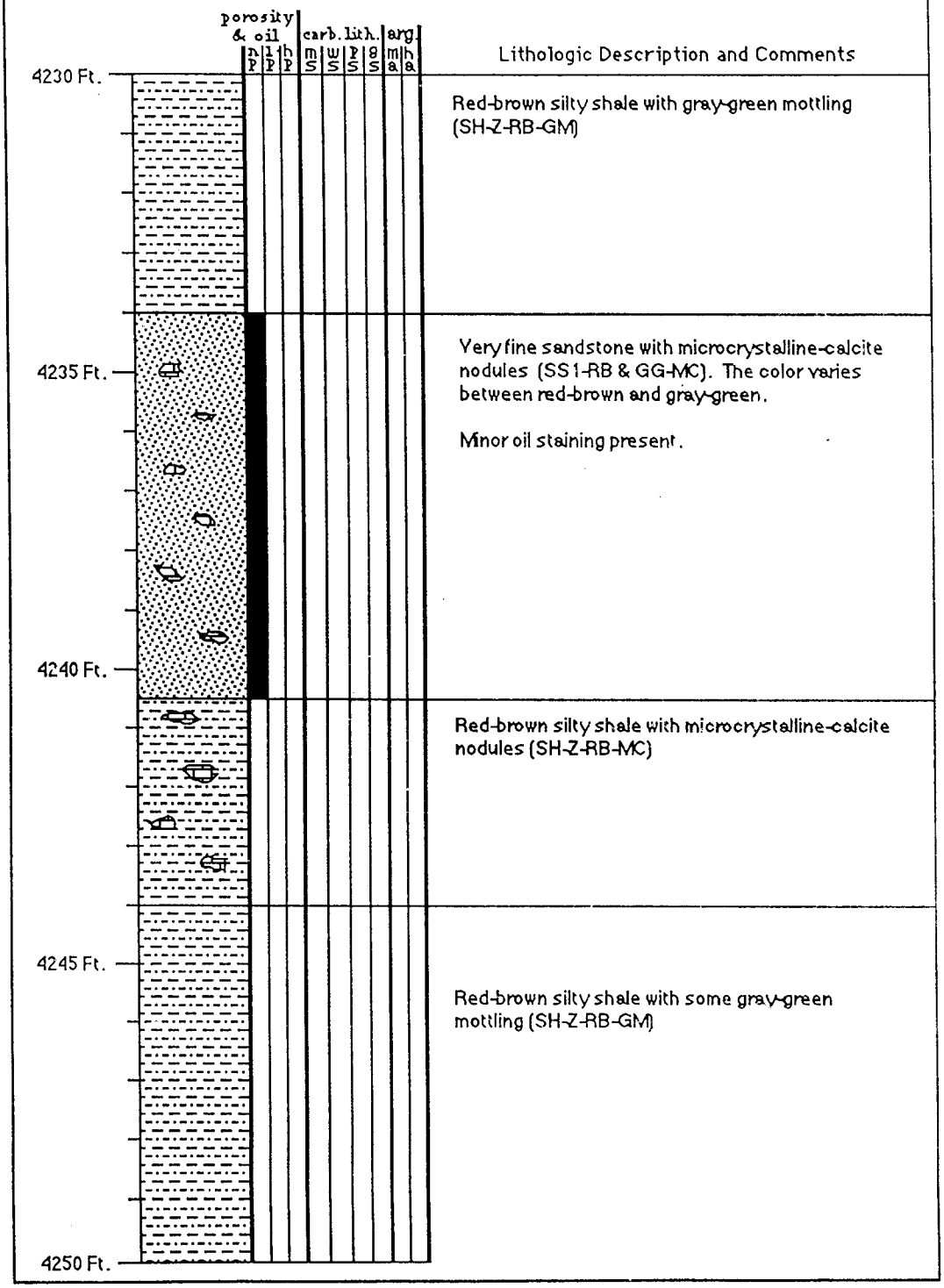

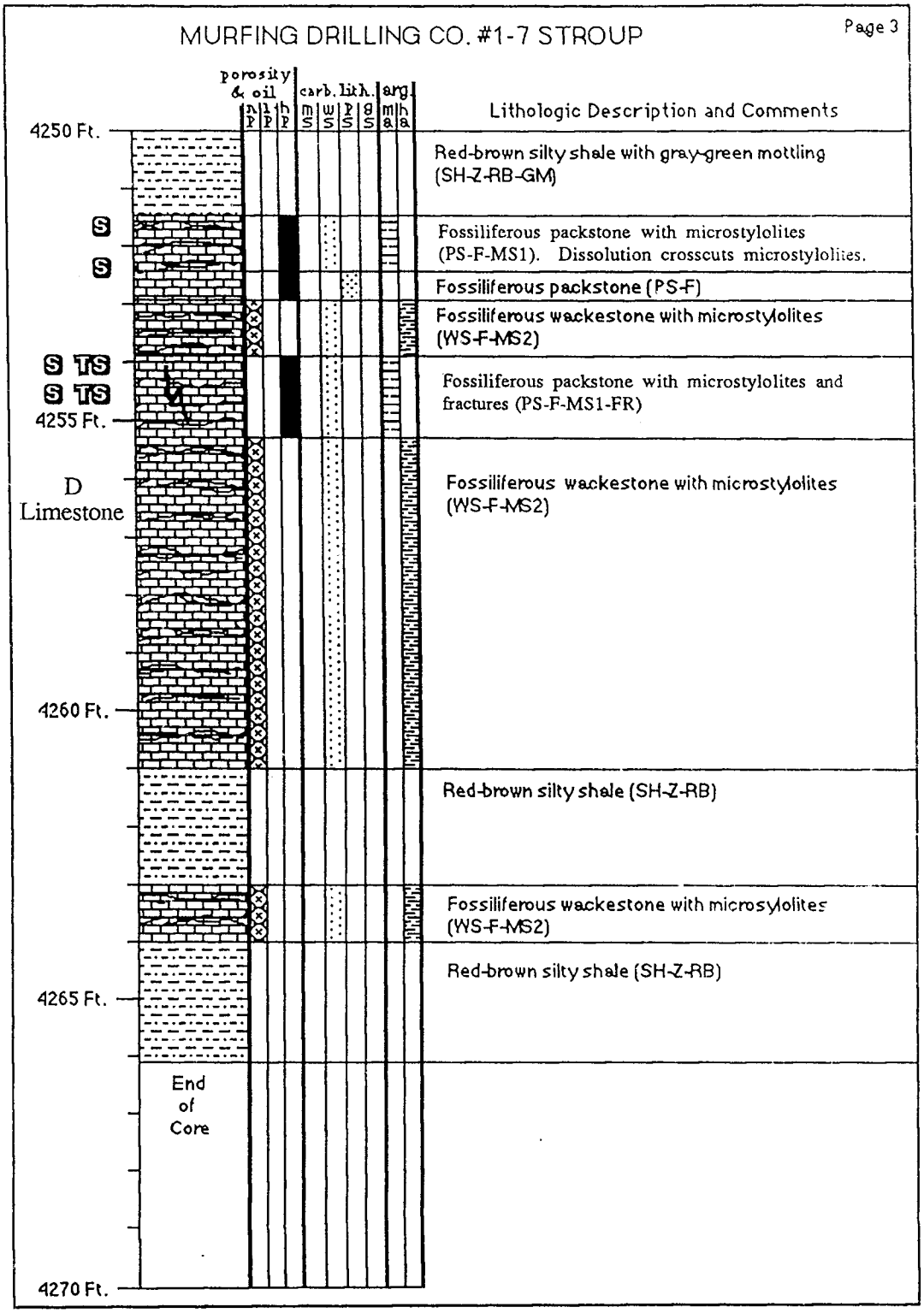
MURFING DRILLING CO. #1-7 STROUP
Page 3
porosity & oil
carb.
lith.
arg.
Lithologic Description and Comments
4250 Ft.
Red-brown silty shale with gray-green mottling (SH-Z-RB-GM)
S
Fossiliferous packstone with microstylolites (PS-F-MS1). Dissolution crosscuts microstylolites.
S
Fossiliferous packstone (PS-F)
Fossiliferous wackestone with microstylolites (WS-F-MS2)
S TS
S TS
Fossiliferous packstone with microstylolites and fractures (PS-F-MS1-FR)
4255 Ft.
D Limestone
Fossiliferous wackestone with microstylolites (WS-F-MS2)
4260 Ft.
Red-brown silty shale (SH-Z-RB)
Fossiliferous wackestone with microstylolites (WS-F-MS2)
Red-brown silty shale (SH-Z-RB)
4265 Ft.
End of Core
4270 Ft.

MURFIN OIL CO. #1 PRENTICE
C NE NE, Sec. 30-T2S-R35W
Seberger Field, Rawlins Co., Kansas
Perforated 4246-47 ft., 4252-58 ft., 4268-72 ft., 4304-06 ft., 4314-16 ft., 4316-17 ft. (4314-17 ft. produced all water)

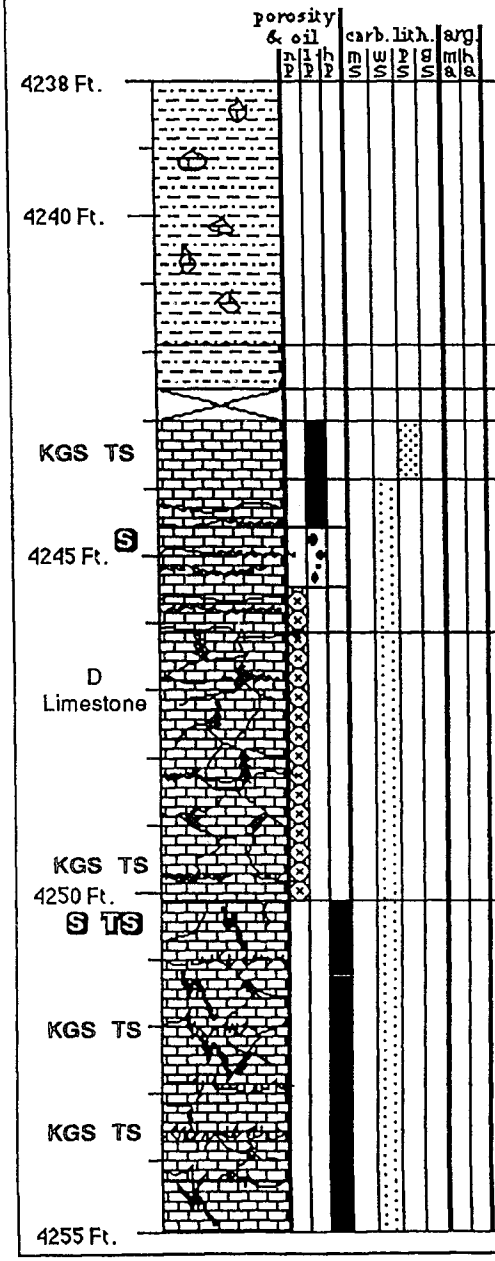

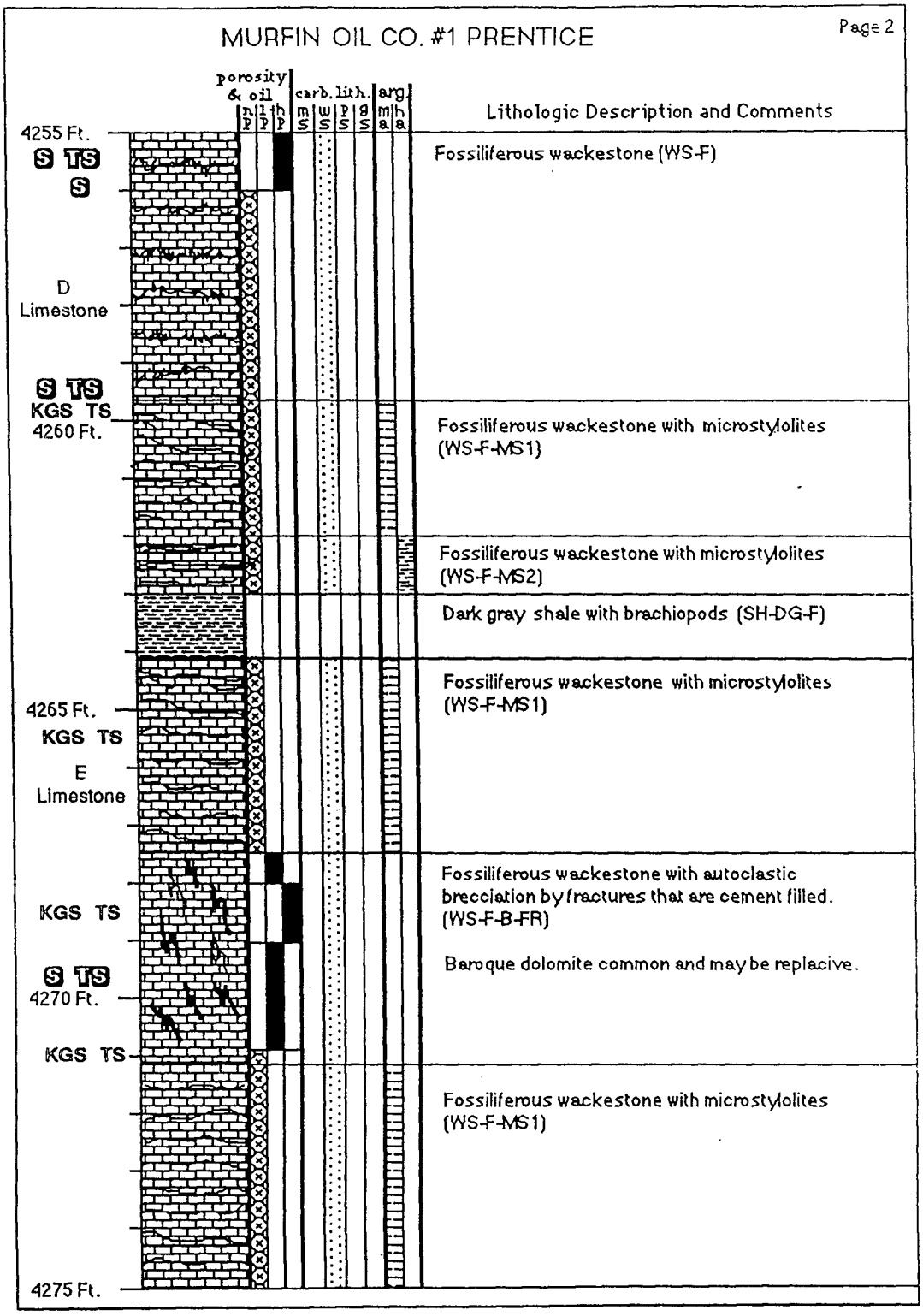
MURFIN OIL CO. #1 PRENTICE
Page 2
porosity & oil
carb. lith.
arg.
Lithologic Description and Comments
4255 Ft.
S TS S
D Limestone
S TS
KGS TS
4260 Ft.
Fossiliferous wackestone (WS-F)
Fossiliferous wackestone with microstylolites (WS-F-MS1)
Fossiliferous wackestone with microstylolites (WS-F-MS2)
Dark gray shale with brachiopods (SH-DG-F)
4265 Ft.
KGS TS
E Limestone
Fossiliferous wackestone with microstylolites (WS-F-MS1)
KGS TS
Fossiliferous wackestone with autoclastic brecciation by fractures that are cement filled. (WS-F-B-FR)
Baroque dolomite common and may be replacive.
S TS
4270 Ft.
KGS TS
Fossiliferous wackestone with microstylolites (WS-F-MS1)
4275 Ft.

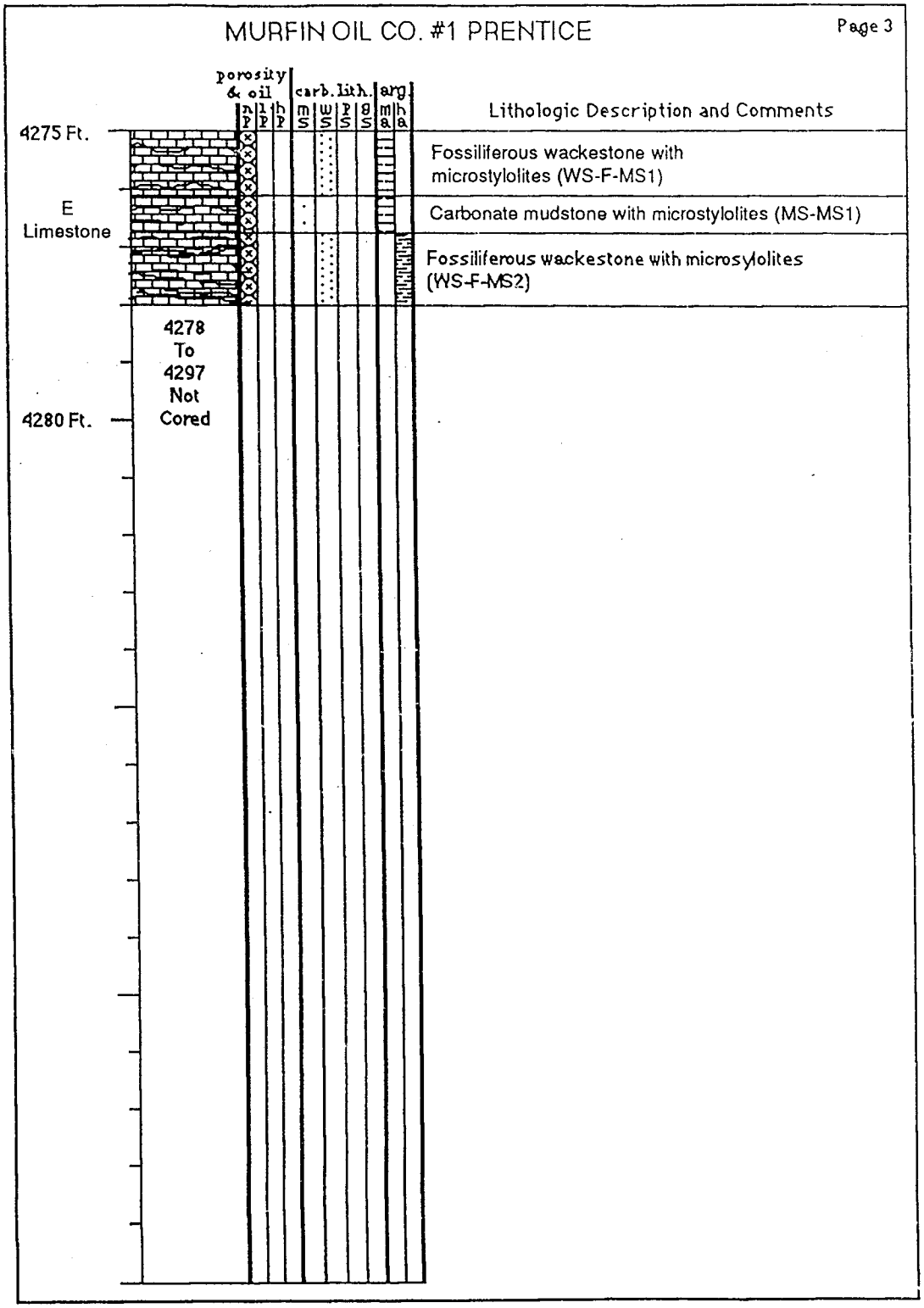
MURFIN OIL CO. #1 PRENTICE
Page 3
porosity & oil
carb. lith.
arg.
Lithologic Description and Comments
4275 Ft.
Fossiliferous wackestone with microstylolites (WS-F-MS1)
E Limestone
Carbonate mudstone with microstylolites (MS-MS1)
Fossiliferous wackestone with microsylolites (WS-F-MS2)
4278 To 4297 Not Cored
4280 Ft.

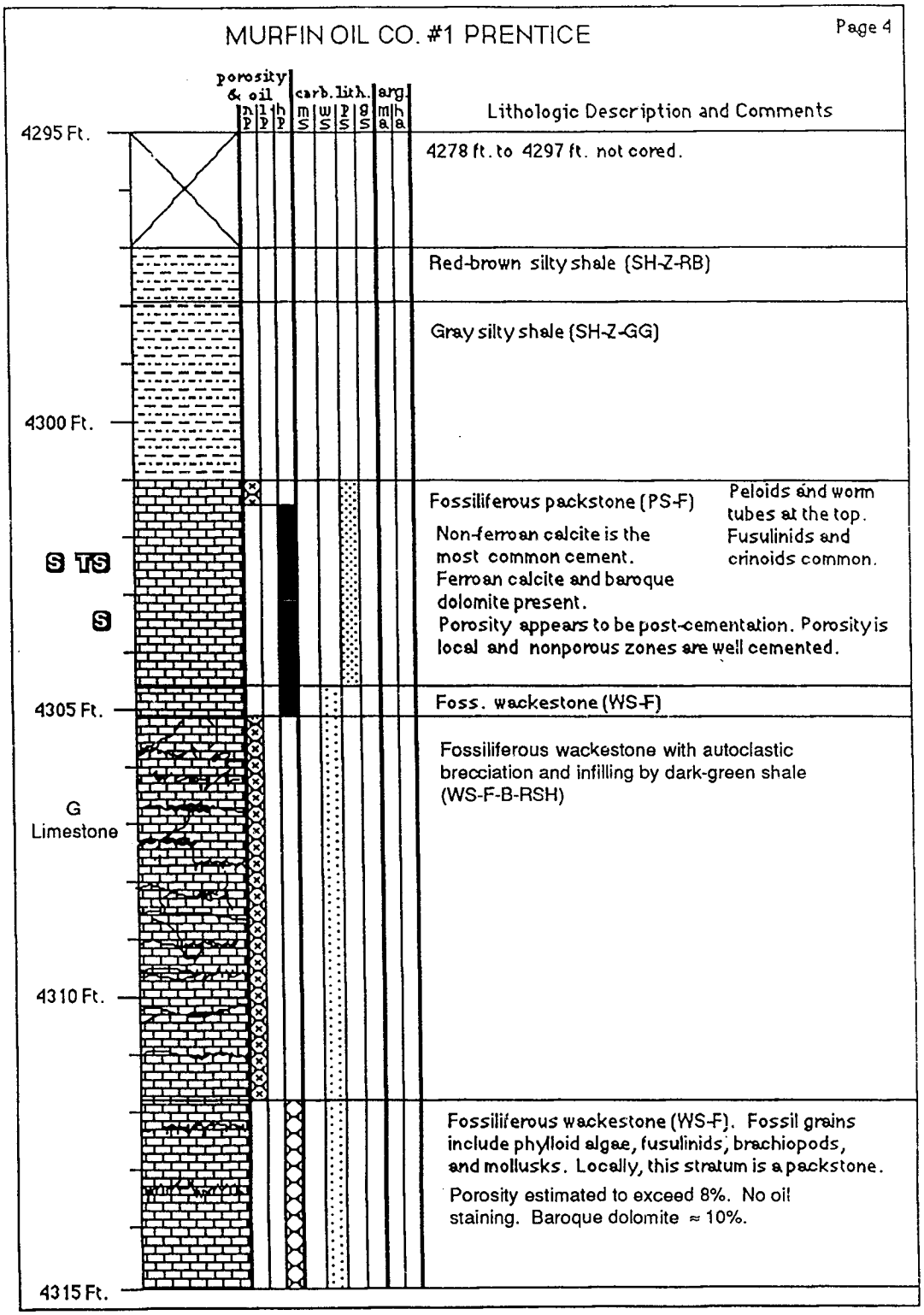
MURFIN OIL CO. #1 PRENTICE
porosity & oil
carb. lith.
arg
Lithologic Description and Comments
4295 Ft.
4278 ft. to 4297 ft. not cored.
Red-brown silty shale (SH-Z-RB)
Gray silty shale (SH-Z-GG)
4300 Ft.
Fossiliferous packstone (PS-F)
Peloids and worm tubes at the top. Fusulinids and crinoids common.
Non-ferroan calcite is the most common cement. Ferroan calcite and baroque dolomite present.
Porosity appears to be post-cementation. Porosity is local and nonporous zones are well cemented.
S TS
S
4305 Ft.
Foss. wackestone (WS-F)
Fossiliferous wackestone with autoclastic brecciation and infilling by dark-green shale (WS-F-B-RSH)
G Limestone
4310 Ft.
Fossiliferous wackestone (WS-F). Fossil grains include phylloid algae, fusulinids, brachiopods, and mollusks. Locally, this stratum is a packstone.
Porosity estimated to exceed 8%. No oil staining. Baroque dolomite ≈ 10%.
4315 Ft.

MURFIN OIL CO. #1 PRENTICE

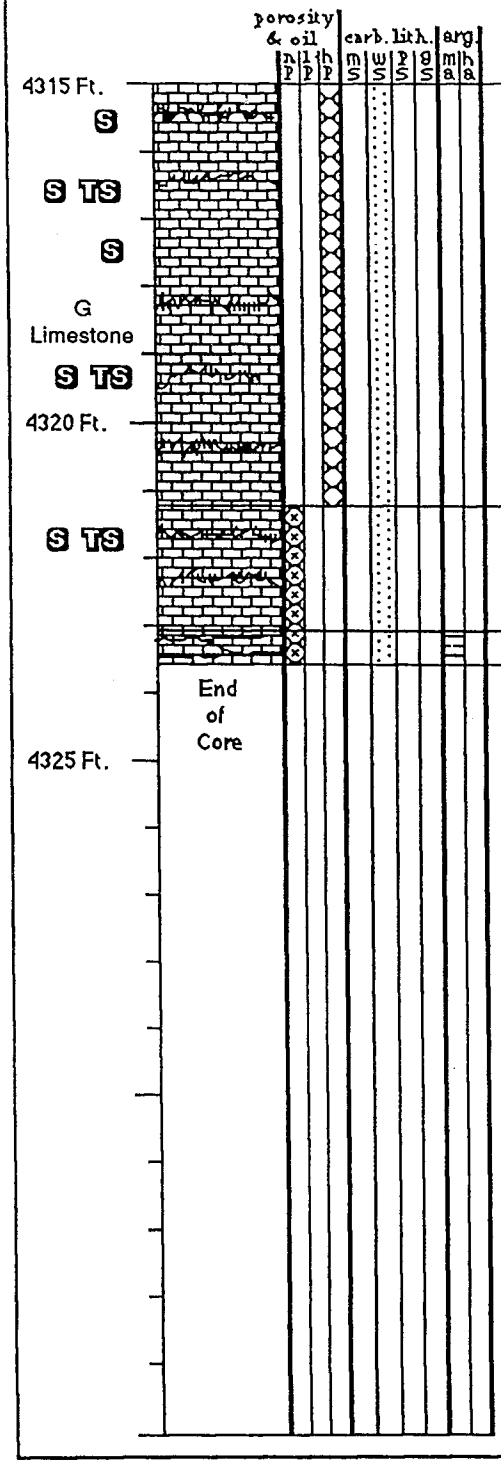

Murfin Drilling Co. #2 Elvin

SE NW SE 14-3S-27W, Decatur Co., Kansas
Drilled and completed for oil prod. in 1978.
Perf. 3593-95.5 (3594.5-97 in Core Descr.),
IPP 152 BOPD + 8 BWPD.

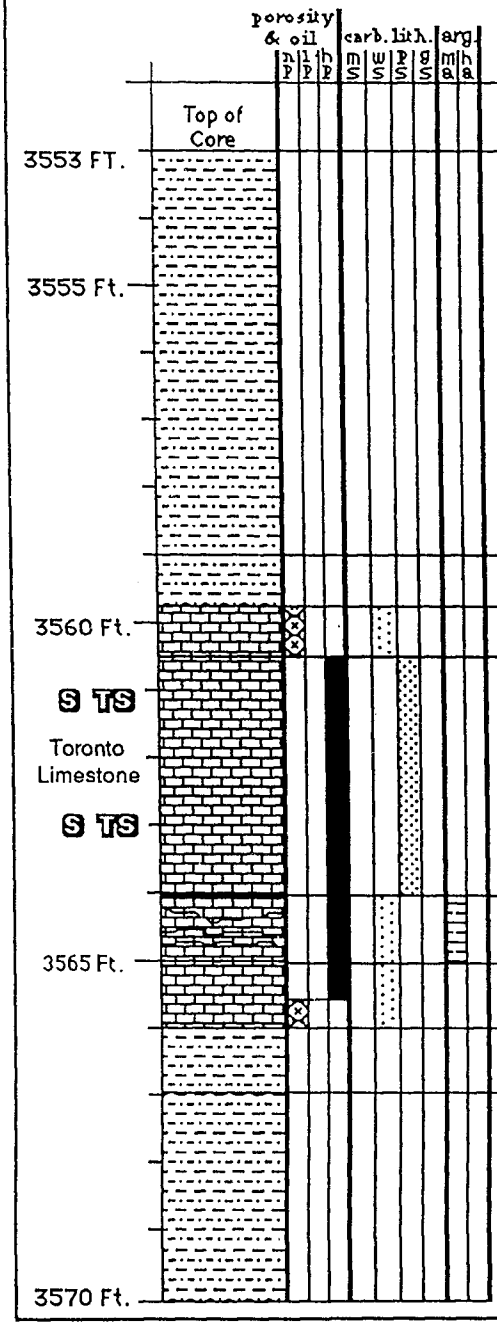

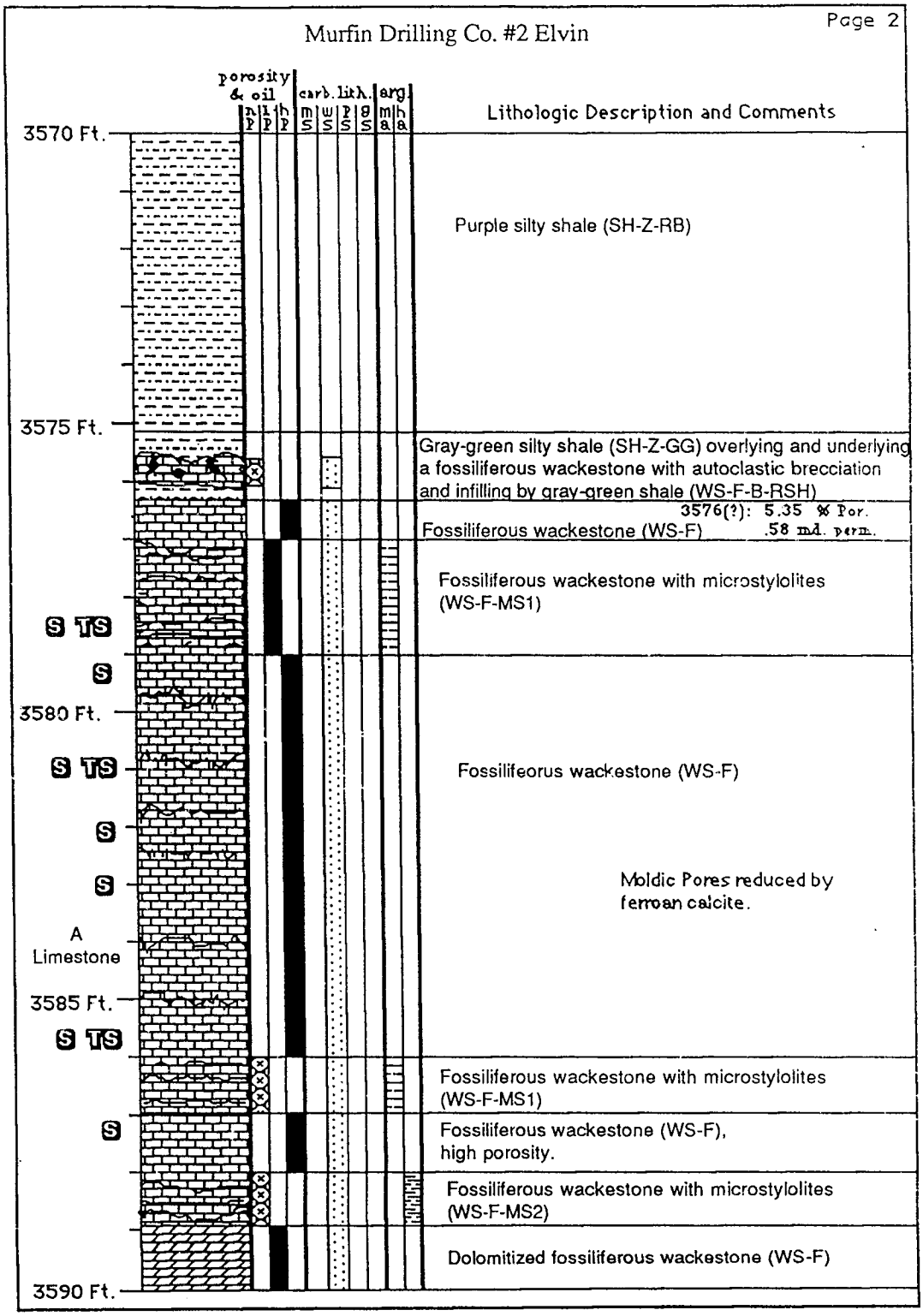
Murfin Drilling Co. #2 Elvin
Page 2
porosity & oil
carb. lith.
arg.
Lithologic Description and Comments
3570 Ft.
Purple silty shale (SH-Z-RB)
3575 Ft.
Gray-green silty shale (SH-Z-GG) overlying and underlying a fossiliferous wackestone with autoclastic brecciation and infilling by gray-green shale (WS-F-B-RSH)
3576(?): 5.35 % Por.
.58 md. perm.
Fossiliferous wackestone (WS-F)
Fossiliferous wackestone with microstylolites (WS-F-MS1)
S TS
S
3580 Ft.
S TS
Fossilifeorus wackestone (WS-F)
S
S
Moldic Pores reduced by ferroan calcite.
A Limestone
3585 Ft.
S TS
Fossiliferous wackestone with microstylolites (WS-F-MS1)
S
Fossiliferous wackestone (WS-F), high porosity.
Fossiliferous wackestone with microstylolites (WS-F-MS2)
Dolomitized fossiliferous wackestone (WS-F)
3590 Ft.

Murfin Drilling Co. #2 Elvin

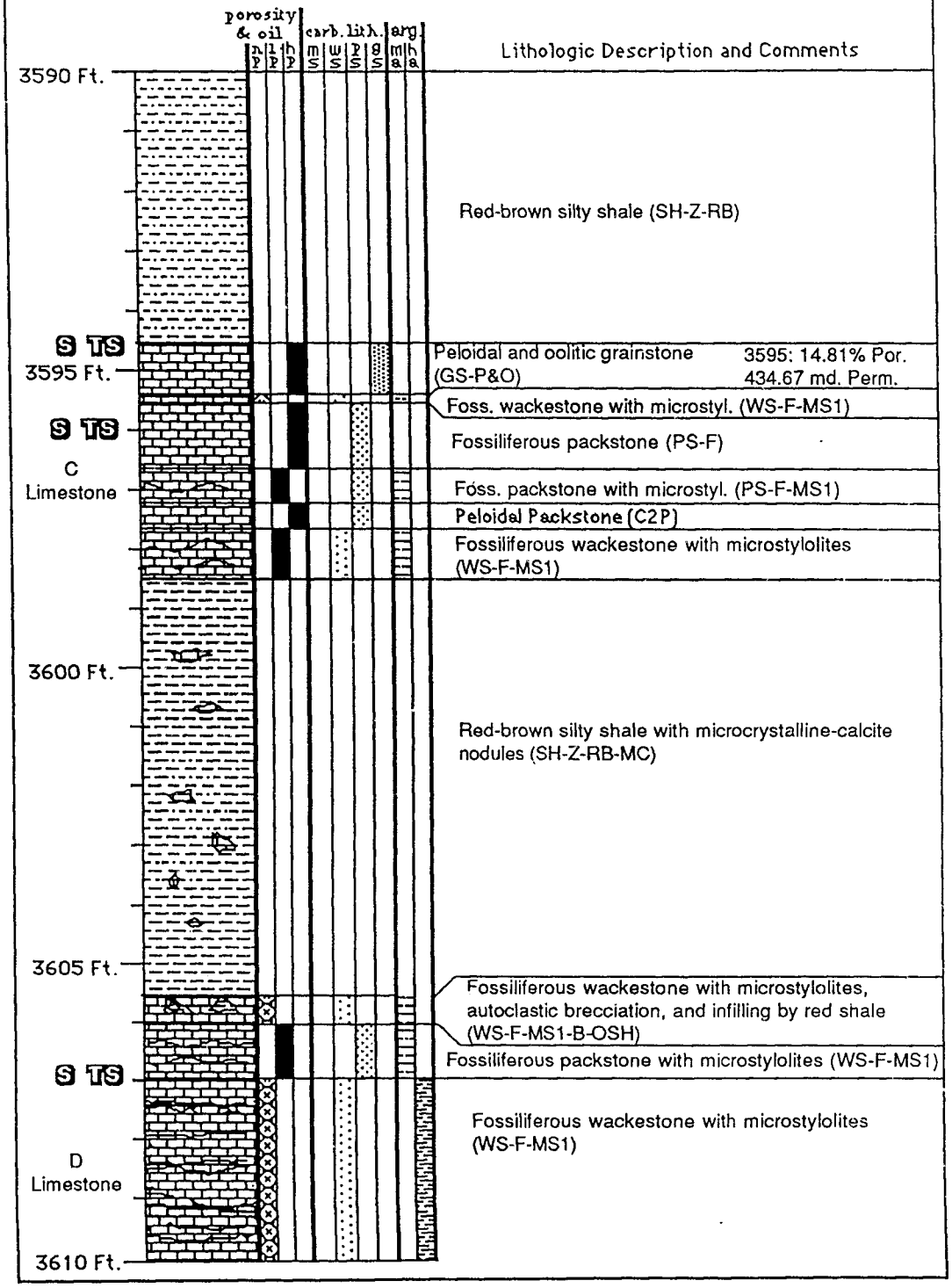

Murfin Drilling Co. #2 Elvin

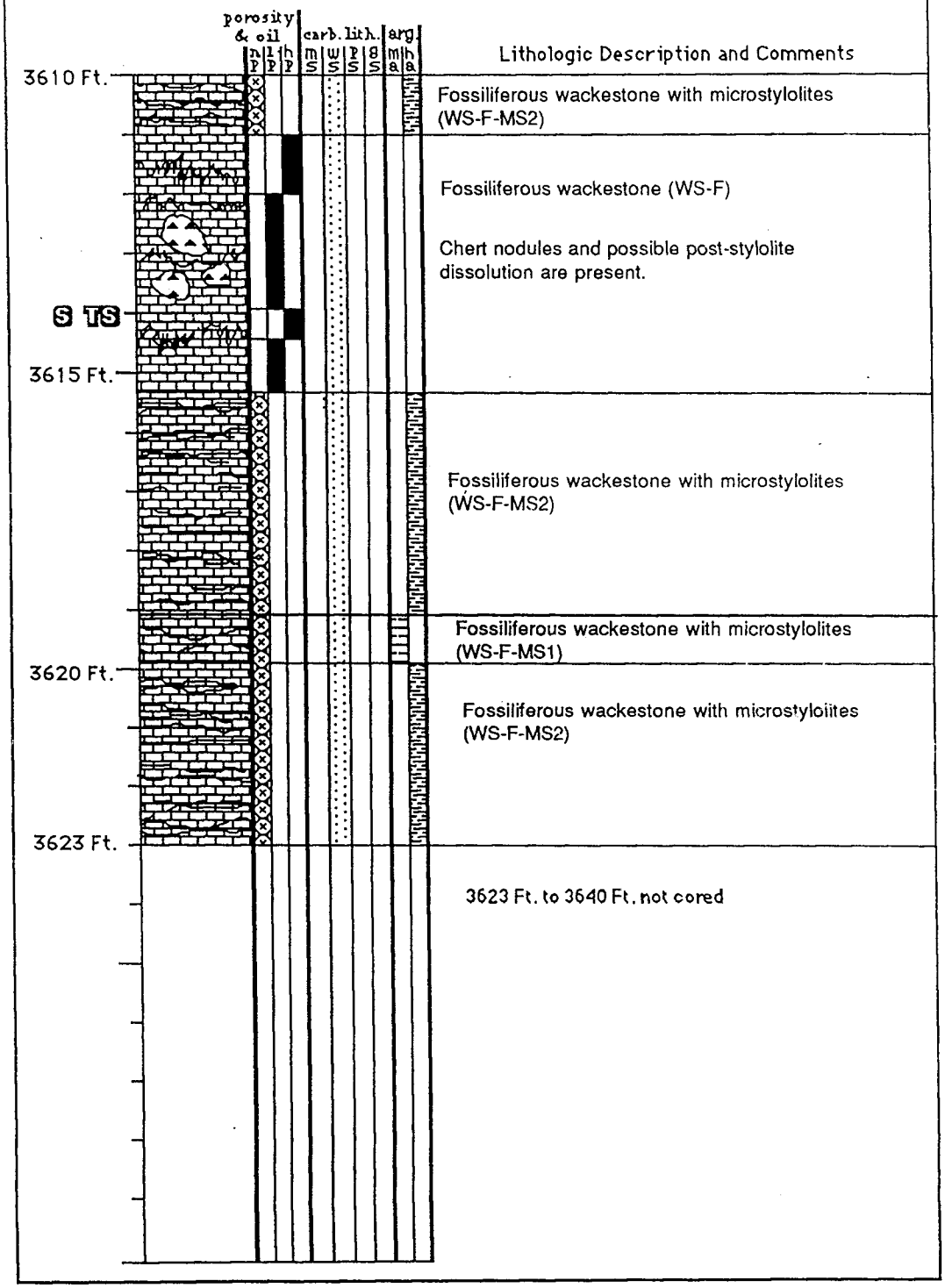

Murfin Drilling Co. #2 Elvin

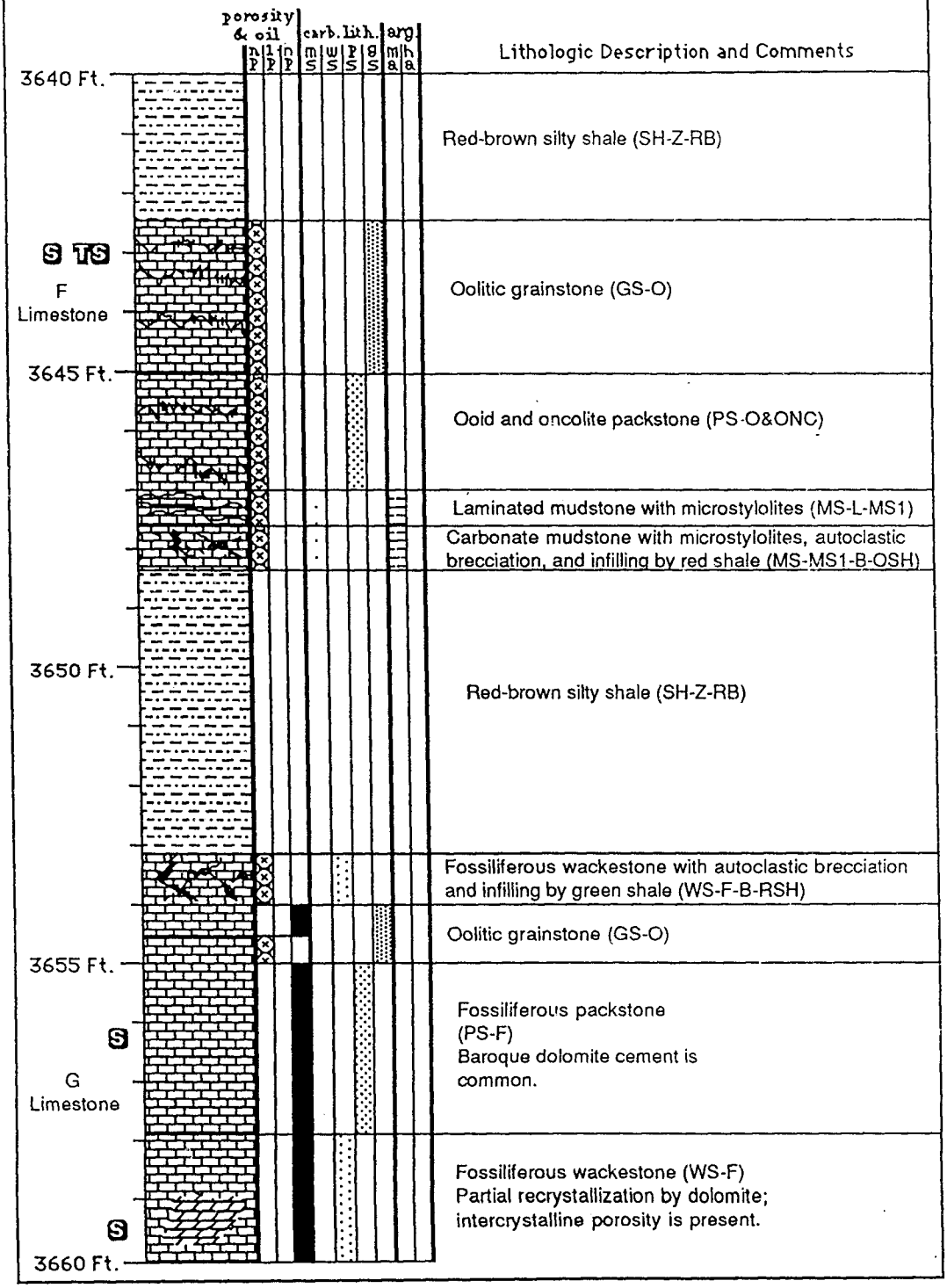

Murfin Drilling Co. #2 Elvin

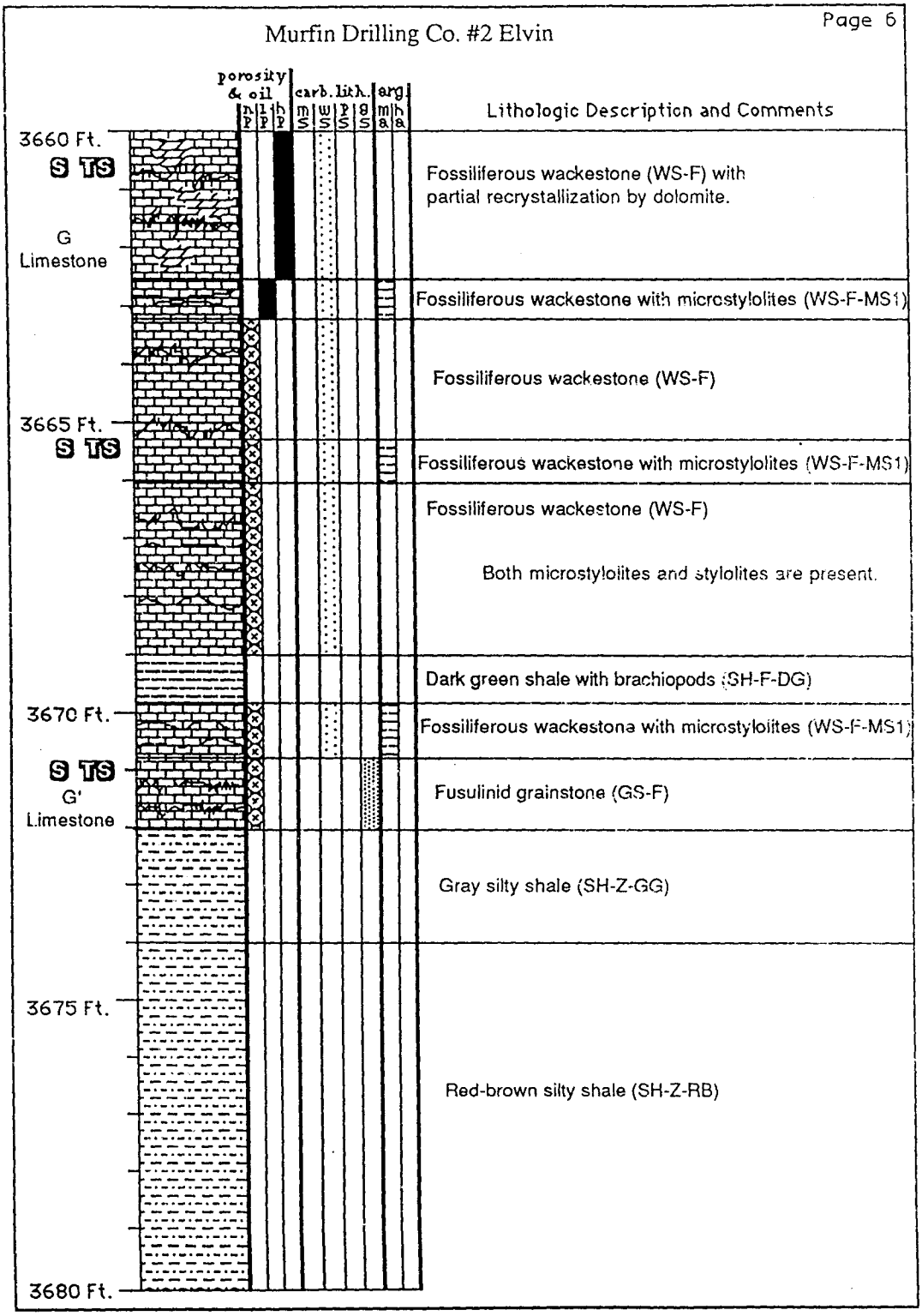

Murfin Drilling Co. #2 Elvin

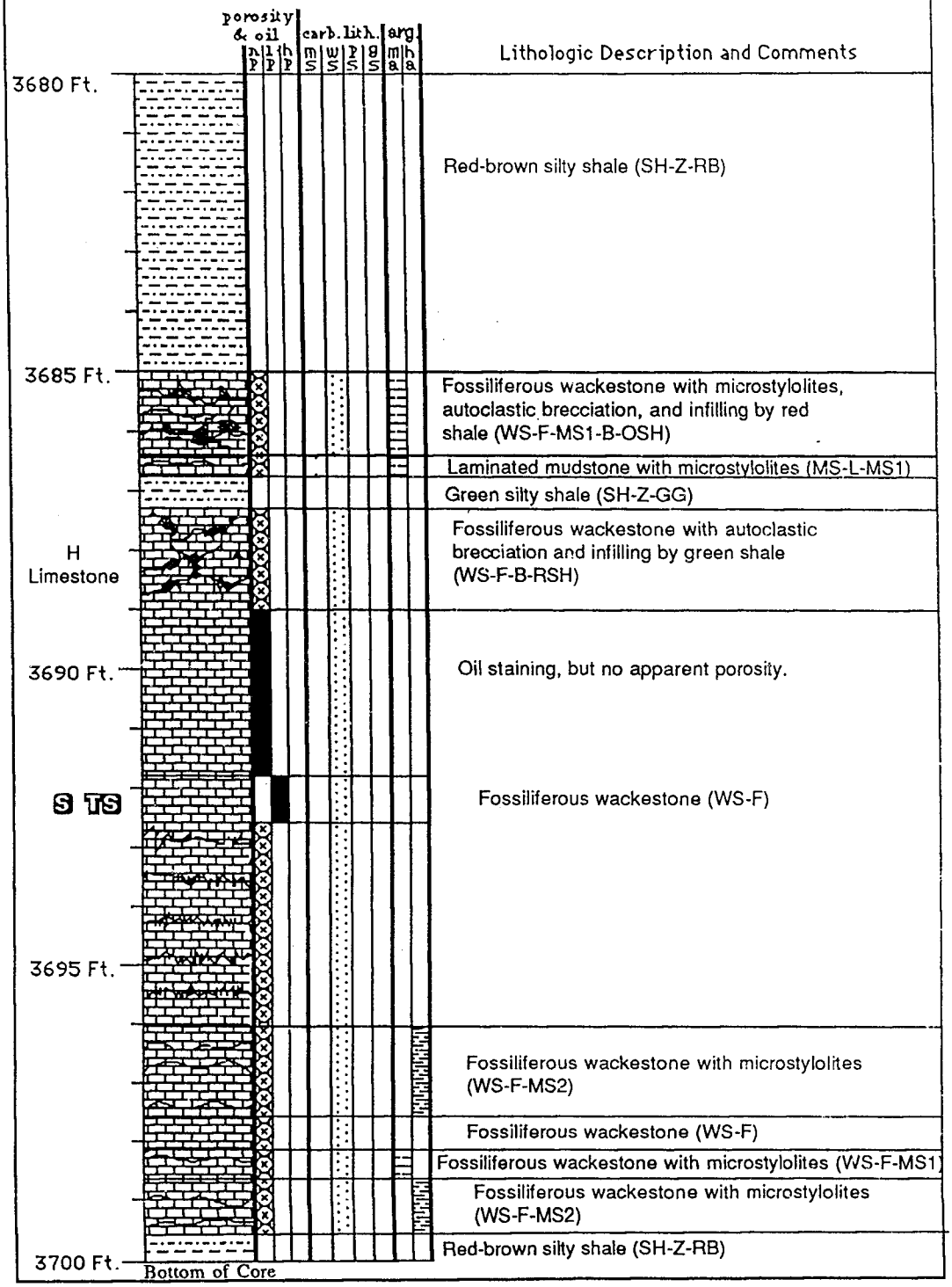

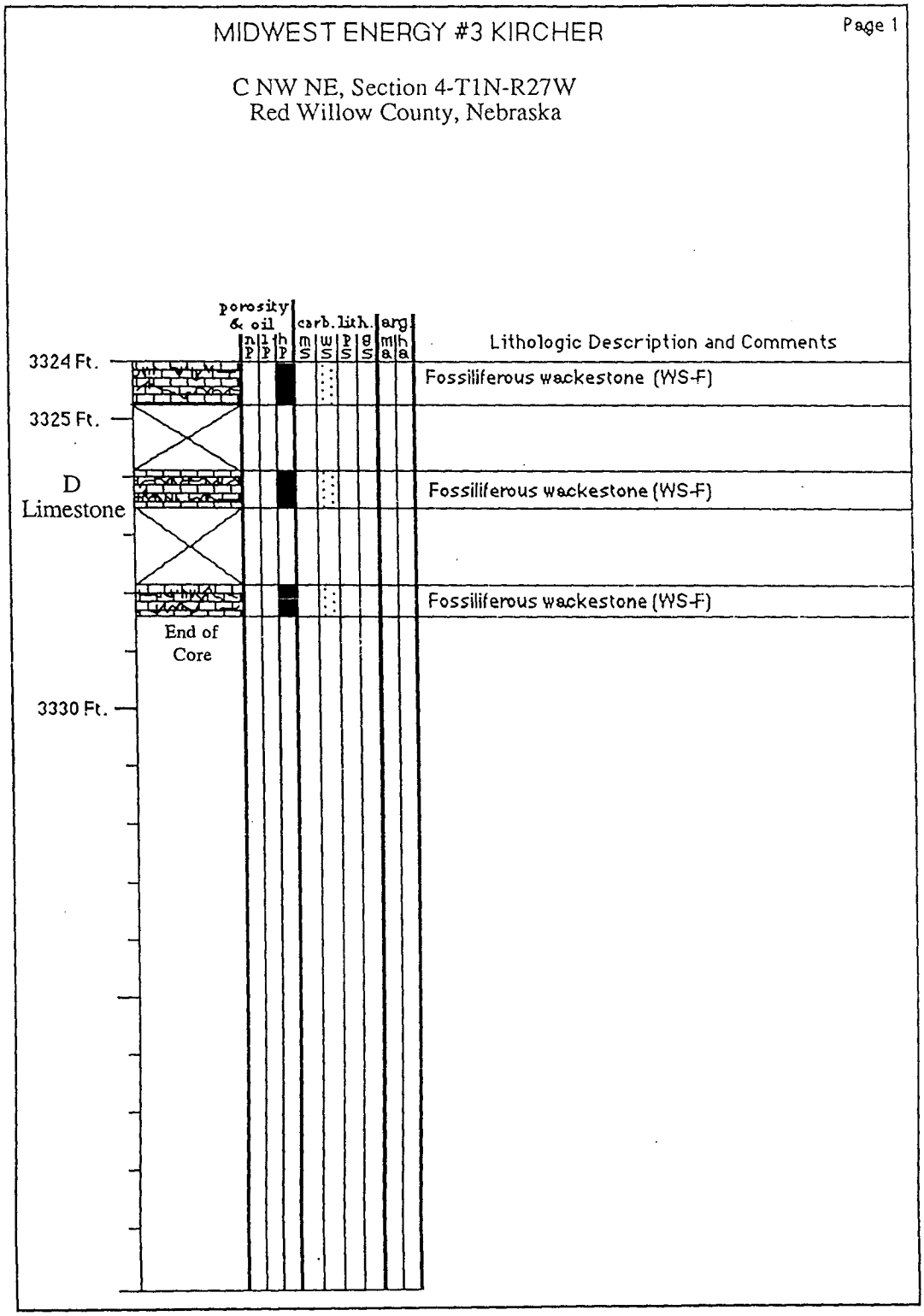
MIDWEST ENERGY #3 KIRCHER
Page 1
C NW NE, Section 4-T1N-R27W
Red Willow County, Nebraska
porosity & oil
carb. lith.
arg.
Lithologic Description and Comments
3324 Ft.
Fossiliferous wackestone (WS-F)
3325 Ft.
D Limestone
Fossiliferous wackestone (WS-F)
Fossiliferous wackestone (WS-F)
End of Core
3330 Ft.

JOHN O. FARMER #1 NICHOLSON

Location: C SW SW, Sec. 12 R1N T27W, Red Willow Co., Nebraska.
Initial production was 25 BOPD + 25% Water.
Production is from the upper and lower D Limestone.

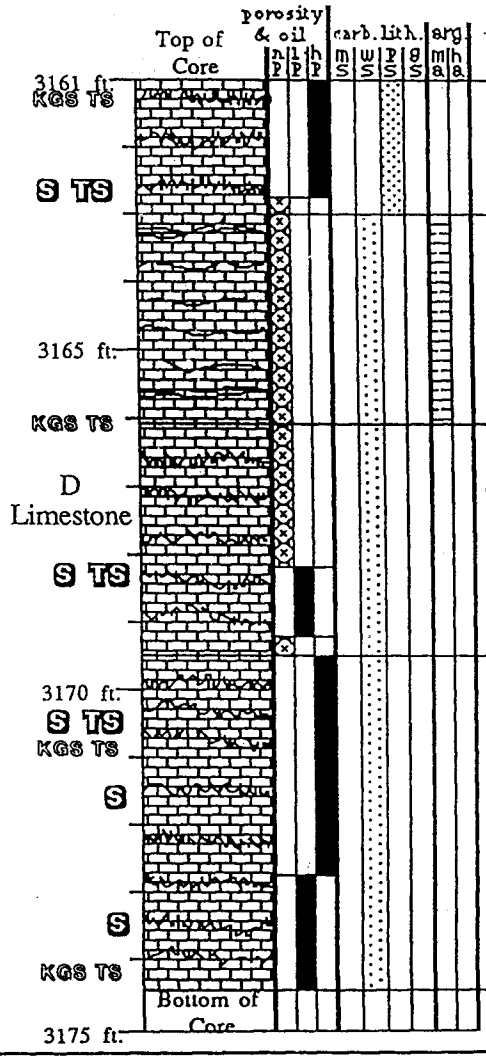

JOHN O. FARMER #2 NICHOLSON

Location: SW SE, Sec. 12-R1N -T27W, Red Willow Co., Nebraska.

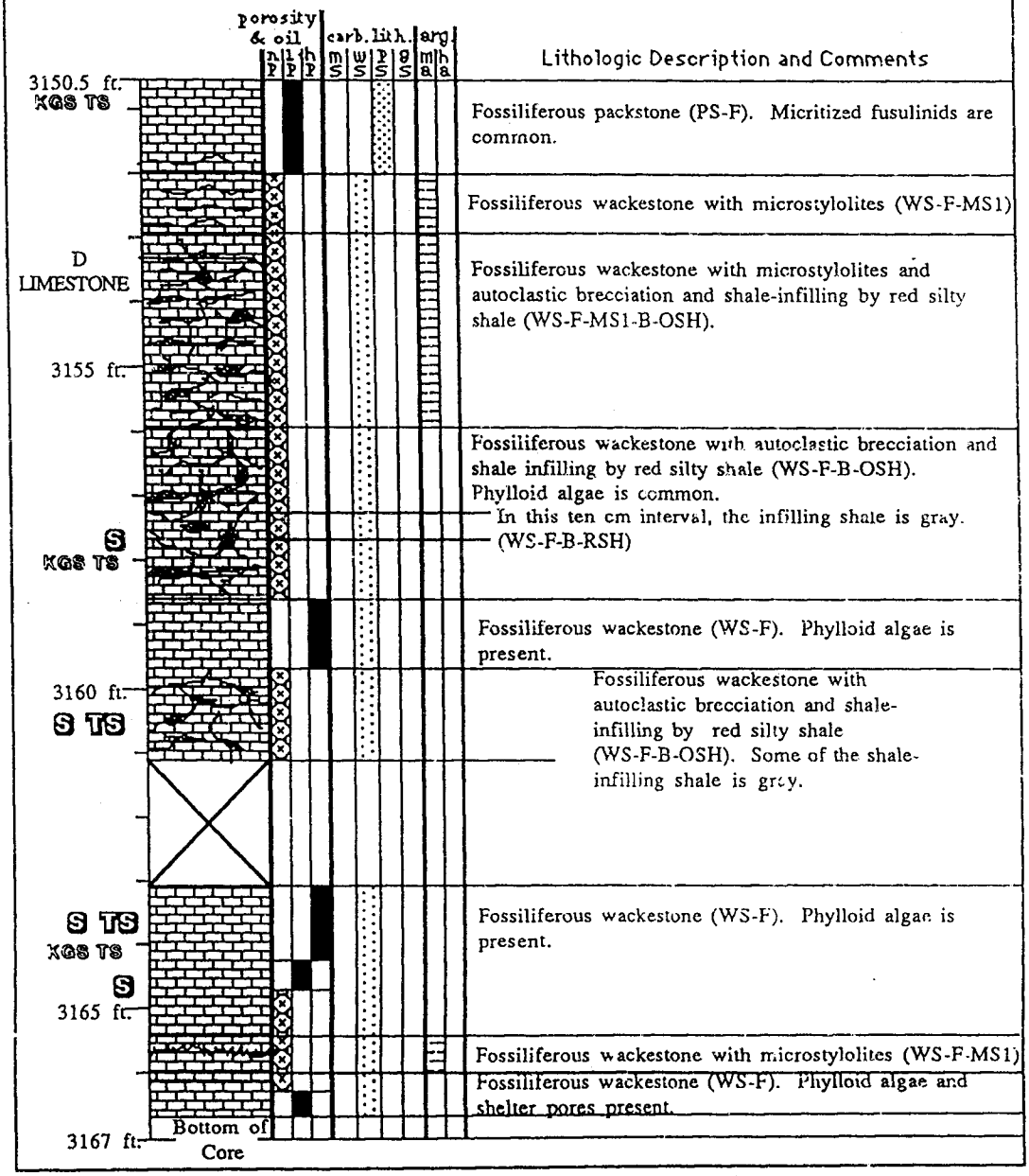

JOHN O. FARMER #3 NICHOLSON

Location: C NE NE, Sec. 14 R1N T27W, Red Willow Co., Nebraska.

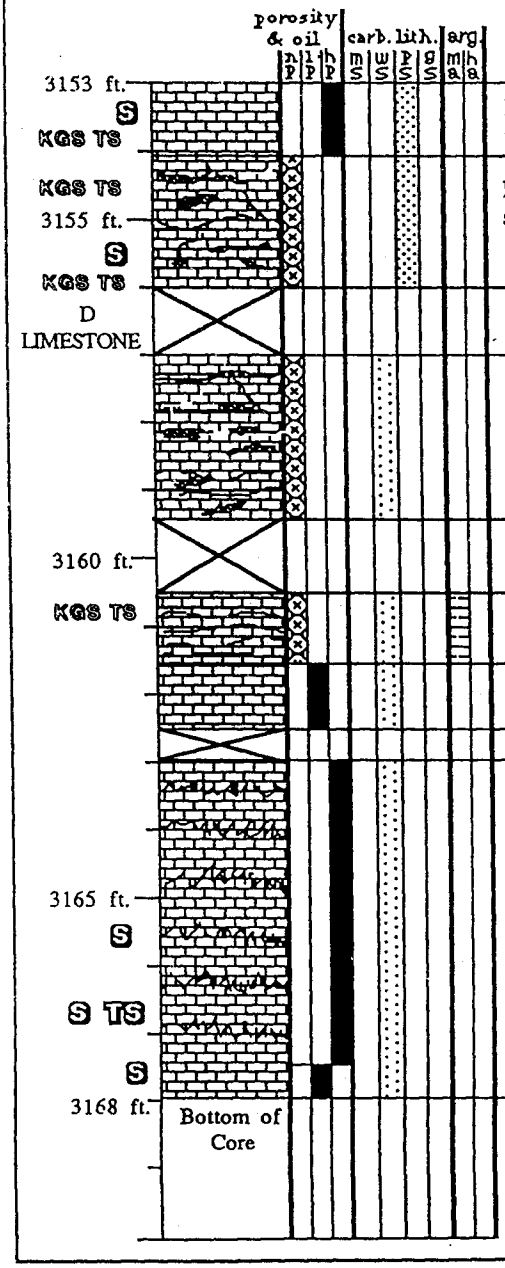

Lithologic Description and Comments
Foss. packstone (PS-F). Fusulinids are common. This interval may be a grainstone.
Fossiliferous packstone with autoclastic brecciation and shale infilling by red silty shale (PS-F-B-OSH)
Fossiliferous wackestone with autoclasitic brecciation and shale infilling by red silty shale (WS-F-B-OSH). Microstylolites are present and are interpreted to have formed from pressure solution of the infilling shale.
Fossiliferous wackestone with microstylolites (WS-F-MS1)
Fossiliferous wackestone (WS-F). Moldic pores are filled with calcite. The open porosity is microporosity.
Fossiliferous wackestone (WS-F). Phylloid algae may be present. Near the top, microporosity is common, larger MO or VUG pores are more common below 3164 ft.

JOHN O. FARMER #5 NICHOLSON

Location: C SW NE, Sec. 14-R1N- T27W,
Red Willow Co., Nebraska.

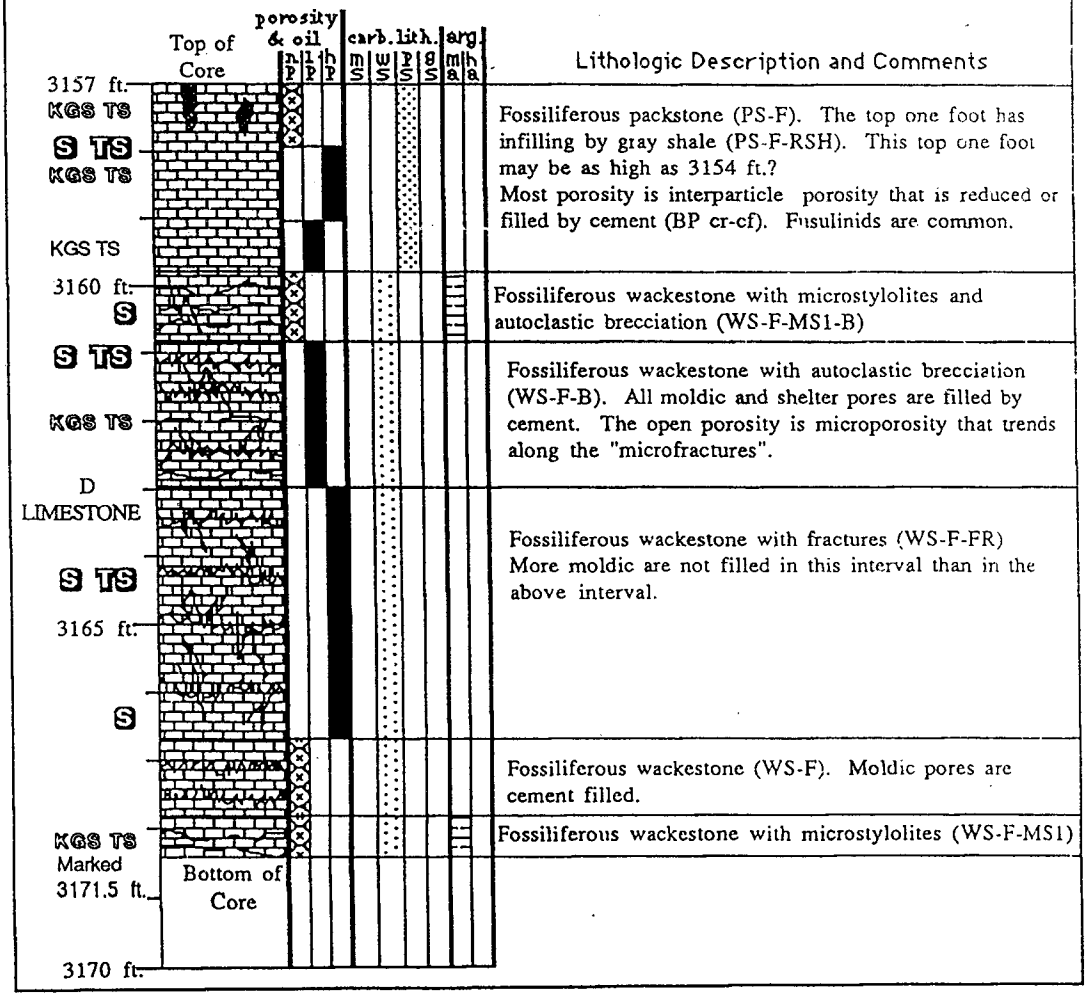

SKELLY OIL CO. #7 C.G. KISLING

C NW NW, Sec. 10-T1S-R34W
Rawlins Co., Kansas
Cahoj Field

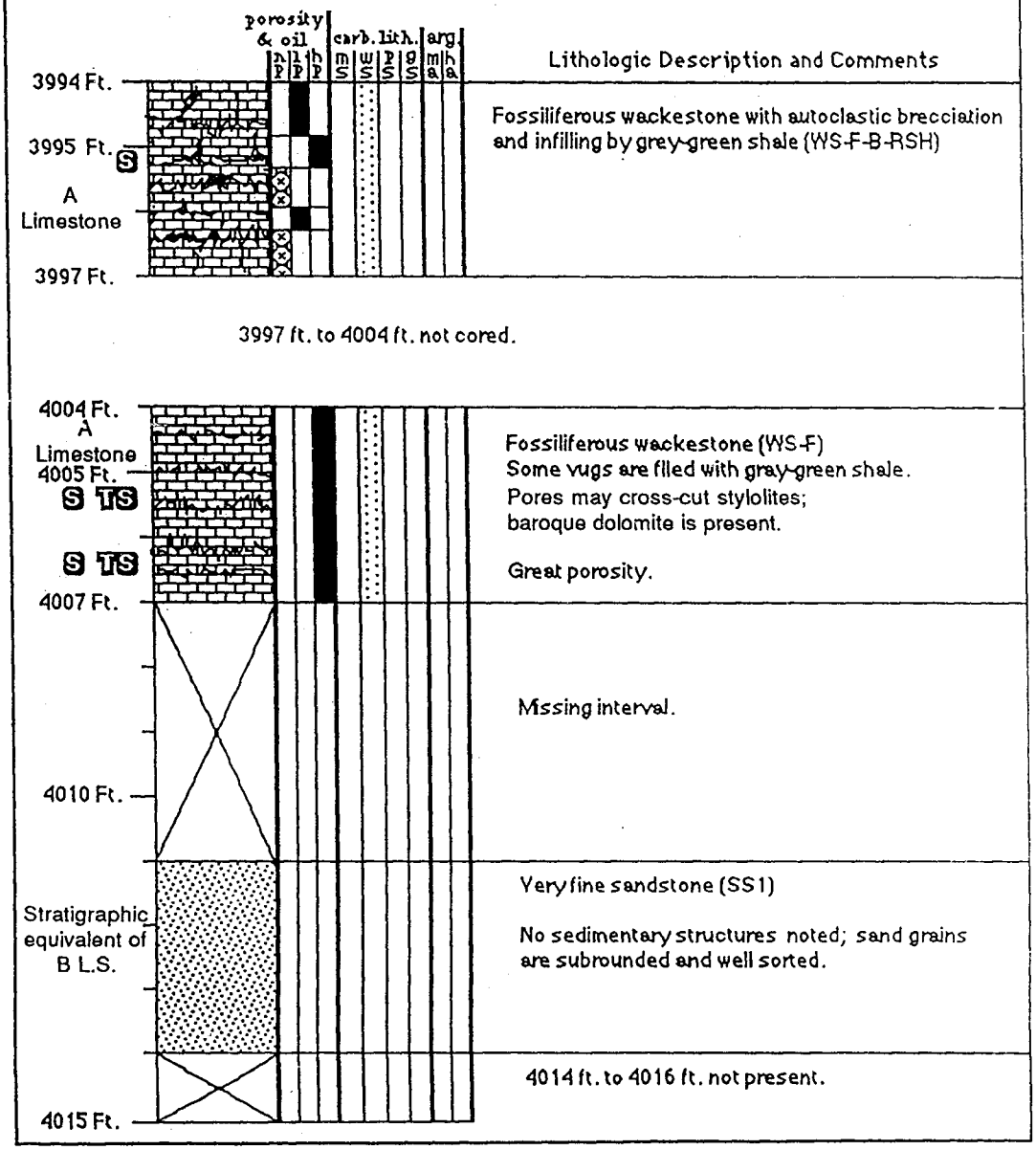

SKELLY OIL CO. #7 C.G. KISLING

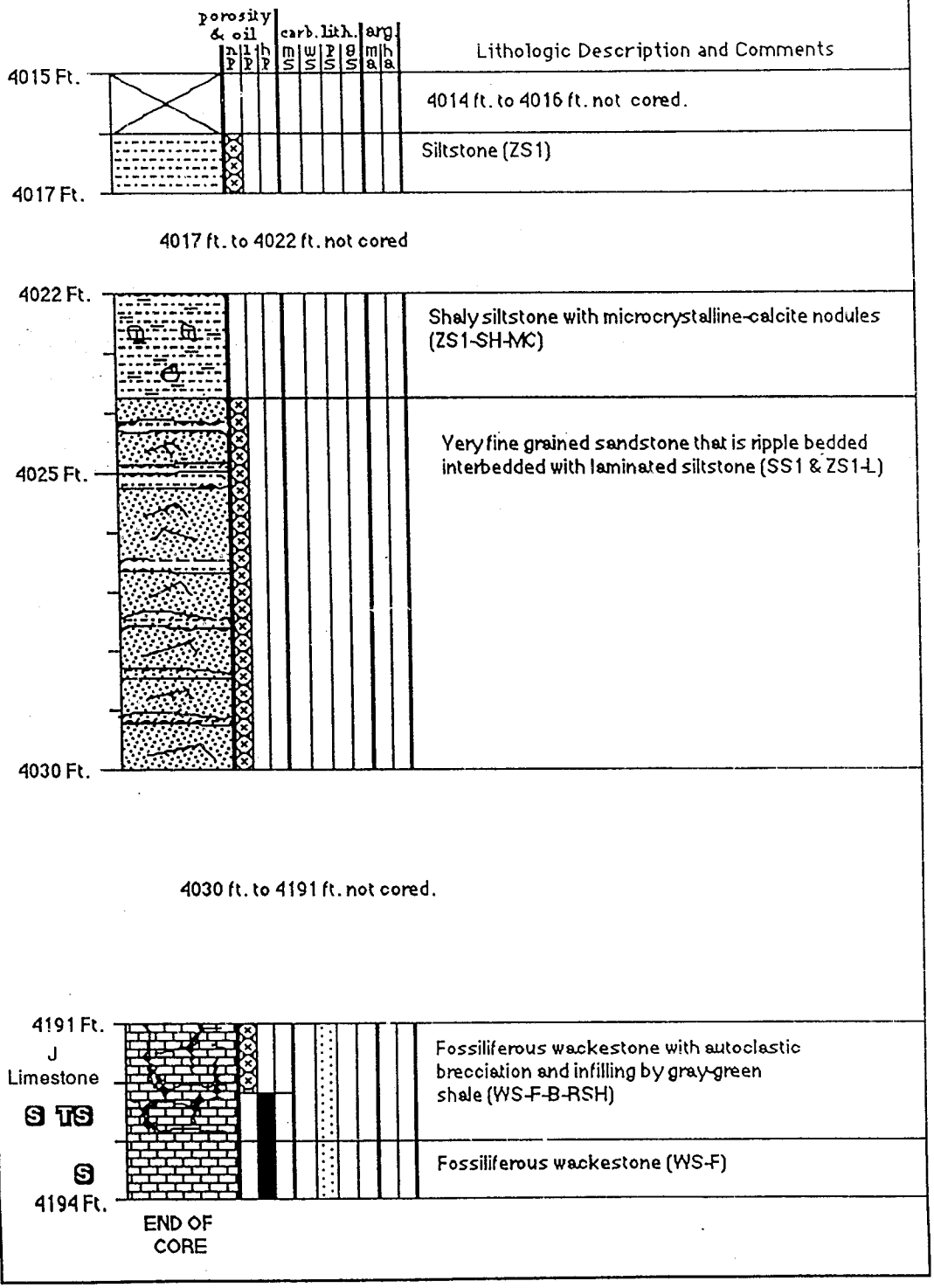

THEODORE GORE CO. #2 SCHAFFERT

Location: C SW SE, Sec. 28-T3N-R32W
This well produced 103 IBOPD at 3815-17 ft This well is part of the Republican River Field.

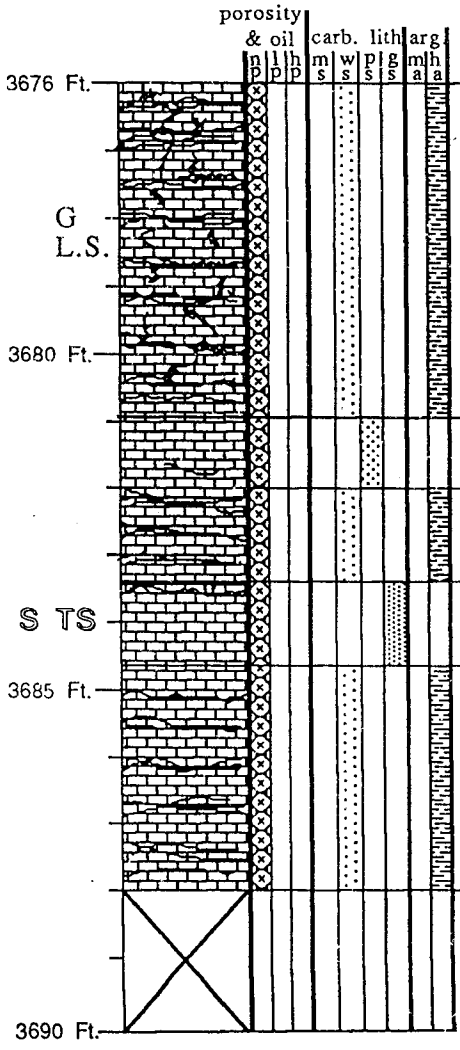

Lithologic Description and Comments

Fossiliferous wackestone with microstylolites and autoclastic brecciation with infilling by red shale (WS-F-MS2-B-OSH)

Fossiliferous packstone (PS-F)

Fossiliferous wackestone with microstylolites (WS-F-MS2)

Fossiliferous grainstone (GS-F). There is a zone of autoclastic brecciation with infilling by gray shale at the top of this lithology.

Fossiliferous wackestone with microstylolites (WS-F-MS2)

3688 ft. to 3813 ft. was not cored.

THEODORE GORE CO. #2 SCHAFFERT

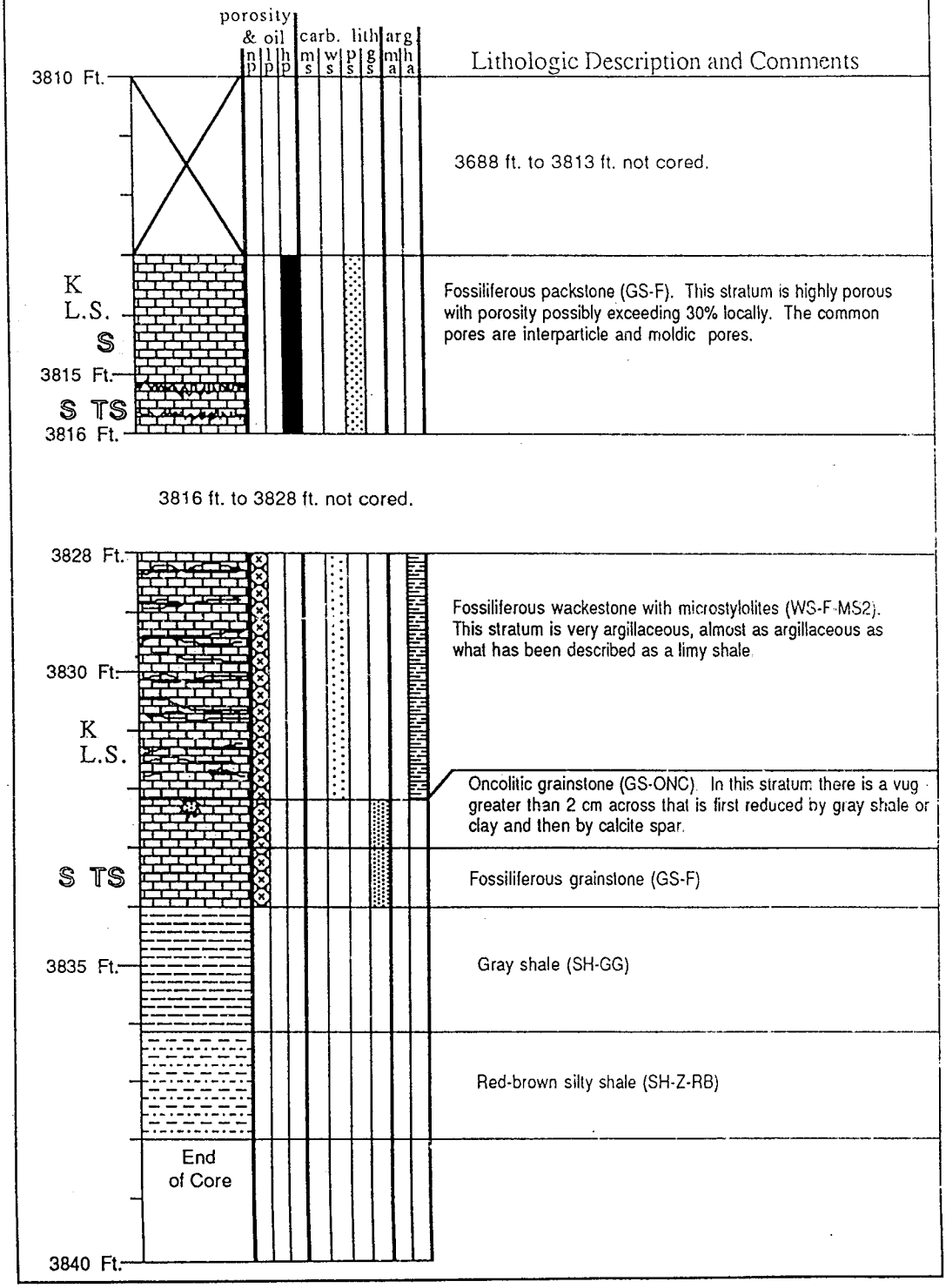

MURFIN DRILLING CO. #1 SOUCHEK

Perforated:
3960-66 ft.
3968-73 ft.
4004-10 ft.
4029-32 ft.
4052-58 ft.
4105-10 ft.
4121-25 ft.
4143-54 ft.

SE SE NE 2-T1S-RR34W
Cahoj Northeast Field
Rawlins, Co., Kansas
IPP 152 BOPD
Completed 10-6-1975
The Cahoj NE field has produced 592,091 BO (as of 1983) since being discovered in 1970. The Cahoj field, 6 miles to the southeast, has produced 7,065,017 BO (1983) since discovery in 1959.

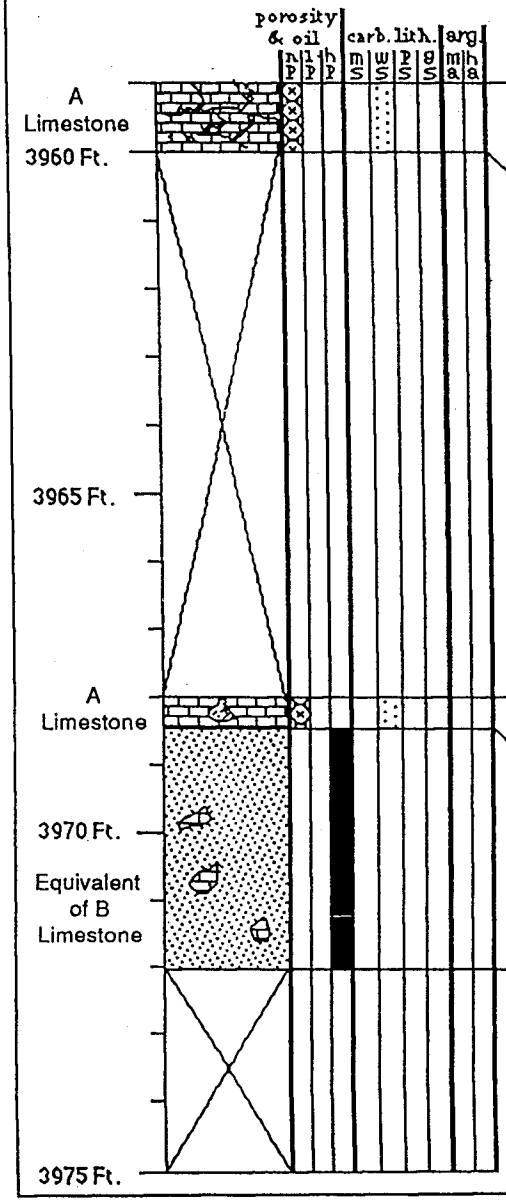

Lithologic Description and Comments

Fossiliferous wackestone with autoclastic brecciation and infilling by green shale (WS-F-B-RSH)
Mold-filling cements are ferroan calcite

Porosity and Permeability data from Hunt (1981)

Depth	Sample #	Porosity	Permeability
3968 ft.	S2A	0.00%	0.00 md
3968 ft.	S2B	2.6 %	0.00 md
3970 ft.	S3A	23.1 %	2.29 md
3970 ft.	S3B	22.5 %	2.16 md
3971 ft.	S1A	27.9 %	9.12 md
3971 ft.	S1B	27.2 %	8.86 md

3960 ft. to 3968 ft. not cored.

Foss. wackestone with autoclastic brecciation and infilling by very-fine sandstone (WS-F-B-SS)

Brown to red very-fine sandstone with oil staining (SS1-RB)
Concretions are composed of non-ferroan calcite, non-ferroan dolomite, ferroan calcite, and baroque dolomite.

Some silt may be present.

MURFIN DRILLING CO. #1 SOUCHEK

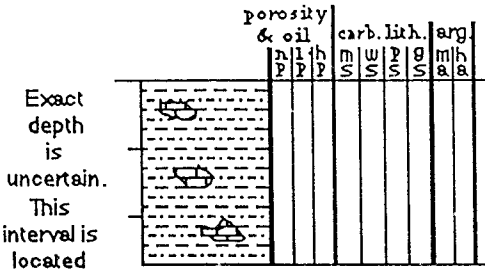

Lithologic Description and Comments

Exact depth is uncertain. This interval is located between 3972 ft. and 4004 ft.

Red-brown silty shale with microcrystalline-calcite nodules and green mottling (SH-Z-RB-MC-GM)

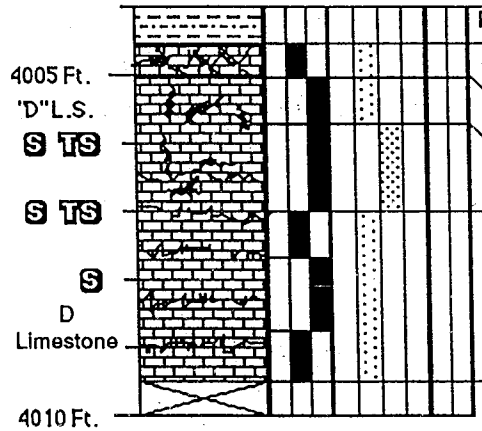

Red-brown silty shale with green mottling (SH-Z-RB-GM)

Foss. wackestone with autoclastic brecciation and infilling by green shale (WS-F-B-RSH)

Foss. wackestone with infilling by green shale (WS-F-RSH)

Peloidal and fossiliferous packstone with infilling by green shale (PS-P & F-RSH)

Fossiliferous wackestone (WS-F)

The interval from 4009.5 ft to 4029 ft. was not present in the core boxes.

Porosity and Permeability data from Hunt (1981):

Depth	Sample #	Porosity	Permeability
4006 ft.	S4	10%	4.37 md
4006 ft.	S5A	21.8%	10.24 md
4006 ft.	S5B	12.7%	7.23 md
4008 ft.	S6A	2.7%	0.00 md
4008 ft.	S6B	5.5%	0.00 md
4010 ft.	S7A	12.9%	7.50 md
4011 ft.	S8A	8.3%	0.00 md
4029 ft.	S9A	1.7%	0.00 md
4029 ft.	S9B	1.8%	0.00 md
4032 ft.	S10A	2.1%	0.00 md
4032 ft.	S10B	4.0%	0.00 md

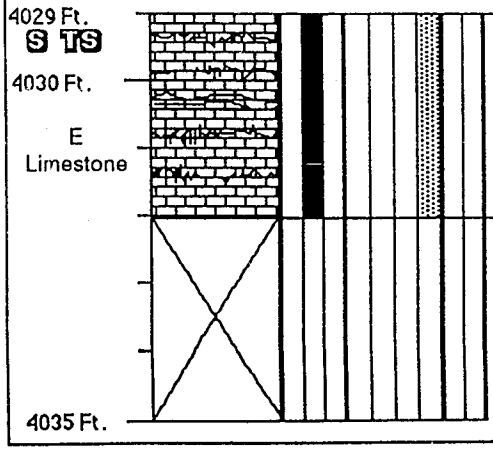

Fossiliferous grainstone (GS-F) with oil staining and porosity estimated to be less than 8%.

4032 ft. to 4100 ft. not cored.

MURFIN DRILLING CO. #1 SOUCHEK

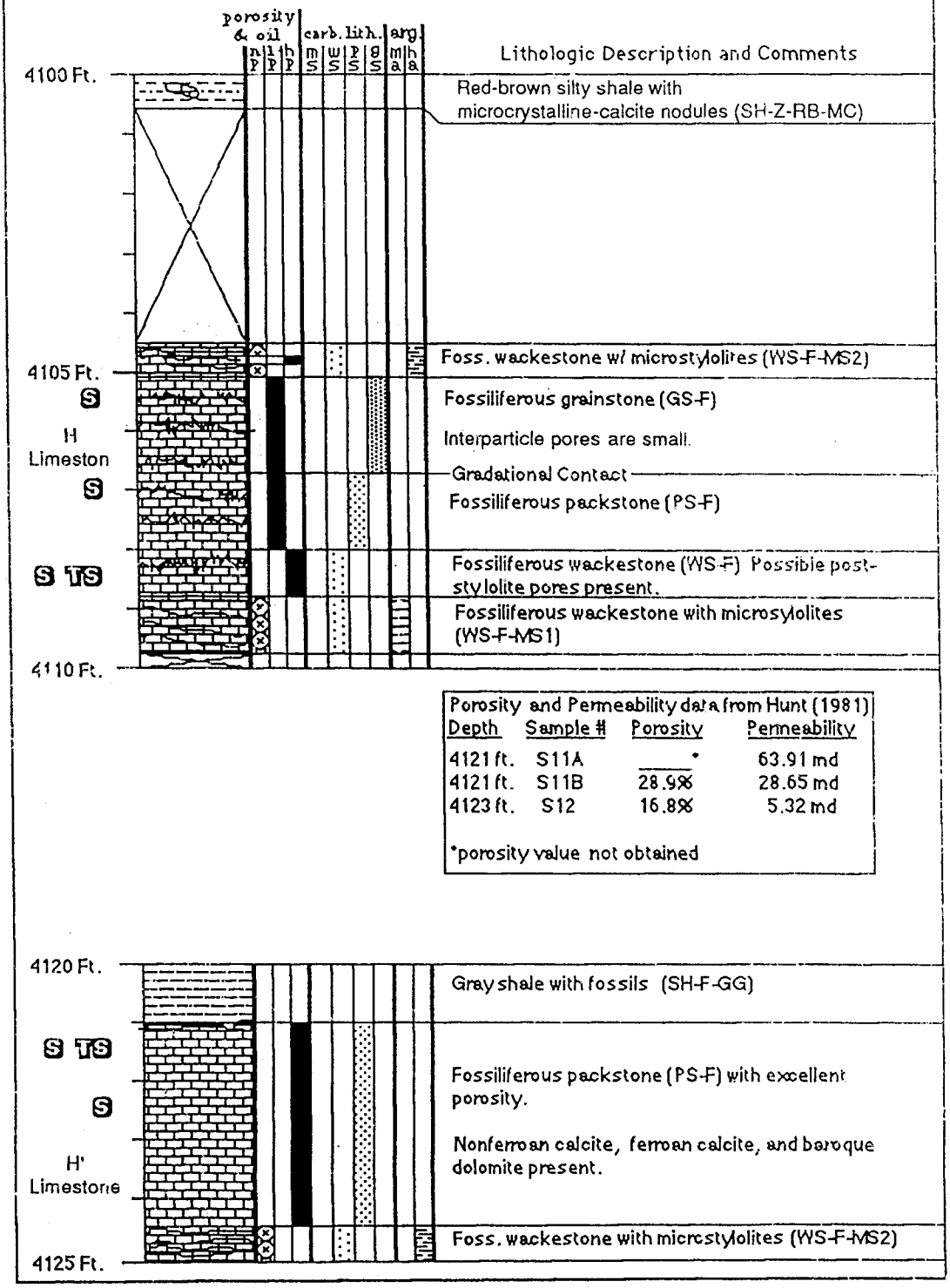

Porosity and Permeability data from Hunt (1981)

Depth	Sample #	Porosity	Permeability
4121 ft.	S11A	*	63.91 md
4121 ft.	S11B	28.9%	28.65 md
4123 ft.	S12	16.8%	5.32 md

*porosity value not obtained

MURFIN DRILLING CO. #1 SOUCHEK

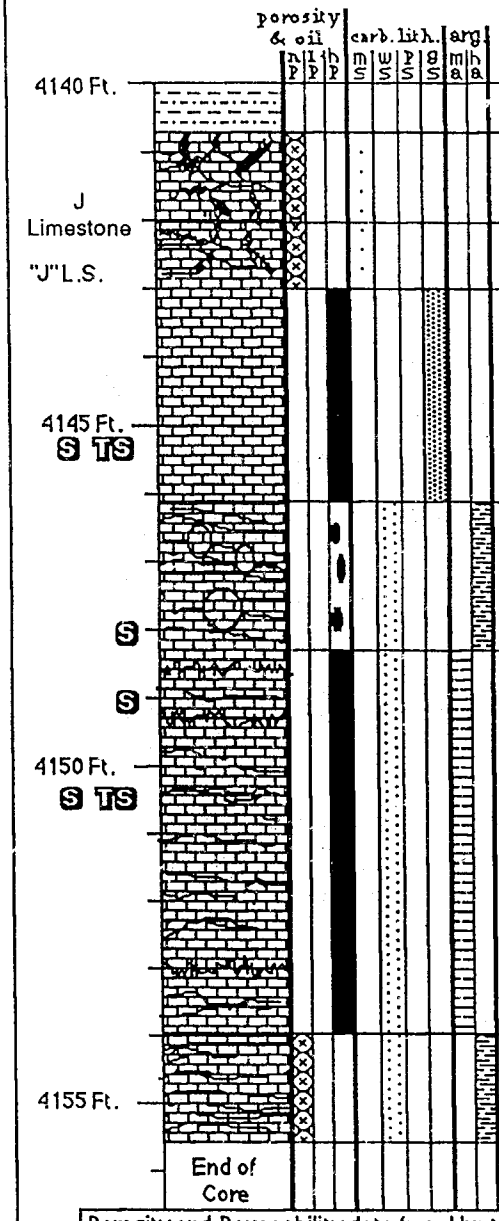

Porosity and Permeability data from Hunt (1981)

Depth	Sample #	Porosity	Permeability	Depth	Sample #	Porosity	Permeability
4144 ft.	S13A	15.0%	22.51 md	4148 ft.	S16A	17.1%	3.51 md
4144 ft.	S13B	20.1%	46.07 md	4148 ft.	S16B	15.7%	0.87 md
4145 ft.	S14A	31.2%	45.41 md	4148 ft.	S17A	25.8%	67.8 md
4145 ft.	S14B	35.1%	77.83 md	4148 ft.	S17B	____*	67.57 md
4148 ft.	S15A	18.5%	0.00 md	4148 ft.	S18A	38.0%	67.94 md
4148 ft.	S15B	17.6%	0.00 md	4148 ft.	S18B	30.2%	58.81 md
*porosity value not obtained				4153 ft.	S19	18.1%	13.76 md

SHAKESPEARE OIL CO. #2 RUDOLPH

NE NE NE, Section 9-T3S-R41W
Cheyenne County, Kansas

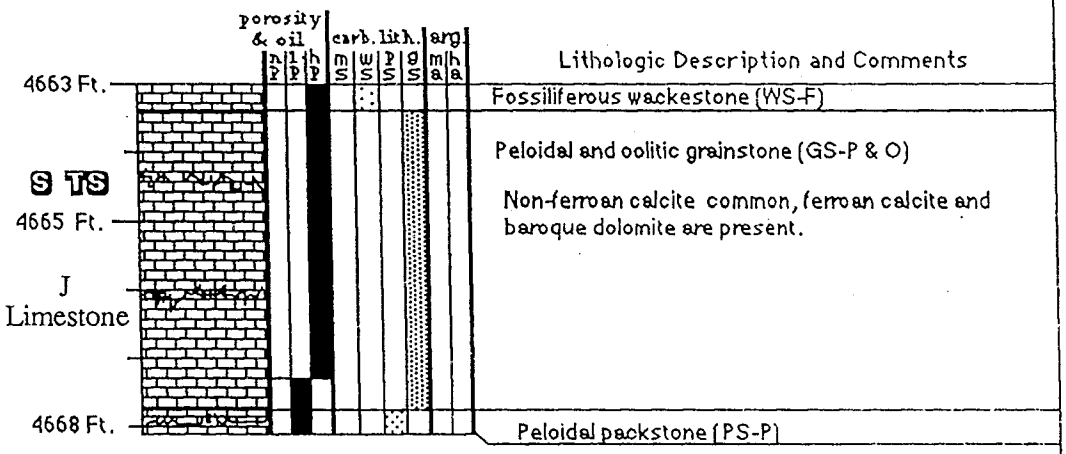

THEODORE GORE CO. #1 WERTZ
SE NW, Section 6-T2N-R32W
Hitchcock County, Nebraska
Republican River Field
Drilled June, 1976

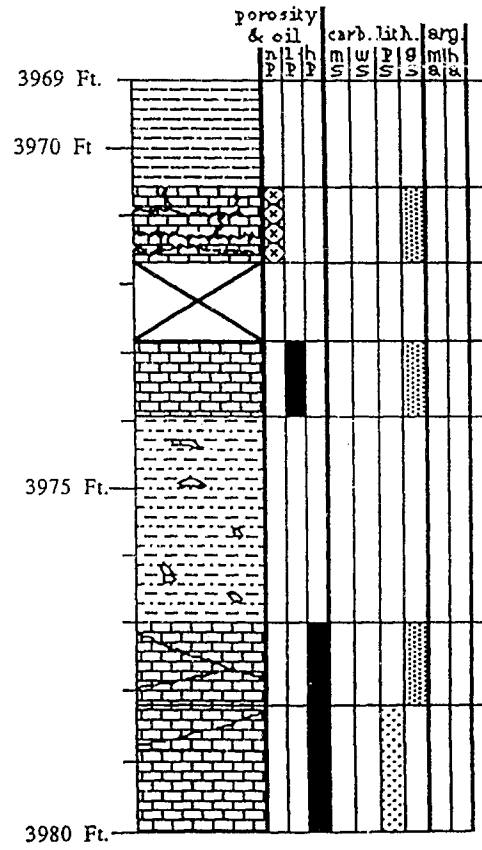

Lithologic Description and Comments

Red-gray shale (SH-RB)

Fossiliferous grainstone with autoclastic brecciation and infilling by gray shale (GS-F-B-RSH)

Fossiliferous grainstone (GS-F)

Red-brown silty shale with microcrystalline-calcite nodules (SH-Z-RB-MC)

Peloidal and fossiliferous grainstone (GS-P&F). Microcrystalline calcite is present in "tubes".

Fossiliferous packstone (PS-F)

No stylolites.

THEODORE GORE CO. #1 WERTZ

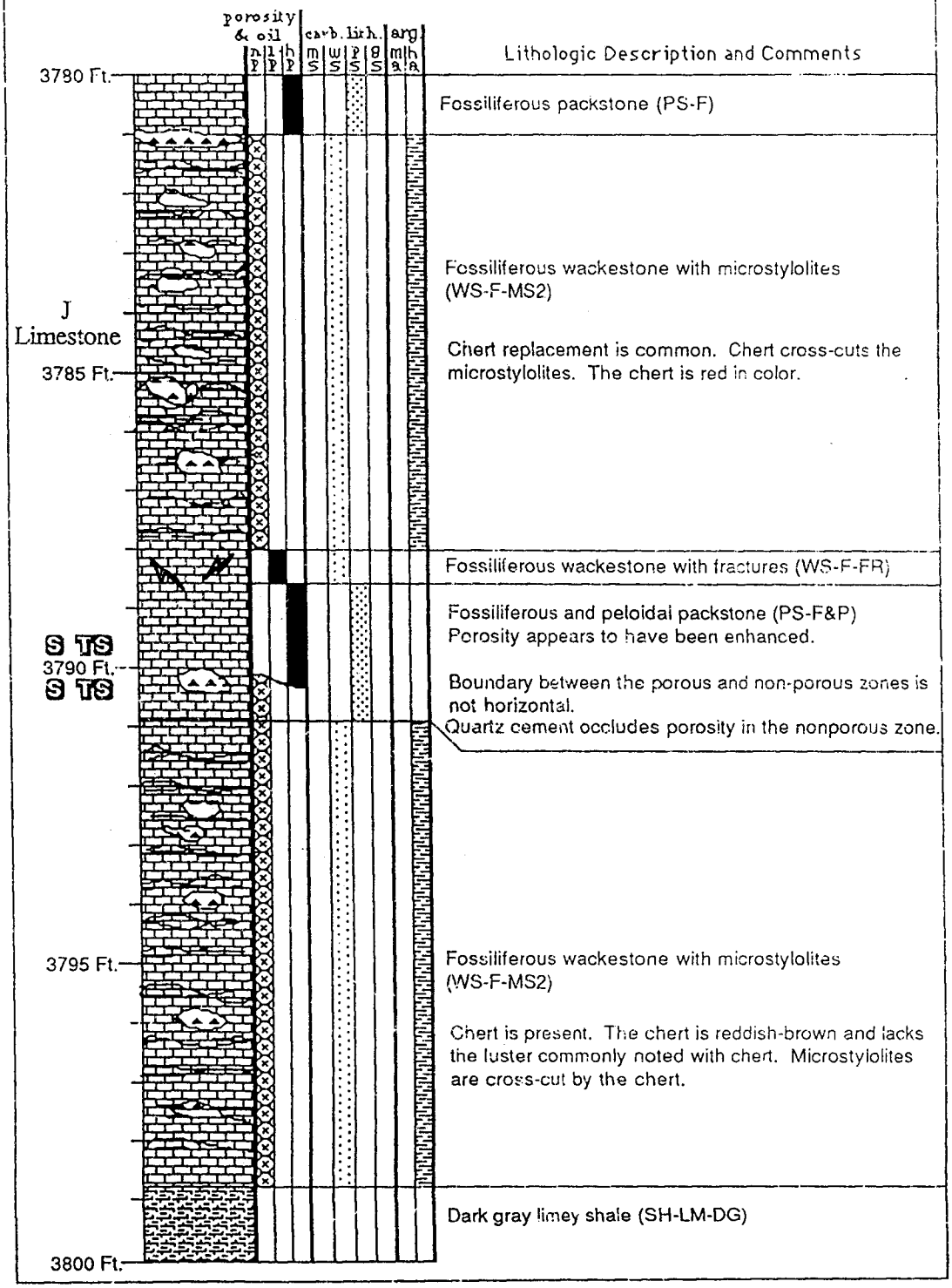

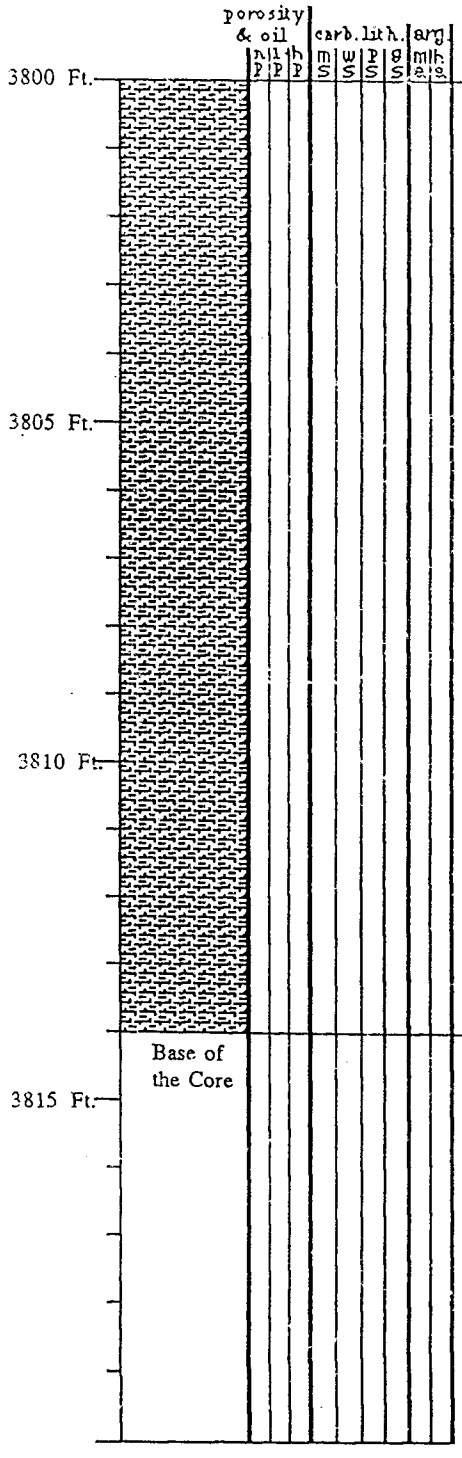

Lithologic Description and Comments

Dark-gray limey shale (SH-LM-DK)

This stratum is a comparable to the microstylolitized wackestones, but this stratum is much more argillacesous to the point that shale is more dominant than the carbonate.

Near the top of this stratum, carbonate mud fills possible burrows.